NASA Contractor Report 3375

Satellite Power Systems (SPS) - LSST Systems Analysis and Integration Task for SPS Flight Test Article

H. S. Greenberg

CONTRACT NAS8-32475
FEBRUARY 1981

NASA

NASA Contractor Report 3375

Satellite Power Systems (SPS) - LSST Systems Analysis and Integration Task for SPS Flight Test Article

H. S. Greenberg
Rockwell International
Downey, California

Prepared for
Marshall Space Flight Center
under Contract NAS8-32475

NASA
National Aeronautics
and Space Administration

Scientific and Technical
Information Branch

1981

FOREWORD

This report contains the structural requirements established for a 1224-meter (side dimension) hexagonal frame and a 20 by 200 meter solar array blanket structure, each of which is the major structure in an SPS test article. These requirements were established from systems definition of the mission and major systems equipment requirements for each test article.

The study was performed by the Space Operations and Satellite Systems Division of Rockwell International in response to NASA/MSFC Contract NAS8-32475, Exhibit E, dated March 25, 1980. The work was accomplished under the technical direction of Mr. James K. Harrison, Advanced Systems Office, George C. Marshall Space Flight Center.

The study was performed under the direction of H. Stanley Greenberg, Study Manager, who may be reached at (213) 594-3687. The following persons made significant contributions toward the completion of the analyses reported herein:

Dr. A. Love	- Microwave
A. Gordon	- Power, Data Management and Communications
D. Camillone	- Attitude Control and Stabilization
K. Kunz	- Auxiliary Propulsion
D. Reed	- Structural Design
Dr. E. French	- Thermal Control

CONTENTS

ILLUSTRATIONS

TABLES

1.0 INTRODUCTION

This report presents the systems definition and resulting structural requirements for the primary structure of two SPS test articles that are fundamental steps in the Satellite Power System (SPS) development cycle. These test articles are:

- SPS Test Article I—A proof-of-concept test article first proposed to NASA/MSFC in a Rockwell briefing presented on December 19, 1979. Documentation of the briefing material is contained in Rockwell Report SSD 80-0108-5, Volume V, ***Satellite*** *Power Systems (SPS) Concept Definition Study, Exhibit "D", Final Report* (August 1980)

- SPS Test Article II—A test article developed in the Space Construction System Study by Rockwell for NASA/JSC under Contract NAS9-15718. The study data are documented in Rockwell Report SSD 79-0077, *Space Construction Systems and Mission Descriptions, Task I, Final Report* (April 26, 1979).

1.1 BACKGROUND

For several years NASA has pursued a program to develop the capability to build large lightweight structures in space using three basic methods of construction: space fabrication, deployable, and erectable. The most suitable method of construction for a particular application is dependent on the configuration size and shape and the mission driven structural requirements.

To develop this *in-situ* capability NASA is, therefore, studying the structural requirements aspects of platform concepts for several prospective user groups that can profit from this new technology, including the Satellite Power Systems (SPS) program. In these studies the structural design requirements are first determined and then conceptual designs are developed to satisfy these requirements.

1.2 STUDY OBJECTIVES

The objective of this study was to determine the structural requirements for SPS Test Articles I and II. Both articles are fundamental structures and intermediate design steps in the SPS development cycle.

The two test articles, having vastly different size, shape, loading, and dimensional stability requirements, provide a dramatic illustration of the significance of mission induced structural requirements variations on the design requirements.

2.0 SPS TEST ARTICLE I

This section describes the SPS Test Article I mission, mission equipment, and subsystems equipment pertinent to the design of this test article's major structure, the hexagonal frame. The frame's overall strength, stability, stiffness, and dimensional stability requirements and equipment and utilities accommodations are described in Section 2.1.5. A brief summary of Section 2.1.5 is included, for convenience, in Section 2.1.3.

The test article shown in Figure 2.0-1 was derived from the following requirements.

1. A recommendation to demonstrate by 1990 the feasibility of the space construction of a structurally suitable and significantly large SPS structure.

2. Proof of the solid-state electronics concept engineering parameters delineated in Section 2.2.1.

3. Transmission of a significant level of power to the ground rectenna (18.8 kW).

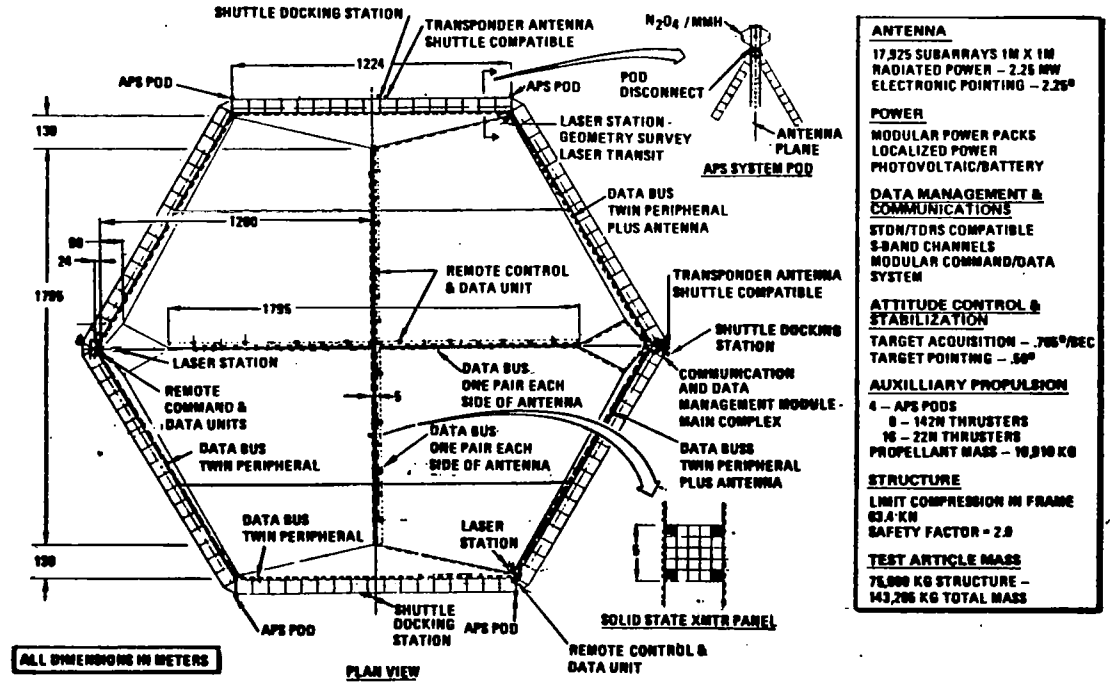

Figure 2.0-1. Test Article I Configuration

4. In view of the large investment, retention and use of the demonstration structure in the future solid-state configuration (Figures 2.2-27 and 2.2-28).

The hexagonal frame planform size was directly determined from the first and-fourth requirements, and satisfied the other requirements.

2.1 SYSTEM DEFINITION

2.1.1 MISSION OBJECTIVES AND DESCRIPTION

Test Objectives

The SPS Test Article I demonstration test objectives are as follows:

- Construction of a significantly large SPS structure
- Measurement of the structure fabrication quality in regard to deviations from straightness
- Verification of structural suitability
- Delivery of 18.8 kilowatts of power from LEO to ground
- Retrodirective phase control of array for
  - Microwave antenna beam formation
  - Electronic beam steering up to ±2.25°
- Solid-state power amplifier performance and efficiency of dc/RF conversion
- Solar array, power conditioning, and battery performance
- Legacy in the form of capability for later upgrading to a full-blown SPS satellite in geosynchronous orbit

Mission Scenario

The SPS test article mission scenario is illustrated in Figure 2.1-1; the highlights of each phase are discussed below.

Frame Construction (Construction time—up to six months)

Data from the Space Construction Study[1] indicated a total structure construction time of 36 hours to fabricate the structural beams (one beam machine), join the transverse to longitudinal beams, and install and pretension the X-bracing. For a tri-beam hexagonal frame with a perimeter length of 7488 m, simple extrapolation indicates a construction time of 112 days. Use of more than one beam machine can reduce this value; however, it is estimated that other constructions could require additional time—hence, a six-month construction period is required.

[1] *Space Construction Systems and Mission Descriptions, Task I, Final Report,* NASA/JSC, Contract NAS9-15718, Rockwell International, SSD 79-0077 (April 26, 1979).

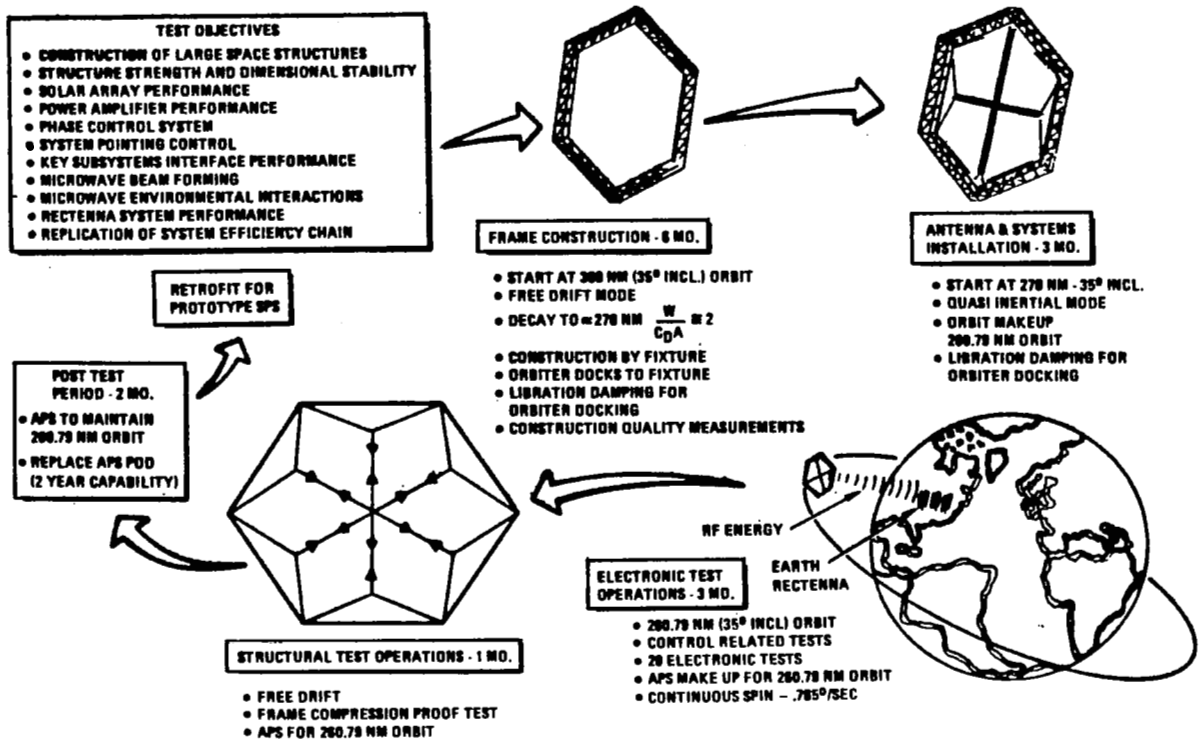

Figure 2.1-1. Mission Description and Construction Scenario

The need for an initial 300-nmi construction orbit was based on the orbit decay data shown in Figure 2.1-2. The W/C_DA estimated for the Test Article space-fabricated frame is 2.0. (A pentahedral truss utilizing dixie-cup columns would be higher, i.e., approximately 3.0.) The requirement imposed on the use of the OMS kits and the reduction of cargo bay volume is appreciated and dependent on detailed knowledge of the construction.

A free-drift mode was selected to minimize propellant requirements.

Antenna Systems Installation (Construction time—three months)

The construction time is three months and is based on the requirement to make the 17,925 subarray monitor and control electrical connections. This will allow about seven minutes per connection which is expected to be adequate.

Orbiter docking—To accommodate delivery and installation of the antenna solid-state panels, Orbiter docking ports are located as shown in Appendix A (Drawing 42635-18029).

Orbiter makeup propellant for this phase and for the remaining six months is based on the data of Table 2.1-1 for $W/C_DA = 1$ (example space-fabricated structure and antenna array).

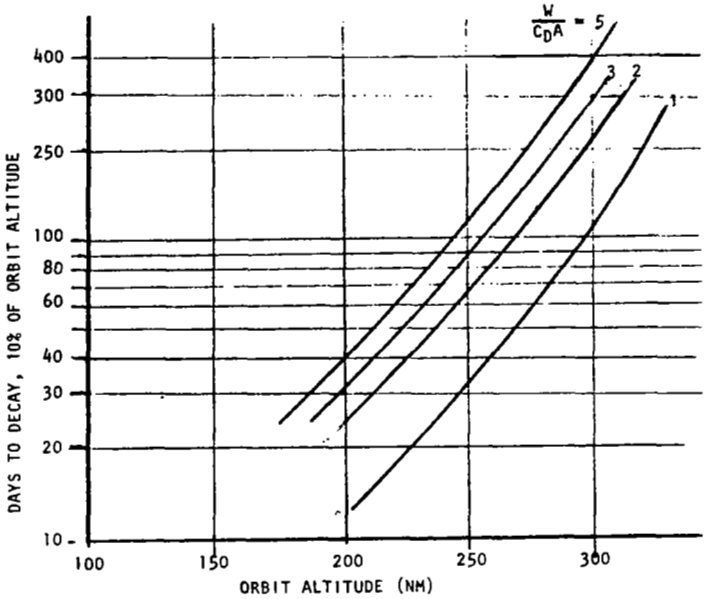

Figure 2.1-2. Orbit Decay Vs. W/C_DA (lb/ft^2)

Table 2.1-1. Orbit Makeup Vs. W/C_DA
(483 km orbit, inclination = 35°)

W/C_DA		Propellant
N/m^2	(lb/ft^2)	(kg/kg/day)
47.9	1.0	0.000081
71.8	1.5	0.000054
95.8	2.0	0.000040
119.8	2.5	0.000033

Electronic Tests/Test Maneuver

The test article is in a 483 km (260.79 nmi), 35° inclination orbit. The rectenna is located at 35°N latitude. For this case the test article will pass through the zenith point of the rectenna every 15th orbit. This is the point of closest approach. The critical features and parameters of the test maneuver are shown in Figure 2.1-3. The figure at the left indicates the need for a pitch maneuver of 0.765°/sec during the test. The results of a computer simulation, shown at the right, illustrate the deviation between the pitch angle required for continuous target acquisition and a constant induced pitch rate for the satellite. Correction can be achieved by electronic beam pointing through the use of phase control at individual subarrays. For the selected subarray size of one meter by one meter, electronic beam steering through ±2.25° is possible at the expense of up to 1.6 dB loss in antenna gain. The 2.25° allowable deviation is the sum of 1.7° (from Figure 2.1-3) and an allowance of 0.55° for mechanical pointing error.

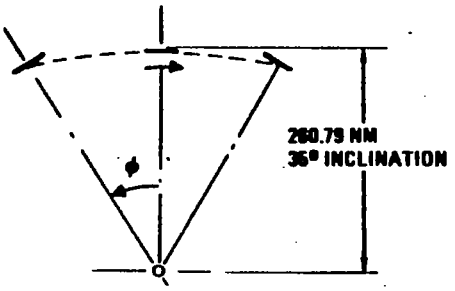

- ϕ AT START OF TEST = 41.3°
- TEST TIME = 108 SECONDS
- PITCH RATE = .765°/SEC
- MAXIMUM DEVIATION OF 1.7° INCLUDES GRAVITY GRADIENT AFFECTS
- PERMISSIBLE ADDITIONAL MECHANICAL POINTING ERROR = .55°

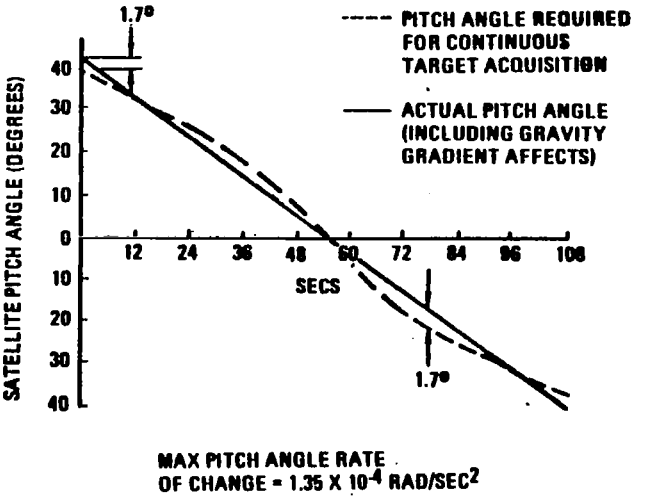

Figure 2.1-3. Test Maneuver

Twenty such test maneuvers are required, in which case continuous spinning of the test article results in the minimum propellant usage.

Structural Test Operations

Subsequent to completion of the electronic test phase, the tension cable system geometry can be replaced with a system representative of the future prototype design and a proof test to the limit loads of the future prototype structure (33-1/3% increase in test article loads) can be performed. Replacement of the SPS test article cable arrangement is necessary since a NASTRAN hexagonal frame stability analysis indicates the buckling coefficient ϕ is dependent on cable geometry (Figure 2.1-4).

Post-Test Period (two months)

Sufficient propellant is provided in the basic APS module to provide orbit makeup for two months subsequent to the structural test period. After the end of the two-month period, the empty APS pods will be removed and replaced with APS modules capable of maintaining the 483 km orbit for two years. For this reason, orbiter docking ports are provided adjacent to the APS pods.

2.1.2 MISSION EQUIPMENT REQUIREMENTS SUMMARY

Mission equipment is defined to be those systems or subsystems that are located on a satellite solely to satisfy the mission experimental objectives. Equipment installed to fully (or even partially) support the basic satellite operations is not included. In the case of Test Article I, the microwave subsystem discussed in Section 2.2.1 is considered the single relevant subsystem.

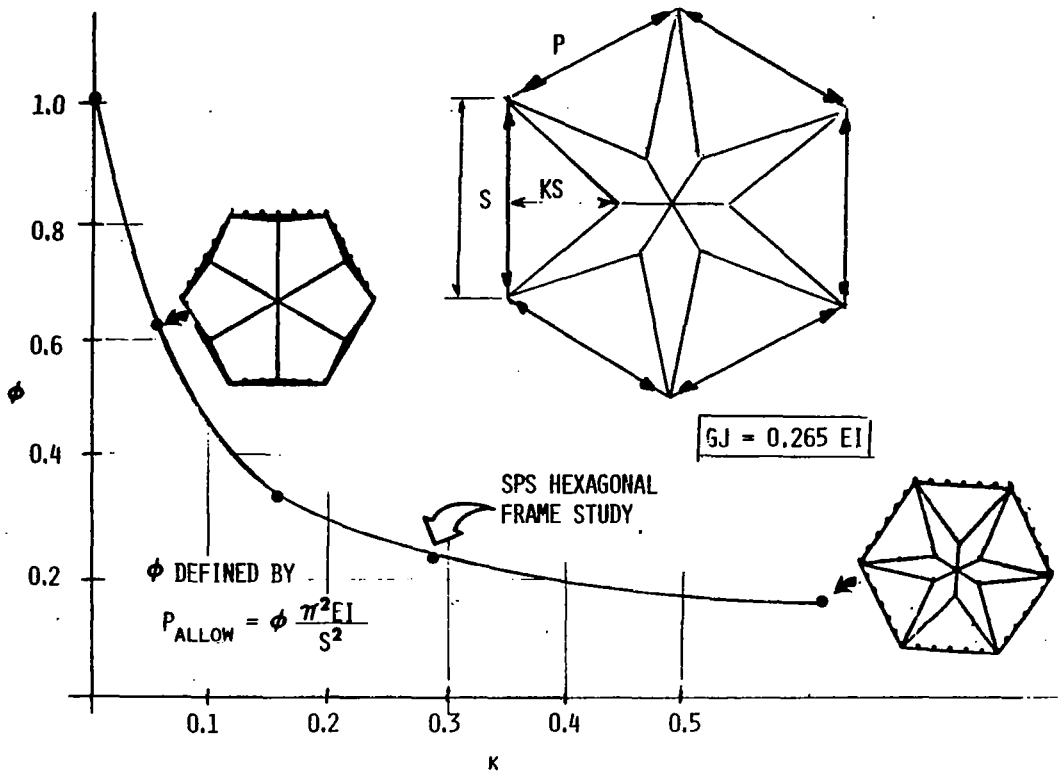

Figure 2.1-4. Variation of Stability Coefficient ϕ With Tension Cable Geometry

The SPS Test Article I microwave system accepts energy from a photoelectric solar cell/battery power subsystem and transmits this energy as microwave energy to a ground receiver where the energy is then converted to a form compatible with standard utility networks. The test antenna consists of 17,925 one-meter by one-meter subarrays arranged in a Mills Cross configuration with each leg 5 m wide and 1795 m long. Figure 2.1-5 illustrates this arrangement on the satellite and also shows the location of the associated power sources for each 25-m^2 segment of the antenna. All subarrays operate at the same RF power density level, arbitrarily specified to be 125 W/m^2. Total mass of the microwave antenna is estimated to be 0.454×10^5 kg, including the associated power packs and a growth allowance of $0.099 \chi 10^5$ kg (22%).

2.1.3 SUBSYSTEMS EQUIPMENT REQUIREMENTS SUMMARY

Described in this section are the power, data management and communications, stabilization and control, and auxiliary propulsion subsystems to be supported by the structure, and a summary of the structural requirements listed in Section 2.1.5.

Power Subsystem

Requirements

- Sun availability, 1-2 hours (equivalent) per 24-hour period

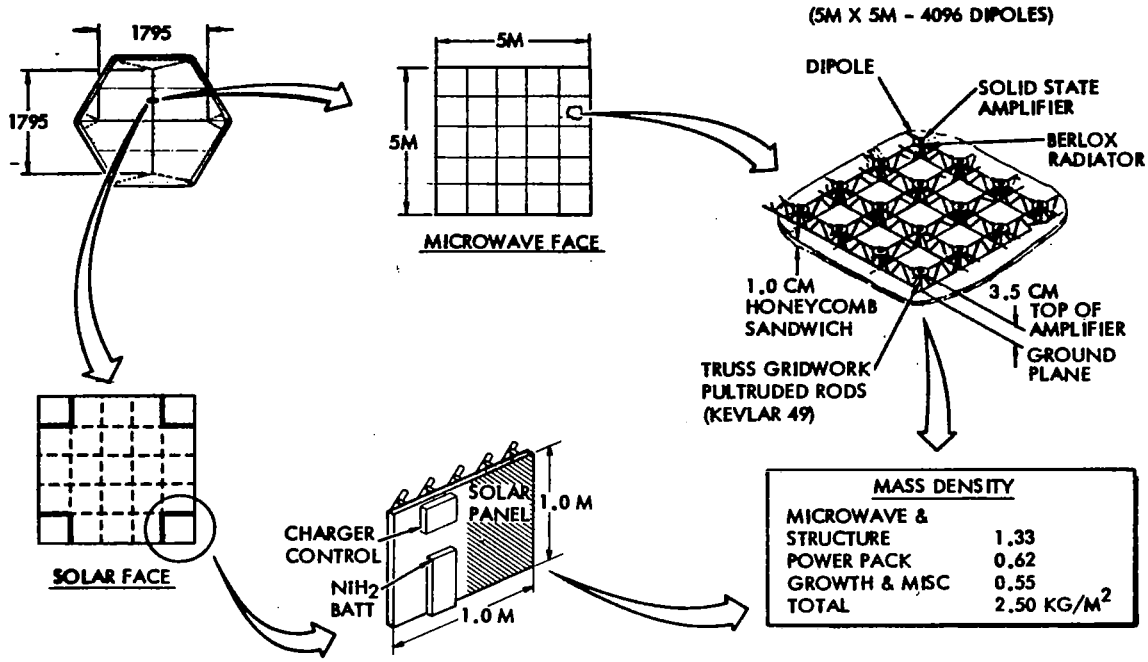

Figure 2.1-5. Mission Equipment—Test Article I

- Load requirements (each 24 hours)

  (10 V dc) Microwave antenna—160 W/m^2 up to 4 minutes

  (28 V dc) APS—200 W (2 hours)
  50 W (continuous)

  (28 V dc) Communication—800 W (continuous)

  (28 V dc) Instrumentation and data management—5-40 W (continuous)

  (28 V dc) Attitude determination—104 W (continuous)

Five differing power packs have been defined to satisfy the varying (and physically separated) satellite operational requirements: (1) the main data management and communications module power pack; (2) the APS power pack; (3) the attitude determination module power pack; (4) the microwave subarray power pack; and (5) the instrumentation and data management power pack. The electrical and physical characteristics of each of the power pack types are summarized in Table 2.1-2. The satellite will require one of the DMC power packs, four of the APS packs, one ADS pack, 717 microwave packs, and at least 45 instrumentation packs required wherever an instrumentation group and a remote interface must be installed.

Data Management and Communications

Requirements

The primary mission test requirements have not imposed any special loads upon either the communications channels or the on-board data system. Therefore, the only constraint will be that the selected communication concept must be

Table 2.1-2. Power Pack Equipment Summary

TYPE	NO. SETS	LOCATION	UNIT MASS (kg)	TOTAL MASS (kg)	DIMENSION W×L×D (m)	COMMENTS
A. DATA MANAGEMENT AND COMMUNICATION (DMC)	1	AT ONE OF TWO FRAME JUNCTIONS NOT POSSESSING APS INTERFACE	(1027)	(1027)		
DMC ELECTRONICS			350		1×2×0.5	SINGLE PACKAGE
BATTERY			464			
BATTERY ELECTRONICS			63			
SOLAR ARRAY		ON STRUCTURE NEAR MODULE	50		10×10×0.02	MOUNTED PARALLEL TO MW ARRAY
B. APS	4		(43.32)	(173.3)		
BATTERY		ON RCS PODS	35.7		0.25×0.25×0.5	SINGLE PACKAGE
BATTERY ELECTRONICS			4.0			
SOLAR ARRAY		ON STRUCTURE ADJACENT TO RCS PODS	3.62		1×7.24×0.02	MOUNTED PARALLEL TO MW ARRAY;
C. ATTITUDE DETERMINATION	1		(107.0)	(107.0)		
BATTERY		SATELLITE ROTATION AXIS	91.4		0.5×0.5×0.5	
BATTERY ELECTRONICS			8.2			
SOLAR ARRAY		ON STRUCTURE ADJACENT TO MODULE	7.4		4.0×3.7×0.02	MOUNTED PARALLEL TO MW SUBARRAY
D. MICROWAVE	2868	4 DISTRIBUTED AND MOUNTED ON REAR OF EACH 5×5-m MW SUBARRAY	(3.85)	(11,042)		4 PER 25 m^2 MW SUBARRAY (0.62 kg/m^2 AVG SPREAD OVER MW SUBARRAY
BATTERY			2.6		0.5 m^2 (4 PLCS)	LOCATED ON 4 CORNERS OF 25-m^2 SUBARRAY (1 m^2 EACH CORNER)
BATTERY ELECTRONICS			1.0			
SOLAR ARRAY			0.25		1×0.5×0.02 (4 PLCS)	
E. INSTRUMENTATION & D.M.	45		(21.98)	(1320)		
BATTERY		AS REQUIRED, >45 PLACES	14.6		0.5×0.5×0.5	
BATTERY ELECTRONICS			6.0			
SOLAR ARRAY		ON STRUCTURE NEAR EACH MODULE	1.38		1×2.75×0.02	MOUNTED PARALLEL TO MW SUBARRAY

compatible with the existing communications capabilities in the operations time frame, and that the selected data management concept utilize the appropriate state-of-the-art hardware and software. Accordingly, the data management and communications concept utilized on the SPS Test Article I satellite is required to be Orbiter, Space Tracking and Data Network (STDN), and Tracking and Data Relay Satellite (TDRS) compatible. Figure 2.1-6 summarizes the available communications paths, and Table 2.1-3 summarizes the communications requirements.

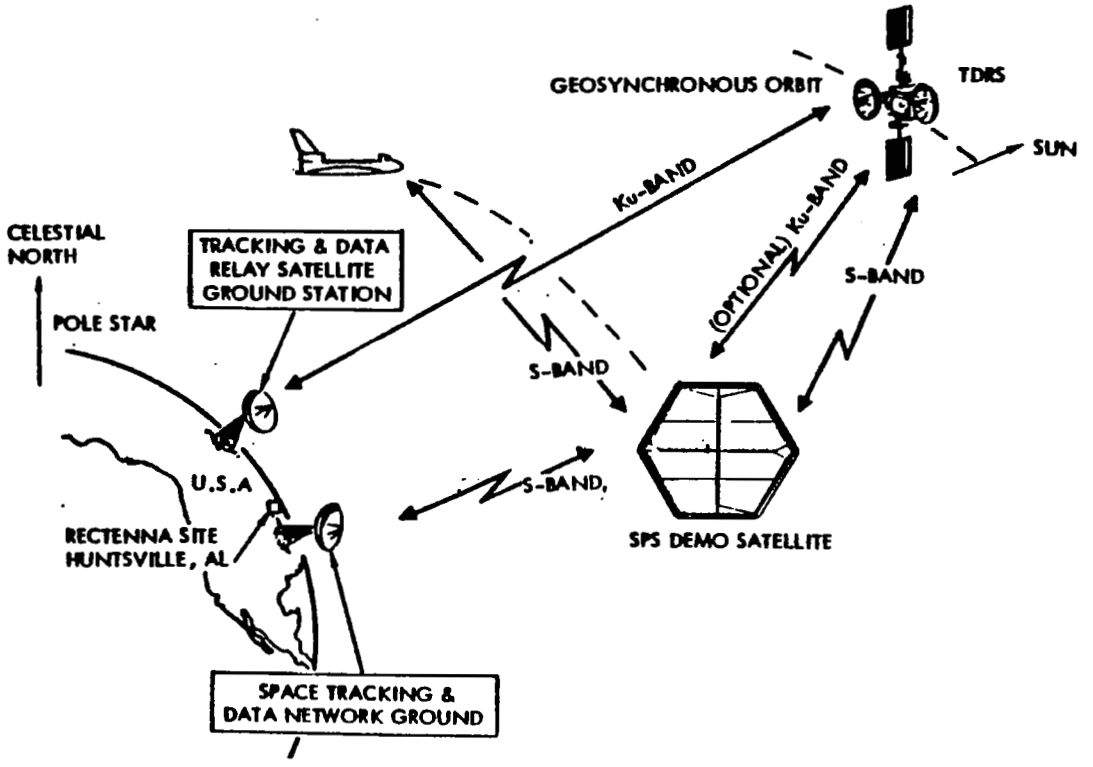

Figure 2.1-6. Communication Links for SPS Test Article I

Table 2.1-3. Communications Requirements

• Orbit altitude	482 km (260 nmi)
• Power transmit—duty cycle	Once in each 24-hour period
• Communications link	
- Transmit orbit (continuous)	±5.4 min. about power LOS ground zero
- All other orbits	1 time/orbit 5 min. average
• Data rate	10 kbit/s
• Command rate	≥2 kbit/s
• Data bus	
- Material	Fiber optic
- Bit rate	1 Mbit/s

Equipment

The equipment arrangement is described in Figure 2.1-7. The communications utilize S-band transceivers compatible with existing ground-based (STDN) networks, orbiter channels, and with proposed TDRSS links. The controller/processor section may be implemented by utilizing the processor (and software) proposed for the NASA/Goddard Multi-Mission Modular Spacecraft (MMS) with necessary customizing software as required. The data bus concept selected is similar to that utilized by the MMS with two major modifications: (1) a multi-channel (six) bus controller would replace the present MMS concept, and (2) the data bus itself would be implemented using state-of-the-art fiber optics.

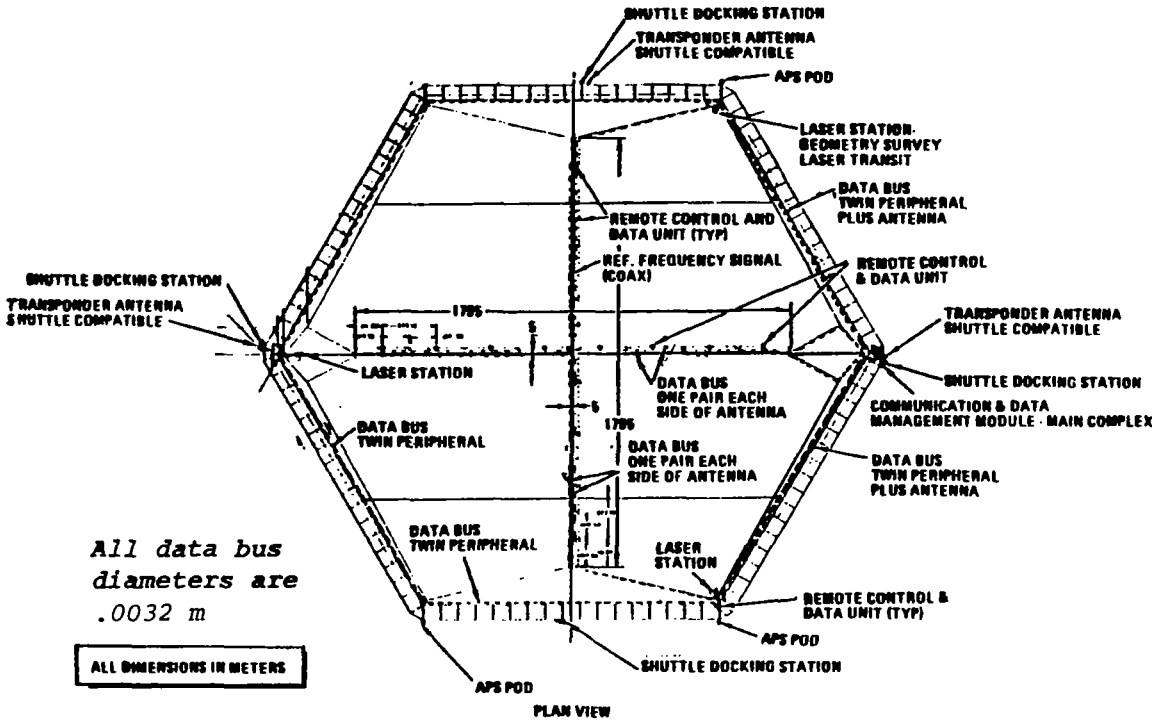

Figure 2.1-7. Equipment Arrangement

Table 2.1-4 summarizes the physical characteristics (preliminary mass and power) of the DMC subsystem.

Stabilization and Control

The following requirements are the basis for the selection of the baseline ACSS:

Attitude error	±0.5°
Attitude rate error	<.004°/sec
Spin rate	0.765°/sec

Table 2.1-4. DMC Mass and Power Summary

S-BAND COMM.	MASS (KG)	POWER (W)	NOTES
PM TRANSPONDER	31.6	63	POWER REQUIREMENTS SET BY ASSUMING 1 EA ON AT SAME TIME
PM-PROCESSOR	16.2	30	
DOPPLER EXTRACTOR	14.8	16	
POWER AMPLIFIER (100 W) 2 EACH	28.8	400	
PREAMPLIFIER	23.2	25	
FM TRANSMITTER	6.0	120	
FM PROCESSOR	10.4	9	
SWITCH ASSY	3.0	2	
WIRING	30.0	-	
ANTENNA (7)	2.0	-	
	~170.0	~700	USED FOR POWER PACK SIZING
DATA MGMT			
DATA PROCESSOR (2)	60	40/2 STDBY	50% DUTY CYCLE
MEMORY (4)	60	40/2 STDBY	20% DUTY CYCLE
TIMING UNIT (1)	20	5	BUILT-IN REDUNDANCY
SYSTEM CONTROLLER (1)	20	20	
BUS CONTROLLER (6)	120	10	
REMOTE CONTROL/DATA (AS REQ'D)	(2 EA)	10/2 STDBY	EST. FOR POWER MODULE SIZING
	~282	~100	RCD PWR DISTRIBUTED
FIBER OPTIC CABLE	NEGL.	-	
INSTRUMENTATION	300	-	DISTRIBUTED

Equipment Description

The mission requires six months of activity by the ACSS. The ACSS features an APS using an N_2O_4/mmH bi-propellant system for control (Figure 2.1-8).

A diagram of the ACSS equipment is shown in Figure 2.1-9. The baseline control system features a precision attitude reference system, coarse alignment system, flight computer, and interface unit. The output of the control system provides the commanded signals to an active three axis APS. The ACSS consists of all standard equipment with the exception of the flight computer and interface unit.

The details of the ACSS are summarized in Table 2.1-5. The precision attitude reference system is comprised of the DRIRU-11 inertial reference unit (IRU), two fixed-head star trackers, and associated software.

Auxiliary Propulsion (see Figure 2.1-8)

Functional Requirements

- Three-axis attitude control (APS)
- Translation velocity corrections

Mission Requirements

- Attitude stabilization—quasi-inertial, 3 months' construction

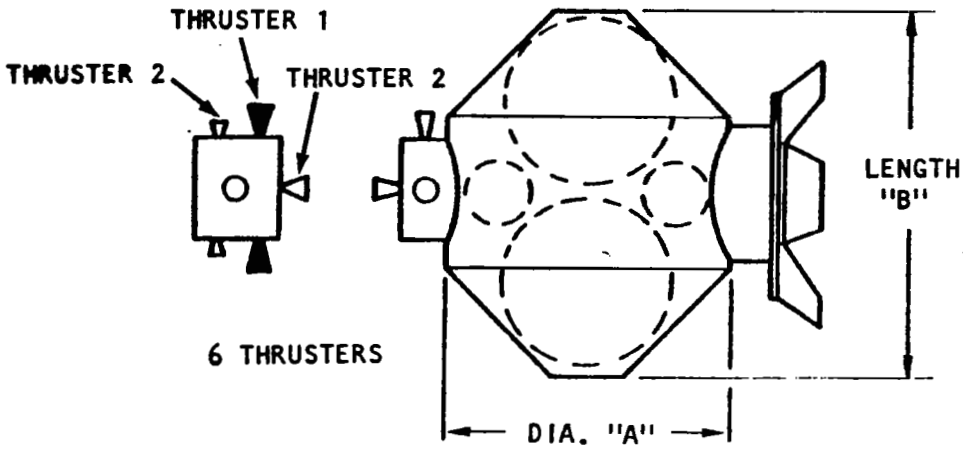

STRUCTURE TOTAL MASS (kg)	DIA. 'A' (m)	LENGTH 'B' (m)	THRUST 1 (N)	THRUST 2 (N)	PROPELLANT MASS (kg)	DRY MODULE MASS (kg)	TOTAL MASS (kg)
75,000	2.3	3.2	142	22	10,910	3,970	14,880
112,500	2.6	3.6	200	29	15,336	5,581	20,917
150,000	2.8	3.9	258	36	19,737	7,214	26,951
187,500	3.0	4.2	316	42	24,183	8,848	33,031
225,000	3.2	4.4	374	49	28,584	10,436	39,080

PROPELLANT AND DRY MODULE WEIGHTS ARE FOR FOUR MODULES.

Figure 2.1-8. APS Pod Characteristics

- Spinning mode—antenna test period, 3 months
- Orbit makeup—test period and pre- and post-periods

  483 km (260.79 nmi)—9 months total

- Spin/despin operation

Structural System Requirements Summary

The data listed below summarizes the major structural requirements of the hexagonal frame that are listed in Section 2.1.5.

1. The frame is the mounting platform for all the mission and subsystems equipment listed above and defined on drawings 42635-18029 and 18031.

2. The frame must sustain the thermal gradient and libration damping induced loads that occur during the frame construction period.

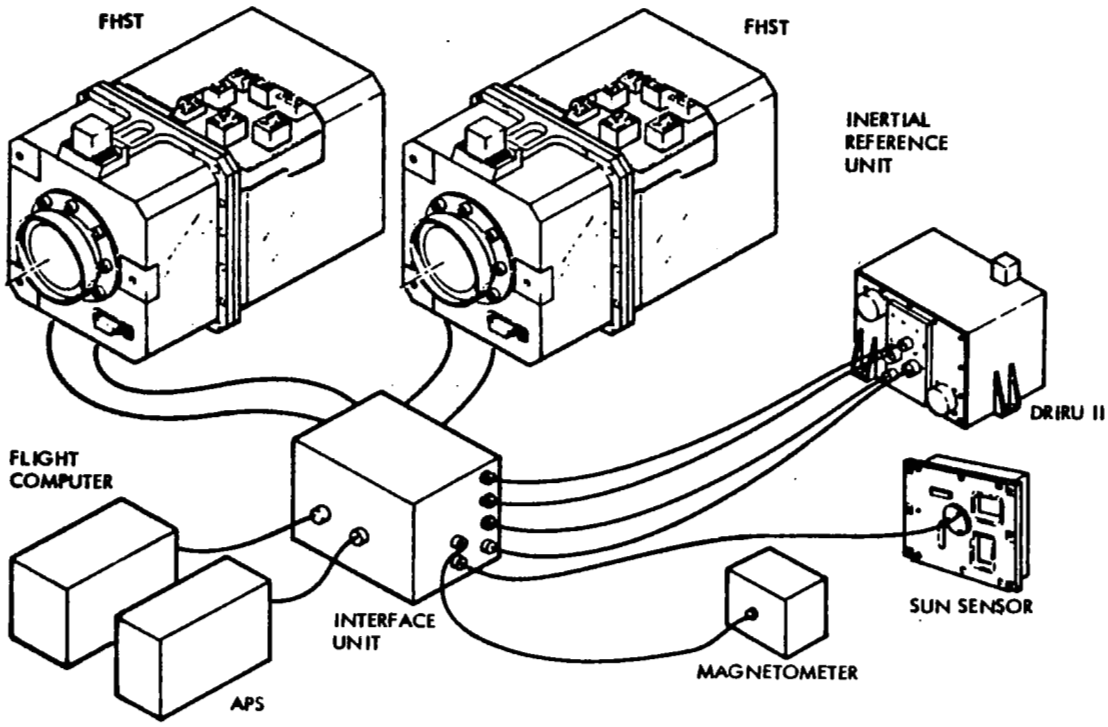

Figure 2.1-9. Attitude Control and Stabilization Subsystem

Table 2.1-5. Elements of the ACSS

ITEM	NO. REQ'D	MASS (kg)	DIMENSIONS EACH (cm)	TOTAL MASS (kg)	POWER (W)
PRECISION REFERENCE SYSTEM					
• DR IRU-II	1	16.9	22.6×31.2×22.9	16.9	22.5
• MOD II FIXED-HEAD STAR TRACKER	2	9.1	15.9×19.6×43.9	18.2	42.0
COARSE ALIGNMENT					
• FINE-POINTING SUN SENSOR	1	2.6	-	2.6	2.2
• MAGNETOMETER	1	0.9	14.2×16.5×6.8	0.9	2.0
INTERFACE UNIT	1	14.0	31×31×61	14.0	35.0
			TOTAL	52.6	103.7

3. The frame must sustain the loads that occur during installation of the data bus lines and systems equipment packages, including APS pod installation and orbiter docking.

4. The frame must sustain the most severe combination of a limit compression load of 84.3 kN (18,950 lb) in conjunction with thermal gradient and centripetal induced loads (spin rate = .765°/sec).

5. The frame must have a minimum modal frequency compatible with the attitude control system. The minimum frequency requirement will be satisfied by the frame EI and GJ provided to satisfy (4). See Section 2.2.6 for further detail.

6. During operation in the prototype SPS solid state configuration the maximum displacement (Figure 2.1-13) of cable attachment points 2, 4, 6 normal to the plane of points 1, 3, 5 is not to exceed 15 cm.

7. The frame must sustain the separate conditions of APS firings listed below.

   Spin-up or despin—pitch, four 142.3 N thrusters
   Attitude control—pitch and yaw, four 22.2 N thrusters
   Attitude control—roll, two 22.2 N thrusters
   Orbit makeup—two 22.2 N thrusters (in-plane)

2.1.4 SPS TEST ARTICLE I CONFIGURATION

The SPS Test Article I configuration is shown on Drawing 42635-18029 (Appendix A). Table 2.1-6 summarizes the test article mass for a structure such as a tri-beam and the APS pod mass changes for heavier hexagonal frame structures. For convenience, Figure 2.0-1 presents a summary of the major configuration characteristics and functional equipment.

The test article uses a hexagonal frame structure to stabilize the array of primary tension cables configured to support a Mills Cross antenna. The antenna dimensions are 1795 m wide and 5 m wide, containing 17,925 one-meter by one-meter subarrays. The radiated power is 2.25 mW with 18.8 kW delivered to the ground antenna at the closest approach. The subarrays are composed of dipole radiating elements and solid-state power amplifier modules such as that proposed for the SPS "sandwich" concept. The nickel-hydrogen battery packs mounted on the back face (Figure 2.1-10) provide power storage capability compatible with the mission power requirements. The total antenna/solar cell/battery/structure distributed mass is 2.5 kg/m^2.

Electronic beam steering, provided by phase control of the individual subarray, is ±2.25°. This is required for the test maneuver described in Figure 2.1-3 and is compatible with the attitude control and structural systems.

The same test maneuver requires a test article pitch rate of 0.765°/sec. For minimum propellant usage the test article continuously rotates about the axis (Figure 2.1-11) of minimum mass moment of inertia.

The attitude control and stabilization system used four APS pods containing N_2O_4/mmH bipropellant for control. The control system features a precision attitude reference system, coarse alignment system, flight computer, and interface unit. The output of the control systems provides the command signals to an active three-axis APS. The ACSS consists of all standard equipment with the exception of the flight computer and interface unit. The precision attitude reference system is comprised of the DRIRU-11 inertial reference unit (IRU),

Table 2.1-6. SPS Test Article I—Weight Summary

No.	Component	Mass (kg)
1	Hexagonal frame (includes 20% for details	75,000
2	Tension cable system (tension devices, fittings)	4,820
3	Solid-state microwave/solar cell/battery integrated panels (2.5 kg/m^2)	45,450
4	Miscellaneous equipment	3,135
5	APS pod (inert)	3,970
	Total dry mass	132,375
6	APS propellant	10,910
	Total mass	143,285

For frame masses greater than 75,000 kg, use following total (for 4) APS pod masses (5) and (6):

Hex Frame Mass	(5) Pod Inert (kg)	(6) Propellant (kg)
112,500	5,581	15,336
150,000	7,214	19,737
187,500	8,848	24,183
225,500	10,436	28,584

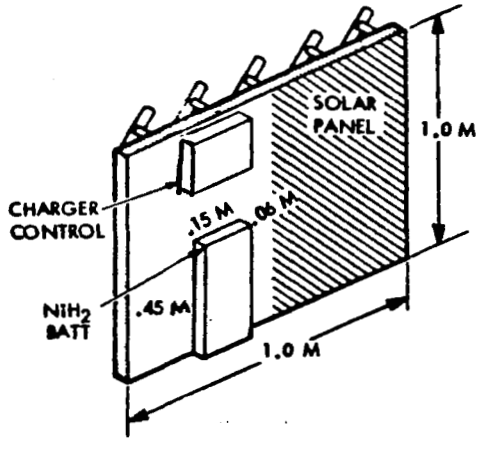

ORBITAL DATA

- 260 nmi ORBIT (483 km)
- 35° INCLINATION
- 90-MIN PERIOD
- 33-MIN ECLIPSE

BATTERY DATA

- OPERATING RANGE: -10° TO +10°C
- NO-DAMAGE RANGE: -20° TO +20°C
- THERMAL CAPACITY: 920 j/kg/°C
- MASS 2.6 kg
- DISSIPATION: 250 W FOR 4 MIN (ONCE A DAY)

Figure 2.1-10. Battery Thermal Control for SPS Experiment

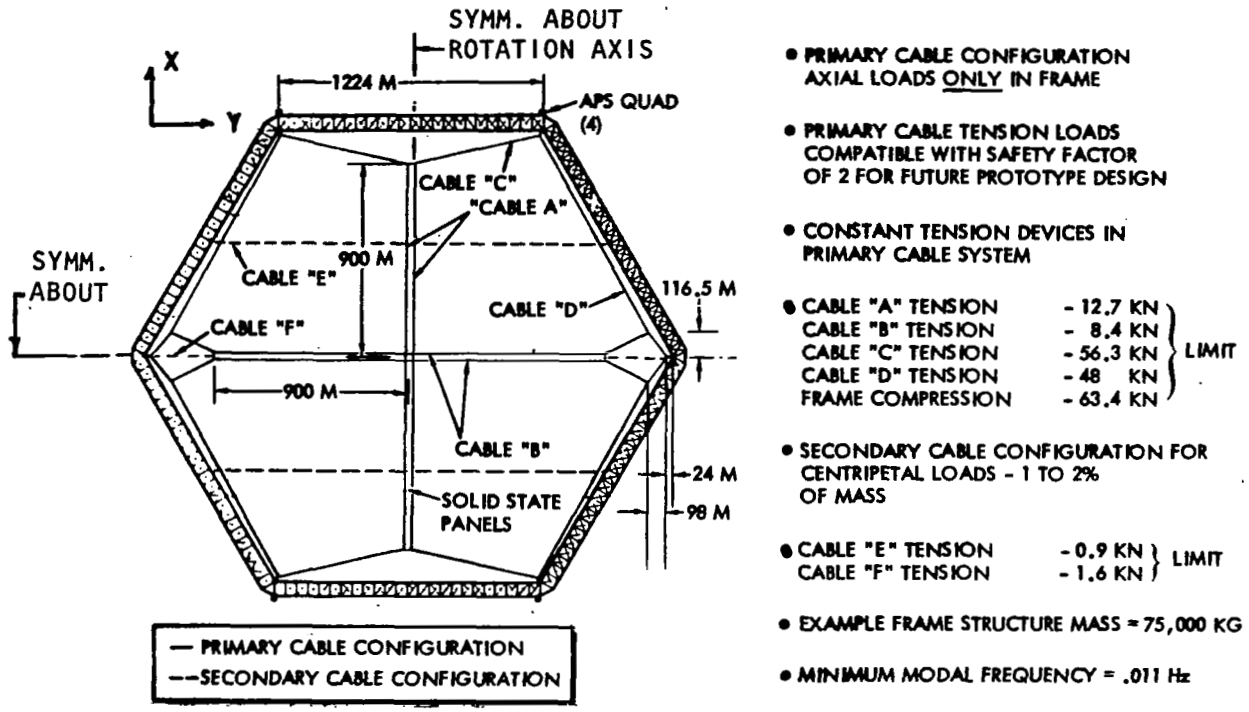

Figure 2.1-11. SPS Test Article I
Major Structural Characteristics

two fixed-head star trackers, and associated software, and is located on the frame structure at the axis of rotation. The flight computer and its associated software process the IRU and star tracker data and compensate for known measurement errors to compute attitude and attitude rate information which, in turn, generates APS control commands. The sun sensor and magnetometer are a part of the coarse alignment system. The sensors are used for platform acquisition and reorientation.

Each APS pod, for the SPS Test Article structure, is assumed to contain 2728 kg (6000 lb) of propellant and have a total mass of 3720 kg (8182 lb). Each pod contains six thrusters (Figure 2.1-8) provided for the following maneuvers (Figure 2.1-11).

- Two 142.3 N (32 lb) thrusters for spin/despin torque about the pitch axis (X axis)
- Two 22.2 N (5 lb) thrusters for control torques about the (X and Y axes)
- Two 22.2 N (5 lb) thrusters for control about the Z-axis and orbit makeup maneuvers

The communication system utilizes S-band transceivers compatible with existing ground-based (STDN) networks, Orbiter channels, and with TDRSS links. The controller/processor section may be implemented by utilizing the processor (and software) proposed for the NASA/Goddard Multi-Mission Modular Spacecraft (MMS) with necessary customizing software as required. The data bus configuration is

shown to be similar in concept to that of the MMS except for two major modifications: (1) a multi-channel (six) bus controller would replace the present MMS concept, and (2) the data bus itself would be implemented using state-of-the-art fiber optics.

- The major structural features are shown in Figure 2.1-11. The hexagonal frame structure, defined by the side dimension length of 1224 m (4651 ft), is provided to support the primary array of tension cables shown. The pairs of cables, "A" and "B", support the 1795 m × 5 m Mills Cross configuration of 5 m by 5 m antenna subarrays. The cable tension loads induce a limit axial compression in the frame of 63.4 kN (14,250 lb). The secondary array of tension cables is provided to reduce (to small values) the in-plane beinding moments resulting from the test article spin rate of 0.765°/sec. Appropriate constant tension devices (negators or equivalent) can be used to maintain the primary cable load tensions.

The primary cables that extend to the six corners of the hexagonal frame are attached to the frame by radial directed support devices. These devices are dependent on the particular construction concept used and must have out-of-plane adjustment capability compatible with the dimensional stability requirements defined in Section 2.1.5.

A total of eight NASA androgynous docking ports are provided at the four APS pods and at four stations as shown on Drawing 42635-18031.

The docking ports at the pods are provided for future replacement of the pods at the conclusion of the post-test period. The four other docking ports are provided to permit Orbiter docking for delivery of equipment during the antenna installation phase.

2.1.5 HEXAGONAL FRAME STRUCTURAL REQUIREMENTS

The structural requirements for the hexagonal frame structure (Dwg. 42635-18031) of the SPS Test Article I are summarized here.

The requirements encompass the hexagonal frame overall strength, stiffness (modal frequency) and dimensional stability requirements and the local structural requirements for the electrical power and data management utilities, and equipment packages summarized in Section 2.1.3. Further, specific options to the requirements are presented.

Overall Strength and Stability Requirements

(1) During the construction in the free-drift mode the hexagonal frame must sustain, without permanent deformation, the most severe combination of drag and thermal-induced loads, and the loads associated with libration damping to accommodate orbiter docking to the construction fixture. Completion of the last bay of the hexagonal frame and joining with the first bay shall (through appropriate design) induce no significant residual loads or, alternatively, the operational loads analysis shall include the residual loads.

(2) During the installation of tension cables, the antenna subarrays and remaining systems that were not installed during the foregoing period of frame construction, the structure must sustain the most severe combination of equipment installation loads, drag, and thermal induced loads [483 km orbit (260.7 nmi)] and the loads associated with libration damping and/or orbiter docking to the hexagonal frame. During this time the configuration is in a quasi-inertial mode or, if advantageous, a free-drift mode. During this period, the primary cable configuration need not be fully tensioned.

(3) For use in SPS Test Article I, the structural elements that comprise the frame structure must sustain, without detrimental deformation, a limit axial compression of 63.4 kN (14,250 lb)* in conjunction with the most severe combination of thermal gradient, centripetal, and APS thruster firing loads. The thermal gradient induced loads are unique to the frame material, thermal coating α/ε values, and construction characteristics and, have not been determined in this study. The spin-induced loads are determined from the spin rate of 0.765°/sec, the mass data of Table 2.1-6, and the structural configuration of Figure 2.1-12. The APS thrust loads are presented in Section 2.1.3.

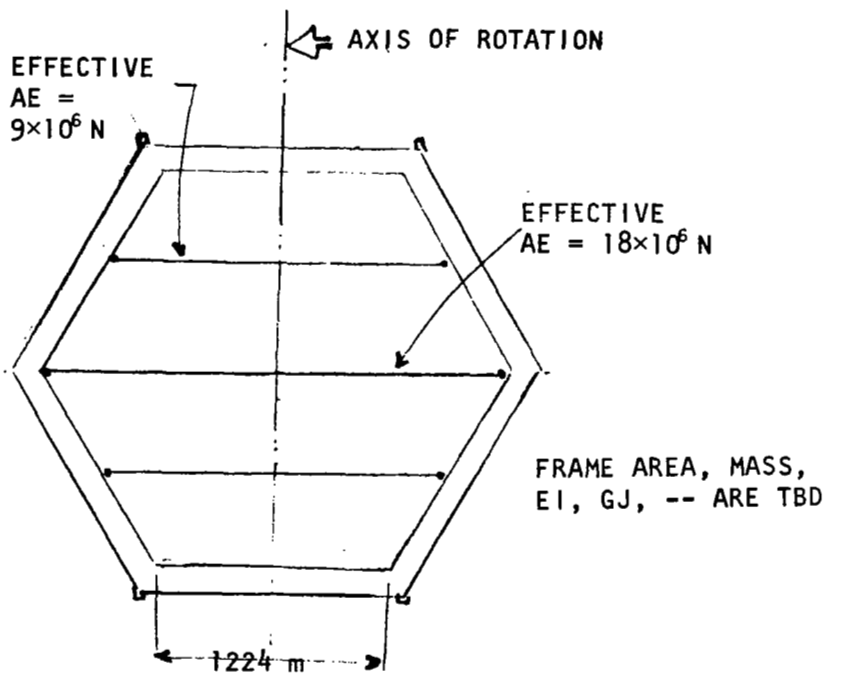

Figure 2.1-12. Effective Structural Configuration for Centripetal Loads

*This load is based upon use of a safety factor of 2 for the test article. The prototype limit load of 84.3 kN (18,950 lb) is based on a safety factor of 1.5.

(4) For use in the prototype design, supported as shown in Figure 2.1-13, the structural elements that comprise the frame structure must sustain, without deformation, a limit axial compression of 84.3 kN (18,950 lb) in conjunction with the most severe combination of thermal gradient induced loads. The thermal gradients can be determined from the basic SPS mission description (Section 2.2.6). Also, from Section 2.2.6, the net effective uniform pressure imposed on the fully populated solid-state array due to concentrated solar pressure (CR = 5), gravity gradient, and microwave pressure is 45×10^{-6} N/m^2 (0.94×10^{-6} lb/ft^2).

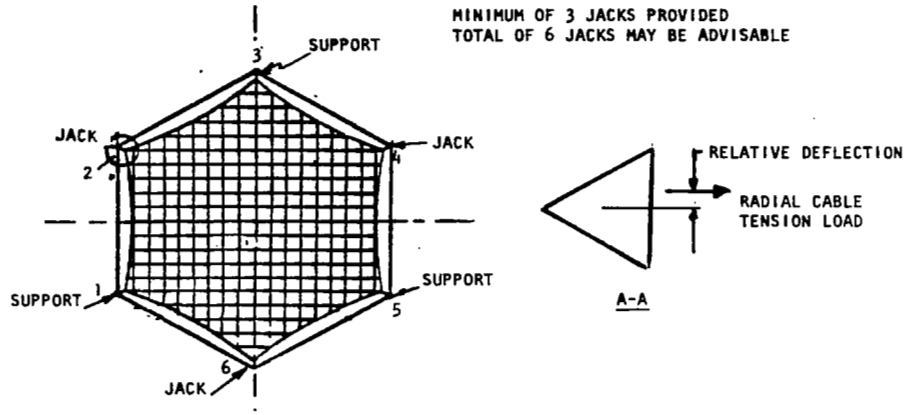

Figure 2.1-13. Prototype SPS Hexagonal Frame Configuration

For both the test article and the prototype design, the strength analysis shall include the additional element loadings due to initial frame fabrication deviation from straightness (and/or planar flatness) and thermal induced deflections. Of particular concern is the frame torsional and bending moments resulting from the resulting offset between frame center of gravity and the cable tension loads (Figure 2.1-13). Further, the magnification of these deflections due to the appropriate limit axial compression shall be considered.

(5) The frame structural materials and thermal coating design properties employed in the strength and stability analysis must be maintained during exposure to the environment described in Section 2.1.1.

Stiffness Requirements

For use in the test article, the frame stiffness must be sufficient so that the entire test article structural configuration has modal frequency values and shapes compatible with the stabilization and control system. This requirement is satisfied by the overall frame EI/GJ characteristics to satisfy requirements (3) and (4). See Section 2.2.6 for further detail.

The same comment is applicable to use of the frame in the prototype design.

Dimensional Stability Requirements

The dimensional stability criteria listed below may be satisfied by use of three adjustable supports located as shown in Figure 2.1-13. (Three additional jacks may be used if advantageous.) Use of the adjustment capability can be limited to elimination of fabrication induced deviations and initial cambering (passive figure control) or used throughout operation (active figure control).

The most stringent requirement pertains to use of the frame in the prototype SPS design. In this application the maximum deviation of any one of the tension cable adjustable support points (2,4,6) normal to the plane of the three support points (1,3,5) shall be limited to 15 cm.

The requirements for use in the test article (Section 2.2.6), while not expected to be as critical, are presented for completeness. Figure 2.1-14 presents the test article frame configuration. The maximum relative deflection between any three corners of the frame relative to the plane of the other three corners shall not exceed 24 cm.

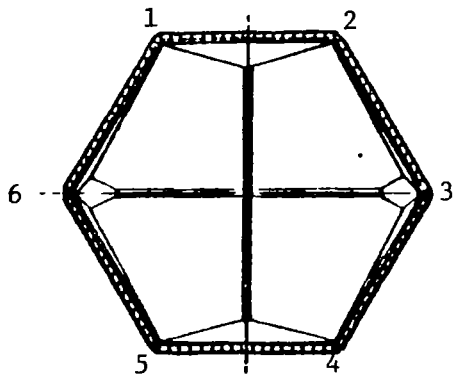

Figure 2.1-14. Test Article Tension Cable Support Points

Local Structural Requirements

Included in the local structural requirements are the loads incurred during attachment of APS modules and orbiter docking to the frame, either during the antenna system installation or post-test mission phase. The transient loads depend on the technique utilized (docking or berthing), relative approach velocity, local structural stiffness, and the basic local structural capability of the particular design. The docking loads are not within the scope of this study and are not presented here. However, the docking technique and orbiter and RMS approach velocity criteria are presented herein. In all cases, the NASA androgynous docking systems are employed.

Drawing 42635-18031 illustrates the equipment to be mounted on the hexagonal frame structure.

Utilities Attachment

The hexagonal frame construction must support the data bus and equipment shown on Drawing 42635-18031.

Structural Interface Requirements

Interfaces 1 and 2—Antenna Support Cable Attachment

This interface lies between the basic structure and the fitting that receives the pair of intersecting antenna array support tension cables. The interface must be capable of sustaining the resultant delivered limit radial tension load of 65.9 kN (including centripetal forces) for the test article, and 84.3 kN for the SPS prototype design.

The structural design must also provide for adjustment normal to the plane of the frame that is compatible with the previously stated dimensional stability requirements.

Interface 3—APS Pod Attachment (four required)

The total interface is located as shown on the drawing and contains a male/female docking device for attachment of the APS pod to the structure and another device to permit orbiter docking for future removal of this pod. The data bus and power line for the APS pod are also shown.

The interface must be capable of sustaining the loads, without detrimental deformation, occurring during APS installation, orbiter docking, APS firing, and during spin (centripetal loads). The APS thruster sizes are shown in Figure 2.1-8 and need not be concurrent. The design provides for removal of the APS pods. For this operation the orbiter is docked to the frame and the RMS is used to place the retrofit module (Figure 2.1-15) to the structure. The existing RMS technical features itemized below shall be used for the loads analysis of this operation.

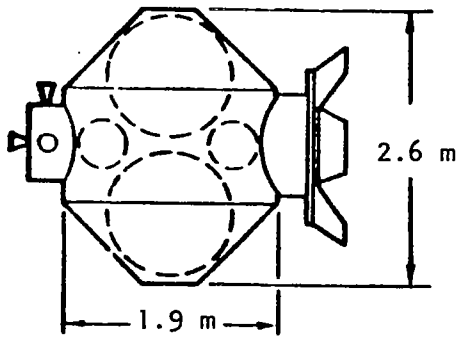

TOTAL POD MASS = 2076 kg

Figure 2.1-15. APS Pod for Post-Test Two-Year Period

- Maneuvering Speed

  - Maximum tip* velocity—fully loaded—0.2 ft/sec
  - Maximum tip velocity—unloaded—2 ft/sec
  - Maximum stopping distance with or without payload—2 ft

  (*This velocity is for a reference 32,000-lb payload.)

- Positioning Accuracy

  - Tip position (automatic mode), ±2 in., ±1°
  - Operator controlled, ±0.5 in. accuracy

The orbiter/payload contact conditions shown in Table 2.1-7 shall be used for the orbiter-to-frame docking loads analysis.

Table 2.1-7. Orbiter/Payload Contact Conditions

RELATIVE CONTACT VELOCITY (-Z)	0.5 fps (0.05 fps, LOWER LIMIT)
RELATIVE LATERAL VELOCITY (X, Y)	0 ± 0.1 fps
RELATIVE ANGULAR VELOCITY (3 AXES)	±1.0°/SEC ABOUT ANY AXIS
RELATIVE LATERAL MISALIGNMENT (ORBITER X, Y)	0 ± 0.5 ft
RELATIVE ANGULAR MISALIGNMENT (ORBITER PITCH, ROLL)	0 ± 5° ABOUT EACH AXIS
RELATIVE ROTATIONAL MISALIGNMENT (ORBITER YAW)	0 ± 7°

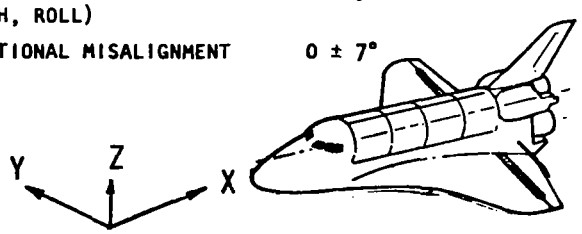

Interfaces 4, 5, 6, and 7—Shuttle Docking

These interfaces contain the male and female components of the docking orts shown on Drawing 42635-18031. This interface must be capable of sustaining the transient loads incurred during docking of the orbiter during the systems installation and post-test mission phases. The orbiter/payload contact onditions shown in Table 2.1-7 shall be used in the loads analysis.

Interfaces 4 and 5 also contain provisions for equipment storage during onstruction.

Interfaces 4, 5, and 6 contain solar cells to be supported from the basic tructure.

The ACCS equipment is located at Interface 7.

Options

The following options may be used relative to the foregoing requirements.

Thruster Size Reduction

The 142.4 N thruster forces may be reduced to 71.2 N (if critical to the particular construction joint design. The 71.2 N value is sufficient to satisfy the requirements of Section 2.2.4 and will require a longer burn time for test maneuver spin-up and despin.

Removal of Cable "E" in Secondary Tension Cable Configuration (Figure 2.1-11)

This is, of course, possible to simplify cable installation, but will result in increased frame bending loads.

Free-Drift Mode during Systems Installation

If advantageous, the systems installation may be performed in the free-drift mode, rather than the quasi-inertial mode.

2.2 SYSTEMS ANALYSES

This section contains the microwave, power, data management and communications, attitude stabilization and control, auxiliary propulsion systems, and structural analyses that were used to establish the requirements and characteristics of these systems.

2.2.1 MICROWAVE

Summary

The SPS Test Article I microwave system accepts energy from a photoelectric solar cell/battery power subsystem and transmits this energy as microwave energy to a ground receiver where the energy is then converted to a form compatible with standard utility networks. The Test antenna consists of 17,925 one meter by one meter subarrays arranged in a Mills Cross configuration with each leg 5 m wide and 1795 m long. Figure 2.1-5 illustrates this arrangement on the satellite and also the location of the associated power sources for each 25 m^2 segment of the antenna. The figure also illustrates the appearance of the amplifier/antenna face (front) of the array. Also shown is the mass breakdown of the array which has a total mass estimated to be 0.454×10^5 kg, including a growth allowance of 0.55 kg/m^2. In addition to the layout and mass requirements summarized above, a flatness specification of ≤ 24 cm is imposed to avoid ambiguous phase conjunction solutions to antenna phase control.

Microwave Subsystem Demonstration Requirements and Objectives

The demonstration concept is based on a LEO satellite which converts energy from the sun into microwave energy and transmits it, during a portion of its

orbit, to an earth-based rectenna. Batteries are used to store the dc power generated by a set of photovoltaic panels. At appropriate times, the dc battery power is converted to microwave power by solid-state oscillator/amplifier modules operating at 2450 MHz. These devices excite two crossed dipole arrays whose orthogonal beams are focused on the rectenna as the satellite passes over its site.

If the satellite's orbital inclination is equal to the latitude of the rectenna site then, at certain times, the satellite will pass through the zenith point of the rectenna and this, of course, represents the closest possible approach. Figure 2.2-1 shows that under these conditions, nearly two minutes of power transmission and phase control testing can be conducted at the elevation angles and slant ranges noted. Test operations take place while the satellite is within ±41° of the rectenna's zenith.

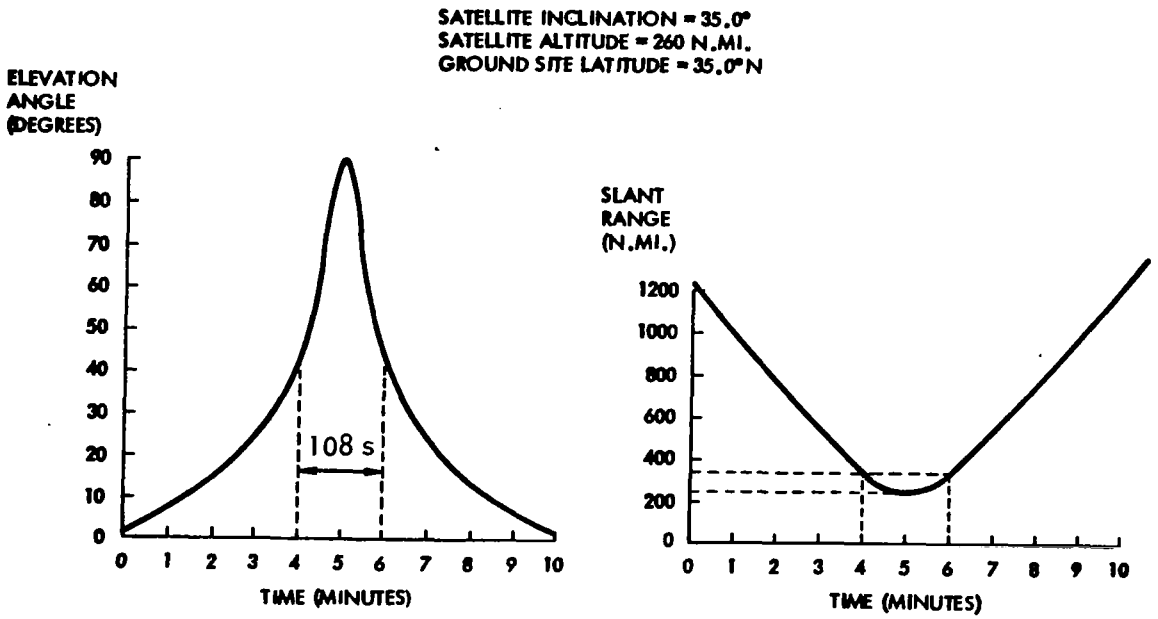

Figure 2.2-1. Flight Data Relative to Ground Site

At an altitude of 482 km (260 nmi) and inclination of 35° the satellite completes exactly 15 orbits each day and thus will make one appearance per day over a rectenna located at 35°N latitude. However, due to orbital regression, it is estimated that measurements could be taken over a single fixed site only nine days out of 48. To supplement these opportunities, provisions have been made to include batteries on board the satellite, thereby allowing daily testing to be conducted. Variations in received power levels will be experienced as functions of elevation angles and slant range; however, since the exact positions of those will be known, actual measurements can be correlated with the calculated performance specifications.

An additional factor that must be accounted for is satellite pitch angle. The results of a computer simulation, shown in Figure 2.2-2, illustrate the deviation between the pitch angle required for continuous target acquisition

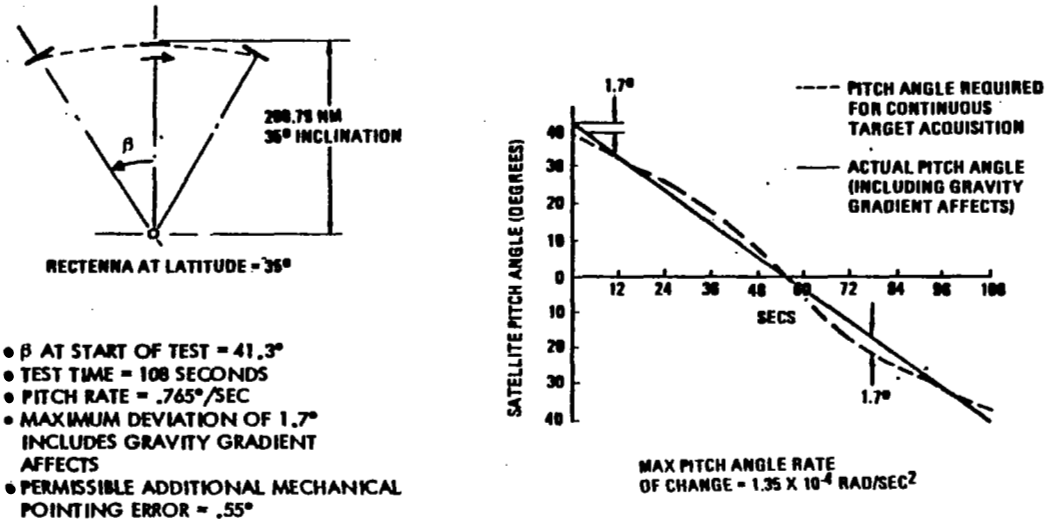

Figure 2.2-2. Test Maneuver

and a constant induced pitch rate for the satellite. Providing the deviation is not too large, correction can be achieved by electronic beam pointing created by phase control of individual subarrays. If subarray size is 1 m by 1 m, then electronic beam steering through ±2.25° is possible at the expense of up to 1.6 dB loss in antenna gain. The 2.25° allowable deviation is the sum of 1.7° from Figure 2.2-2 and an allowance of 0.55° for mechanical pointing error.

The microwave subsystem demonstration requirements and objectives are as follows:

- Delivery of 18.8 kW of power from LEO to ground
- Retrodirective phase control of array for
  - Microwave antenna beam formation
  - Electronic beam steering up to ±2.25°
- Solid-state power amplifier performance and efficiency of dc/RF conversion
- Solar array, power conditioning, and battery performance
- Legacy in the form of capability for later upgrading to a full-blown SPS satellite in geosynchronous orbit

Antenna Flatness

As already noted, some form of active retrodirective phase control of individual subarrays must be employed to ensure proper beam formation and focusing as well as correct pointing. Phase conjugation of a pilot tone signal emanating from the rectenna will be assumed for this purpose. This technique then automatically compensates for deviations from flatness between subarrays. To avoid ambiguity problems it will be assumed that the deviations do not exceed ±λ. Hence, there is a requirement for mechanical flatness <24 cm over the arms of the antenna.

Subsystem Description

The microwave transmitting antenna, shown in Figure 2.2-3, is a Mills Cross which is used in radio astronomy to achieve high angular resolution without going to the expense and complication of a filled aperture. In the present case the crossed arrangement of linear arrays results in a high power density main beam which can be focused on a ground receiving station.

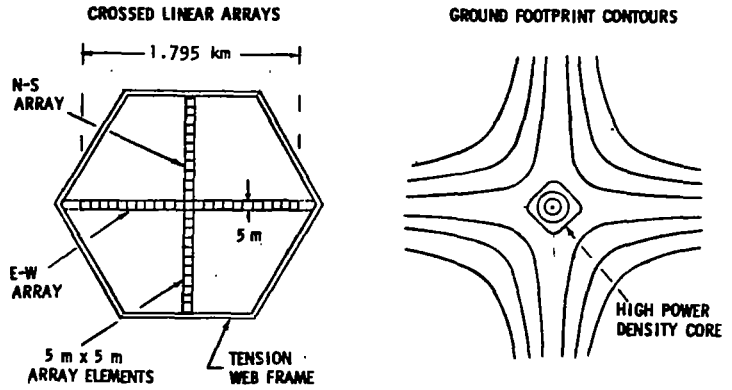

Figure 2.2-3. Test Concept Configuration—LEO/Ground

Each arm of the cross is 1.795 km long but only 5 m wide. The arms are made up of 717 panels, each 5 m by 5 m and consisting of twenty-five 1 m by 1 m subarrays. The subarrays are composed of dipole radiating elements and solid-state power amplifier modules such as have been proposed for the so-called sandwich concept. All subarrays operate at the same RF power density level, which has somewhat arbitrarily been taken to be 125 W/m^2. The reason for this choice is that the original concept did not include provision for batteries; the sandwich-type construction was then estimated to be capable of an RF power density of 1300 W/m^2 (solar flux) times 0.12 (solar cell efficiency) times 0.8 (solid-state amplifier efficiency). This estimate assumed the solar flux to be normally incident on the photovoltaic cells, which is not only unduly restrictive, but is actually incompatible with the orbital parameters of Figure 2.2-2. With the inclusion of batteries, there is no longer a strong dependence on sun angle and the RF power density could be increased above the 125 W/m^2 level if desired.

If the two linear arrays are aligned north-south and east-west, as indicated in Figure 2.2-4, then two fan beams will be radiated normal to the plane of the arrays. At the intersection of the fan beams there will be a core region of high power density. At the closest approach, i.e., when the satellite is in the zenith direction from the rectenna, the ground footprint contours appear as shown at the right in Figure 2.2-3. The geometry of the orbit and typical orbit tracks are shown in Figure 2.2-4. It is clear that the ground-based rectenna must be located in the high power density core of the footprint. It is necessary then, to determine the size of this core area and the power density distribution within it.

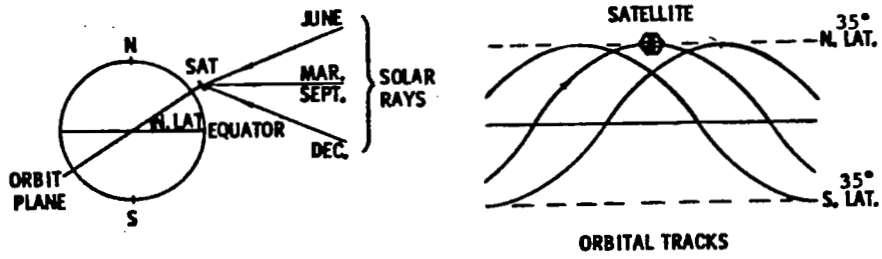

Figure 2.2-4. Test Satellite in Low Earth Orbit

Subsystem Design Analysis

For a linear array of length 1.8 km, the far field begins at a distance of about 53,000 km at 2450 MHz, based on the $2D^2/\lambda$ criterion. At closest approach the rectenna is only 482 km from the satellite and is, therefore, well inside the Fresnel zone of the crossed arrays. For this reason each array must be focused on the rectenna and, since the range varies during the 108-second duration of the test, the focusing mechanism must compensate for the variable range. Focusing is accomplished by providing a non-uniform phase distribution over each array such that the "aperture distribution" across the antenna is not a plane wave but a spherical wavefront with a radius of curvature equal to the range from satellite to rectenna. In this case the radiated wavefront converges on the rectenna, which lies in the focal plane of the array, and footprint and gain calculations in the focal plane can be made by using the normal Fraunhofer (i.e., far-field) pattern relationships. The spherical wavefront across one of the linear arrays is shown in Figure 2.2-5. At closest approach, where R = 482 km, the spherical wave differs from planarity by approximately 0.84 m, or about 7 λ.

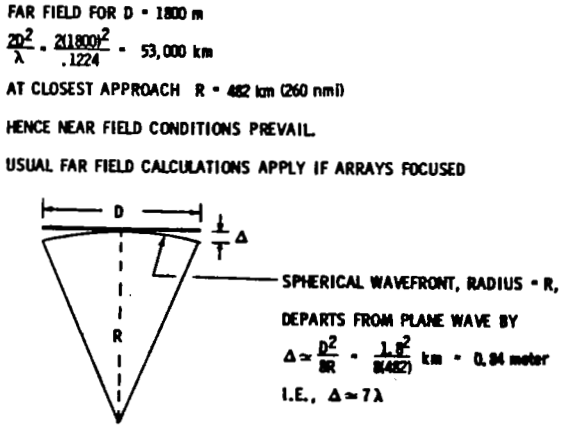

Figure 2.2-5.
Array Focusing

Under focused conditions, then, one linear array will radiate a fan beam having a peak flux density of

$$S_R = G \frac{S_T A}{4\pi R^2}$$

where A is the array area (9000 m^2), S_T is the array power density (125 W/m^2) and R is the range (482 km at closest approach). The gain of the array is given by

$$G = \frac{4\pi A}{\lambda^2}$$

so that the peak flux density at the rectenna is given by

$$S_R = S_T \left(\frac{A}{\lambda R}\right)^2 \qquad (2.2\text{-}1)$$

$$= 2.90 \text{ W/m}^2.$$

When the two crossed arrays are operated coherently, this peak flux density will increase by a factor of four, as will be seen later, to 11.6 W/m^2 at the center of the rectenna.

To determine quantitatively the distribution of power density over the rectenna, it will be assumed that each linear array acts as a uniformly illuminated rectangular aperture of dimensions d = 5 m by D = 360 d = 1800 meters. Then, the fields radiated by the two arrays are given by

$$E_1(\theta,\phi) = \frac{\sin u \cos\phi}{u \cos\phi} \cdot \frac{\sin 360\, u \sin\phi}{360\, u \sin\phi}$$

$$E_2(\theta,\phi) = \frac{\sin 360\, u \cos\phi}{360\, u \cos\phi} \cdot \frac{\sin u \sin\phi}{u \sin\phi}$$

where $u = kd \sin\theta$ and ϕ is azimuth angle measured from due north. Subscripts 1 and 2 refer to the east-west and north-south arrays, respectively.

The cardinal plane patterns are obtained by taking $\phi = 0$ for the N-S plane and $\phi = \pi/2$ for the E-W plane. Since the total field is

$$E = E_1 + E_2$$

then the field patterns in the cardinal planes are identical and are given by

$$E(\theta) = \frac{\sin u}{u} + \frac{\sin 360\, u}{360\, u} .$$

In the intercardinal planes, given by $\phi = \pm 45°$, the patterns are again identical,

$$\text{i.e.,} \quad E(\theta) = 2\, \frac{\sin u/\sqrt{2}}{u/\sqrt{2}} \cdot \frac{\sin 360\, u/\sqrt{2}}{360\, u/\sqrt{2}} .$$

Now power density is proportional to the square of electric field strength and at the rectenna the proportionality constant is, from Equation (2.2-1), 2.9 W/m^2. Thus the power density distribution over the rectenna, under ideal pointing and focusing conditions, is given by

$$S_R(\rho) = 2.9 \left[\frac{\sin u}{u} + \frac{\sin 360\, u}{360\, u}\right]^2 \text{W/m}^2 \qquad (2.2\text{-}2)$$

in the cardinal planes and

$$S_R(\rho) = 11.6 \left(\frac{\sin u/\sqrt{2}}{u/\sqrt{2}} \cdot \frac{\sin 360\, u/\sqrt{2}}{360\, u/\sqrt{2}} \right)^2 \text{ W/m}^2 \qquad (2.2\text{-}3)$$

in the intercardinal planes. In these equations ρ represents radial distance measured from the center of the rectenna. Using the small sine approximation to relate ρ and u gives

$$\rho = 3760\, u \text{ meters} \qquad (2.2\text{-}4)$$

Equations (2.2-2), (2.2-3), and (2.2-4) can now be used to calculate power density patterns in the focal plane (i.e., over the rectenna site). Such patterns are shown in Figure 2.2-6. In the cardinal planes the pattern has sharp nulls at ρ = 46.4 meters, but no such nulls are evident in the cardinal planes where the patterns oscillate above and below a mean level which is 6 dB below the beam peak.

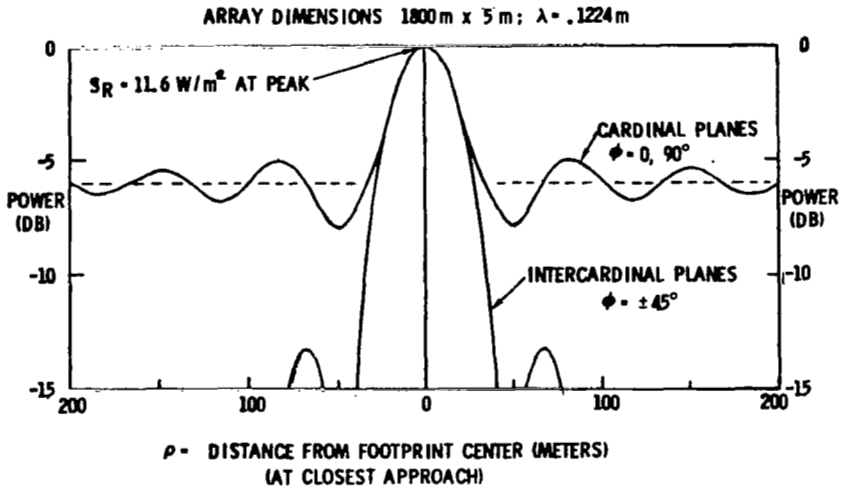

Figure 2.2-6. Crossed Array Patterns in Focal Plane

Contours of constant power density in the focal plan have also been estimated using Equations (2.2-2), (2.2-3), and (2.2-4) and are shown in Figure 2.2-7. From this figure it is evident that a rectenna with a diameter of 66 m will collect essentially all the power in the main lobe of the transmitted beam. The total amount of power so collected is given by

$$\rho = \int \int S_R(\rho,\phi)\rho \, d\rho \, d\phi \, ,$$

and the integral is approximated by taking an average value for $S_R(\rho,\phi)$, i.e.,

$$S_R(\rho,\phi) = \overline{S_R(\rho)}$$

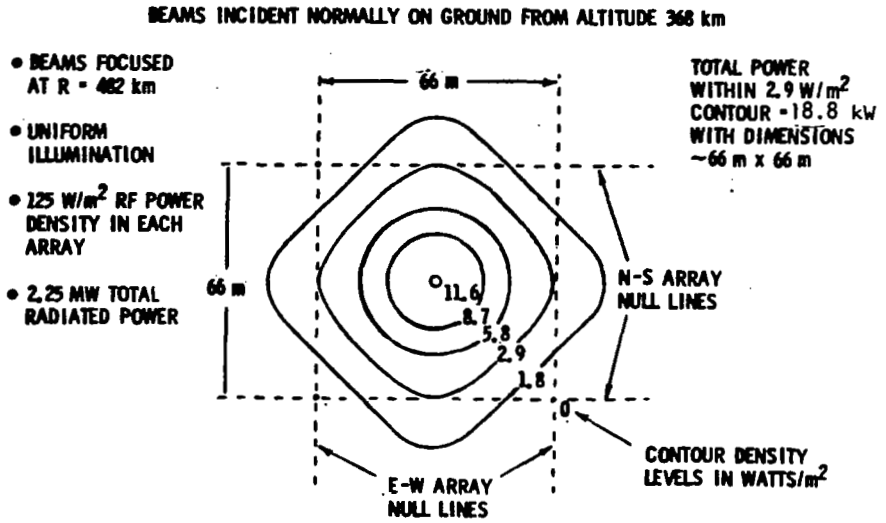

Figure 2.2-7. Power Density Contours within Footprint Core

where $\overline{S_R(\rho)}$ is shown by the dashed curve in Figure 2.2-8. With this approximation the integral becomes

$$P = 2\pi \int_0^{\rho} \overline{S_R(\rho)}\, \rho d\rho$$

and when evaluated graphically gives P = 18.8 kW for ρ = 33 meters. This, then, is the power delivered to the rectenna at closest approach. If rectification efficiency is 85%, then the available dc output power will be 16 kW.

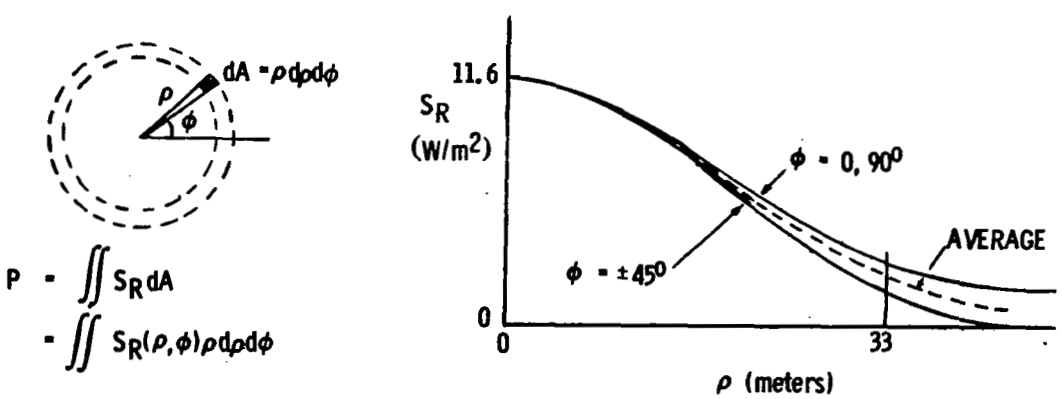

APPROXIMATE THE INTEGRATION BY USING $S_R(\rho,\phi) = \overline{S_R(\rho)}$

THEN $P = 2\pi \int_0^{\rho} \overline{S_R(\rho)}\, \rho d\rho$

GRAPHICALLY, P = 18,800 W FOR ρ = 33 meters

Figure 2.2-8. Total Power Calculation

During the course of the 108-second demonstration (see Figure 2.2-2) the range and the angle of incidence (β) on the rectenna will change and the delivered power will vary accordingly. To determine the extent of the variation it will be assumed that retrodirective pointing control operates in an ideal manner so as to ensure that the transmitted beam is always pointed to, and focused on, the rectenna. It is easy to see that the range loss varies as $\cos^2\beta$ while the loss due to projected rectenna area varies as $\cos\beta$. The net result is that delivered power varies as $\cos^3\beta$. Since $\beta = 41.3°$ at the beginning and end of the test, the delivered power is then 3.7 dB below the maximum and is reduced to 8.0 kW. Superimposed on this power-level variation is an additional possible loss due to the need for electronic beam steering. It was earlier pointed out that the maximum loss due to this effect is 1.6 dB. Hence, the worst case range of delivered power levels is from 5.5 to 13.0 kW.

2.2.2 POWER

Summary

Preliminary analysis of the power requirement for the SPS Test Article I satellite has identified several unique mission and design constraints. The first constraint is the realization that the large dimensions (2-km character) of the satellite could cause prohibitive power losses if a conventional power generation/distribution approach is selected. The second constraint is that if photoelectric power conversion devices, e.g., solar cells, are used, the continuous pitching motion of the satellite in the direction of orbital motion will result in a cyclic generation of operational power.

Another potential problem is in the relationship between power generation and power utilization. Of particular concern is the need to provide power to the microwave power transmitter at a fairly high level (3.028 MW) for a period not to exceed 240 seconds, once during any 24-hour period.

Consideration of the above constraints has led to the selection of a "power pack" concept for the SPS Test Article I satellite. The power pack consists of a GaAs solar array, a battery group, and associated control and charging electronics. Depending upon the array area required the solar array may be mounted upon the pack surface or strung like a "bed sheet" from the adjacent structure.

Five power packs have been defined to satisfy the varying and physically separated satellite power requirements (Table 2.2-1): (1) the main data management and communications module power pack, (2) the APS power pack, (3) the attitude determination module power pack, (4) the microwave subarray power pack (Figure 2.1-5), and (5) the instrumentation and data management power pack. Table 2.2-2 summarizes the electrical and physical characteristics of each of the power pack types. The satellite will require one of the DMC power packs, four of the APS packs, one ADS pack, 717 antenna packs, and at least 45 instrumentation packs, required wherever an instrumentation group and a remote interface must be installed. Table 2.2-3 summarizes the location, number, and form factor that may be considered probable for each of the power pack types. The mass of the communication module is included in the summary (Type A)

Table 2.2-1. Power Distribution Requirements

REQUIREMENTS/ASSUMPTIONS

- SUN FACING TIME EQUIVALENT: 1-2 HR OVER 24-HR PERIOD
- POWER REQUIREMENTS FOR 24-HR PERIOD

(10 V dc) MICROWAVE ANTENNA—160 W/m^2 UP TO 4 MINUTES IN DURATION

(28 V dc) APS—200 W (2 HR), 50 W (CONTINUOUS)

(28 V dc) ADS—104 W (CONTINUOUS)

(28 V dc) COMMUNICATION—700 W (CONTINUOUS)

(28 V dc) INSTRUMENTATION AND DATA MANAGEMENT—5-40 WATTS (CONTINUOUS)

Table 2.2-2. Power Distribution Characteristics

TYPE	LOAD	POWER LEVEL	ENERGY (Wh)	BATTERY CELL SIZE (AH)	SYST. VOLTAGE (V dc)	NO. BATT.	BATTERY CAP. TOTAL (Wh)	SOLAR CELL AREA (m^2)	BATTERY (kg)	SOLAR CELLS (kg)	CHARGER (kg)	PRORATED (kg/m^2)
A	COMMUNICATION	800 W (CONT.)	25,152	100	28	13	36,400	114	464	50	63	
B	APS	200 W (2 HR) 50 W (CONT.)	1,600	100	28	1	2,800	7.24	35.7	3.62	4.0	
C	ATT. DETERMIN.	104 W (CONT.)	3,270	100	28	2	5,600	14.8	91.4	7.4	8.2	
D	MICROWAVE ANT.	160 W/m^2 (4 MIN.)	390	18	10	4	720	2	10.4	1	4.0	0.62 (OVER 25 m^2)
E	INSTRUMENTATION & DATA MGMT	5-40 W (CONT.)	604	18	28	2	1,008	2.75	14.6	1.38	6.0	

NOTES: NiH_2 BATTERIES
28 V dc—23 CELLS
10 V dc—8 CELLS
f = 1.57—BATTERY TECHNOLOGY IMPROVEMENT FACTOR (Wh/kg)
SOLAR CELLS = 0.5 kg/m^2
BATTERY CHARGER & ELECTRONICS = 2.5 kg/kW (LARGE SIZE); 10.0 kg/kW (SMALL SIZE)
NOMINAL DEPTH OF DISCHARGE = 60%
CHARGE TIME = 1 HR WITH NOMINAL 2 HR ALLOWED

Table 2.2-3. Power Pack Equipment Summary

TYPE	NO. SETS	LOCATION	UNIT MASS (kg)	TOTAL MASS (kg)	DIMENSION W×L×D (m)	COMMENTS
A. DATA MANAGEMENT AND COMMUNICATION (DMC)	1	AT ONE OF TWO FRAME JUNCTIONS NOT POSSESSING APS INTERFACE	(1027)	(1027)		
DMC ELECTRONICS			350		1×2×0.5	SINGLE PACKAGE
BATTERY			464			
BATTERY ELECTRONICS			63			
SOLAR ARRAY		ON STRUCTURE NEAR MODULE	50		10×10×0.02	MOUNTED PARALLEL TO MW ARRAY
B. APS	4		(43.32)	(173.3)		
BATTERY		ON RCS PODS	35.7		0.25×0.25×0.5	SINGLE PACKAGE
BATTERY ELECTRONICS			4.0			
SOLAR ARRAY		ON STRUCTURE ADJACENT TO RCS PODS	3.62		1×7.24×0.02	MOUNTED PARALLEL TO MW ARRAY;
C. ATTITUDE DETERMINATION	1		(107.0)	(107.0)		
BATTERY		SATELLITE ROTATION AXIS	91.4		0.5×0.5×0.5	
BATTERY ELECTRONICS			8.2			
SOLAR ARRAY		ON STRUCTURE ADJACENT TO MODULE	7.4		4.0×3.7×0.02	MOUNTED PARALLEL TO MW SUBARRAY
D. MICROWAVE	2868	4 DISTRIBUTED AND MOUNTED ON REAR OF EACH 5×5-m MW SUBARRAY	(3.85)	(11,042)		4 PER 25 m^2 MW SUBARRAY (0.62 kg/m^2 AVG SPREAD OVER MW SUBARRAY
BATTERY			2.6		0.5 m^2 (4 PLCS)	LOCATED ON 4 CORNERS OF 25-m^2 SUBARRAY (1 m^2 EACH CORNER)
BATTERY ELECTRONICS			1.0			
SOLAR ARRAY			0.25		1×0.5×0.02 (4 PLCS)	
E. INSTRUMENTATION & D.M.	45		(21.98)	(1320)		
BATTERY		AS REQUIRED, >45 PLACES	14.6		0.5×0.5×0.5	
BATTERY ELECTRONICS			6.0			
SOLAR ARRAY		ON STRUCTURE NEAR EACH MODULE	1.38		1×2.75×0.02	MOUNTED PARALLEL TO MW SUBARRAY

because it is assumed that the DMC, the battery, and the battery electronics will be combined into a single package.

Design

Preliminary review of the SPS Test Article I satellite has indicated that power requirements may be considered in two categories: (1) continuous for satellite and mission operations support subsystems, and (2) very intermittent for the microwave antenna subarrays with a duty cycle of 240 seconds once every 24 hours, maximum. Mission experiments, however, may not necessarily be conducted during consecutive 24-hour periods. A second major requirement was that the satellite would operate at an altitude of approximately 482 km (260 nmi). Furthermore, the satellite would be placed into a continuous spinning mode in the orbital direction with a spin rate of 0.765 degrees/second. Prior to the mission period the satellite may be in a quasi-inertial altitude control mode with a permitted 19-degree wobble.

An additional factor that will receive consideration is the desire to simulate the SPS solid-state power configuration to the greatest extent possible.

Requirements Analysis

The initial step in the analysis was to determine the power requirements for each of the satellite support subsystems and the microwave antenna. The power consumption requirements were determined and grouped into five categories, four of which require power on a continuous basis, with the fourth (the antenna subarray) utilizing power in 120-240 second bursts once every 24 hours. A summary of the requirements analysis performed and impact on the solar array is presented in Table 2.2-4.

Table 2.2-4. Power Requirements and Solar Array Summary

MODULE	REQUIRED POWER	ENERGY (f) *	ENERGY (Wh)	POWER AVAIL. (W/m^2)	CHARGE TIME (hr)	ARRAY AREA REQ. (m^2)
MICROWAVE ANTENNA	160 W/m^2 FOR 4 MIN.	1.45	390	221	1 2	1.76 0.88
APS	50 W CONTINUOUS 200 W (2 HR)	1.31	1600	221	1 2	7.24 3.62
ATTITUDE DETERMINATION	104 W CONTINUOUS	1.31	3270	221	1 2	14.80 7.4
COMMUNICATIONS	800 W CONTINUOUS	1.31	25,152	221	1 2	114.0 57.0
INSTRUMENTATION AND DATA MANAGEMENT	5-40 W CONTINUOUS (120-960 Wh) 460 Wh AVG	1.31	604	221	1 2	2.73 1.37

**f is an array improvement factor (by 1990).*

The basic block diagram of the power pack is shown in Figure 2.2-9.

The use of an articulated (sun following) array was considered for the communications power pack, but this approach was rejected because of the complexity and reliability impact even though the array area requirements would be significantly reduced.

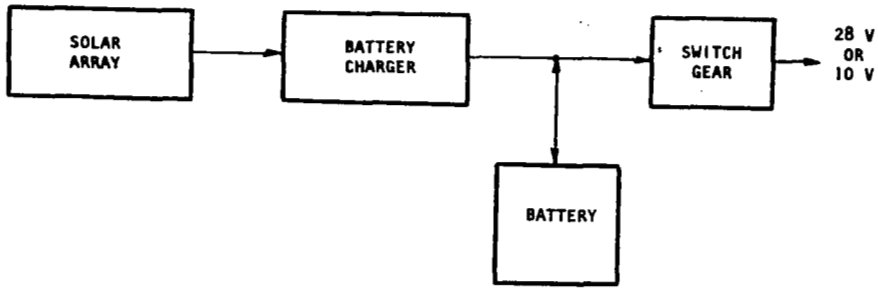

Figure 2.2-9. Power Distribution Block Diagram

Solar Array

The basic efficiency assumptions applicable to the power pack solar array are illustrated in Figure 2.2-10. The major points of interest are the assumption that the solar cell temperature can be maintained at an average temperature of 70°C. Overall efficiency of the solar array is 16.33%, resulting in a power density output of 221 W/m^2 if a solar input of 1353 W/m^2 is specified.

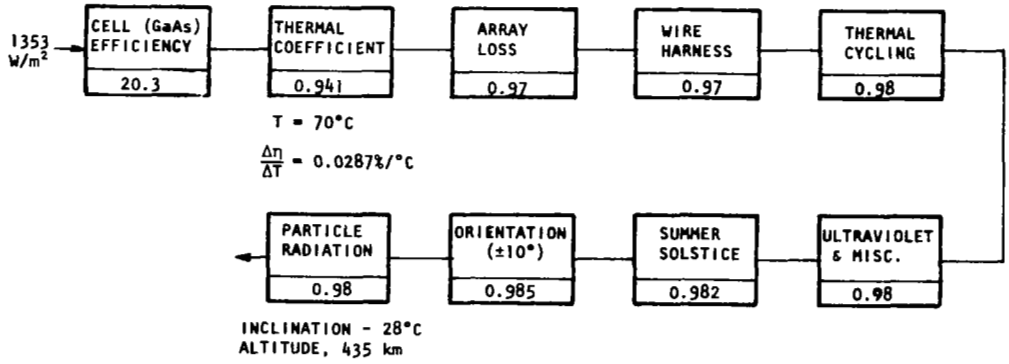

Figure 2.2-10. Power Pack Solar Array Efficiency Assumptions

Batteries

The batteries selected were based on advanced nickel-hydrogen technology with a cell voltage of 1.25 V/cell. Thus, for a 28-V system a battery consists of 23 cells in series, while a 10-V battery utilizes 8 cells. The possible charge rate as a function of battery size is summarized in Table 2.2-5. The volume occupied by a single battery pack in the 100-AH range is 42,580 cm^2. The smaller 10-V cell dimensions are 22.4×8.9×71.2 cm (14,194 cm^3). A typical seven-cell NiH configuration is shown in Figure 2.2-11.

Table 2.2-5. Battery Charge Rates ($Ni-H_2$)

CAPACITY (AH)	CHARGE RATE		
	C/4	C/6	C/10
30	7.5A	5.0A	3.0A
50	12.5	8.3	5.0
60	15.0	10.0	6.0
100	25.0	16.6	10.0

Figure 2.2-11. Nickel-Hydrogen Battery Cells

Table 2.2-6 summarizes the result of an industry survey to determine today's state of the art for Ni-H_2 energy storage elements; at the same time, discussion with various experts in the industry resulted in an estimated improvement factor of 1.53 for the proposed technology cutoff period. Thus for a 100-AH battery, a value of 78.5 Wh/kg was deemed reasonable.

Table 2.2-6. Battery State-Of-The-Art Technology (1980)

CAPACITY		DIAMETER	LENGTH	WEIGHT	DENSITY
AH	WH	(cm)	(cm)	(kg)	(WH/kg)
9	11.25	6.35	10.16	0.284	39.6
12	15.0	6.35	11.43	0.341	43.99
25	31.25	8.38	12.7	0.7	44.6
30	37.5	8.89	23.1	0.909	41.25
50	62.5	8.89	27.94	1.318	47.4
100	121.7	8.89	22.4	2.43	50.0
400	500.0	11.48	76.2	9.09	55.0

Thermal Control Requirements

This section presents a brief analysis of the thermal control requirements. The study was directed toward assessing the severity of the potential thermal problem and providing insight into potential solutions. Because of time limitations and the fact that details of the test configuration and its operational schedule have not been completely defined, the analytical model employed has been greatly simplified.

Power for the power transmission experiments on the SPS Test Article I will be supplied by nickel-hydrogen battery packs mounted on panels containing the solar arrays used for charging. These batteries are expected to be critical components from the standpoint of thermal control. They must be maintained within ±10°C while undergoing strong variations in heat input due to solar incidence variations, eclipses, and brief periods of battery discharge at high power levels. Measures such as insulation, which would prevent overcooling during eclipse, would aggravate the problem of overheating during battery discharge.

Battery Physical Characteristics

The SPS Test Article I satellite microwave subarray consists of twenty-five 1 m^2 honeycomb panels arranged in a five-by-five matrix. The four corner panels contain solar arrays, a battery compartment, and control compartment on the sun-facing side (Figure 2.2-12). All panels have arrays of dipole antennas on the side not facing the sun.

Since the detailed geometry of the battery compartments had not been defined prior to this analysis, it was necessary to make the following assumptions. The outer envelope is rectangular, with the dimensions shown in Figure 2.2-12. The sides and outward-facing surface are made of aluminum sheet, thick enough to avoid significant temperature gradients. Individual storage cells are mounted directly to the inner side of the aluminum sheet so as to provide good thermal coupling. The compartment as a whole is well-insulated from the panel to which

it is attached. For thermal modeling purposes, the battery compartment is treated as an isothermal box with internal heat generation, attached to the panel by an adiabatic surface. It gains and loses energy by radiation through its exposed sides.

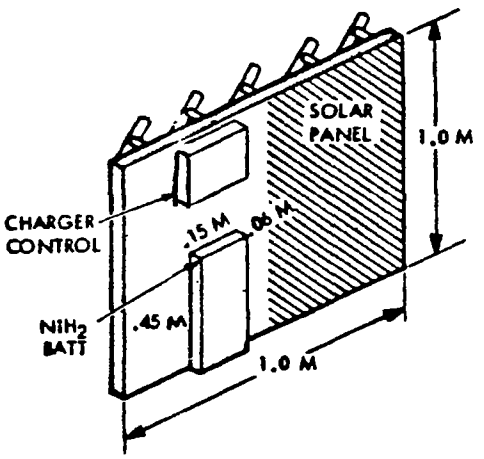

ORBITAL DATA

- 260 nmi ORBIT (483 km)
- 35° INCLINATION
- 90-MIN PERIOD
- 33-MIN ECLIPSE

BATTERY DATA

• OPERATING RANGE:	-10° TO +10°C
• NO-DAMAGE RANGE:	-20° TO +20°C
• THERMAL CAPACITY:	920 j/kg/°C
• MASS	2.6 kg
• DISSIPATION:	250 W FOR 4 MIN (ONCE A DAY)

Figure 2.2-12. Battery Thermal Control

Each battery has a mass of 2.6 kg and will deliver 1000 W of electrical output for a four-minute discharge period during once-a-day RF beam tests. Typically, nickel-hydrogen batteries have the following characteristics: Their preferable operating range of ±10°C, but they can be exposed to ±20°C without significant deterioration in lifetime or performance; based upon the mass distribution among battery components (electrodes, electrolyte, pressure shell, etc.), the average specific heat has been estimated to be 920 J/kg/°C. Recent experimental data on charge and discharge efficiencies show values in the range 16-17%. In this study the more conservative value of 20% has been used.

During the study, two flight modes were identified as applicable to the test satellite. In the first (spinning) mode, the array will be spinning slowly about an axis perpendicular to the orbit plane. In the second (inertial) mode, the array is basically oriented toward the sun, but wobbles ±19° about an axis perpendicular to the orbit plane. Subsequently, the first mode was selected as the most suitable design.

Battery Compartment Temperatures

A simplified transient heat balance equation may be written for the battery compartment as a whole, assuming the system is essentially isothermal.

$$\left[S(t)\ \alpha + I_e\ (t)\right]\ A_p - \sigma\varepsilon(A_p + A_s)\ T^4 = C\ \frac{dT}{dt} \qquad (2.2\text{-}1)$$

where:

A_p	Compartment plan area	m^2
A_s	Area of compartment sides	m^2
C	Thermal capacity	J/K
I_e	Incident earth radiation	W/m^2
L	Latent heat of fusion	J/kg
M	PCM mass	kg
S	Incident solar radiation	W/m
t	Time	sec
T	Temperature (compartment)	K
α	Solar absorptivity	
ε	Infrared emissivity	
σ	Stefan-Boltzman constant	$W/m^2\ K^4$

The functions $S(t)$ and $I_e(t)$ are the time-varying values of incident solar and earth radiation, respectively.

Equation 2.2-1 requires a numerical solution in general because of the complicated time-dependence of the radiation inputs. However, in the present case, the system has a fairly high thermal capacity. This means that temperature will vary only a few degrees from an orbital average value. Therefore, the second term in Equation 2.2-1, which represents radiation to space is nearly constant with time. If this assumption is made, Equation 2.2-1 is easily integrated over one orbital period to give average temperatures in terms of average radiation inputs. The time-dependent term, of course, integrates to zero over a complete orbit (cycle).

$$\left(\overline{S}\,\alpha + \overline{I}_e\,\varepsilon\right) A_p = \sigma\varepsilon(A_p + A_s)\overline{T}^4 \qquad (2.2\text{-}2)$$

The time-averaged values of solar and earth radiation depend upon eclipse duration and the variation in incident angles. For both flight modes they vary with solar declination and, hence, time of year. The values chosen here for temperature estimates are appropriate to the summer solstice:

Mode	$\overline{S}$ (Solar)	$\overline{I}_e$ (Earth)
Spinning	857	69
Inertial	431	94

Equation 2.2-2 was solved for average temperature with α/ε as a parameter. Figure 2.2-13 shows the results. As may be seen, a desirable average temperature of 0°C can be obtained with either flight mode using reasonable values of surface optical properties.

MODE I (SPINNING)

- AVERAGE SOLAR EXPOSURE (BATTERY SIDE ONLY): 1353/π W
- AVERAGE EARTH RADIATION: 94 W

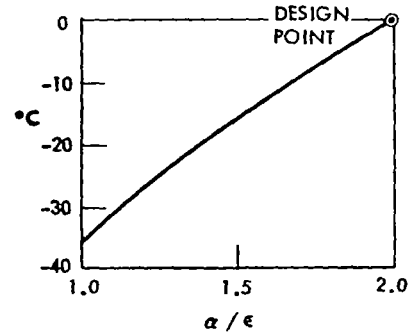

MODE II ("INERTIAL")

- AVERAGE SOLAR EXPOSURE (BATTERY SIDE): 1353 W FOR 57 MIN
- AVERAGE EARTH RADIATION: 188 W FOR 33 MIN

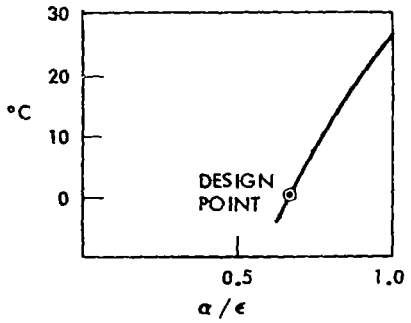

Figure 2.2-13. Orbital Average Temperatures for Battery Assembly

Transient Temperature

Equation 2.2-1 can be used to estimate the amplitude of the temperature cycle, in the absence of battery dissipation during discharge. (The low-level dissipation during charging has been neglected for simplicity.) Assuming, as before, that the loss term is constant and neglecting earth radiation in comparison with radiation loss gives the following expression for temperature drop during the cooling cycle.

$$T_{max} - T_{min} = \frac{\sigma\varepsilon\ (A_p + A_s)\ \overline{T}^4\ \Delta t}{C} \qquad (2.2\text{-}3)$$

For $\overline{T}$ = 273°K, ε = 0.21 and Δt = 33 minutes (1980 seconds) yields a temperature drop of 8°C. Inclusion of earth radiation decreases the drop to about 6°C. Thus, in the absence of battery discharge, the system temperature will cycle ±3°C during a typical orbit (Figure 2.2-14).

During battery discharge, the energy dissipated (250 W) is much larger than either net heating or cooling during the normal cycle. The temperature rise during discharge is approximately

$$\Delta T_{dis} = \frac{250\ \Delta t}{C} \qquad (2.2\text{-}4)$$

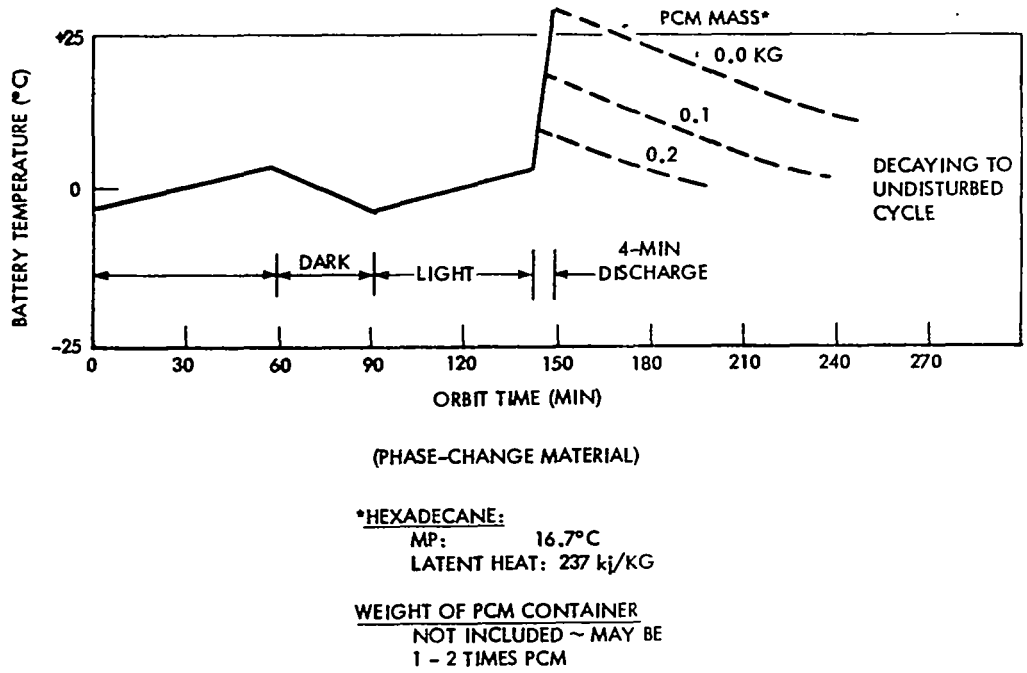

Figure 2.2-14. Battery Temperature Transients during Orbit

For a four-minute (240-second) discharge period, the rise is 25°C. This could overheat the batteries and reduce their lifetime—particularly if the discharge occurred at the end of a heating cycle.

As Equation 2.2-4 suggests, a straightforward way to reduce the temperature rise is to increase the thermal capacity. This can be done with minimal weight impact by the use of phase change material (PCM). There are many types of PCM. One type which has received extensive laboratory testing and which has been flown in space is the paraffins—high-molecular-weight, saturated hydrocarbons. They have good heats of fusion, low volume change, and are available as a homologous series with closely spaced melting temperatures. An appropriate PCM for the present application is hexadecane with a latent heat of fusion of 237 kJ/kg and a melting point of 16.7°C. Tetradecane has a similar heat of fusion and a melting point of 5.5°C.

Provided the final temperature is above the melting point, the ideal temperature rise with M kilograms of PCM added is

$$\Delta T_{dis} = \frac{250\ \Delta t - ML}{C} \qquad (2.2\text{-}5)$$

As shown in Figure 2.2-14, very little PCM mass is required to reduce the temperature rise dramatically. In practice, ideal PCM performance is reduced by temperature hysteresis effects and the requirement for a metallic container which may weigh one to two times the PCM itself. Nevertheless, the use of PCM appears to be a practical means of preventing excessive battery temperature in this application.

2.2.3 DATA MANAGEMENT AND COMMUNICATIONS (DMC)

Summary

Initial analysis of the mission and satellite requirements indicates that present state-of-the-art technology can be utilized to implement all elements of the data management and communications (DMC) subsystem. The assumed satellite configuration and major interfacing elements are illustrated in Figure 2.2-15.

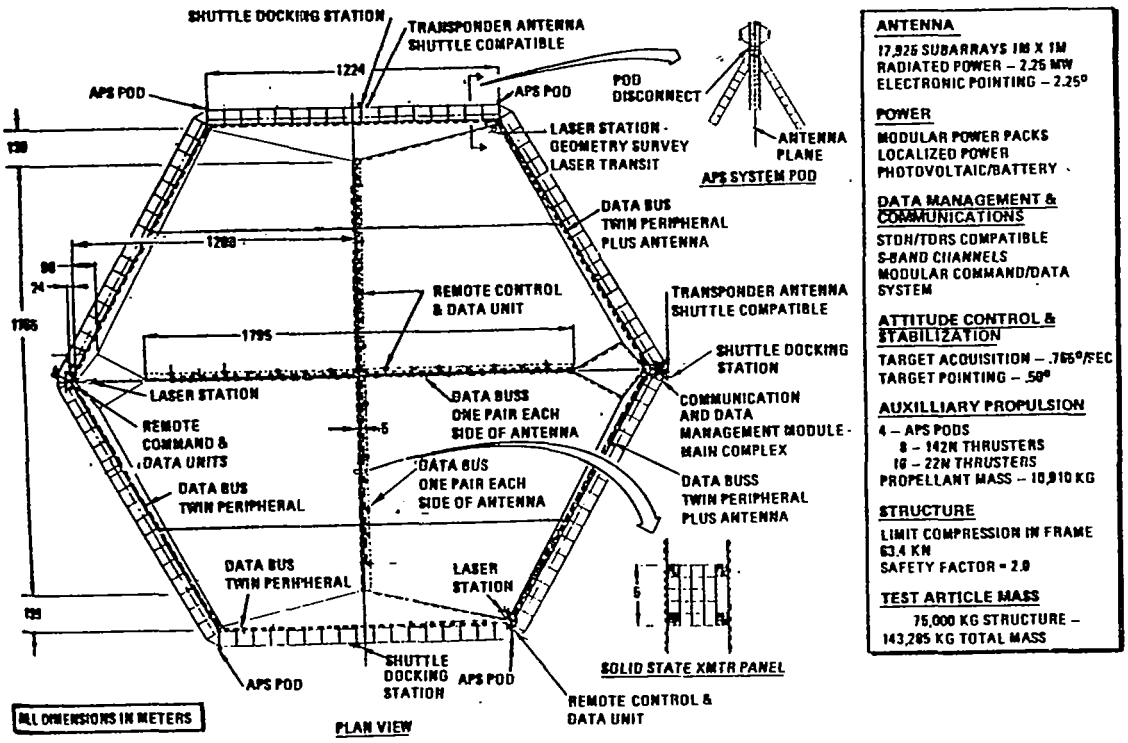

Figure 2.2-15. Satellite Configuration

The preliminary concept selected for the DMC subsystem is shown in Figure 2.2-16. The communications utilize S-band transceivers compatible with existing ground-based (STDN) networks, orbiter channels, and with proposed TDRSS links. The controller/processor section may be implemented by utilizing the processor (and software) proposed for the NASA/Goddard Multi-Mission Modular Spacecraft (MMS) with necessary customizing software as required. The data bus concept selected is similar to that utilized by the MMS with two major modifications: (1) a multi-channel (six) bus controller would replace the present MMS concept, and (2) the data bus itself would be implemented using state-of-the-art fiber optics. Table 2.2-7 summarizes the physical characteristics of the DMC subsystem, while Table 2.2-8 indicates the available or optimal data link channels (two-way).

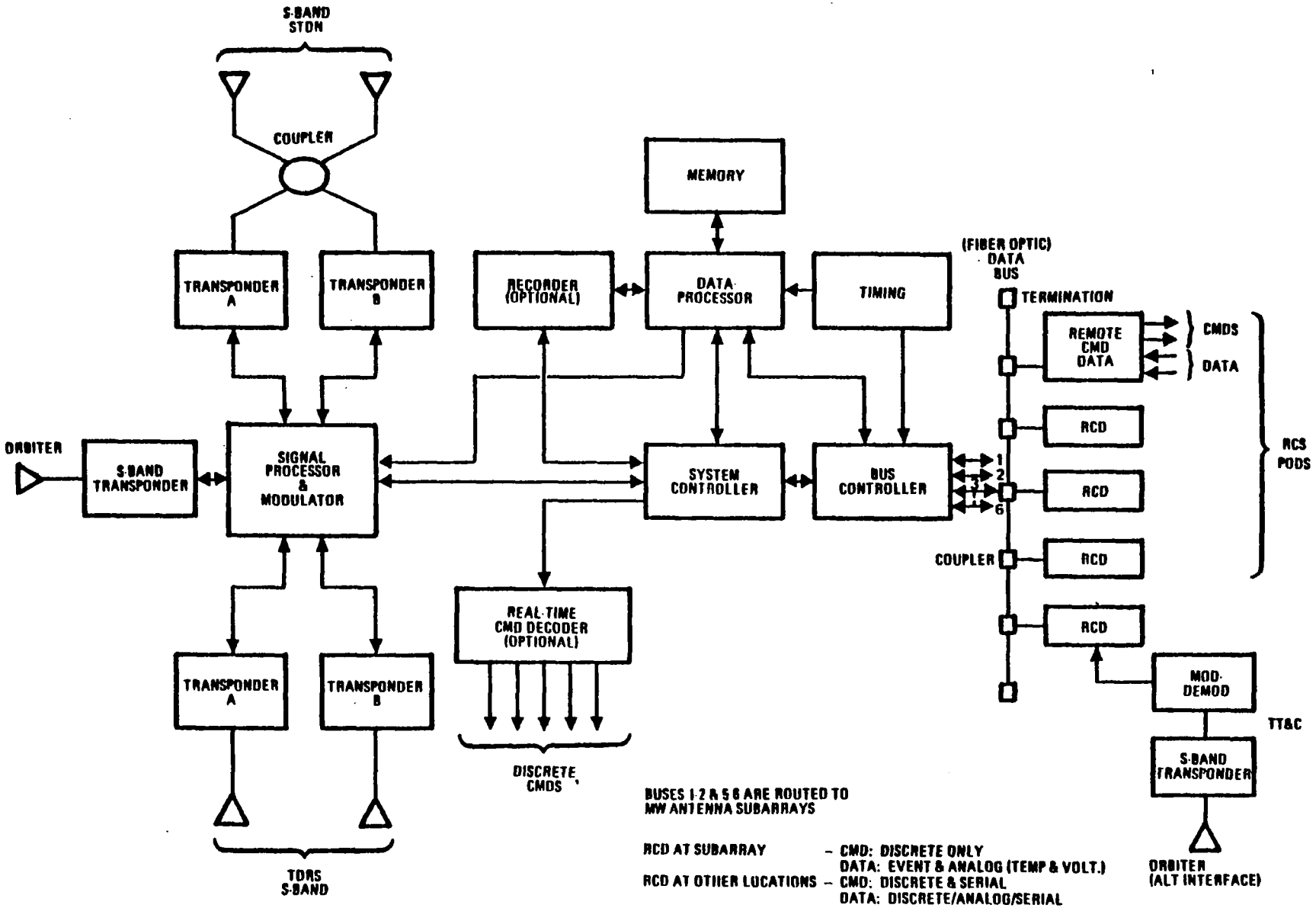

Figure 2.2-16. Basic DMC System

Table 2.2-7. DMC Mass and Power Summary

S-BAND COMM.	MASS (KG)	POWER (W)	NOTES
PM TRANSPONDER	31.6	63	POWER REQUIREMENTS SET BY ASSUMING 1 EA ON AT SAME TIME
PM PROCESSOR	16.2	30	
DOPPLER EXTRACTOR	14.8	16	
POWER AMPLIFIER (100 W) 2 EACH	28.8	400	
PREAMPLIFIER	23.2	25	
FM TRANSMITTER	6.0	120	
FM PROCESSOR	10.4	9	
SWITCH ASSY	3.0	2	
WIRING	30.0	-	
ANTENNA (7)	2.0	-	
	~170.0	~700	USED FOR POWER PACK SIZING
DATA MGMT			
DATA PROCESSOR (2)	60	40/2 STDBY	50% DUTY CYCLE
MEMORY (4)	60	40/2 STDBY	20% DUTY CYCLE
TIMING UNIT (1)	20	5	BUILT-IN REDUNDANCY
SYSTEM CONTROLLER (1)	20	20	
BUS CONTROLLER (6)	120	10	
REMOTE CONTROL/DATA (AS REQ'D)	(2 EA)	10/2 STDBY	EST. FOR POWER MODULE SIZING
	~280	~100	RCD PWR DISTRIBUTED
FIBER OPTIC CABLE	NEGL.	-	
INSTRUMENTATION	300	-	DISTRIBUTED

Table 2.2-8. SPS Test Article I Satellite Link Parameters

LINK	ONE WAY OR TWO WAY?	FREQUENCY	DATA RATE	NOTES
S-LINK				
PM TO ORBITER (OR DIRECT TO STDN OR SCF)	TWO	RETURN 2200-2300 MHz FORWARD 2025-2120 MHz	192 Kb/s 72 Kb/s	THIS LINK IS RELAYED TO STDN, SCF, OR TDRS. SCF HAS 256 Kb/s (RETURN) RF POWER = 6 W ANTENNA = 4 QUAD OMNIS
FM TO GROUND (STDN OR SCF)	ONE	RETURN 2250 MHz (10 MHz BANDWIDTH)	4 Mb/s	RF POWER = 10 WATTS ANTENNA = 2 HEMIS. OMNIS
PM TO TDRS (THROUGH TDRSS)	TWO	RETURN 2200-2300 MHz FORWARD 2025-2120 MHz	192 Kb/s 72 Kb/s	RF POWER = 100 WATTS ANTENNA = 4 QUAD OMNIS TIME COVERAGE: ≥ 95%
Ku-LINK				
TO ORBITER OR TO TDRSS	TWO	RETURN 14.85-15.15 MHz	50 Mb/s DIGITAL OR 4.5 MHz ANALOG TV 2 Mb/s PAYLOAD 192 Kb/s TELEMETRY	RF POWER = 50 WATTS ANTENNA = PARABOLIC (0.9 M DIAMETER) TIME COVERAGE: ≥ 95%
		FORWARD 13.75-13.80 GHz	216 Kb/s COMMANDS	HAS DATA & PN RANGE

Communications

Communications requirements for the SPS Test Article I satellite are summarized in Table 2.2-9. The channels that are available are shown in Figure 2.2-17.

Table 2.2-9. Communications Requirements

• Orbit altitude	482 km (260 nmi)
• Power transmit—duty cycle	Once in each 24-hour period
• Communications link	
- Transmit orbit (continuous)	±5.4 min. about power LOS ground zero
- All other orbits	1 time/orbit 5 min. average
• Data rate	10 kbit/s
• Command rate	≥2 kbit/s
• Data bus	
- Material	Fiber optic
- Bit rate	1 Mbit/s

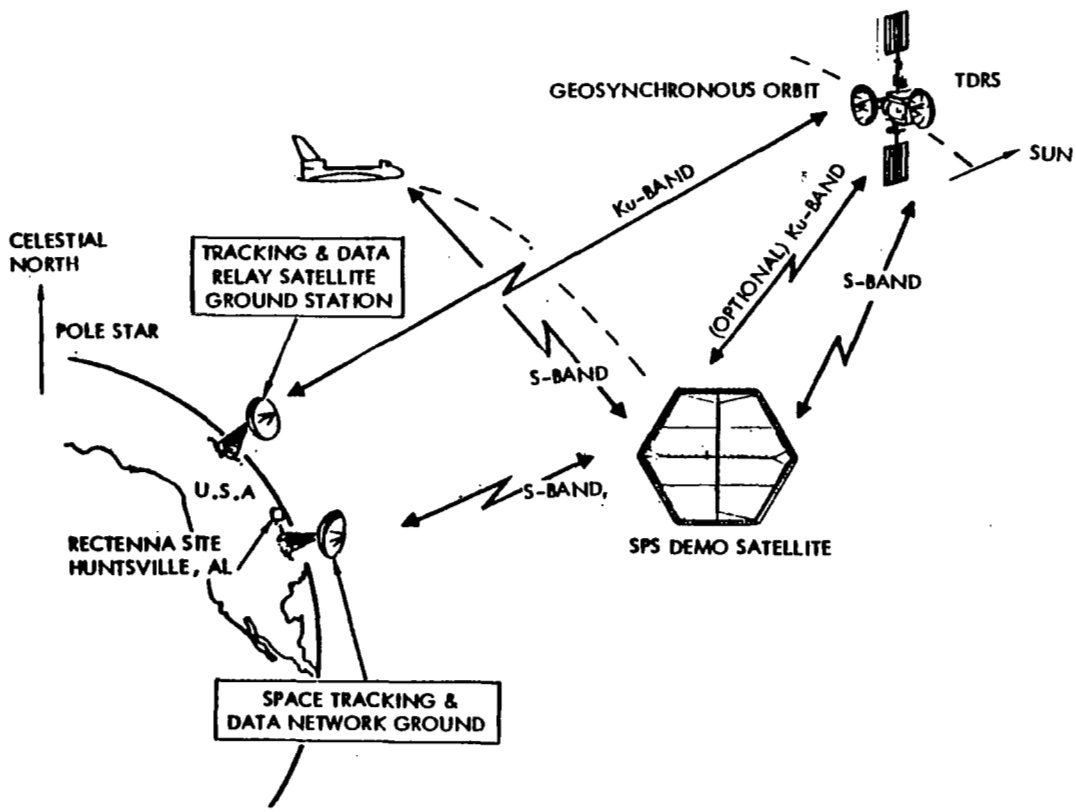

Figure 2.2-17. Communication Links Available for SPS Test Article I

The operating orbit for the satellite has been selected at LEO with a nominal attitude of approximately 482 km (260 nmi). The satellite would utilize S-band RF links to provide two-way command and data plus tracking capability. If Ku-band capability is also implemented, the complete system would provide a maximum command reception rate of 512 Kbits/sec. Ku-band utilization would also permit the use of CCTV and high data rate transmission with a maximum rate of 50 Mbits/sec.

S-band RF links (and Ku-band also, if implemented) may be established with existing NASA ground stations (STDN) or routed through the Tracking and Data Relay Satellite System (TDRSS).

The suggested on-board communication links for the demonstration satellite were shown in Table 2.2-8. There are three S-band links: (1) PM to orbiter, STDN or SCF; (2) FM direct to ground; and (3) PM to TDRSS and then TDRS on the ground. The return link on (1) is split into high (2250-2300 MHz) and low (2200-2250 MHz).

Link margins are given in the special issue on *Space Shuttle Communications and Tracking*, IEEE Transactions on Communications, November 1978 (pp. 1474, 1521 and 1604). Table 2.2-7 provided mass and power estimates. The total without growth provisions, for the S-band communication subsystem including wiring and antennas is estimated to be 170 kg in mass and 700 W of power.

For completeness, the capability of the TDRSS Ku-band was also defined in Table 2.2-8 although the need for this capability has not, at this time, been demonstrated.

Note (Figure 2.2-16) that Links (1) and (2) have less than 40% real-time coverage, whereas Links (3) and the Ku-band have more than 95% due to the SPS satellite being in low earth orbit and the good coverage provided by TDRSS.

Data Management

The data management subsystem is comprised of two major subsections—the data management processor subsection and the data and command distribution network.

The data management subsection includes the primary system controller, the primary (or central) on-board data processor and its auxiliary equipment, and the real-time command decoder to provide those hard-wired control interfaces (if any) required to place the satellite in a safe, standby mode of operation during unpredicted anomaly periods. Because of the very large dimensions involved the use of remote microprocessors co-located with critical support subsystems (such as attitude control modules) is also postulated.

The data and command distribution subsection of the data management subsystem consists of a data bus controller which is the microprocessor controlled interface between the data processing system and the data management section, a fiber optic primary data bus (two-way) system, and the many remotely located command and data interface units (RCD's) located at each of the various subsystem locations (such as APS pods) and at various positions along the microwave

transmitting array. The remote interface module will be installed whenever the total of data points and control inputs within a 100-m radius "zone" exceed some specified number.

Figure 2.2-18 illustrates the proposed data systems network, showing the coneept of dual redundancy and isolation of the structural data system from the

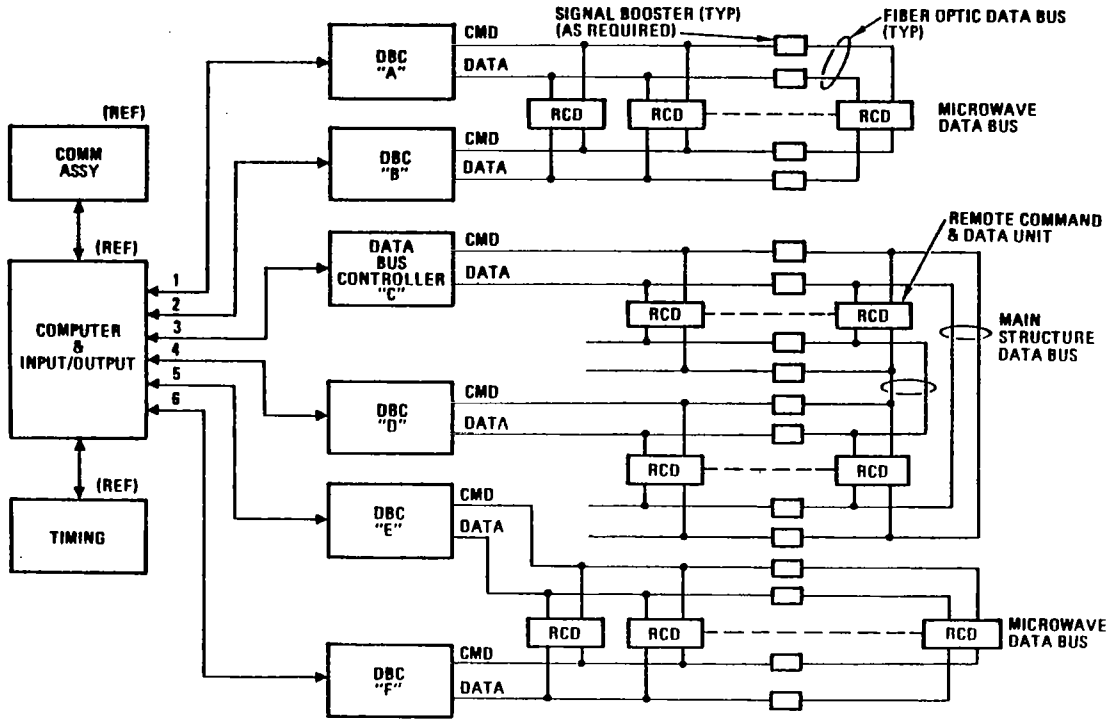

Figure 2.2-18. Satellite Command/Data Distribution System

data system on the microwave array. Figure 2.2-19 shows the location of some of the elements on the satellite structure.

The main group, contained in a single module with the communications equipment, would be located at one of the docking ports. The estimated 0.32-cm-diameter multifiber optical data bus located on the structure would then be routed along the perimeter of the antenna in both directions from the central module along the primary structure. Since the cables are non-metallic (if a metallic radiation shield is used, an outer non-metallic sheath would be added), a simple lightweight clip may be used to fasten the optical cable to the structure wherever required. Because of their simple construction and small size, the clips will have no major influence on their adjoining structure. Periodically, remote interface units or repeater units will be connected in series with the optical cable. The repeaters will be used whenever line loss becomes excessive but where an interface unit is not required. A repeater unit will be included in each remote interface unit to achieve the same purpose.

A reasonable number of interfaces for a single remote unit could be somewhere between 256 and 512. For a more complex interface, such as the APS pod,

one or two remote units would be dedicated to the specific interface, and would very likely be co-located with the interfacing equipment group.

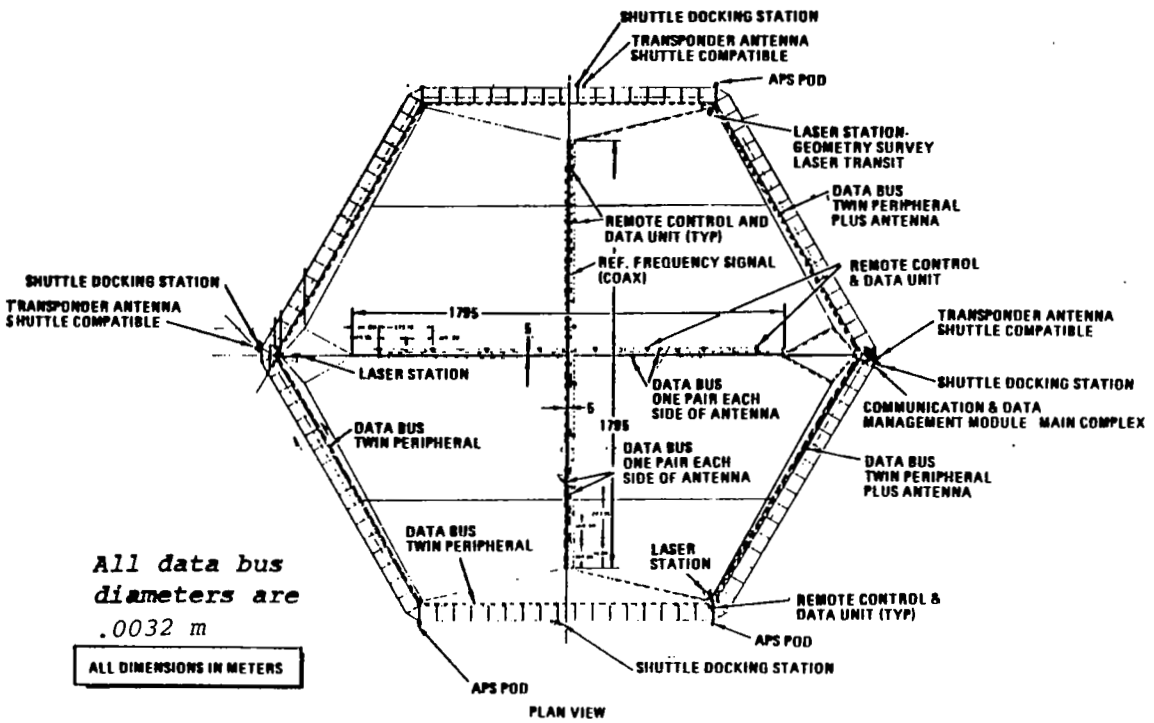

Figure 2.2-19. Element Location on Satellite Structure

The data bus interface to the microwave antenna would follow the array tension cabling with the redundant buses being routed on each side of the transmitting array and coming from each end of the Mills cross (Figure 2.2-19) to ensure maximum reliability and safety. The remote units would be mounted on the rear surface of the subarray with one unit located approximately every 200 m.

The actual interconnections from the remote unit to the remote sensors or control inputs would be metallic—probably aluminum conductors—to reduce costs. The total number of remote units required cannot be estimated until specific details identifying instrumentation and control requirements are defined. However, it is estimated that at least 45 units will be needed.

Table 2.2-7 provides mass and power estimates for the data management elements. The total, without growth provisions and without the mass of the metallic conductor interface between subsystem and remote unit, is estimated at approximately 280 kg and 100 W (continuous).

The total mass of the fiber optic data buses is estimated to be less than 50 kg. Since this mass is distributed on the entire satellite, the specific impact on the structure may be neglected.

The estimated instrumentation mass of 300 kg (distributed) assumes the installation of 106,000 individual sensors and conditioners with an average

mass of 0.028 kg (1 oz.) per sensor and conditioner set. The actual number of sensor interfaces will be less, with some individual sensors having a mass as much as 10 kg. (An example of a sensor with this mass would be a laser transit device that would be used to determine structural, cable, or subarray deflection.)

2.2.4 ATTITUDE CONTROL AND STABILIZATION SUBSYSTEM (ACSS)

Introduction

The attitude control and stabilization subsystem (ACSS) provides control of SPS Test Article I during the antenna installation and test operation phases. The mission is six months. The ACSS features an APS using an N_2O_4/MMH bipropellant system for control. Two separate concepts are employed for each of the two phases. During the antenna installation phase, the test article is in a quasi-inertial mode. It is spin-stabilized in the test operation phase.

A diagram of the ACSS equipment is shown in Figure 2.2-20. This equipment is located on the axis of the pitch rotation (Drawing 42635-18031). The control system features a precision attitude reference system, coarse alignment system, flight computer, and interface unit (Figure 2.2-21). The output of the control systems provides the commanded signals to an active three-axis APS. The ACSS consists of all standard equipment with the exception of the flight computer and interface unit. No major technology development program is anticipated.

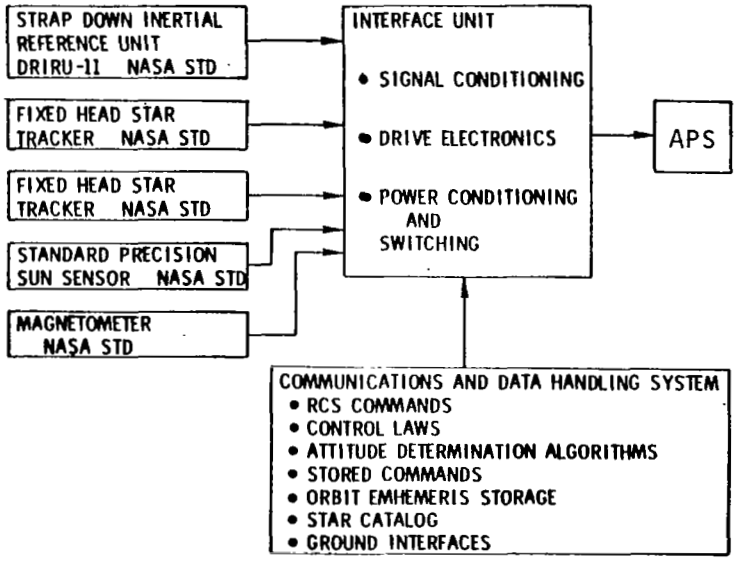

Figure 2.2-20. ACSS Block Diagram

The details of the ACSS are summarized in Table 2.2-10. The precision attitude reference system is comprised of the DRIRU-11 inertial reference unit (IRU), two fixed-head star trackers, and associated software. The software processes the IRU and star tracker data and compensates for known measurement errors to compute attitude and attitude rate information which generates APS

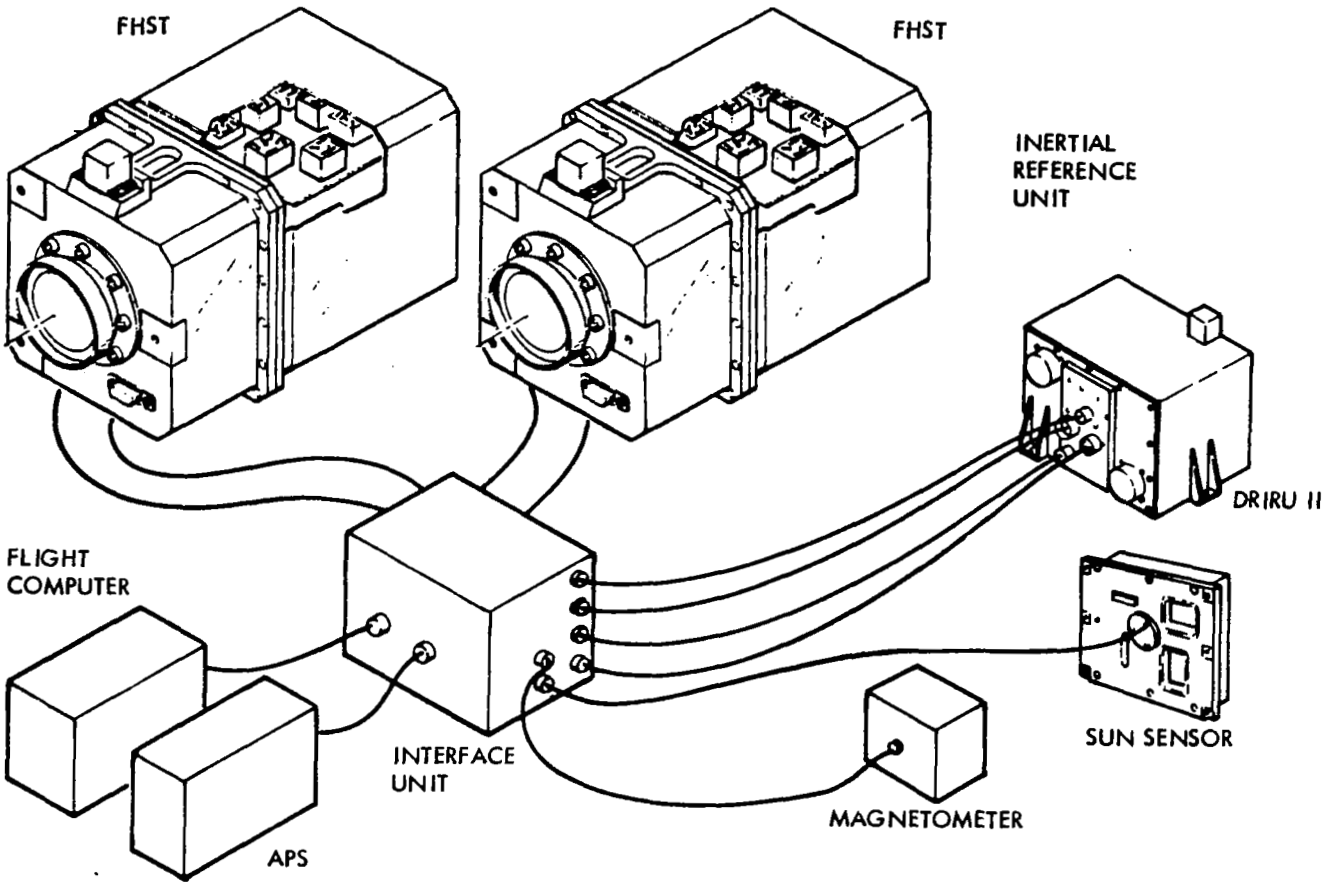

Figure 2.2-21. Attitude Control and Stabilization Subsystem

Table 2.2-10. Elements of the ACSS

ITEM	NO. REQ'D	MASS (kg)	DIMENSIONS EACH (cm)	TOTAL MASS (kg)	POWER (W)
PRECISION REFERENCE SYSTEM					
• DR IRU-II	1	16.9	22.6×31.2×22.9	16.9	22.5
• MOD II FIXED-HEAD STAR TRACKER	2	9.1	15.9×19.6×43.9	18.2	42.0
COARSE ALIGNMENT					
• FINE-POINTING SUN SENSOR	1	2.6		2.6	2.2
• MAGNETOMETER	1	0.9	14.2×16.5×6.8	0.9	2.0
INTERFACE UNIT	1	14.0	31×31×61	14.0	35.0
			TOTAL	52.6	103.7

control commands. The sun sensor and magnetometer are part of the coarse alignment system. The sensors are used for platform acquisition and reorientation.

Attitude Control Requirements

The following requirements are the basis for the selection of the ACSS: (1) attitude error, ±0.5°; (2) attitude rate error, ±0.004°/sec; and (3) spin rate, 0.765°/sec. The ACSS provides a pointing accuracy capability within the specified requirements with a minimum of hardware development. The attitude reference system of the IRU, plus the star tracker and attitude determination algorithm, measure attitude to an accuracy of 20 arc-sec and an attitude rate (0.001-0.1) arc-sec/sec. Compensation of measurement errors resulting from structural deformation caused by thermal gradients and APS firings is accomplished by the algorithm. Static alignment errors are biased out in the computation. The compensation is updated by processing in-flight structural deformation data. The three-axis APS is capable of pointing accuracy of ±0.1°. With this accuracy, an attitude rate error of ±0.004°/sec is permissible within the 0.5° pointing accuracy requirement without performance degradation (i.e., I_{SP} level is maintained); a minimum impulse is achievable which results in attitude rate change that is an order of magnitude less than the specified rate error. The baseline ACSS using standard NASA components is feasible.

Attitude Mode Selection

Several control modes were considered in the selection of the preferred concept for the test operation. For all of the concepts, the quasi-inertial (QI) mode was used for the antenna installation phase, although subsequent study indicated a free-drift mode would suffice with minor propellant reduction. During installation, the pointing requirements are not stringent and the gravity-gradient torque is the dominant disturbance on the spacecraft; hence, the QI mode results in small RCS propellant requirements and achieves near-inertial attitude synchronized to the gravity-gradient torque.

An important factor in selecting the preferred concept for test operations was the magnitude of the propellant requirements. The propellant requirements principally result from control of the large gravity-gradient torques and from any maneuvers required during the testing orbit (i.e., to maneuver the vehicle prior to test and return vehicle to its non-testing orbit attitude). The aerodynamic and solar pressure torques are small because of the geometrical symmetry of the spacecraft resulting in a small c.p-c.g offset.

Referring to Table 2.2-11, four control concepts were considered in the study. The first two modes—solar inertial and Y-POP inertial—had propellant penalties exceeding 30% spacecraft mass over six months. In these modes, large propellant penalties resulted from the gravity-gradient torque control and the maneuvers required to orient the test article for test. In the QI mode, the propellant penalty for gravity-gradient torque was substantially reduced, but the maneuver requirements remained to obtain the testing attitude. The spin-stabilized concept resulted in a substantial propellant reduction and was selected on that basis.

Table 2.2-11. Propellant Mass for Attitude and Stabilization Candidates

	TOTAL PROPELLANT (KG)	% SPACECRAFT MASS OVER 6 MONTHS
THREE-AXIS ACTIVE CONTROL		
• SOLAR INERTIAL	PROHIBITIVE	PROHIBITIVE
• INERTIAL Y-POP	40,900	30
• QUASI-INERTIAL	25,000	18.4
SPIN STABILIZATION - SPIN STABILIZED ABOUT MINOR AXIS WITH ACTIVE NUTATION DAMPING (SPIN AXIS POP)	8,643	6.3

INCLUDES 3 MONTHS QUASI-INERTIAL MODE DURING ANTENNA INSTALLATION
INCLUDES SPINUP & DESPIN FOR TEST

The propellant reduction achieved in the spin-stabilized concept resulted from several reasons. In the spin-stabilized mode no major maneuver is required to orient the spacecraft over the test site. The spin rate selected is 0.764°/s which is 12 times the orbit rate, and the required spin rate during test is 0.765°/s. Hence, a slight adjustment in spin rate is required in the testing orbit. The adjustment results in a small propellant requirement.

The spin axis which is always the minor inertia axis is inherently unstable. However, the divergent time constant which is a function of spin axis moment of inertia and propellant tank properties is sufficiently long, which results in a small propellant requirement for active nutation damping. Spinning about the intermediate axis of inertia was rejected since it results in unstable motion with a fast divergent time constant.

Details that contributed to the propellant penalty for the spin stabilization mode are presented in Table 2.2-12. An additional disturbance torque resulting from orbit precession is included in this mode. The propellant

Table 2.2-12. Spin Stabilization Propellant Requirements (75,000 kg Frame)

		PROPELLANT (KG)
• ORBIT MAKEUP (9 MONTHS)		2,267
• QUASI-INERTIAL MODE (3 MONTHS)		2,225
• SPIN CONTROL (3 MONTHS)		
• ORBIT PRECESSION	3084	
• GRAVITY GRADIENT DISTURBANCE TORQUES	1012	
• NUTATION DAMPING	NEGLIGIBLE	6,418
• SPINUP & DESPIN	1161	
• CONTINGENCY SPINUP & DESPIN	1161	
TOTAL		10,910

penalty to control this torque accounted for 48% of the total propellant requirement. The other 52% of the propellant was equally divided to control the gravity gradient torques and to spin and despin the spacecraft. The results are based on inertia properties that are larger than the present values. The propellant penalty of 6418 kg shown (Table 2.2-12) is conservative for the satellite mass of 143,285 kg. The actual value would be reduced by approximately 11%, which results in a propellant penalty of 705 kg.

The attitude control requirements for the ACSS during the 108-second test period are achievable in the spin-stabilized mode. The control of the environmental disturbance torques will contribute a small propellant penalty. There is sufficient stiffness to maintain the orientation of the spin axis. The nutation of the spin vector is negligible because of the long divergent time constant.

Control System and Structural Dynamics Interaction

The potential for interactions between the control system and structural dynamics increases with spacecraft size and weight. This interaction, if unaccounted for, may degrade pointing accuracy and cause system instability. The present and easiest method to prevent such interaction is by ensuring large frequency separation between the first modal frequency and control bandwidth. Typically, the separation is such that the first modal frequence is 5 to 10 times the control frequency. The analysis indicates that a 0.0078-Hz bandwidth is required to compensate for the gravity-gradient torque. The 0.0078-Hz bandwidth also provides the necessary stiffness to satisfy the 0.5° attitude pointing error. The lowest modal frequency associated with the gravity-gradient torque is 0.0176 Hz which results in a frequency separation of 2.26. Although the frequency separation is less than desired, there seems to be no major control bandwidth/bending frequency interaction problem.

If a reduction in frequency separation arises and more than a few modes must be stabilized, there will be a need for active modal control of the structural vibration response. Active modal control will increase the complexity of the control system. More sensors and actuators will be required to control the vibration response than the traditional methods. The dynamic modeling of control system and structure will increase in size and complexity. The assessment of the control system requirements would require more extensive analysis, which is beyond the scope of this study.

Alternate Considerations

Momentum storage devices, such as control moment gyros (CMG's) were considered to perform the control function. The gravity-gradient disturbance torques give rise to large momentum requirements. The number of CMG's needed to satisfy the momentum requirement is prohibitive. This was based on using Skylab CMG's which have high momentum storage capacity (3000 nms) and have been flight qualified. Momentum storage devices required for this application would result in a significant technology development program. On this basis, momentum storage devices were rejected for attitude control.

APS Minimum Thruster

The APS is a 24-thruster configuration consisting of four pods. In each pod there are four 22.2 N thrusters and two 142.4 N thrusters. The 142.4 N thrusters provide for the translational control and gravity-gradient control. The analysis indicated that 71.2 N thrusters are sufficient for gravity gradient control. These thrusters are not used prior to the test maneuver. A reduction in thrust level gives rise to increased burn time for spin/despin maneuvers. Thus, some flexibility in thruster configuration design exists.

2.2.5 AUXILIARY PROPULSION SYSTEM (APS)

An auxiliary propulsion system (APS) is provided for control of SPS Test Article I in the low earth orbit (LEO) during a nine-month active life, during which the microwave antenna is tested. The APS provides control for both translation maneuvers and for attitude orientation and spinning mode control in conjunction with the attitude control stabilization subsystem (ACSS).

Summary

The key features of the APS for the SPS Test Article I design are summarized in Table 2.2-13. The APS module is illustrated in Figure 2.2-22 together with parametric scaling data for test articles with frames of mass greater than 75,000 kg.

Table 2.2-13. APS Summary (75,000 kg Frame)

• Propellant	N_2O_4/MMH
• Pressurization gas	Helium
• Total impulse	31.49×10^6 N-sec (7.08×10^6 lb-sec)
• Number of modules	4
• Number of thrusters	24
• Thrust, each	
16 thrusters	22.2 N (5 lb_f)
8 thrusters	142.3 N (32 lb_f)
• Propellant weight	10,910 kg (24,000 lb_m)
• Total weight	14,880 kg (32,728)

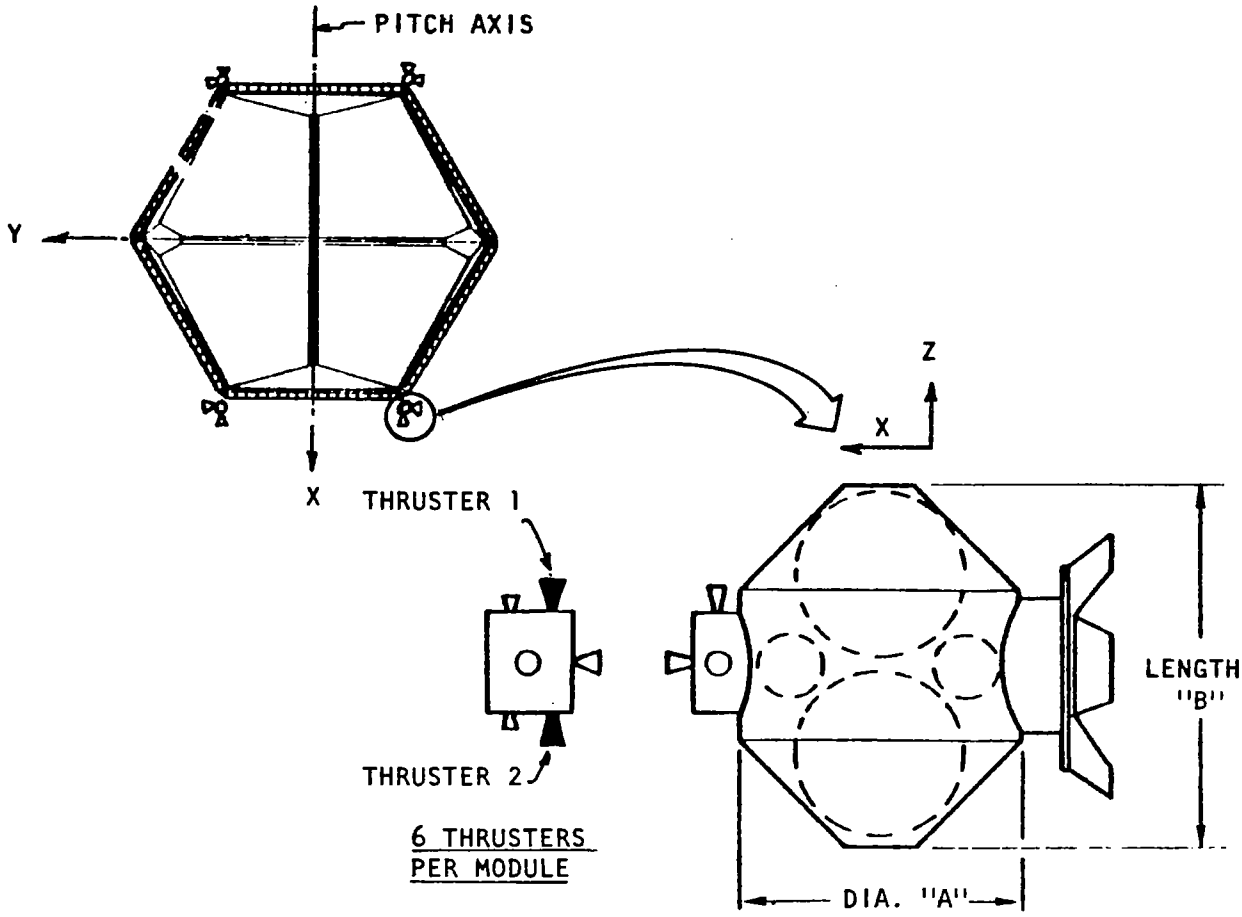

STRUCTURE TOTAL WT. (kg)	DIA. 'A' (m)	LENGTH 'B' (m)	THRUST 1 (N)	THRUST 2 (N)	PROPELLANT WEIGHT (kg)	DRY MODULE WEIGHT (kg)	TOTAL WEIGHT (kg)
75,000	2.3	3.2	142	22	10,910	3,970	14,880
112,500	2.6	3.6	200	29	15,336	5,581	20,917
150,000	2.8	3.9	258	36	19,737	7,214	26,951
187,500	3.0	4.2	316	42	24,183	8,848	33,031
225,000	3.2	4.4	374	49	28,584	10,436	39,080

PROPELLANT AND DRY MODULE WEIGHTS ARE FOR FOUR MODULES.

Figure 2.2-22. Typical APS Module

Requirements

The APS requirements are derived from the mission and from the ACSS requirements. As shown in Table 2.2-14, the first mission phase of six months' duration (frame construction) does not require the APS, which may be installed either in

Table 2.2-14. APS Functions

Mission Phase	Duration
1. Frame Construction • Free-drift mode • Orbit decay, 549 km to 494 km (300 nmi to 270 nmi)	6 mo. (no APS)
2. Installation Systems and Antenna • Quasi-inertial mode • Orbit makeup maintains 483 km (260 nmi) altitude	3 mo.
3. Spin-Up, 0.765 deg/sec	
4. Test Operations • Spinning mode • Orbit makeup maintains 483 km (260 nmi) altitude	3 mo.
5. Despin	
6. Structural Test • Orbit makeup maintains 483 km (260 nmi) altitude	1 mo.
7. Post-Test Period • Orbit makeup maintains 483 km (260 nmi) altitude	2 mo.

the first or second phase. The APS translation functional requirements consists of orbit makeup ΔV to maintain an orbital altitude of 483 km (260 nmi) for the remainder of the mission—a period of nine months. During the spinning mode, the APS ΔV thrusters are fired for orbit makeup whenever the thrusters are aligned along the velocity vector. The APS attitude control functional requirement consists of three-axis attitude stabilization with couples to provide control about the pitch, yaw, and roll axes; and spin-up and despin about the minor axis (X-axis, POP). The three-axis attitude stabilization is required during both the quasi-inertial mode when antenna and systems installation occurs, and during the spinning mode when test operations occur. However, APS thrusting is not allowed during the orbital pass (once a day) for the microwave test (one out of 15 orbits/day). Propellant requirements for the test article design can be obtained from Table 2.2-15, which shows the relative amount of total impulse required for each major mission element. Based on a specific impulse of 2893 N-sec/kg for small thrust radiation-cooled thrust chambers, a total propellant weight of 10,910 kg (24,000 lb) is required for the test article containing a 75,000-kg frame.

Description

A 24-thruster configuration with propellants are grouped in four modules and located at four corners of the hexagonal shaped platform. This configuration

provides an APS that meets the mission and functional requirements. The module locations were selected to provide a minimum mass moment of inertia about the axis of rotation.

Table 2.2-15. Total Impulse Requirements

		N-sec
1.	Orbit makeup	6.556×10^6
2.	Attitude stabilization (quasi-inertial)	6.357×10^6
3.	Spin-up/despin	3.359×10^6
4.	Attitude stabilization (spinning mode)	11.856×10^6
5.	Contingency	3.359×10^6
	Total	31.487×10^6

Figure 2.2-22 illustrates a typical APS module containing an oxidizer tank, a fuel tank, and helium pressurization tanks located within a structural shell that acts as a micrometeoroid shield and provides for thermal control. On one side of the APS module, an assembly of six thrusters is located, with a docking port on the opposite side for mating and attachment to the platform structure.

The assembly of six thrusters (per module) consists of two 142.3 N (32 lb_f) thrusters (±Z-axis), and four 22.2 N (5 lb_f) thrusters (±Z-axis, +X-, or -X axis, and +Y or -Y axis). In using four modules, thruster firings are accomplished in couples about each axis, and thruster redundancy is provided. For three-axis attitude stabilization, four ±Z-axis thrusters are fired for pitch (X-axis) and yaw (Y-axis) control; and two ±Y thrusters are fired for roll (Z-axis) control. Spin-up (and despin) is accomplished by firing four ±Z thrusters (142.3 N) for a burn time of 40.7 minutes to reach the 0.765°/sec spinning rate. Orbit makeup is done by firing two +Y and -Y thrusters, each once per orbit (14 times/day) for a burn time of 19.5-sec duration, each, during the quasi-inertial mode. However, during the spinning mode, orbit makeup is done in a similar fashion, except two firings per orbit of 9.7 seconds each for +Y thrusters (same for -Y thrusters after 180° rotation) are done to minimize cosine losses. The Y-thrusters are aligned within ±5 degrees of the spacecraft velocity vector for a duration of 13 seconds during the spinning mode. There are 24 opportunities per orbit to fire the ±Y-thrusters for orbit makeup (four opportunities are utilized with the 9.7-second burn durations). The baseline thrust levels were selected to provide reasonable timelines and good performance.

Storable propellants (N_2O_4/MMH) were selected for the APS to be compatible with the long-duration propellant storage for the nine-month mission and still provide reasonable performance. Bi-propellant APS thrusters are being qualified that provide a steady-state specific impulse of 2893 N-sec/kg (295 sec) in a radiation-cooled design at pulse durations in excess of 100 milliseconds. This performance value was used in sizing propellant quantities, since relatively long pulse durations are required. Total burn time required on the 22 N thrusters is an area for technology improvement.

A weight summary of the APS module for the test article vehicle is shown in Table 2.2-16.

Table 2.2-16. APS Module Weight Summary (75,000 kg Structure)

Weight per Module	kg	lb
Propellant	2728	6000
Inert	992	2182
Total	3720	8182
Total Weight (4 modules)		
Propellant	10,912	24,000
Inert	3,968	8,728
Total	14,880	32,728

APS weight data for test articles with a frame mass greater than 75,000 kg are delineated in Figure 2.2-22. APS weights are based on total vehicle mass properties.

APS Thrust Transients

A typical thrust transient for low-thrust APS thrusters is shown in Figure 2.2-23 and is provided for use in structural dynamics analysis. The data are based on test firing a low-thrust bi-propellant thruster with relatively slow-acting valves which are appropriate for this application. These curves are applicable to the range of thrust values and burn times used herein.

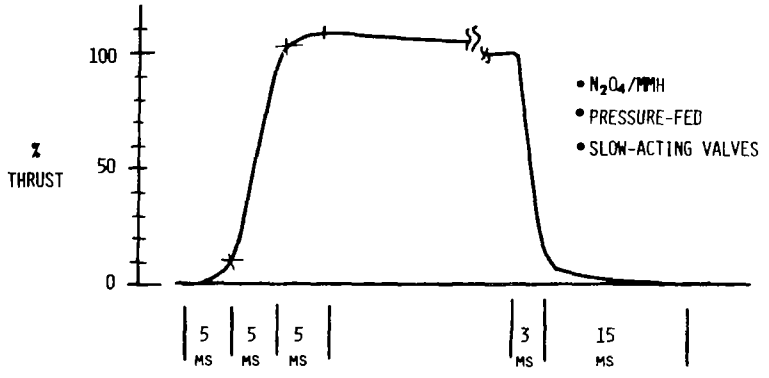

Figure 2.2-23. Typical APS Thrust Transient

2.2.6 STRUCTURES

This section describes the structural analysis performed in support of the definition of SPS Test Article I, evaluation of the resulting structural system credibility, and for establishment of the significant structural requirements delineated in Section 2.1.5.

Test Article Structure Description

The basic structural configuration is illustrated in Figure 2.2-24. A hexagonal frame structure, defined by the side dimension length of 1224 m (4651 ft), is provided to support the primary configuration of tension cables shown. The pairs of Cables "A" and "B" support the 1795 m by 5 m Mills Cross configuration of 5 m by 5 m antenna subarrays. The basic "closed-forced system" of limit tension loads in these cables is shown in Table 2.2-17. These tension loads induce a limit axial compression in the frame of 63.4 kN (14,250 lb).

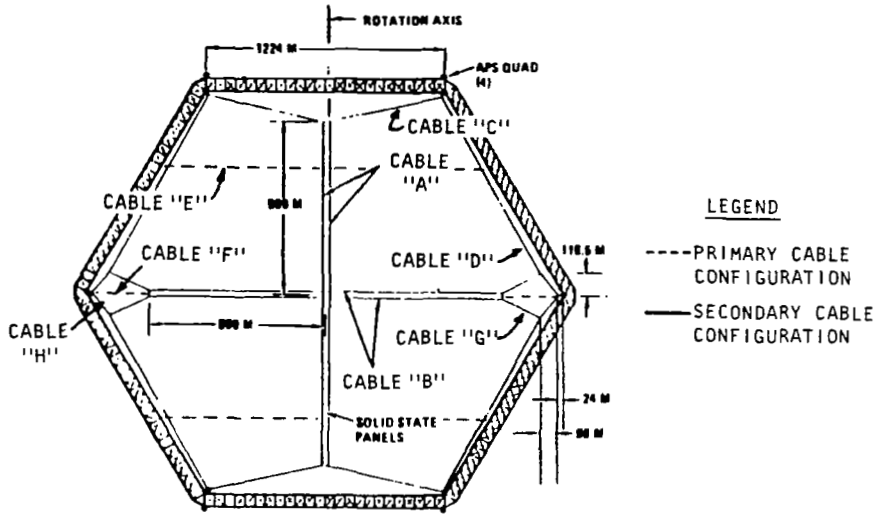

Figure 2.2-24. Test Article I Structural Configuration

Table 2.2-17. Primary Cable Configuration Limit Tension Loads

Cable	Limit Tension (kN)
A	12.7
B	8.4
C	56.3
D	48.0
G	9.7
H	48.9

The secondary array of tension cables are provided to reduce (to relatively small values) the in-plane bending moments resulting from the test article spin rate of 0.765°/sec. The resulting secondary tension cable and basic frame loads are shown in Table 2.2-18 for a 75,000 kg frame. Figure 2.2-25 illustrates the loads sign convention and structure model. Appropriate constant tension devices (negators or equivalent) are used to maintain the foregoing primary cable configuration loads.

Table 2.2-18. Frame and Secondary Cable Configuration Centripetal Loads

LOCATION	AXIAL LOAD, A (N)	SHEAR, V (N)	BENDING MOMENT, M (N m)	COMMENTS
1	1282	0	39,300	TENSION IN CABLE E = 920 N
2	204	-356	39,300	
3	-13	-173	-40,540	TENSION IN CABLE F = 1610 N
4	-142	-307	407	
5	-134	-236	-52,980	
6	-307	-534	62,380	

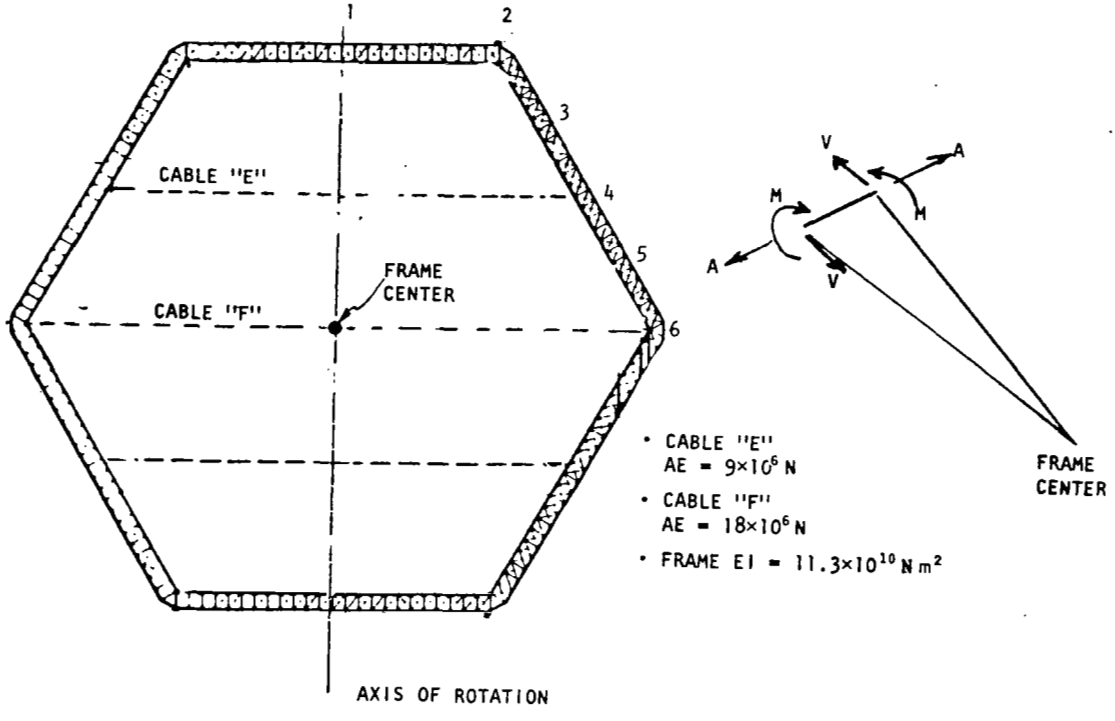

Figure 2.2-25. Centripetal Loads Model

The pairs of primary cables that extend to the six corners of the hexagonal frame are attached to the frame by radially directed support devices. The nature of these devices is dependent on the particular construction, and must have out-of-plane adjustment capability compatible with the dimensional stability requirements defined earlier in Section 2.1.5. NASA androgynous docking ports are provided for the four APS pods and eight orbiter docking stations (Drawing 42635-18031) with provision of attachment of miscellaneous equipment to be in accordance with the requirements stated in Section 2.1.5. Finally, the structural configuration has the four minimum modal frequency values and mode shapes shown in Figure 2.2-26. These data are based on the

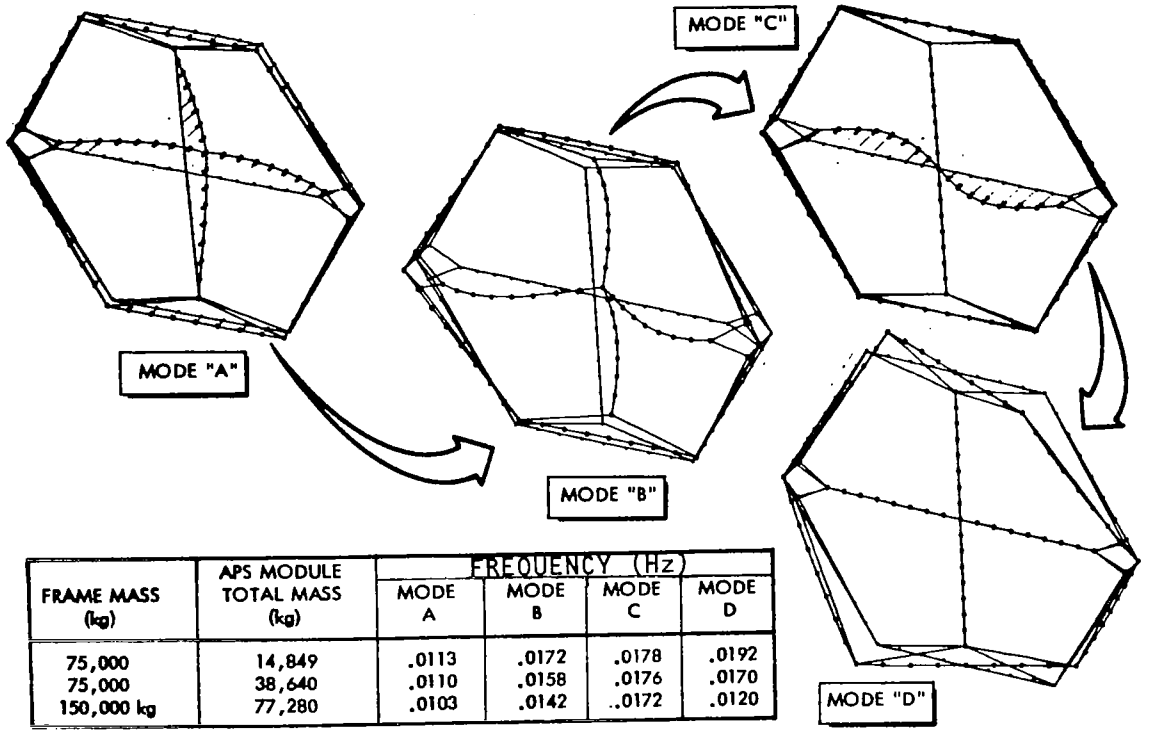

FRAME MASS (kg)	APS MODULE TOTAL MASS (kg)	FREQUENCY (Hz) MODE A	MODE B	MODE C	MODE D
75,000	14,849	.0113	.0172	.0178	.0192
75,000	38,640	.0110	.0158	.0176	.0170
150,000 kg	77,280	.0103	.0142	..0172	.0120

Figure 2.2-26. Modal Frequencies Mass Sensitivity

primary tension cable loads (Table 2.2-17) and the mass distribution of Table 2.1-6 for a tri-beam frame with the structural characteristics shown below:

- Frame depth: 68 m
- AE = 1.5×10^{8} N
- EI = 11.3×10^{10} N m^2
- GJ = 3.0×10^{10} N m^2
- KAG = 0.83×10^{8}N

Structure Concept Development

The foregoing concept was derived from the following two considerations:

- A recommendation to demonstrate by 1990 the feasibility of the space construction of a large SPS structure and proof of the solid-state electronics concept.

- In view of the large investment, reuse of the demonstration structure in the future solid-state configuration shown in Figure 2.2-27.

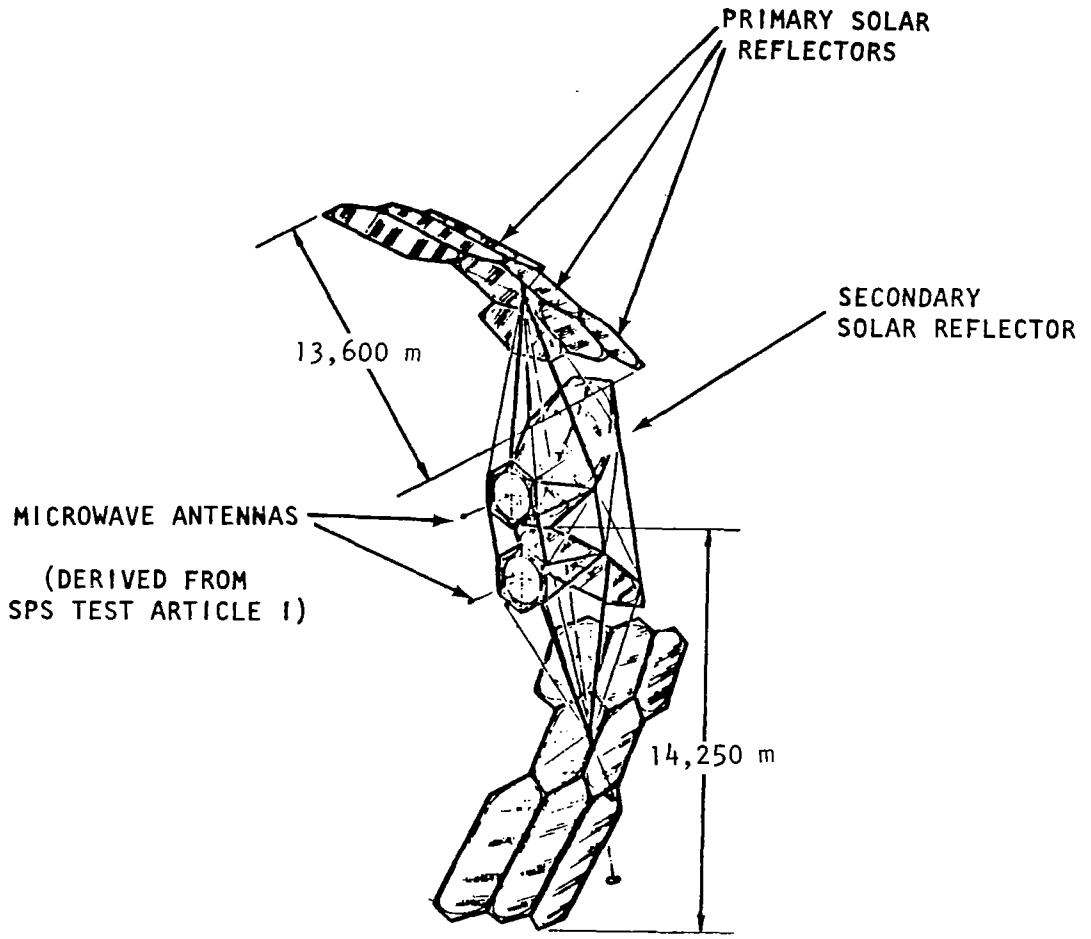

Figure 2.2-27. Current Solid-State SPS Configuration

The hexagonal frame configuration shown in Figure 2.2-24, therefore, was determined from structural analysis of the future prototype SPS solid-state application requirements. The primary tension cable arrangement was configured to support the largest size Mills Cross antenna, i.e., 1795 m, such that only axial compression loads were imposed in the frame. Since this is a test article, the primary tension cable loads (Table 2.2-17) were limited so that the resulting axial compression in the frame is no more than 75% of the future prototype limit load, resulting in an ultimate safety factor of 2.0. The highest possible primary tension cable loads were used to provide the highest possible structure modal frequency and minimum departures from flatness.

The centripetal loads acting on the frame, resulting from the 0.765°/sec spin rate necessary to perform the electronic test, resulted in the placement of the secondary cable system. The secondary tension cable system reduced the maximum in-plane lateral bending moments such that additional cap loads are small compared to that from the basic axial compression loads. Use of the secondary cable system also reduced frame in-plane shears. To maintain the foregoing prescribed closed-force system of loads between the frame and primary tension cable system, constant tension devices are required.

Selection of the four APS pods' sizes and location of docking ports were discussed in Section 2.1.4.

The following paragraphs describe the establishment of the prototype design and the structural investigation to determine the suitability of this configuration to satisfy the flatness and control compatibility requirements.

SPS Future Prototype Design Analysis

The SPS future prototype analysis is based on the use of two 1700 m aperture diameter antennas as shown previously in the solid-state configuration of Figure 2.2-27 and in Figure 2.2-28 below.

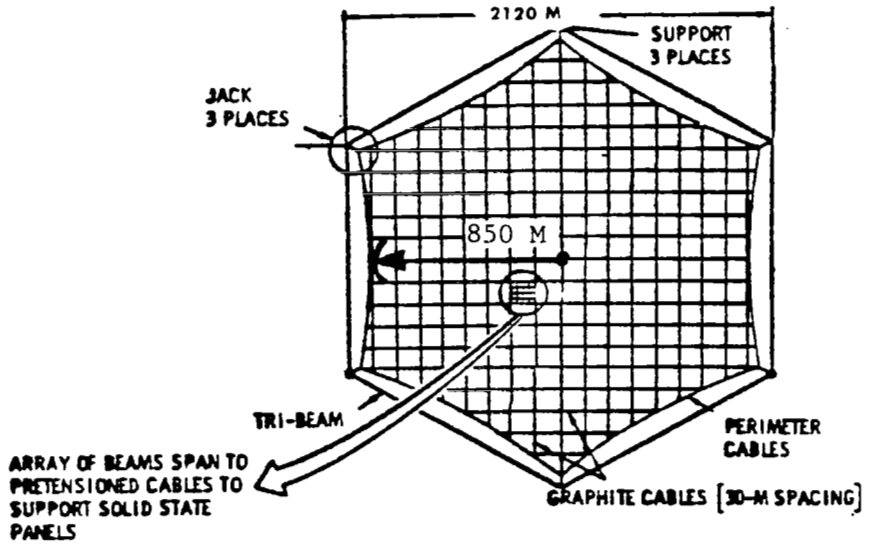

Figure 2.2-28. Microwave Antenna Structure Concept

In this concept, solid-state amplifiers structurally integral with the solar cell array and referred to as a *solid-state sandwich design* are attractive because they minimize the power distribution system. The microwave surface is directed toward earth with the solar cells mounted on the back face and illuminated by a system of primary and secondary reflector surfaces as shown. An orthogonal array of cables, tension-stabilized by the peripheral compression-carrying frame, provides a primary structural support system with no encroachment on either surface. The detailed structural analysis study of the prototype design, performed by

Rockwell for the Satellite Power System (SPS) Concept Definition Study, is presented in Appendix B. The electronics studies also conducted within that contract have established the microwave surface flatness requirements to be maintained within 21 cm. Figure 2.2-29 illustrates the frame weight versus surface deviation data derived by application of the design methodology of Appendix B to the configuration shown in Figure 2.2-27.

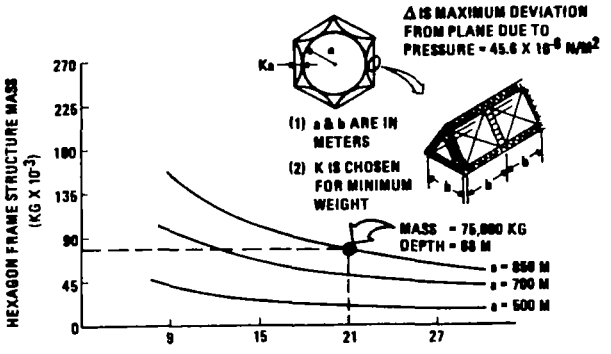

Figure 2.2-29. Frame Mass Vs. Solid-State Permissible Surface Deviation (cm)

The method of analysis discussed in Appendix B (for an example tri-beam) provides the design described in Figure 2.2-30. From this detailed analysis, the total frame weight is 81,500 kg, or 8-1/2% more than the quoted 75,000 kg, but does not affect the results of this study. (The propellant calculations were 11% conservative per Section 2.2.4.) The design requirements used were a = 850 m, Δ = 21 cm, W = 45.0×10^{-6} N/m^2. From the previous optimization analysis, K = 0.20. The only modification (which is minor) to the appendix analysis model was the increase in the allowance for the total of cable attachment length at the frame corners, and the frame inner edge to frame center dimension. The increase was from 0.015 a to 0.07 a, and effects a 3.5% increase in frame weight. From these data, the structural characteristics shown previously were derived.

Other constructions such as a pentahedral truss (essentially a statically determinate structure) comprised of either dixie-cup struts and unions or designs using the machine-made beams developed by Grumman, McDonnell-Douglas, or General Dynamics will have different mass, EI, and GJ characteristics based on the results of construction versus weight tradeoffs such as that shown in Appendix B (Figure B-11). These comments are pertinent to the modal frequency analysis subsequently discussed herein.

Analysis for Test Article I Requirements

The significant structural requirements established by Test Article I are:

(1) To provide sufficient tension in primary tension cables "A" and "B" to maintain the surface flatness of the Cross antenna array to the values shown in Figure 2.2-31 during the test maneuvers. Implied in this requirement is the separation frequency between the spin induced disturbances and the control system bandwidth, and structure frequency.

(2) To sustain, without detrimental deformation, the combination of centripetal induced and basic "closed forced system" pretension loads. Gravity-gradient and drag loads are negligible by comparison.

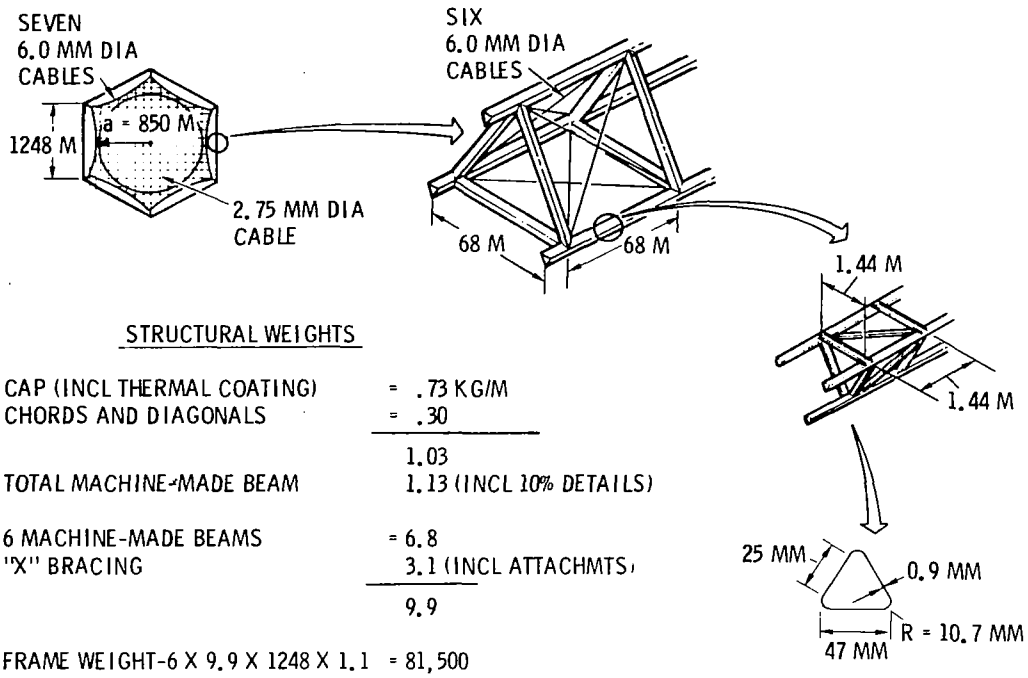

STRUCTURAL WEIGHTS

CAP (INCL THERMAL COATING)	= .73 KG/M
CHORDS AND DIAGONALS	= .30
	1.03
TOTAL MACHINE-MADE BEAM	1.13 (INCL 10% DETAILS)
6 MACHINE-MADE BEAMS	= 6.8
"X" BRACING	3.1 (INCL ATTACHMTS)
	9.9

FRAME WEIGHT-6 X 9.9 X 1248 X 1.1 = 81,500

DESIGN FOR DEVIATION = 21 CM

STRESS VERIFICATION -

- LOADS

$$N = \frac{Wa^2}{4\Delta} = 45 \text{ N/M (LIMIT)}$$

30 x 30 M CABLE TENSION = 1.35 KN
LIMIT STRESS FOR 2.75 MM DIA CABLE = 222 MPa

$$H = \frac{Na(1+k)^2}{6k} = 46 \text{ KN (LIMIT)}$$

$$C = H + Na = 84 \text{ KN (LIMIT)} \qquad C_{ULT} = 1.5 \times C = 126 \text{ KN}$$

$$T_{max} = \left|(46)^2 + (26.5)^2\right|^{1/2} = 53 \text{ KN}$$

LIMIT STRESS FOR 6.0 MM CABLES = 271 MPa

- COMPRESSION STABILITY

$$\text{Cap } \sigma_e = \frac{\pi^2 E_L \rho^2}{C^2} = \frac{\pi^2 \times 13.8 \times 10^4 \times (.015)^2}{(1.44)^2} = 148 \text{ MPa}$$

$$\sigma_{cc} = \frac{4\pi^2\sqrt{E_L E_T}\left(\frac{t}{d}\right)^2}{12(1-\nu^2)} = \frac{4\pi^2\sqrt{13.8 \times .85} \times 10^4 \times}{12(.95)}\left[\frac{.9}{25}\right]^2 = 154 \text{ MPa}$$

$$\text{COMBINED } \sigma_{all} \text{ (JOHNSON PARABOLA)} = 154\left[1 - \frac{154}{4 \times 148}\right] = \underline{114 \text{ MPa}}$$

$$\text{APPLIED ULTIMATE STRESS} = \frac{126}{9 \times .126} = \underline{111 \text{ MPa}}$$

$$\text{MACHINE-MADE BEAM COLUMN } \sigma_{all} = \frac{.95\pi^2 \times 13.8 \times 10^4 \times (0.59)^2}{(68)^2} \times 1.15 = 111 \text{ MPa}$$

$$\text{TRI-BEAM } \sigma_{all} = .95 \cdot \frac{.233\pi^2 \times 13.8 \times 10^4 \times (27.8)^2}{(1248)^2} = \underline{149 \text{ MPa}}$$

Figure 2.2-30. Hexagonal Frame Illustrative Data (Design for Deviation = 21 cm)

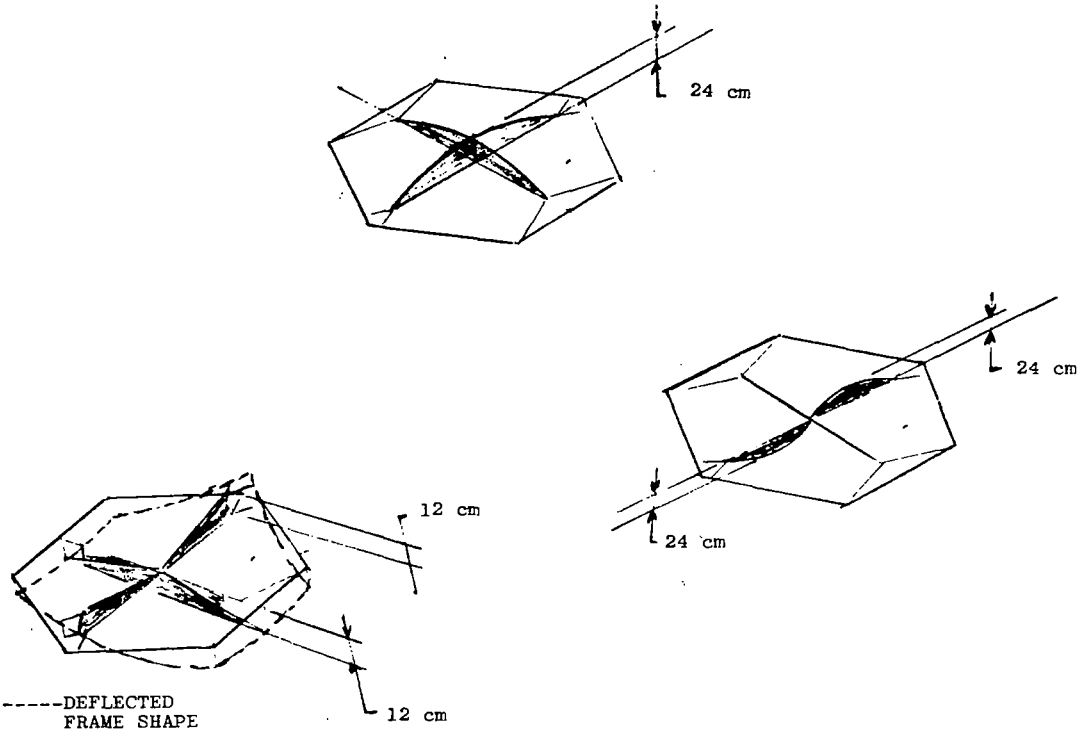

Figure 2.2-31. Permissible Mills Cross Antenna Deviations

Maintenance of Surface Flatness

The antenna surface flatness can be perturbed by drag, APS thruster firings for attitude and pitch rate adjustments, and frame thermal gradient induced relative deflections of the frame corners. Gravity gradients alone will cause no deflection of the cables, since, unique to this structure (because it is planar) the gravity-gradient loads produce only rigid body accelerations.

The issue of frequency separation is addressed herein (and in Section 2.2.4). The spinning rate of 0.765°/sec results in gravity-gradient and drag disturbances with frequencies of 0.00425 and 0.00212 Hz (Figure 2.2-32). The first and third modal frequency values shown (Figure 2.2-26) were obtained from NASTRAN analysis using the NASTRAN (McNeal Schwendler version) with the model shown in Figure 2.2-33. For simplicity, the model represents the 5 m panel and pairs of cables as a single cable with the appropriate distributed mass. The frequency associated with differential motion between the cables will be higher than the third mode and is not critical. Within this context, the 5-m-wide panels can be supported on cables spaced 10 m apart with only a negligible structure weight addition, if necessary. The essence of the foregoing is that the minimum frequency separation between the highest disturbance frequency and the lowest mode is 0.011/0.00425 = 2.59, and the minimum frequency separation between the disturbance and modes that could be excited is 0.0178/0.00425 = 4.1, and 0.011/0.00212 = 5.1. A perspective on the significance of these low levels of frequency separation is perceived only through a static evaluation of the magnitude of these disturbances.

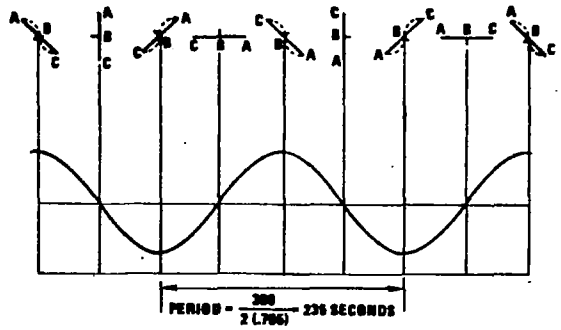

Frequency = 0.00425 Hz

GRAVITY GRADIENT DISTURBANCES

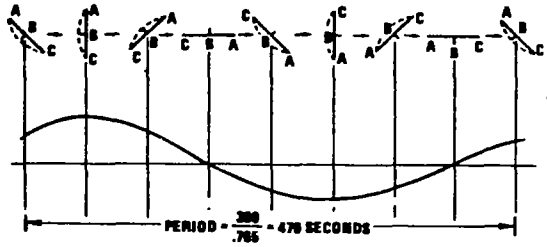

Frequency = 0.00212 Hz

DRAG DISTURBANCE

Figure 2.2-32. Spin Induced Disturbances

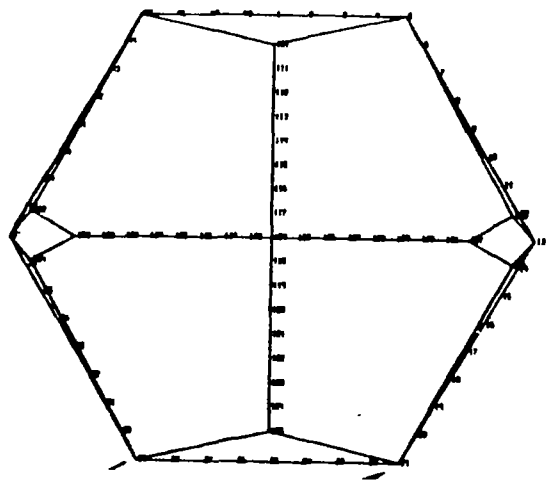

Figure 2.2-33. NASTRAN Model of Frame and Antenna

The static deflection due to drag is conservatively estimated as follows:

- For the 260.79 nmi orbit, 1990 time period, the nominal value of atmospheric density is 2.2×10^{-15} slug/ft^3
- Using $P_D = 1/2\ C_D\rho V^2$ where $C_D \cong 1$, V = 7595 m/sec
  Then, $P_D = 32.7\times10^{-6}$ N/m^2 (6.8×10^{-7} lb/ft^2)
- The uniform load applied to tension cable "B" is
  32.7×10^{-6} (2.5) = 0.82×10^{-4} N/m (5.6×10^{-6} lb/ft)
- The maximum differential deflection $\Delta \cong \dfrac{0.82\times10^{-4}\ 900^2}{2\times8400}$

  $\cong$ 0.004 m = 0.4 cm (nominal)
- The maximum differential deflection for a 2σ environment will be 4.2×0.4 = 1.7 cm

The maximum deflection due to firing of the APS thrusters for pitch rate or attitude corrections was determined from a transient analysis developed from the modal analyses. The APS firing used the 22.2 N (5 lb) thrusters inducing a torque about the spin axis. The APS pod thrust versus time data shown were used. The maximum differential deflection obtained from the data in Figure 2.2-34 is 6.1 cm. These values are clearly well below the surface flatness requirements of 24 cm and within the capability of the control system design discussed in Section 2.2.4.

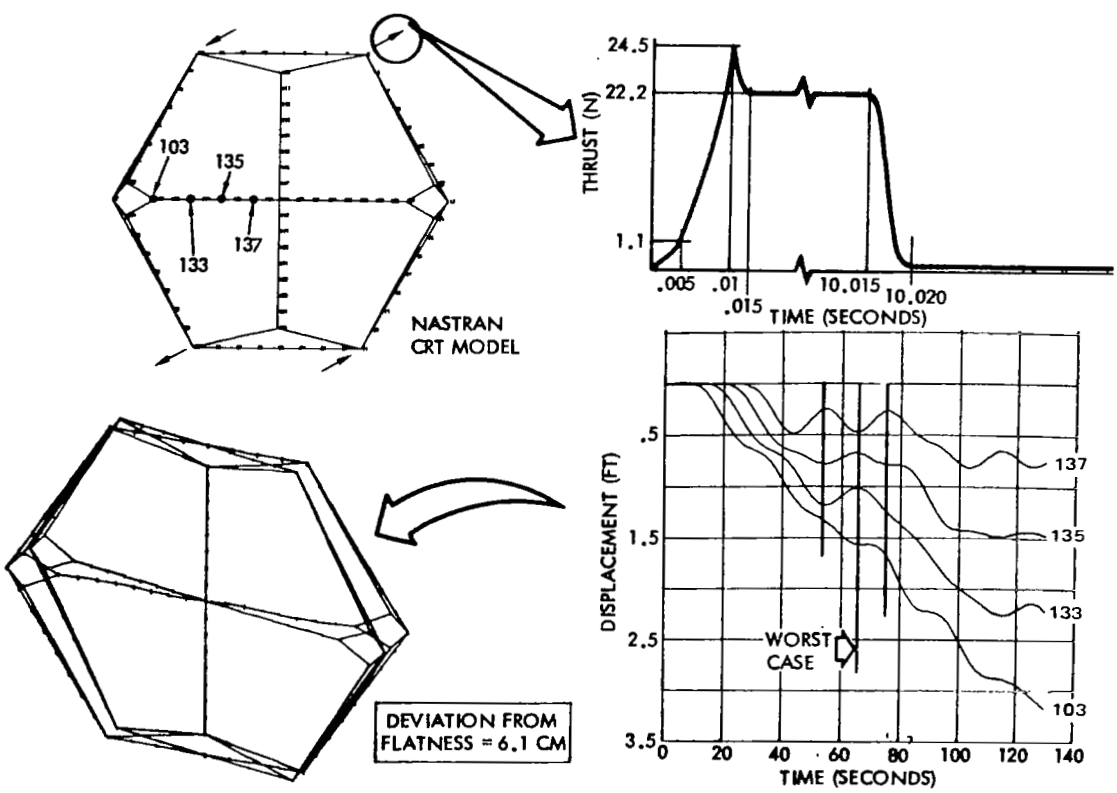

Figure 2.2-34. Transient Analysis Results—ACSS Maneuvers

Recognizing the likely variation of frame weight with construction variation, particularly if a construction desirable frame depth restriction is imposed, modal analyses were performed for frames and APS pods of increased mass (Figure 2.2-26). The antenna cross, tension cable systems, and miscellaneous equipment were maintained the same. Of primary importance, the frame EI and GJ characteristics were maintained. The data verify the relative insensitivity of the pertinent lowest modal values to the frame and APS masses. The pertinent modal values are primarily dependent on the primary tension cable system and not the frame structural behavior. For this reason, a minimum modal frequency requirement is not specified in Section 2.1.5, but rather satisfaction of the specified overall strength and stability requirements will result in a frame design with EI and GJ characteristics that are compatible with the control system design and flatness restrictions.

Centripetal Loads

The centripetal loads resulting from the test maneuver spin rate of 0.765°/sec were shown in Table 2.2-18. The frame bending moments are proportional to frame mass, providing the frame in-plane EI and cable AE values quoted are maintained. Analysis of the loads without cable "E" illustrated the desirability of including this cable despite the additional requirement of cable erection and attachment. These cables should be installed with negligible pretension loads (10 to 20 N). It is also pertinent to note the use of constant tension devices in the primary tension cable configuration will ensure maintenance of the pre-spin "closed forced system loading."

Overall Frame Stability Criteria

As stated previously, the structural characteristics of EI, GJ, and AE presented were determined by the analysis method described in Appendix B, particularly the data of Figure B-11 (ϕ vs. GJ/EI) for the model with cables. In the interest of analysis consistency among the future follow-on study contractors, it is recommended to NASA that these data be used as the basis of the overall frame stability analysis. Selection of the most suitable GJ/EI and resulting ϕ will be dependent on the particular design's mass versus construction characteristics.

Earth Orbit Modal Frequency Concern

Finally, of concern to the construction operation, is the modal frequency of the frame during construction in the free-drift mode. Figure 2.2-35 illustrates the minimum modal frequency of the hexagonal frame in its weakest configuration (just prior to frame closure), which is five times the frequency of earth orbit gravity-gradient disturbances (0.0035 Hz), and feasible particularly since there is no target acquisition.

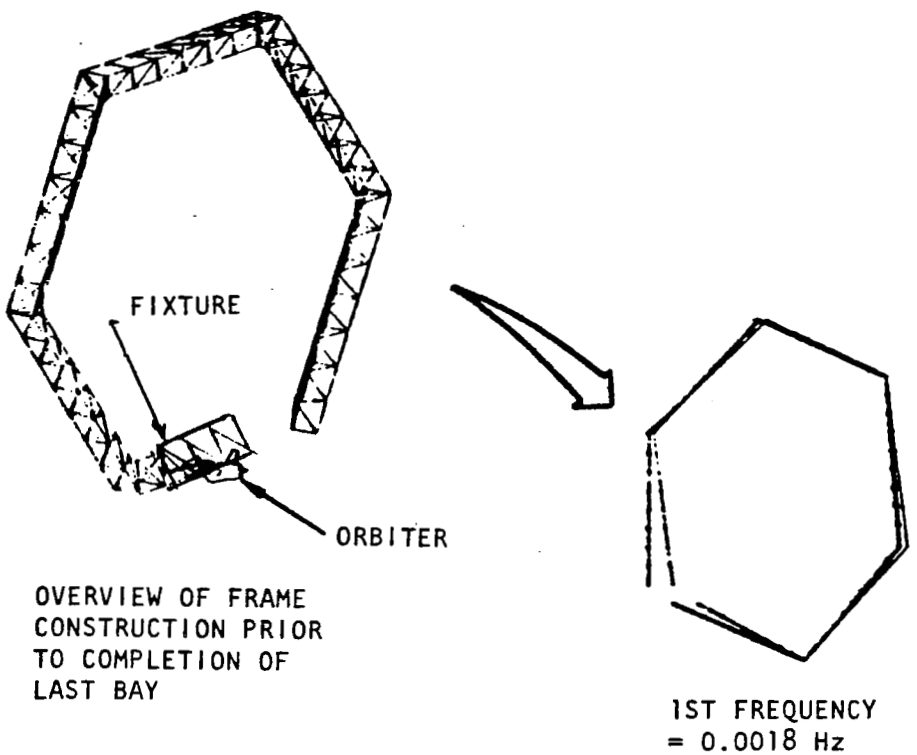

Figure 2.2-35. Construction Phase Minimum Modal Frequency

3.0 SPS TEST ARTICLE II

This section describes the SPS Test Article II mission, mission equipment and subsystems equipment pertinent to the design of this test articles major structure, the solar blanket support structure. The structures overall strength, stability, stiffness, dimensional stability and local equipment and utilities accommodation requirements are described in Section 3.1.5. A brief summary of Section 3.1.5 is included for convenience, in Section 3.1.3.

The test article shown in Figure 3.0-1, was derived from the requirements to accommodate:

1. A solar blanket area of 400 m^2, required to provide power for the microwave antenna to accomplish the test objectives stated in Section 3.1.1.

2. Construction from an orbiter-mounted fixture, where installation of the solar blankets utilizes the RMS with its reach limitations directing the structure width to essentially 20 m and a blanket length of 200 m.

3. Finally, satisfaction of the strength and stability, and minimum modal frequency requirements (see Section 3.2.6) was possible with a structure minimizing space construction complexity.

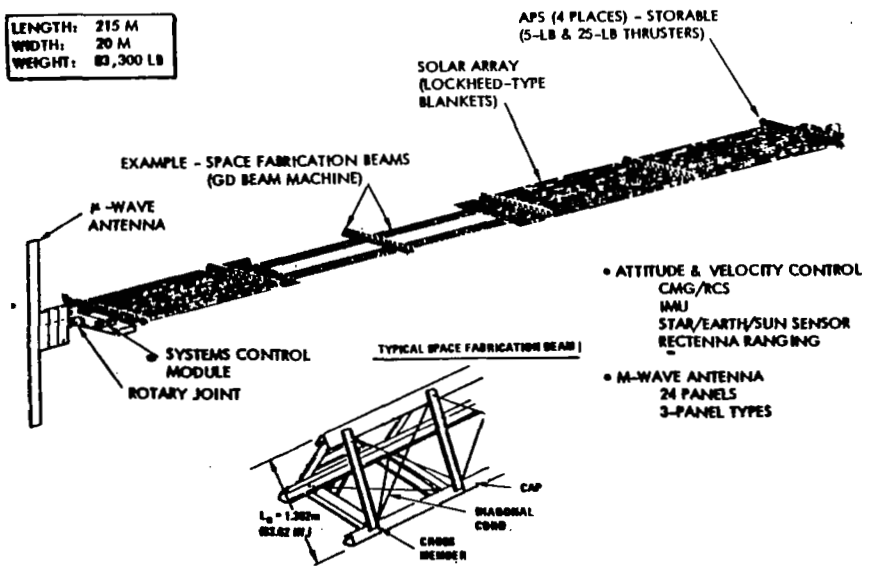

Figure 3.0-1. General Configuration—SPS Test Article II

3.1 SYSTEM DEFINITION

3.1.1 MISSION OBJECTIVES AND DESCRIPTION

Test Objectives

The SPS Test Article II test objectives are as follows:

- Simulation of heat rejection in the high thermal flux environment of the beam-forming electronics at the center of the antenna
- Verification of the retro-directive phase control concept for beam formation and beam focus/containment
- High-voltage photovoltaic power generation
- System construction tests
- Evaluation and behavior of lightweight space structures

Mission Scenario

The SPS Test Article II mission scenario is illustrated in Figure 3.1-1; the highlights of each phase are discussed below.

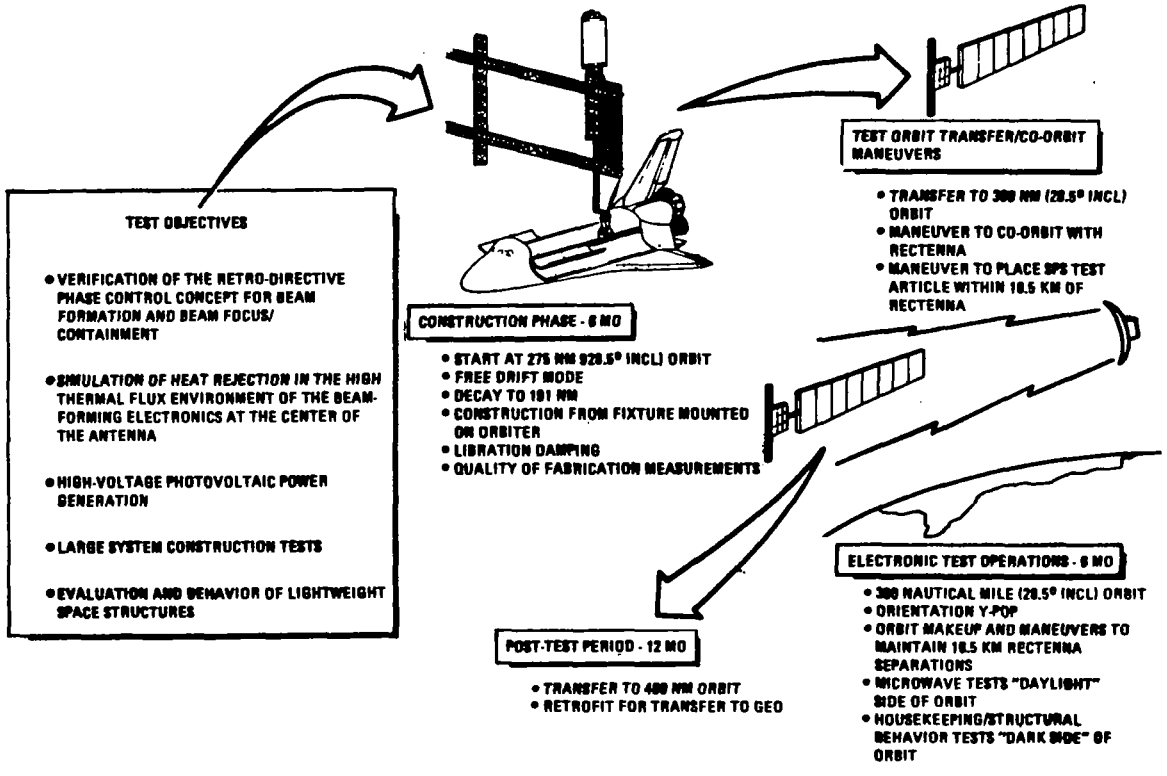

Figure 3.1-1. SPS Test Article II Mission Scenario

Construction Phase (6 months)

Construction starts at an altitude of 509 km (275 nmi) in a free drift mode. Figure 3.1-2 illustrates the orbit decay of the candidate start of construction orbits. The altitude drop for each step in the construction sequence was determined from decay rate data. The final altitude for each step was used as the initial altitude for the next step. Each step or segment of the overall construction sequence was assumed to be comprised of two basic parts. The first is a seven-day interval with the orbiter attached in which the actual construction operations are performed, the second part is a 23-day interval representing the coast time between Shuttle revisits where the drag configuration does not include the orbiter. Thus, an overall construction process involving Shuttle launches on 30-day centers was assumed.

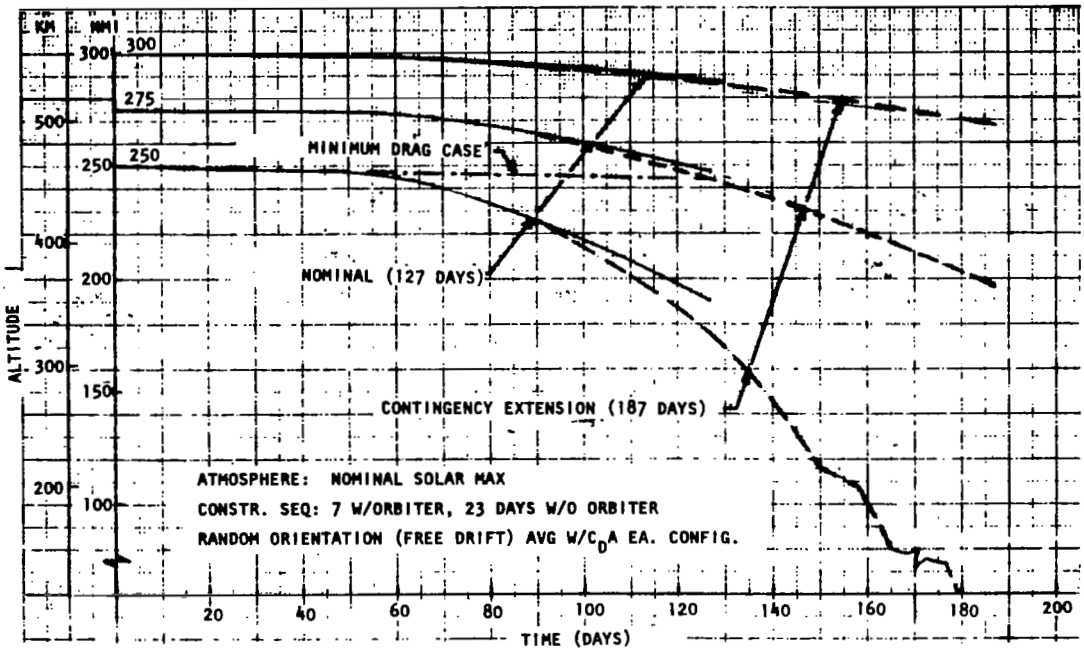

Figure 3.1-2. Orbit Decay During SPS Test Vehicle Construction

The data shows that the orbital altitude, at the end of 6 months, is 191 nmi.

Test Orbit Transfer and Co-Orbit Maneuvers

The mission profile calls for the orbital delivery of a rectenna vehicle following construction and checkout of SPS Test Article II. The rectenna is the receiving element of the space-to-space microwave beam performance test and is a separate flight vehicle. Definition of this important element is outside the scope of the SPS Test Article II definition reported herein.

Once the rectenna vehicle is suitably placed in the test orbit, SPS Test Article II would be maneuvered to the same orbit with the appropriate standoff

distance. An "orbit adjustment" phase is included which is comprised of a series of small correction maneuvers to achieve the proper "co-orbital" accuracies between the two vehicles. These correction maneuvers are provided by the SPS test vehicle rather than the rectenna system.

- The stationkeeping maneuvers were also assumed to be performed by SPS Test Article II. These maneuvers are needed to maintain the 16.5 km (8.9 nmi) separation distance between the SPS test vehicle and the rectenna. This separation distance is bounded by beam spreading/loss of side lobe capture on the high side, and near field effects on the low side. A stationkeeping "deadband" of ±1 km was assumed. This could require maneuvers as frequent as three or four times per day, depending upon the drag/weight differences between the two vehicles.

In addition to stationkeeping, the first mode for the microwave tests requires precision pointing of the antenna toward the rectenna receiving system. Further, the solar array area must be sun oriented. Thus, a rotary joint is provided between the antenna and the solar array to provide their respective viewing requirements.

Electronic Test Operations (6 months)

An orbit altitude of 555 km (300 nmi) was selected for the microwave tests. This was deemed the lowest feasible altitude consistent with the large area, low W/C_DA characteristics of the configuration. A higher orbit may prove to be required, but the lowest practical orbit was selected here in recognition of the payload performance/transportation costs associated with higher orbits.

A six-month mission duration was estimated to be adequate for the performance of the planned microwave tests. This provides over 2700 orbit revolutions with nearly four full cycles of sun/orbit geometries. As a preliminary estimate, these multiple cycles of the space orbital environment should be adequate to meet the various test objectives including the microwave performance assessments, electrical power generation tests and measurements of structural behavioral/response to both thermal cycling and thruster pulses.

Post-Test Period (12 months)

A higher, 740 km (400 nmi), orbit is also shown after the microwave test mission is completed. This was introduced in recognition of the potential value of long duration ($\geq$1 yr) advanced technology experimentation which could be conducted in the post microwave test phase. Experiments during this extended period could include solar electric propulsion, remote servicing, and many others. Following this period, the system could then be transferred to a lower, more Shuttle-accessible orbit for re-outfitting to a new mission configuration.

3.1.2 MISSION EQUIPMENT REQUIREMENTS SUMMARY

Mission equipments are defined to be those systems/subsystems that are located on a satellite solely to satisfy the mission experimental objectives. Equipments installed to fully (or even partially) support the basic satellite

operations are not included. In the case of this Test Article, the microwave subsystem discussed in Section 3.2.1 is considered the single relevant subsystem.

The SPS test article II antenna, as shown in Figure 3.1-3 consists of two contiguous but independent parts. The thermal test portion is comprised of 9 subarrays, each 2.92 m × 2.92 m and made up of 33 waveguides each having 33 radiating slots. The central subarray radiates 121 kW, provided by 2450 MHz klystron tubes mounted on its rear surface (Figure 3.1-4). Each klystron has a nominal rating of 1 kW RF output and 121 such tubes are arrayed in the form of an 11×11 matrix. It is emphasized that this slotted waveguide subarray could equally well be excited by four 50 kW tubes in a 2×2 matrix without requiring any major changes. The central subarray is surrounded by 8 identical 2.92 m × 2.92 m subarrays, but these are each excited by 16 1-kW klystrons in a 4×4 matrix. Total RF power input to the 9 element array is therefore 16×8+121 = 249 kW.

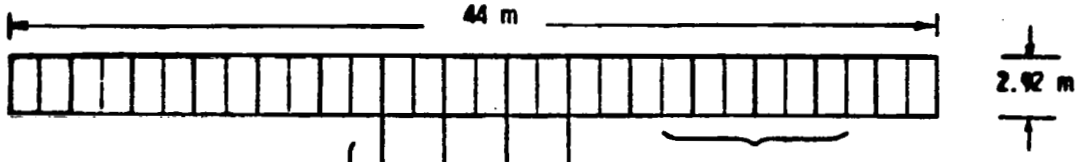

THERMAL TEST ARRAY

- 9 SUB-ARRAYS, EACH 2.92 x 2.92 m. WITH 33 x 33 SLOTS.
- 8 OUTER SUB-ARRAYS HAVE 16 KLYSTRONS EACH 1 kW OUTPUT
- CENTRAL SUB-ARRAY HAS 121 ONE kW TUBES
- TOTAL RF POWER 16 x 8 + 121 = 249 kW

PHASE CONTROL TEST ARRAY

- 30 ELEMENTS EA. 2.92 x 1.46 m.
- EACH ELEMENT = ONE HALF OF BASIC 33 x 33 SLOT SUB-ARRAY HAVING EITHER 33 x 16 OR 33 x 17 SLOTS (ALTERNATING).
- SINGLE 1 kW KLYSTRON PER ELEMENT. TOTAL RADIATED RF POWER 30 kW.

- ALUMINUM WAVEGUIDE .05 cm (.020 in) WALL: TOTAL MASS 970 kg.

Figure 3.1-3. SPS Test Article II Antenna

Each klystron requires 1280 W of dc input power plus about 120 W for heater and focusing solenoid for a total of 1400 W. During thermal testing a total of 249 tubes will be in operation so that maximum dc power requirements are about 350 kW.

The phase control test portion is a linear array of 30 subarrays each 2.92 m × 1.46 m. It is 2.92 m wide and about 44 m long. Two of these 1.92 m × 1.46 m subarrays adjacent to each other make up a unit that is identical to one of the 33×33 slot subarrays used in the thermal test array. However, each

of these 2.92 m × 1.46 m subarrays is fed by only a single 1-kW klystron tube so that total RF power into the array is 30 kW. Each klystron, and therefore each of the 30 elements in the linear array, is subject to phase control for the purpose of beam formation and pointing control.

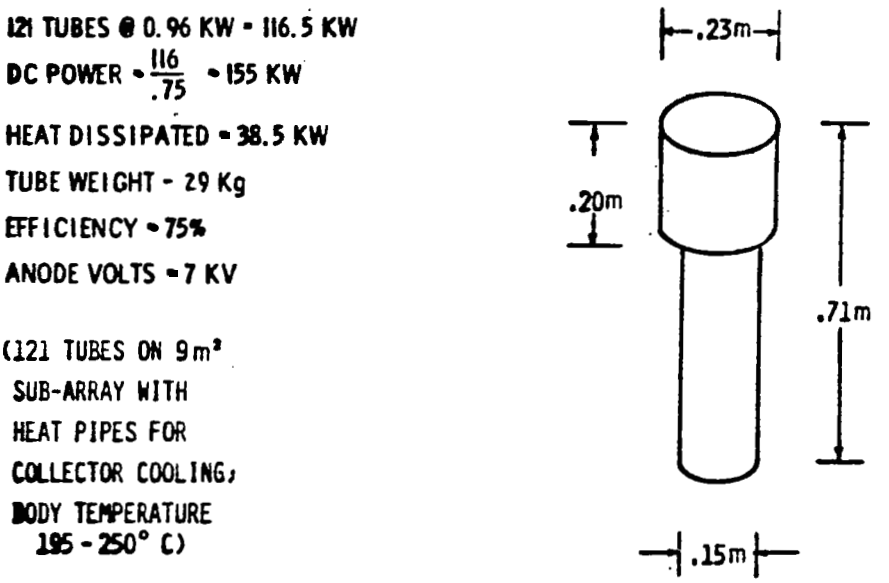

Figure 3.1-4. 1-kW Klystron Tube

Each subarray is an assemblage of slotted waveguide radiators each of which is of the standing wave, resonant slot type. The array is excited by one or more slot coupled transverse feeder guides placed on the back (i.e., non-radiating) side of the subarray. The arrangement is shown in Figure 3.1-5 wherein only a single transverse feeder guide is shown for simplicity.

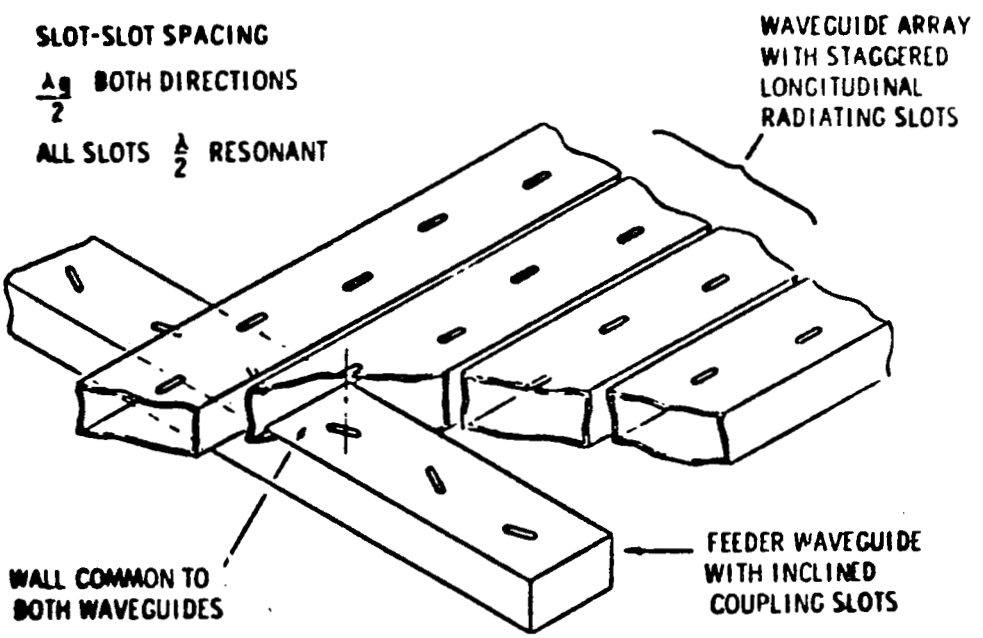

Figure 3.1-5. Transverse Feeder Guide for Slot Array

3.1.3 SUBSYSTEMS EQUIPMENT REQUIREMENTS SUMMARY

Described in this section are the power, data management and communications, stabilization and control, and auxiliary propulsion subsystems to be supported by the structure, and a summary of the structural requirements listed in Section 3.1.5.

Power Subsystem

Requirements

The requirements of power for the antenna, telemetry, tracking, and command are shown in Table 3.1-1.

Table 3.1-1. Electrical Power Generation, Distribution and Control Subsystem

Item	Characteristic
Power Generation	$4000m^2$ Solar Array
	130 Watts/m^2 End-of-Life Output
	High Efficiency Hybrid Solar Cell
	20 Year Life
Electrical Power Distribution	520 kW Power @ 200 Volts dc
	5% Regulation
	Transmission Efficiency = 94%
Energy Storage	Nickel-Hydrogen Batteries
	37 kW Hours
Rotary Joint	Slip Rings
	Transfer 488.8 kW @ 204.7V
Test Article	279 Klystrons
Microwave Antenna	dc-dc Converter/Klystron Interface
	334.05 kW @ 204V dc
Telemetry, Tracking & Command (TT&C)	5 kW @ 28 V dc and 200 V dc

The electrical power distribution system (EPDS) receives power from the power generation subsystem, and provides the regulation and switching required to deliver the power for distribution to the various satellite loads or to the storage batteries. The subsystem consists of main feeders, secondary feeders, tie bars, summing buses, regulators, voltage converters switch gear, remote power contactors, slip rings, brushes and subsystem cabling. Batteries and battery chargers are included for eclipse periods.

A weight summary of the Electrical Power Distribution System for the SPS Flight Test Article is shown in Table 3.1-2. Finally, Figure 3.1-6 indicates the location of the various EPDS equipments.

Table 3.1-2. SPS Flight Test Article II EPDS Weight Summary

Solar Array	4,091.1
EPS Wire Harness	1,503.1
Blanket Switch Box (25)	892.5
Electrical Power Distribution Panel (2)	962.4
Battery Systems	
Batteries	942.8
Chargers	103.2
Wire Harness & Control	88.3
Ion Propulsion EPD System	
Wire Harness	1,798.3
Propulsion Switch Boxes	584.4
Antenna System	1,472.5
Secondary Structure	1,243.9
	13,682.5 kg

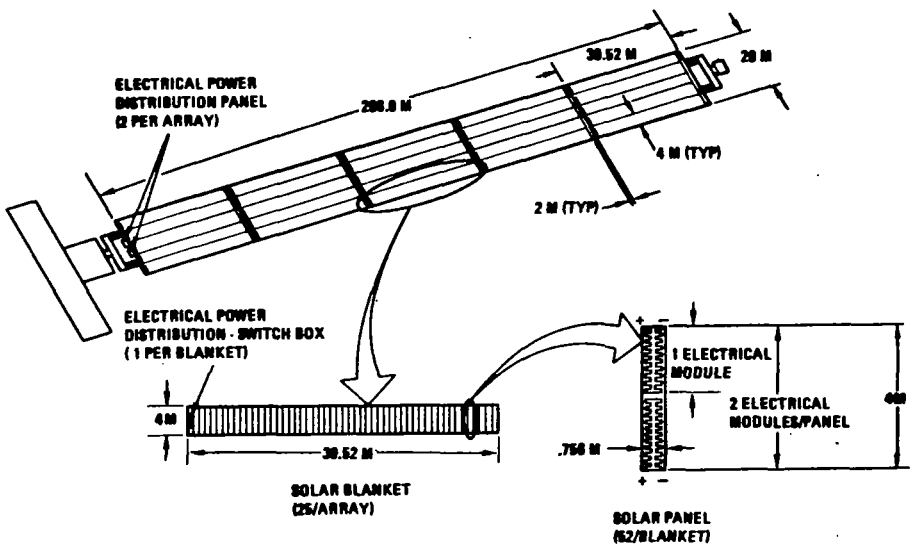

Figure 3.1-6. EPDS Equipment Locations

Data Management and Communications

Requirements

During low earth orbit or during geosynchronous orbit, the communications and tracking system of SPS Flight Test Article II requires S-band and Ku-band

links to provide, in addition to tracking, reception of commands at a maximum rate of 216 k bits/s. The system also requires a transmission capability for telemetry, television, and data at a maximum rate of 50 M bits/s. A simultaneous capability to communicate with the co-orbiting rectenna platform, the Space Shuttle Orbiter, GPS, or other spacecraft is required.

Equipment

S-Band Links

There are three S-band links: (1) PM to orbiter, STDN or SCF, (2) FM direct to ground, and (3) PM to TDRSS and there to TDRS on the ground. The return link on (1) is split into high (2250-2300 MHz) and low (2200-2250 MHz).

Ku-Band Links

The Ku-band subsystem for the SPS Flight Test Article operates as a two-way communications system with the ground through the Tracking and Data Relay Satellite System (TDRSS). The advantage of the Ku-band link is the large increase in data.

Table 3.1-3 provides a summary of the mass and power estimate for this test satellite.

Table 3.1-3. SPS Flight Test Article II
LRU Mass and Power Summary

LRU	Mass (kg)	Power (W)
S-Band		
PM transponder	15.8	63
PM processor	8.1	30
Doppler extractor	7.4	16
Power amplifier (100 W)	14.4	400
Preamplifier	11.6	25
FM transmitter	3.0	120
FM processor	5.2	9
Switch assembly	3.0	2
Ku-Band		
Electronic assembly Signal processor Deployed assembly	95.0	489
Total with wiring and antennas	200	1200
Data Management	500	~100
Instrumentation	300	

Stabilization and Control

Requirements

This system must control the vehicle's attitude, point the microwave antenna, control orbit transfer maneuvers, and regulates the vehicle velocity to maintain proper spacing with the co-orbiting rectenna. These requirements must be satisfied during orbit transfer to the 300-nmi operational orbit, six months of antenna testing, transfer from the operational orbit to a 400-nmi holding orbit, a prolonged period in storage, and transfer back down to the 250-nmi construction orbit.

Two attitude control requirements must be met. The solar array must be oriented toward the sun, and the bearing axis of the microwave antenna must be oriented so that the antenna can be accurately pointing toward the co-orbiting rectenna. These requirements are satisfied by aligning the long axis of the vehicle perpendicular to the orbit (Figure 3.1-7) and orienting the solar arrays toward the sun. The required accuracies are (1) roll, ±5°; (2) pitch, ±8°, and (3) yaw, ±3°; and (4) microwave antenna pointing control, 13 arc-min.

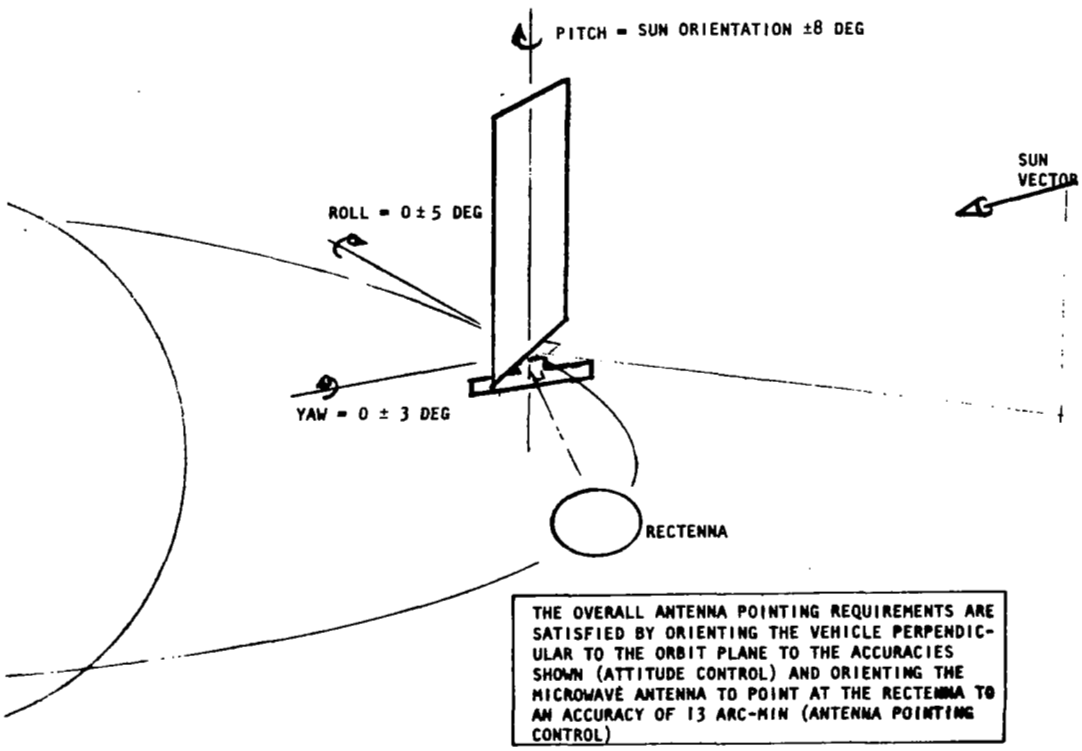

Figure 3.1-7. Attitude Control Requirements for the Microwave Transmission Experiment

Equipment

Details of the AVCS are presented in Figures 3.1-8 and 3.1-9. The control system consists of an attitude reference system and four CMG's in a conic configuration. The control moment gyros (CMG's) are single-degree-of-freedom

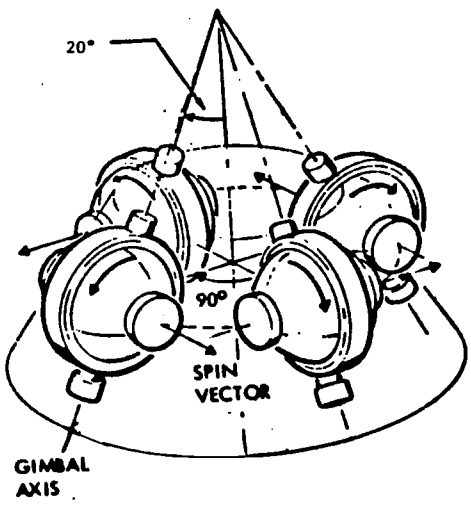

CHARACTERISTICS OF EACH CMG	
• CMG WEIGHT (BASE GIMBAL INCLUDED)	195 LB
• ANGULAR MOMENTUM	1600 FT-LB-SEC
• POWER REQUIREMENTS	
PEAK GYRO INPUT POWER	50 W
PEAK DURING RUN-UP	200 W
STEADY-STATE RUNNING	40 W @ 5300 RPM
• WHEEL OPERATING SPEED	7000 RPM
• SPIN BEARINGS BALL BEARINGS	204H DF PAIR
• TORQUER OUTPUT	15 FT-LB
CMG SIZE	40.1×27.0×30.5 IN.
• TOTAL WEIGHT (INCL. ELECTRONICS)	206 LB

Figure 3.1-8. CMG's for SPS Test Article Attitude Control

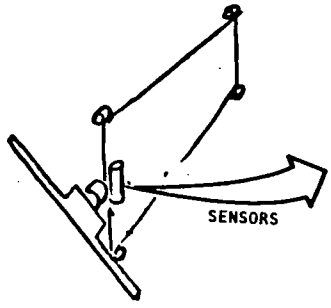

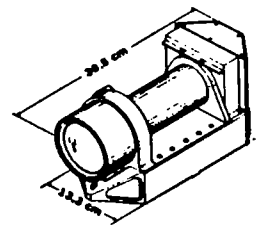

STAR SENSORS

TYPE	TRACKER
FOV	8×8 DEG
POWER	4 WATTS
ACCURACY	10 SEC (1σ)

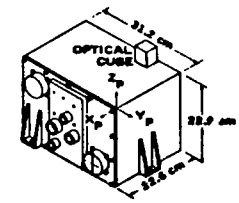

INERTIAL REFERENCE UNIT

POWER	7.5 W/CHANNEL
RANDOM DRIFT	0.015 DEG/HR (3σ)

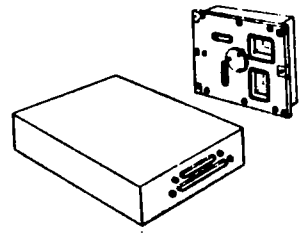

TWO-AXIS SUN SENSOR

FOV	±32 DEG
POWER	2.5 W
RESOL.	<15 SEC
STAB.	1 MIN

Figure 3.1-9. Sensors for SPS Test Article Attitude Control

devices, the characteristics of which are summarized in Figure 3.1-8. The precision attitude reference is comprised of the inertial reference unit (IRU) and star tracker.

Auxiliary Propulsion

Requirements

The translation functional requirements consist of (1) low altitude orbit transfer, (2) rendezvous with the rectenna, and (3) stationkeeping for six months. The APS attitude control functional requirements consist of periodic thrusting for momentum dumping of the control moment gyros (CMG) about the pitch, yaw anf roll axes. The initial orbit transfer maneuver must transport the platform from the construction orbit altitude up to operational test altitude (556 km or 300 nmi). After the microwave test, the platform must be transported to a holding orbit (741 km or 400 nmi) where it is parked until required; then later, the platform is returned to the construction altitude (463 km or 250 nmi) for re-outfitting, refurbishment, and resupply in preparation for a subsequent mission in GEO.

Equipment

The propulsion subsystem for the SPS test article consists of an auxiliary propulsion system (APS). The APS is provided for control of the SPS platform in low earth orbit (LEO) during a six month life, during which the microwave antenna is tested. The APS provides control for both translation maneuvers and for attitude orientation control in conjunction with AVCS (attitude and velocity control subsystem).

The APS is summarized in Table 3.1-4. The APS module is illustrated in Figure 3.1-10.

Table 3.1-4. APS Equipment

Propellants	N_2O_4/MMH
Pressurization Gas	Helium
Total Impulse	15.1 x 10^6 N-sec (3.4 x 10^6 lb-sec)
Number of Modules	4
Number of Thrusters	20
Thrust, Each	
12 Thrusters	111 N (25 Lbf)
8 Thrusters	22 N (5 Lbf)
Total Weight	7196 kg (15,830 lb)

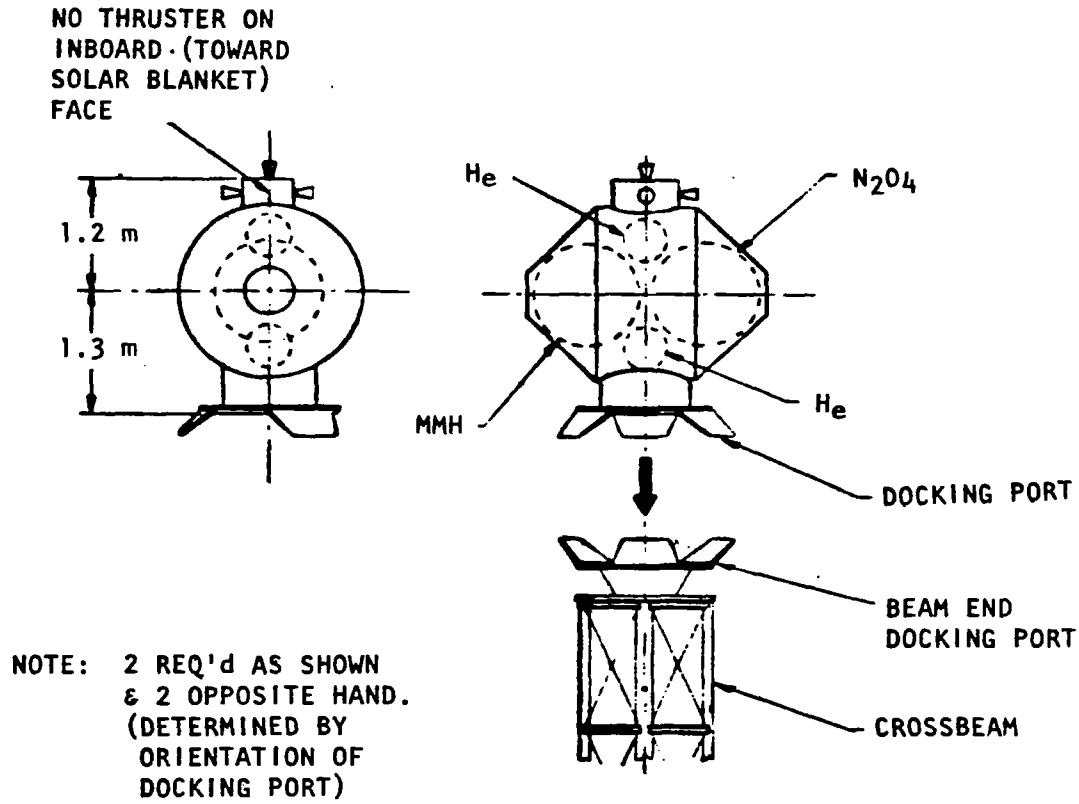

Figure 3.1-10. Auxiliary Propulsion System (APS) Module

Structural System Requirements Summary

The data listed below summarizes the solar blanket support structure major structural requirements that are listed in Section 3.1.5.

(1) The structure is the mounting platform for all the mission and subsystems equipment listed above and defined on drawings 42635-18030 and 18032.

(2) The structure must sustain the most severe combination of gravity gradient, thermal, and libration damping induced loads in conjunction with installation of blankets, power and data lines, J-boxes, and EPD boxes.

(3) The structure must sustain the loads induced with the RMS placement of the systems control module (5000 kg), bridge fitting (1500 kg), and each of 4 APS pods (1798 kg).

(4) The structure must maintain a minimum blanket tension of 17.5 N/m during opration.

(5) The structure must sustain the most severe combination of blanket induced compression in conjunction with gravity and thermal gradient induced loads, and the following separate APS loadings.

- Orbit transfer - four 111 N thrusters (in-plane, longitudinal)
- Stationkeeping - one 111 N thrusters (in-plane, lateral)
- Stationkeeping - two 22.2 N thrusters (transverse)
- Attitude control - four 22.2 N thrusters (pitch, roll)
- Attitude control - two 111 N thrusters (yaw)

(6) The minimum modal frequency of the operational configuration is to be $\geq$ .004 Hz.

(7) There is no significant dimensional stability.

3.1.4 SPS TEST ARTICLE II CONFIGURATION

This SPS test article configuration is described on drawing 42635-18030 (Appendix A). Table 3.1-5 summarizes the test article mass. For convenience, Figure 3.1-11 presents the major configuration equipment characteristics for the LEO and GEO configurations.

This SPS test article consists of a microwave antenna and its power source, a 20 200 m array of Lockheed type silicon solar cell blankets, both of which are supported by the solar blanket array support structure. The microwave antenna is illustrated in Figure 3.1-12 in its folded configuration for Shuttle delivery as well as in its operational configuration. The microwave antenna is attached to the rotary joint.

Table 3.1-5. Mass Summary—SPS Flight Test Article II

	(Mass in kg)
STRUCTURE AND MECHANISMS	(6,472)
Basic Structure	594
Secondary Structure	32
System Control Module	2,268
Mechanisms	(3,576)
Docking Ports	2,838
Rotary Joint Module - MW Ant. End Only (1)	740
ELECTRICAL POWER AND DISTRIBUTION	(13,730)
Solar Energy Collector	(4,091)
Solar Panels	4,091
Battery System	(1,134)
Batteries	943
Charger	103
Wire Harness and Control	88
Distribution	(7,261)
Conductor	(4,822)
EPD Wire Harness	1,503
Ion Propulsion Harness	1,798
Antenna Harness	1,473
Slip Ring/Brushes	48
Equipment	(2,439)
Blanket Switch Box	893
EPD Panel	962
Ion Propulsion Switch Box	584
Supports and Secondary Structure	(1,244)
ATTITUDE CONTROL	(2,050)
Control Moment Gyro	93
Reaction Control System (Inert)	1,957
TT&C	(136)
THERMAL (Battery and Equipment Cooling & Radiator)	(230)
MICROWAVE SYSTEM	(9,141)
Klystrons (279)	8,175
Thermal Test Array	386
Phase Control Test Array	580
INFORMATION MANAGEMENT AND CONTROL	(800)
Data Management	500
Instrumentation	300
TOTAL - SATELLITE, Dry (Initial LEO)	32,559
RCS PROPELLANT	5,239
TOTAL - SATELLITE, Wet (Initial LEO)	37,798
ROTARY JOINT - ELECT PROP. ONLY END (1)	740
TOTAL - SATELLITE, Wet; GEO Mission	38,538
ORBIT TRANSFER PROPULSION	
Inert (6 Modules)	4,967
TOTAL - GEO Burn-out	43,505
Propellant (Mercury)	5,680
TOTAL - GROSS MASS	49,185

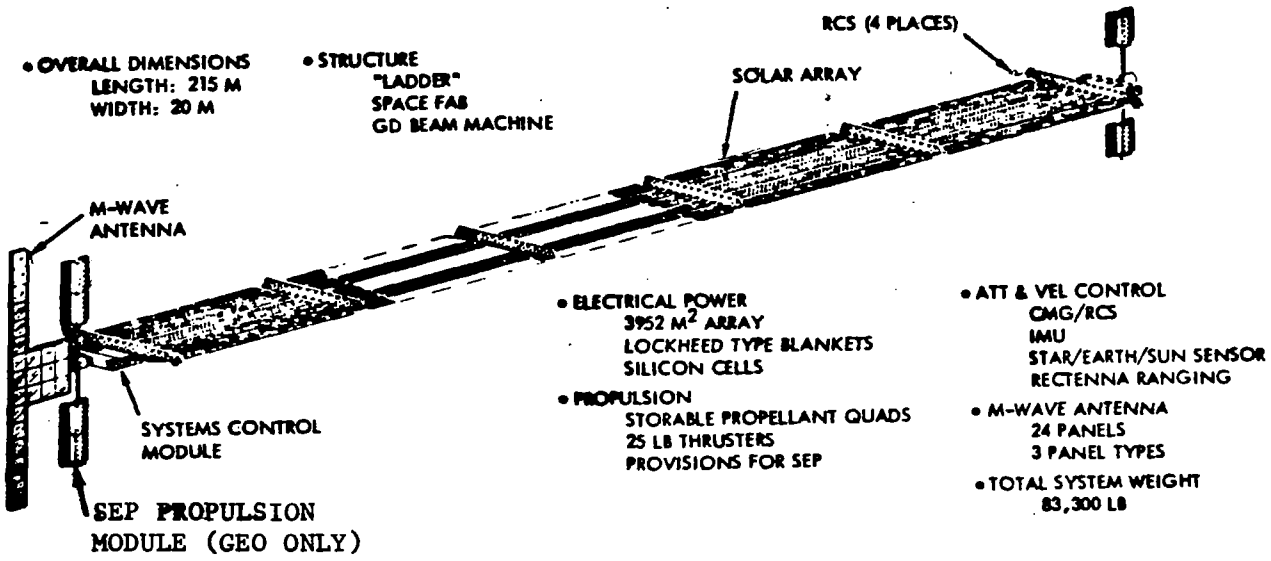

Figure 3.1-11. SPS Test Article II General Configuration

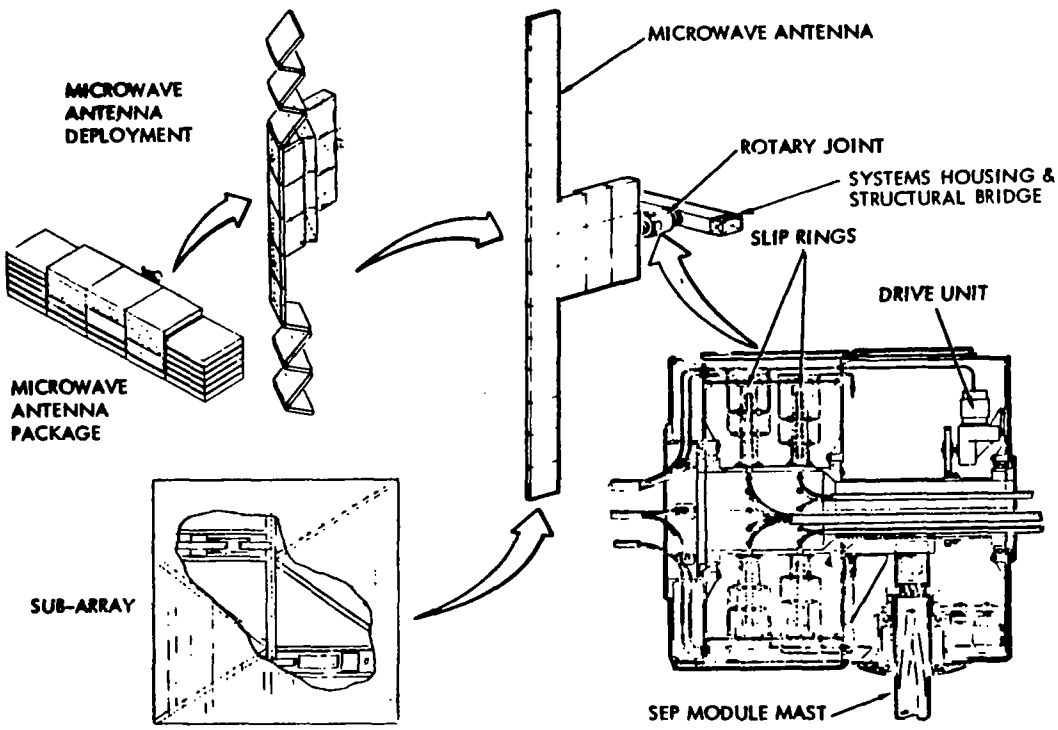

Figure 3.1-12. Microwave Antenna Configuration

For GEO orbit transfer, solar electric modules (SEP) are installed on both ends of the structure. The SEP modules are installed on rotary joints. Consequently, another rotary joint is required at the end of the solar array structure opposite from the microwave antenna in order to accept the SEP modules at this location. This represents the system configuration in GEO.

A control moment gyro/auxiliary propulsion system (CMG/APS) attitude control stationkeeping concept is incorporated. A system control module contains the CMG's, Tracking, Telemetry and Control (TT&C), and power storage batteries with thermal control provided by a radiator and external insulation. Micrometeoroid protection is also incorporated. A bridge fitting at the opposite end of the solar array structure provides the support for the rotary joint and solar electric propulsion modules used for orbit transfer. No other system components are included in this bridge structure.

The solar array consists of 25 4x40 m solar blankets tensioned stressed to a minimum of 17.5 N/m (0.10 lb/in). Each blanket is attached to the transverse beams of the structure. The attachment is provided with fittings to which the solar blankets are attached along the 4 m width of the blanket. Power leads will plug into individual switching boxes. For each of the switch gear boxes power lines will run along the longitudinal beams to interface with the systems control module and continue on to the power slip ring of the rotary joint. This arrangement provides voltage control for each of the 25 blankets.

Four APS pods are provided at the extreme corners of the configuration for orbit transfer, and attitude control. The pod definition is presented in Section 3.2.5. Each pod contains 1309 kg (2881 lb) of N_2O_4/mmH propellant, for a total mass of 1798 kg (3957 lb). Each pod contains 5 thrusters as shown in Figure 3.1-13:

- Three 111 N (25 lb) thrusters for orbit transfer
- Two 22 N (5 lb) thrusters for attitude control and stationkeeping maneuvers

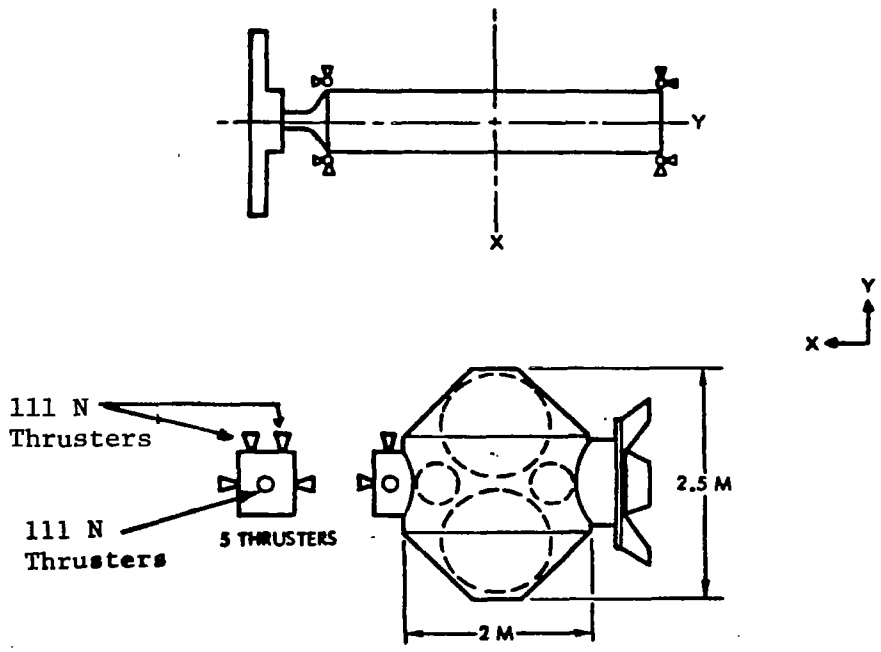

Figure 3.1-13. Auxiliary Propulsion System (APS) Module

The rotary joint provides one degree of freedom rotation between the solar array and the microwave antenna. It also provides the support for the Solar Electric Propulsion (SEP) modules. A slip ring assembly within the rotary joint provides the electrical power transfer across the rotary joint and a second slip ring assembly provides for the transfer of data and control signals. The rotary joint as a unit is attached to the systems control module via a berthing port. An electrical power and data/control signal interface is established at this port. A berthing port also is provided on the other end of the rotary joint unit to accept the microwave test antenna or other test articles if desired.

All of the large modular items such as the APS modules, system control module and bridge fitting are attached to the structure via NASA androgynous type berthing ports. Because all of the berthing activities are accomplished by using the orbiter Remote Manipulator System (RMS), no velocity attenuation system is required. Structural latches are provided only on the mating module. This permits a final checkout of the active latching system on the ground and immediately before assembly in orbit. A utilities interface is provided at each berthing port and each interface will be unique to its particular utilities requirements.

Smaller units such as the electrical junction boxes and the solar blanket switching boxes can be secured to the structure with clamp type devices that are compatible with the structural beam configuration and load capability.

When GEO OPERations are desired, then, and only then, will the SEP modules be installed.

The test article structure, a ladder is comprised of two longitudinal beams (215 m long) spaced 10 m apart and interconnected by a total of six lateral beams. The two longitudinal and six lateral beams shown are the baseline machine-made beams currently being developed for NASA by General Dynamics. In addition, the system control module and the bridge fitting also serve (for the ladder configuration) as bending and torsional strongbacks to increase the configuration stiffness. The strongback bending stiffness significantly supplements the in-plane Vierenhahl behavior of the ladder achieved by welding the laterals to longitudinal members at the four corners of each lap joint (Figure 3.2-18).

3.1.5 SOLAR BLANKET SUPPORT STRUCTURE REQUIREMENTS

The structural requirements for the solar blanket support structure [Drawing 42635-18032 (Appendix A)] of SPS Test Article II are listed below. The structural analyses from which these requirements evolved are discussed in Section 3.2.6.

These requirements are for the overall strength and stability, stiffness (modal frequency) and dimensional stability requirements, as well as the local requirements associated with the attachment of electrical power lines, blankets, J-boxes, EDC switching boxes, APS modules, systems control module, and the bridge fittings summarized in Section 3.1.3. For convenience, the overall and local structural requirements are presented separately. Options to the requirements are also specified herein.

Overall Strength and Stability Requirements

(1) During its construction in the free-drift mode and supported from the orbiter-mounted fixture, the basic solar blanket support structure must sustain, without permanent deformation, the most severe combination of thermal induced loads, and the loads associated with libration damping operations prior to orbiter return docking.

(2) The structure must also sustain the most severe combination of the numerous solar blanket tensioned configurations and APS pod and all other system installation loads in addition to thermal and gravity-gradient induced loads. The minimum required solar blanket tension is 17.5 N/m (0.10 lb/in) however, the design limit tension load shall account for the differential expansion between the structure and solar blanket, unless constant tension devices are used.

(3) The solar blanket support structure shall sustain, without detrimental deformation, the most severe combination of concurrent orbit transfer F_X loads (Cases 1 and 2, Figure 3.1-14), solar blanket tension, and thermal gradient induced loads. The thruster thrust versus time history is delineated in Section 2.2.5.

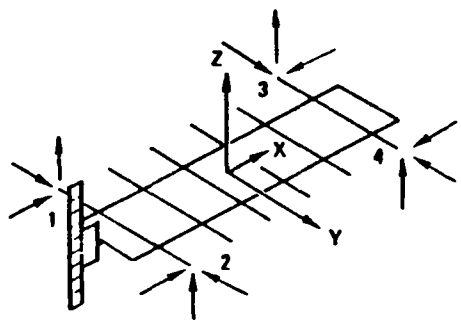

LOAD CONDITIONS (N)

CASE	STATIONKEEPING								ATTITUDE			
LOAD	1	2	3	4	5	6	7	8	9	10	11	12
1_x	222											
1_y			111							111		
1_z							22		-22			22
2_x	222											
2_y				111							111	
2_z							22		-22			-22
3_x		222										
3_y					111						111	
3_z								22	22			+22
4_x		222										
4_y						111				111		
4_z								22	22			-22

Figure 3.1-14. APS Thrust Loads

(4) The solar blanket support structure shall sustain, without detrimental deformation, the stationkeeping and attitude control conditions delineated in Figure 3.1-14, concurrent with blanket tension and thermal induced loads.

(5) In satisfaction of the foregoing requirements (2), (3), and (4) the analysis shall include the additional loading due to axial load magnification of fabrication, transverse load, and thermal gradient induced deviations from straightness.

(6) The solar blanket shall not be damaged by APS pod firing induced deflections.

(7) The structural material and thermal coating design properties employed in the strength and stability analyses must be maintained during exposure to the environments described in Section 3.0.

Stiffness

The structural stiffness of the configuration must be compatible with the control system design and, hence, have a minimum modal frequency no less than 0.004 Hz. The mass distribution is presented in Table 3.1-5.

Dimensional Stability

None.

Local Requirements

Included in the local structural requirements are the loads incurred during attachment of the APS modules, system control module, and bridge fitting. The transient loads depend on the techniques utilized (docking or berthing), relative approach velocity, local structural stiffness, and the basic structural capability of the particular design. The docking loads are not within the scope of this study and are not defined herein. However, the technique used is that of berthing. The orbiter is docked to the construction fixture and the RMS is used to place the above listed components. The RMS features listed in Section 2.1.5 are applicable.

Utilities Attachments

The solar blanket support structure must support the electrical power and data management lines, J-boxes, and EDC switching boxes as shown on Drawing 42635-18032.

Structural Interface Requirements

Interface I—System Control Module Attachment

This interface lies between the male and female portions of the androgynous docking ports, and is the attachment for the system control module. The system control module contains the control moment gyroscope, TT&C unit, electrical power conditioning unit, EPD panels, battery packages, and docking port for attachment of the rotary joint and microwave antenna. The total mass of the structure and contained equipment is 5000 kg. This interface sustains the transient loads incurred during attachment to the solar blanket support structure, and subsequent installation of the microwave antenna and solar electric propulsion device. Also, the interface must sustain the most severe combination of gravity gradient, orbit transfer, stationkeeping, and attitude control maneuver loads resulting from acceleration of the support equipment.

Interface 2—Bridge Fitting Attachment

This interface lies between the male and female portion of the androgynous docking ports and is the attachment for the bridge fitting. The bridge fitting contains a docking port to receive future installation of rotary joint and solar eleetric propulsion device (Figure 3.1-11). The bridge fitting assembly mass is 1500 kg.

The requirements stated for Interface 1, applied to the equipment at this interface, are directly applicable.

Interface 3—APS Pod Attachment

The interface lies between the male and female components of the docking ports shown. This interface must be capable of sustaining, without detrimental deformation, the transient loads occurring during berthing. The interface must also sustain the loads imposed during thruster firing (Figure 3.1-14). The pod thrust versus time characteristics shown in Section 2.2.5 are applicable.

Interface 4—Solar Blanket Attachment

This interface is between the edge of the 40 meter by 4 meter solar blanket arrays and the supporting solar blanket structure, and contains the blanket tension devices. The integrated tension device system, solar blanket system, and solar blanket support structure shall maintain a minimum limit tension of 17.5 N/m throughout all mission phases. Also, the tension device system shall introduce no loads (at the attachment) detrimental to the solar blanket support structure.

Options

Orbit Transfer Thrust

The orbit transfer thrust of 222 N (50 lb) can be reduced with larger burn times if advantageous to the future design studies.

3.2 SYSTEMS ANALYSES

This section contains the microwave, power, data management and communications, attitude stabilization and control, auxiliary propulsion and structural systems analyses that were used to establish the requirements and characteristics of these systems.

3.2.1 MICROWAVE

Summary

The microwave subsystem simulates a modular portion of the Satellite Power System (SPS) for the purpose of conducting power transmission tests in low earth orbit. Two specific tests are of prime importance. In the first, a slotted waveguide array radiates a high power beam (250 kW) and its performance is monitored under thermal conditions that closely approximate those expected

to exist at the center of the actual SPS transmitting antenna. In the second, operating at a considerably lower power level, a long narrow waveguide array radiates a fan beam toward a rectenna that is located at the edge of the far field of the transmitter. Phase front control and beam pointing tests using an active, pilot tone control system will be carried out. Figure 3.2-1 shows the microwave subsystem configuration and indicates important dimensions.

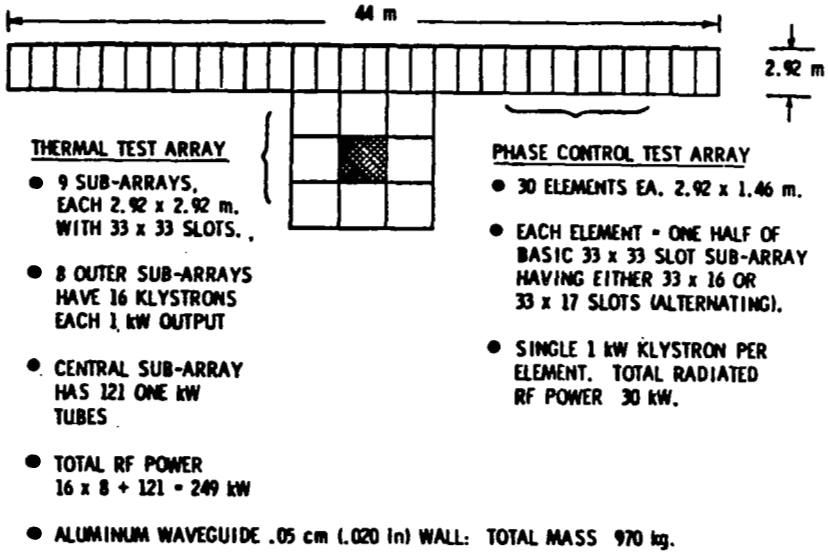

Figure 3.2-1. SPS Test Article II Antenna

Table 3.2-1 presents a summary of the microwave system mass estimate for the test article.

Table 3.2-1. SPS Test Article II—Microwave Mass Summary

	Length (m)	No.	Unit Mass	Total Mass (kg)
THERMAL TEST ARRAY				(7682.0)
Waveguides	2.924	340	0.36 kg/m	357.9
Fittings, etc. (8%)				28.1
Klystrons	-	249	29.3 kg/ea.	7296.0
PHASE CONTROL ARRAY				(1458.7)
Waveguides	2.924	510	0.36 kg/m	536.8
Fittings, etc. (8%)				42.9
Klystrons	-	30	29.3 kg/ea.	879.0
			Overall Total	9140.7

Subsystem Description

The SPS Test Article II antenna (Figure 3.2-1) consists of two parts, a thermal test portion and a phase control portion. The thermal test portion is comprised of nine subarrays, each 2.92 m x 2.92 m and made up of 33 waveguides each having 33 radiating slots. The central subarray radiates 121 kW, provided by 2450 MHz klystron tubes mounted on its rear surface. Each klystron has a nominal rating of 1 kW RF output, and 121 such tubes are arrayed in the form of an 11x11 matrix. It is emphasized that this slotted waveguide subarray could equally well be excited by four 50 kW tubes in a 2x2 matrix without requiring any major changes. The central subarray is surrounded by eight identical 2.92 m x 2.92 m subarrays, each excited by sixteen 1 kW klystrons in a 4x4 matrix. Total RF power input to the nine-element array is, therefore, 16x8+121 = 249 kW.

The phase control test portion is a linear array of 30 subarrays each 2.92x1.46 m. It is 2.92 m wide and about 44 m long. Two of these 2.92x1.46 m subarrays adjacent to each other make up a unit that is identical to one of the 33x33 slot subarrays used in the thermal test array. However, each of these 2.92x1.46 m subarrays is fed by only a single 1 kW klystron tube so that total RF power into the array is 30 kW. Each klystron, and therefore each of the 30 elements in the linear array, is subject to phase control for the purpose of beam formation and pointing control. Each subarray receives a pilot tone emanating from the rectenna. The phases of all the received pilot tone signals are sensed and the necessary control signals are applied to each klystron tube input in such a way that every subarray radiates its 1 kW signal in phase conjugation with respect to the pilot tone signal received by it. This active, retrodirective, control system ensures that the beam from the 30 element array is correctly formed and steered toward the rectenna. Steering, however, occurs only in one dimension. The rectenna is a co-orbiting, independent, free flying vehicle. It is expected that the pilot tone will be received by each of the slotted waveguide subarrays themselves. Thus the weak pilot tone signals must be separated from the strong transmitted signals by means of duplexers, which poses a difficult design problem. As an alternative, separate receiving antennas for the pilot tone might be used at each subarray. These should be cross-polarized relative to the high power transmitted signal so that they pick up only a very small leakage signal. If such separate pilot tone receiving antennas are used it is important that they do not cause any significant increase in spacing between adjacent subarrays in order to prevent the formation of greating lobes.

Subsystem Design Analysis

Each subarray is an assemblage of slotted waveguide radiators each of which is of the standing wave, resonant slot type. The array is excited by one or more slot coupled transverse feeder guides placed on the back (i.e., non-radiating) side of the subarray. The arrangement is shown in Figure 3.2-2, wherein only a single transverse feeder guide is shown for simplicity. The design basis for this array can be explained with the aid of Figure 3.2-3. The radiating and feeder guides have the same dimensions, the height "b" being one half of the width "a", as is customary for rectangular guide. The crosses indicate the locations of the slot centers for both the radiating and the coupling slots.

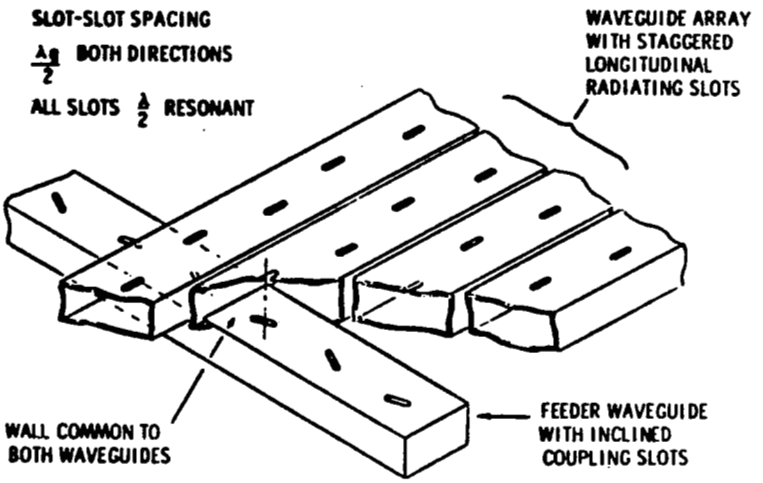

Figure 3.2-2. Transverse Feeder Guide for Slot Array

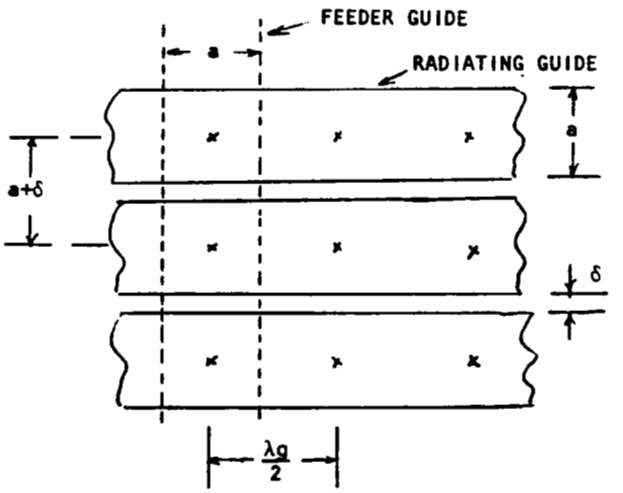

Figure 3.2-3. Resonant Array Design Basis

A standing wave slot radiator requires that the spacing between adjacent slots be equal to $\lambda g/2$ where λg is the guide wavelength. The slotted guide then radiates a broadside beam normal to the plane containing the slots. Several such guides are arranged parallel to one another to form a square subarray that radiates a symmetrical beam normal to its face. The spacing between adjacent guides is denoted by δ and is assumed to include the thickness of the waveguide walls. Thus the spacing between neighboring coupling slots in the feeder guide is $a+\delta$.

In all cases alternate slots must have π radians phase shift which is obtained by the use of staggered longitudinal shunt slots in the radiating guides, and oppositely inclined series slots in the feeder guide. All slots are cut to resonant length ($\sim\lambda/2$) so that slot admittance is simply $g+j0$. Each slot is either displaced from, or inclined to, the guide centerline just enough to make its conductance g equal to $1/N$ where N is the total number of slots in the guide. When the guide is short-circuited at one end, at a distance $\lambda g/4$ from the center of the last slot, all slots appear in parallel. Hence the admittance looking in at the other end is $gN = 1$ and the guide is matched.

The guide can be shorted at both ends, in which case it may be excited by a probe or a slot in the wall opposite to the radiating face. This probe or slot must be located at one of the loops in the "standing wave" pattern in the guide, i.e., at a distance equal to an odd number of quarter guide wavelengths from either end. One, or any number of such excitation points, may be used providing they are located in the above manner.

In order to ensure suppression of grating lobes the spacing between adjacent slots must be less than one free space wavelength. Thus

$$\frac{\lambda g}{2} < \lambda \text{ in the radiating guide and}$$

$$a+\delta < \lambda \text{ in the feeder guide.}$$

Noting that $a = \lambda c/2$, where λc is the guide cut-off wavelength, it is clear that values of $\lambda/\lambda g$ and $\lambda/\lambda c$ in the neighborhood of $1/\sqrt{2}$ are satisfactory so long as δ is small. The feeder guide is also a standing wave resonant slot structure that radiatively couples into the radiating guides. Therefore the spacing between its coupling slots must be equal to one half the wavelength in the feeder guide. Choosing identical dimensions for all guides then requires that

$$a+\delta = \frac{\lambda g}{2}$$

and leads to a symmetrical array with identical spacings in both planes. The above condition, along with the usual waveguide relation

$$\frac{1}{\lambda g^2} + \frac{1}{\lambda c^2} = \frac{1}{\lambda^2} ,$$

has a unique solution which can be expressed as

$$\frac{\lambda}{\lambda g} = \cos\left(\frac{\pi}{4} + \Delta\right) , \qquad \frac{\lambda}{\lambda c} = \sin\left(\frac{\pi}{4} + \Delta\right)$$

where, for small δ, $\Delta \simeq \sin\Delta \simeq \frac{\delta}{\lambda\sqrt{2}}$.

Choosing δ = 0.4 cm with λ = 12.24 cm (2450 MHz) then gives

$$\frac{\lambda}{\lambda g} = .6906 , \quad \frac{\lambda}{\lambda c} = .7232$$

so that $\lambda g/2$ = 8.86 cm and a = 8.46 cm.

Every subarray in the thermal test portion has 33 parallel waveguides each containing 33 radiating slots. The overall dimensions of this 33x33 slot array are 2.920x2.924 m. The central subarray has 11 transverse feeder guides on its back face, each carrying 11 klystron tubes (1 kW ea.) that are probe coupled into the guide at loops in the standing wave pattern. The surrounding 8 subarrays have only 4 feeder guides each being probe fed by 4 klystron tubes. This arrangement is changed slightly for the half-size subarrays in the phase control test portion. Here, the standard 2.92 m^2 subarray described above carries two feeder guides. One of these guides couples to 16 adjacent radiating guides; the other one couples to the remaining 17 radiating guides. In this way the standard subarray is effectively split into two independent units. The units are not quite identical, however, since one has 16x33 slots while the other has 17x33 slots.

The radiation pattern function of a standard subarray is the product of a 33 element array factor and the slot pattern function. Although the slot pattern is different in the E and H planes it is very much broader than the array factor. Thus the latter dominates and the resultant pattern is symmetrical and essentially that of a uniformly illuminated square aperture that is 2.92 m per side. Hence the half-power beamwidth will be 2.1°, the first nulls will occur at 2.4° from the array normal and the level of the first side lobes will be -13.2 dB. The phase control test array, which is 43.8x2.92 m, will radiate a fan beam. In the plane normal to the linear array the beam characteristics are just those of the standard subarray given above. In the plane containing the linear array the pattern is much narrower, the half power width being 0.14° with first nulls occurring at 0.16° from the array normal. First side lobe levels are still -13.2 dB.

In order to perform successful testing in space of the phase control test array, certain tolerances must be placed on the dimensions and orientation of the array and its component subarrays. The most important tolerance requirements are those summarized in Figure 3.2-4. Proper operating of the retrodirective, active control system will compensate for small displacements between adjacent subarrays, providing they remain parallel to each other. Nevertheless, it appears prudent not to allow such displacements to exceed $\lambda/4$ or ±3 cm. Any non-parallelism, i.e., tilt, between adjacent subarrays must be held to ±13 minutes of arc. This is based on an allowable loss in boresight gain not exceeding 3% and is calculated from the loss relation

$$\left(\frac{\sin\Delta X}{\Delta X}\right)^2$$

where $\Delta X = \frac{\pi D}{\lambda}\ \Delta\varepsilon$.

$\Delta\varepsilon$ is the differential tilt angle and D = 2.92 m is the length of a standard subarray.

TILT ANGLE BETWEEN SUB ARRAYS	± 13 min
RMS SURFACE ROUGHNESS	3.4 mm
PARALLEL DISPLACEMENT BETWEEN SUB ARRAYS	± 3 cm
ARRAY ATTITUDE STABILITY	
X AXIS	± 13 min
Y AXIS	± 3 deg
Z AXIS	± 5 deg
(FOR < 3% GAIN LOSS)	

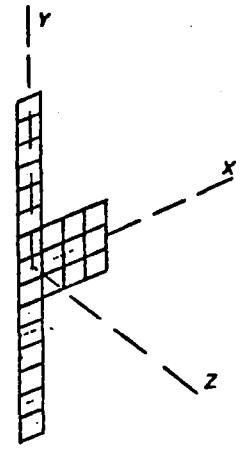

Figure 3.2-4. SPS Antenna Tolerances

The radiating surface of each subarray must be flat with an rms deviation, σ, not exceeding 3.4 mm. Again, this is based on an allowable loss of 3%, using the Ruze formula

$$e^{-\left(\frac{2\pi\sigma}{\lambda}\right)^2} .$$

Attitude stability requirements must be placed on the array orientation and are most stringent for rotation about the X axis. This must be limited to ±13 arc minutes in order to hold the loss to 3% or less. Much looser tolerances can be placed on rotation about either the Y or Z axes, viz, ±3° and ±5° respectively, for the same 3% loss.

Adjacent subarrays must be closely spaced in order to avoid grating lobe formation. The maximum tolerable gap between subarrays is about 2 cm.

Microwave Power Generation

The SPS reference concept is based upon the use of high-power (50 kW) klystron tubes as dc/RF converters. These tubes will operate with depressed collectors and are expected to yield efficiencies of about 83%. However, it is unlikely that such tubes will be available for the 1985 Solar Power Experiment Mission. Therefore, the test article described above is designed to operate with much lower power (~1 kW) klystrons, having lower efficiencies (75%). Such a 960 watt tube is shown in outline in Figure 3.2-5 while Figure 3.2-1 shows how 279 of these tubes are distributed over the slotted waveguide array.

121 TUBES @ 0.96 KW = 116.5 KW
DC POWER = $\frac{116}{.75}$ = 155 KW
HEAT DISSIPATED = 38.5 KW
TUBE WEIGHT - 29 Kg
EFFICIENCY = 75%
ANODE VOLTS = 7 KV

(121 TUBES ON 9m²
SUB-ARRAY WITH
HEAT PIPES FOR
COLLECTOR COOLING;
BODY TEMPERATURE
195 - 250° C)

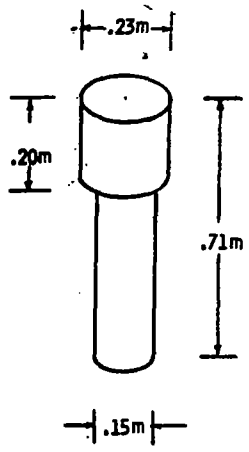

Figure 3.2-5. 1-kW Klystron Tube

As indicated in Figure 3.2-5, the heat dissipated by the central subarray of the thermal test portion of the antenna is 38.5 kW over an area of 9 m^2. This is the same thermal power density that would occur at the center of the SPS reference concept spacetenna which uses 83% efficient klystrons and an RF power density of 20.9 kW/m^2.

Power Requirements

Each klystron requires 1280 watts of dc input power plus about 120 watts for heater and focusing solenoid, for a total of 1400 watts. During thermal testing a total of 249 tubes will be in operation so that maximum dc power requirements are about 350 kW.

3.2.2 POWER

Summary

The characteristics of the major components and loads of the electrical power subsystem were summarized in Table 3.1-1.

The electrical power distribution system (EPDS) receives power from the power generation subsystem, and provides the regulation and switching required to deliver the power for distribution to the various satellite loads or to the storage batteries. The subsystem consists of main feeders, secondary feeders, tie bars, summing buses, regulators, voltage converters, switch gear, remote power contactors, slip rings, brushes, and subsystem cabling. Batteries and battery chargers are included for eclipse periods.

A weight summary of the EPDS for SPS Test Article II was presented in Table 3.1-2.

The location of the various EPDS equipment items was indicated in Figure 3.1-6.

Design

The major requirements are to deliver power at specific voltages and levels on a continuous basis throughout the solar seasons for a duration of 20 years. The solar array will deliver 520 kW of electrical power through a distribution system with a transmission efficiency of 94%. Electrical power at a level of 489 kW is transferred across the rotary joint, through slip rings to the flight test article. The distribution will transmit the electrical power to the flight test article with a transmission efficiency of 98%. Power at a level of 448 kW at 200 volts will be delivered to the dc/dc converter/klystron interface. Figure 3.2-6 illustrates the efficiency chain of the electrical power distribution system.

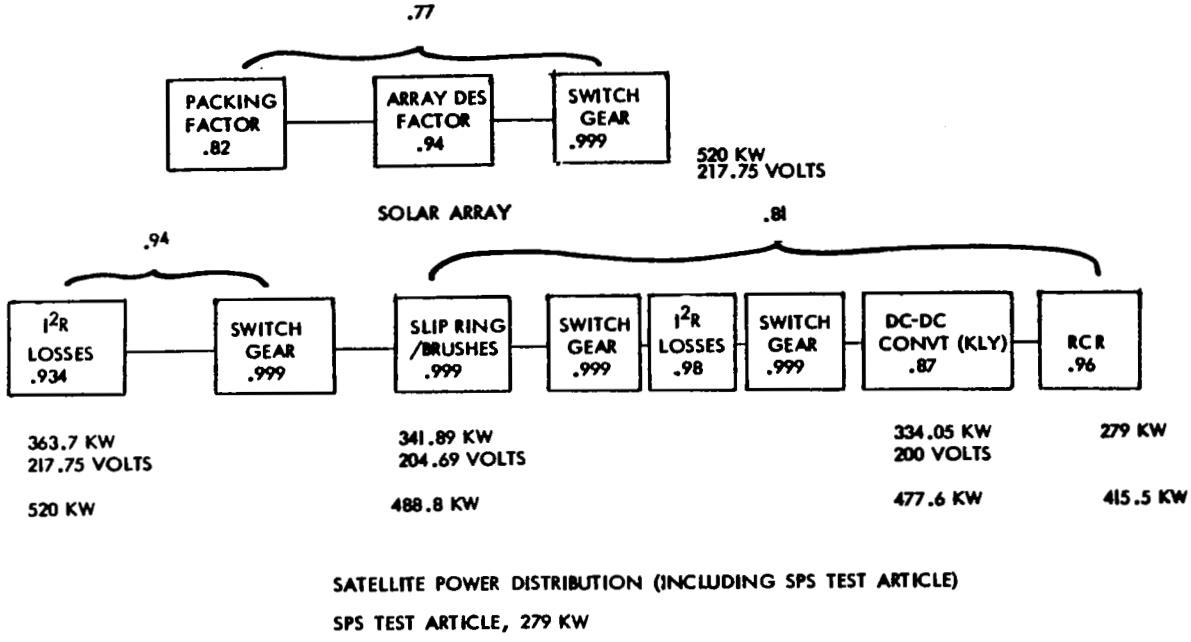

Figure 3.2-6. SPS Flight Test Article II Efficiency Chain

Power Generation

Figure 3.2-7 and Table 3.2-2 summarize the physical format for the solar array. The solar photovoltaic power system follows the direction in Section IX.B of the NASA "Red Book," Solar Power Satellite Concept. Power output per square meter of solar cell blanket is calculated to be 130 W/m^2. Thus, the total dc power generated for a 4000 m^2 solar array would be 520 kW.

The 4000 m^2 is implemented as a 20 m × 200 m solar array. The array is divided into five bays approximately 20 m × 40 m. Each bay has five solar blankets which are 4 m × 40 m. A solar blanket is comprised of 52 solar panels, of dimensions 0.756 m × 4 m. There are two electrical modules per panel. Based on the technology from the PEP solar array, there are 1530 solar cells per electrical module.

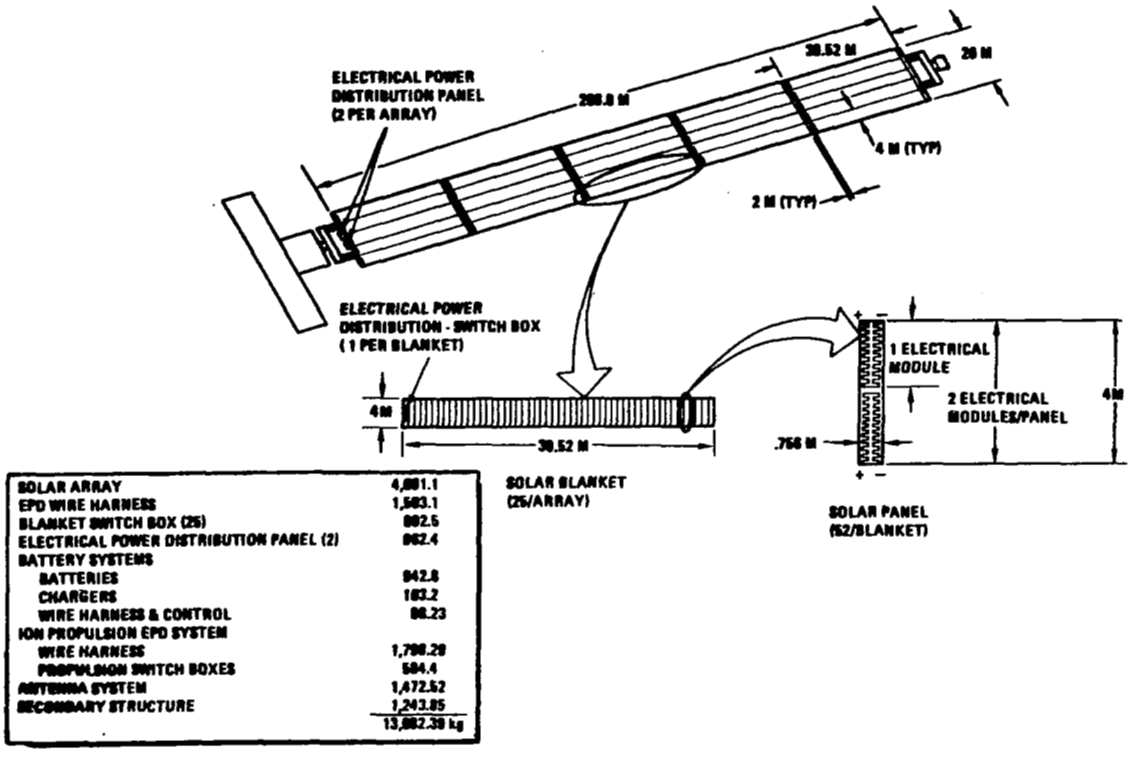

Figure 3.2-7. Solar Array
(20 m × 200 m)

Table 3.2-2. Power Generation Subsystem

Item	Characteristics
Solar Array	4000 Square Meters (20m x 200m) 25 Solar Blankets (4m x 40m) Solar Cell Output EOL 130 W/m^2 Power Output 520 kW
Solar Cell Blanket	160 Square Meters (4m x 40m) 52 Solar Panels (4m x .7564m) 104 Electrical Modules
Solar Panel	3.0256 Square Meters (.7564m x 4m) 2 Electrical Modules/Panel
Electrical Module	1.512 Square Meters (.7564m x 2m)

Utilizing the PEP design concept, the array harness will be a flat cable conductor mounted on the back of the solar array blanket at the two long edges of the blanket. The harness folds up in the same manner as the array panels for retraction and storage. The flat cable conductor insulation is 1-mil-thick Kapton film. Two sheets of Kapton film, bonded together with a thin film of high-temperature polyester adhesive, are used to encapsulate the 1 mm copper conductors. Conductor pairs from six panels will be routed to form a cable which will terminate in a connector at the base of the blanket. Figure 3.2-8 shows a schematic of a typical solar array blanket. The connectors, capable of remote manipulator handling, will be engaged into an electrical power distribution switch box located at the base of each blanket. The number of these connectors will be minimized to augment the remote fabrication operations in space. Feeder cables from the EPD switch boxes are routed to two electrical power distribution panels, located at the base of the array, to form a split bus of equal power. Individual blankets feed power from their respective EPD switch boxes through feeders to the electrical power distribution panel. Switch gear isolate each blanket from the summing bus. As each switch gear is closed, its respective blankets output is connected to the summing bus.

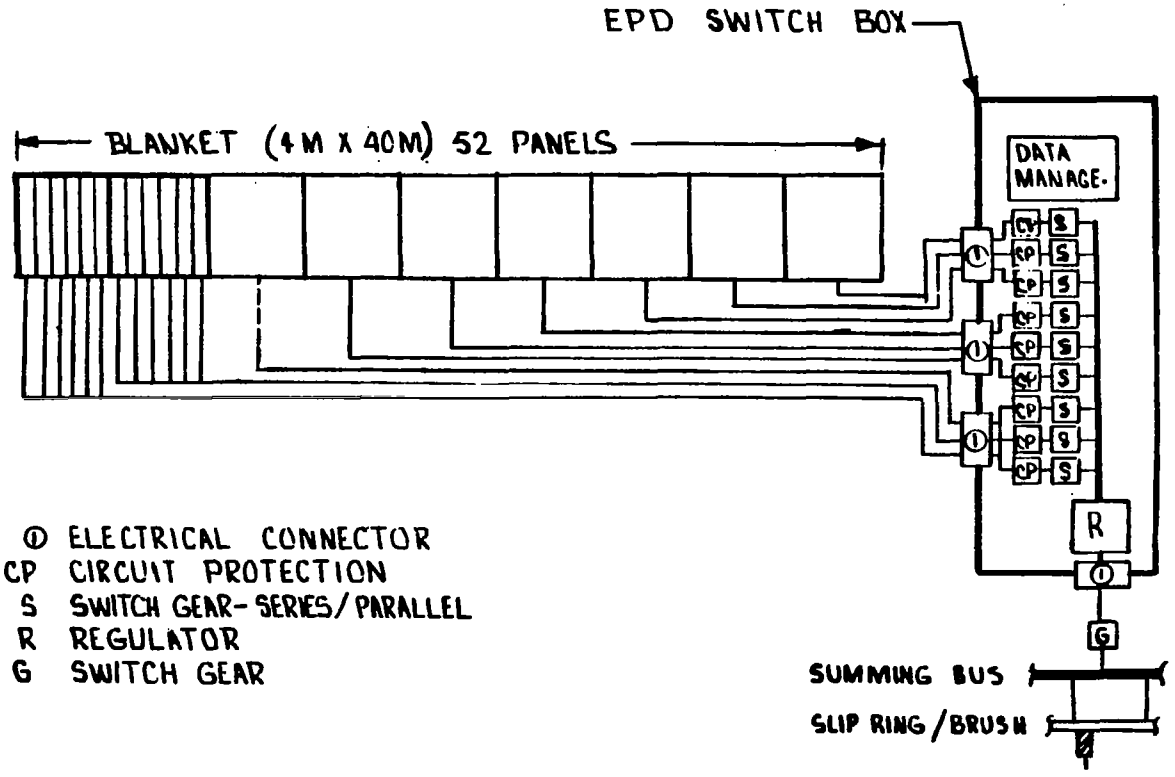

Figure 3.2-8. SPS Test Article II Typical Blanket Element (1 of 25)

Voltage and power output and excess power at the beginning of life (BOL) will be controlled by the isolation switch gear through the data management system within the TT&C system. Voltages, currents, and bus temperatures will

be monitored by the TT&C system to detect any shorts throughout the solar array. Controlled emergency disconnects can occur under the tracking, telemetry, and communication (TT&C) data management system or be effected by breaker control to avoid catastrophic effects. The design is such that no single-point failure may cause a total loss of the SPS function.

Energy Storage

An energy storage system will be utilized during the eclipse periods to provide approximately 37 kWh of electrical power. Batteries and a regenerative fuel cell system have been reviewed as candidate energy storage subsystems. The regenerative fuel cell system was not selected at this time due to the long, costly development program required for the electrolysis unit. Nickel-hydrogen and nickel-cadmium batteries were evaluated as candidates for the energy storage system. Table 3.2-3 provides comparative data which led to the selection of the nickel-hydrogen battery to be used for the energy storage system. Operationally, $Ni-H_2$ and Ni-Cd batteries are similar. However, $Ni-H_2$ cell voltage is 3 mV higher than the Ni-Cd. Also, inherent overcharge and over-discharge capabilities of the $Ni-H_2$ battery simplify cell protection requirements. The Ni-Cd battery requires reconditioning periodically, prior to each eclipse period, due to its memory effect. This is not a problem with the $Ni-H_2$ battery.

Table 3.2-3. Comparison of $Ni-H_2$ to Ni-Cd Batteries

AMP-HOUR EFFICIENCY	SIMILAR, 75 TO 80%
CELL VOLTAGE	$Ni-H_2$ 3.5% HIGHER
SELF DISCHARGE	$Ni-H_2$ SLIGHTLY HIGHER
OVERCHARGE CAPABILITY	$Ni-H_2$ 0.5C, NI-CD 0.1C
OVER DISCHARGE (CELL REVERSAL)	$Ni-H_2$ SUPERIOR, STABLE @ 0.5C
CHARGE CONTROL METHODS	SIMILAR
RECONDITIONING	NOT REQUIRED FOR $Ni-H_2$
OPERATING TEMPERATURE	$Ni-H_2$ 0-20 ° C, 10 ° C DESIRABLE
	NI-CD 5-20 ° C DESIRABLE
	30 ° C SHORTENED LIFE
WEIGHT	$Ni-H_2$ 50% GREATER POWER/POUND
VOLUME	$Ni-H_2$ 2 TIMES GREATER
DEPTH OF DISCHARGE	$Ni-H_2$ @ 80% 2 TIMES LIFE OF NI-CD
POTENTIAL LIFE, PERFORMANCE & COST	$Ni-H_2$ HAS ADVANTAGE

The parameters for the $Ni-H_2$ battery are listed in Table 3.2-4. The current nickel-hydrogen cell, as developed, has a capacity of 50 ampere-hours. The cell is approximately 9 cm (3.5 in.) in diameter and 23 cm (9 in.) long. Figure 2.2-11 is a picture of seven nickel-hydrogen cells in a series connection. The energy storage system will utilize 122 of these cells in series to

Table 3.2-4. Energy Storage System (Nickel-Hydrogen Battery)

Item	Characteristic
Power Requirement	
@ LEO	15,280 Watt-Hours
@ GEO	31,900 Watt-Hours
Capacity	27,093 Watt-Hours
Charging	1.6 Volts
Discharging	1.25 Volts
Charging Rate	C/10
Weight Factor	8.18 Watt-Hours/kg
Depth of Discharge	80%
Cell Size	125 Ampere-Hour
Number Cells/Battery	122
Battery Weight	942.8 kg

form a battery and two batteries will be required. A new cell plate in the stack would be increased. Current technology would be applied along with some test verification.

The battery switch gear and bus tie contactors are located within the electrical power distribution panels shown in Figure 3.2-7. Sensing circuits of the data management system will monitor orbit times and will control when the battery will be connected and disconnected to the buses. As the battery power is connected, sensing circuits will disconnect loads not requiring electrical power during the eclipse periods. Battery power will be switched off in the same manner when the sun energy illuminates the photovoltaic subsystem. The energy storage subsystem will have its energy resupplied by the solar array through the charging system.

Electrical Power Distribution

Figure 3.2-9 shows a simplified block diagram for the electrical power distribution system for SPS Test Article II. Main power feeders are routed from each solar blanket and are summed and divided into two buses. The split bus offers protection from losing all electrical power and provides some

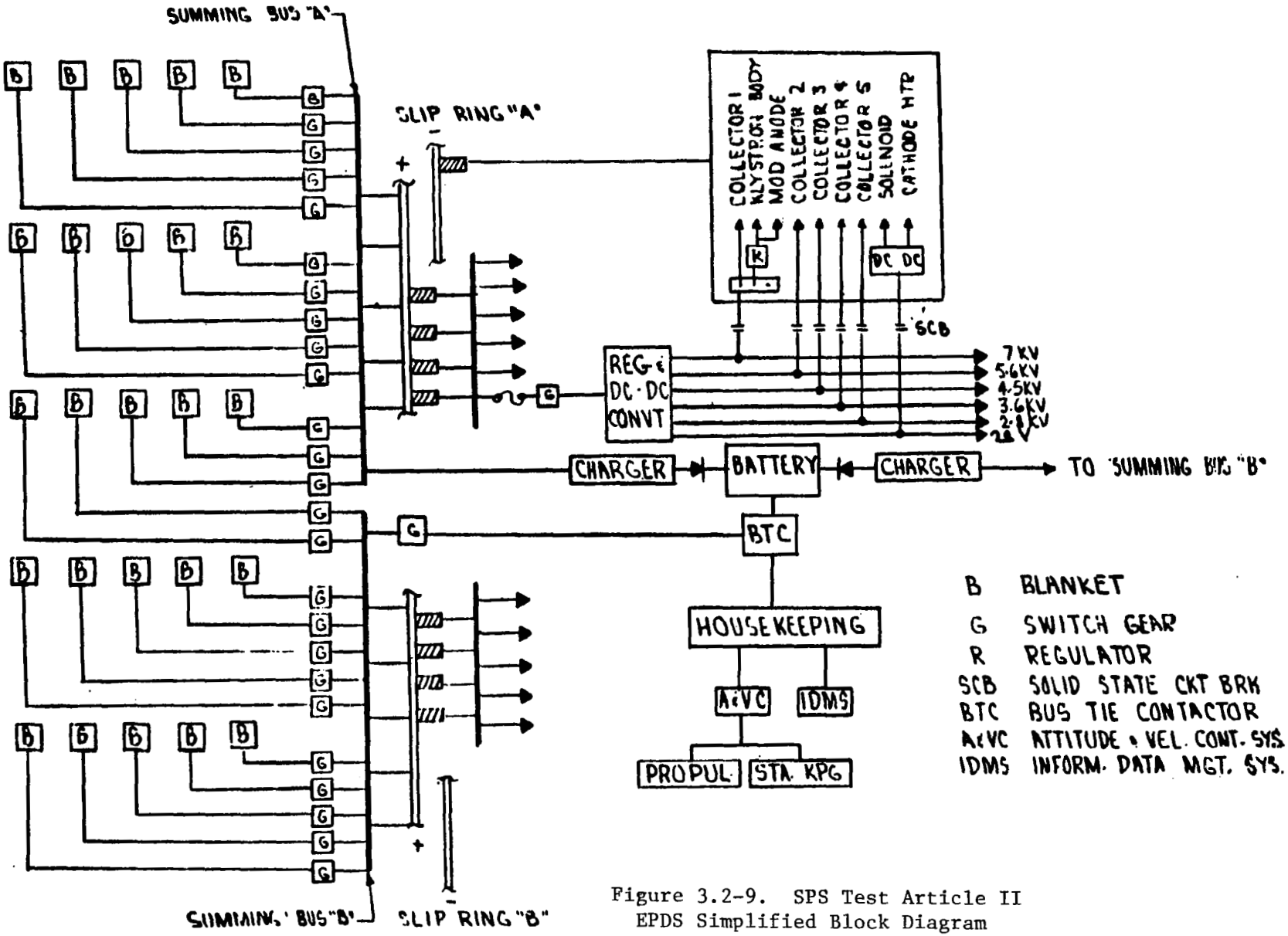

Figure 3.2-9. SPS Test Article II
EPDS Simplified Block Diagram

redundancy in event of a catastrophic event to the solar array. Bus ties from each summing bus of the electrical power distribution panel will interconnect to the power slip rings. The slip rings will transmit the electrical power across the rotary joint and maintain the split bus concept. Risers from each brush of the power slip rings will be tied to a summing bus. Feeders routed through switch gear will connect to dc/dc converters which are located on the microwave test antenna structure. These switch gears isolate each converter for maintenance and are controlled by the data management system for controlled emergency disconnects that may be required in the event short circuits occur within the feeder loop. These switch gear, monitored through the data management system may be used to control the microwave test.

The electrical propulsion system will be powered through the electrical power distribution panel. Switch gears will be located within the panel for isolation of the propulsion system from the summing buses. Power feeders will be routed through the rotary joint, with a loop, to a switch box located on each propulsion mast at the base of the ion thrusters stack. Switch gear and circuit protection devices are provided for isolation and maintenance purposes. The data management system will monitor each ion thruster through data command signals. The attitude velocity control and TT&C systems will have complete control of powering each individual ion thruster and APS unit as required. The battery system has been sized to maintain electrical power on the ion thrusters for a standby status and to apply discharge power 12 minutes prior to the climax of the eclipse period. This action will be controlled by the data management system. Table 3.2-5 shows the distribution of electrical power to the various subsystems.

Table 3.2-5. Distribution of Electrical Power

Item	Power/Energy Generated or Required
Solar Array	520 kW
Battery	37.1 kW-H
Test Article	342 Kw
Telemetry Tracking & Control	5 kW
Attitude & Velocity Control	5 kW
Propulsion	
Orbit Transfer	520 kW
APS	500 W

Electrical power, up to a level of 5 kW, will be supplied to the TT&C system for the housekeeping tasks this system performs. The battery system has been sized to maintain power for all required functions during the eclipse periods. Power will be supplied from the housekeeping bus to each of its loads such as telemetry, rendezvous beacon, attitude and velocity control system, APS, TT&C system, etc. Each of these will be monitored by sensors and controlled through the data management system of the TT&C unit.

3.2.3 DATA MANAGEMENT AND COMMUNICATIONS (DMC)

Summary

During low earth orbit or during geosynchronous orbit, the communications and tracking system of the SPS Test Article II uses S-band and Ku-band links to provide—in addition to tracking—reception of commands at a maximum rate of 216 K bits/sec. The system also provides a transmission capability for telemetry, television, and data at a maximum rate of 50 m bits/sec. S-band links may be established with a ground station, and both S-band and Ku-band may be routed through NASA's Tracking and Data Relay Satellite System (TDRSS). A simultaneous capability to communicate with the co-orbiting rectenna platform, the Space Shuttle Orbiter, GPS, or other spacecraft is also provided on S-band as shown in Figure 3.2-10. The data management subsystem is similar to the system described in Section 2.2.3.

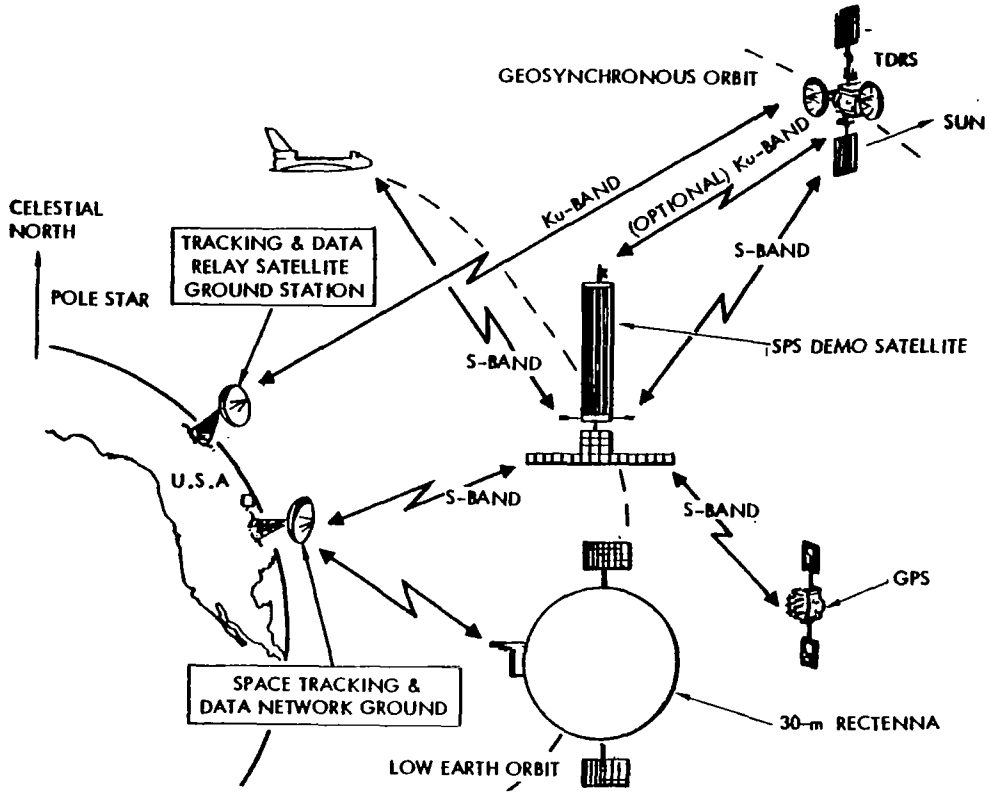

Figure 3.2-10. Communication Links for SPS Test Article II

Table 3.2-6 provides a summary of the mass and power estimate for the SPS Test Article II.

Table 3.2-6. SPS Test Article II LRU Mass and Power Summary

LRU	Mass (kg)	Power (W)
S-Band		
PM transponder	15.8	63
PM processor	8.1	30
Doppler extractor	7.4	16
Power amplifier (100 W)	14.4	400
Preamplifier	11.6	25
FM transmitter	3.0	120
FM processor	5.2	9
Switch assembly	3.0	2
Ku-Band		
Electronic assembly Signal processor Deployed assembly	95.0	489
Total with wiring and antennas	200	1200
Data Management	500	~100
Instrumentation	300	

S-Band Links

As shown in Table 3.2-7, there are three S-band links: (1) PM to orbiter, STDN or SCF; (2) FM direct to ground; and (3) PM to TDRSS and from there to TDRS on the ground. The return link on (1) is split into high (2250-2300 MHz) and low (2200-2250 MHz). If the SPS Test Article II transmits on low, the orbiter relays this signal to TDRSS (or STDN) on high or vice versa. In general, however, the orbiter is not needed for relay and links (1) other than orbiter; (2) and (3) are adequate for most command and telemetry functions. The exception is when higher rates than indicated are needed; then, the Ku-band provides the near-continuous high-data-rate capacity. Link margins are given in the special issue on *Space Shuttle Communications and Tracking*, IEEE Transactions on Communications (November 1978), pp. 1494, 1521, and 1604. The grand totals for S-band and Ku-band communication subsystems, including wiring and antennas, are 200 kg (mass) and 1200 W (power).

Ku-Band Links

The Ku-band subsystem for SPS Test Article II operates as a two-way communications system with the ground, through the TDRSS. The advantage of the Ku-band link is the large increase in data rate capacity both on the forward link as well as the return (Table 3.2-7). This increase in data rate is largely due to the

Table 3.2-7. SPS Test Article II Link Parameters

LINK	ONE WAY OR TWO WAY?	FREQUENCY	DATA RATE	NOTES
S-LINK				
PM TO ORBITER (OR DIRECT TO STDN OR SCF)	TWO	RETURN 2200-2300 MHz FORWARD 2025-2120 MHz	192 Kb/s 72 Kb/s	THIS LINK IS RELAYED TO STDN, SCF, OR TDRS. SCF HAS 256 Kb/s (RETURN) RF POWER = 6 W ANTENNA = 4 QUAD OMNIS
FM TO GROUND (STDN OR SCF)	ONE	RETURN 2250 MHz (10 MHz BANDWIDTH)	4 Mb/s	RF POWER = 10 WATTS ANTENNA = 2 HEMIS. OMNIS
PM TO TDRS (THROUGH TDRSS)	TWO	RETURN 2200-2300 MHz FORWARD 2025-2120 MHz	192 Kb/s 72 Kb/s	RF POWER = 100 WATTS ANTENNA = 4 QUAD OMNIS TIME COVERAGE: $\geq$ 95%
Ku-LINK				
TO ORBITER OR TO TDRSS	TWO	RETURN 14.85-15.15 MHz	50 Mb/s DIGITAL OR 4.5 MHz ANALOG TV 2 Mb/s PAYLOAD 192 Kb/s TELEMETRY	RF POWER = 50 WATTS ANTENNA = PARABOLIC (0.9 M DIAMETER) TIME COVERAGE: $\geq$ 95%
		FORWARD 13.75-13.80 GHz	216 Kb/s COMMANDS	HAS DATA & PN RANGE

0.9-meter parabolic antenna with 1.6° beamwidth and 38.5 dB gain. An uncertainty in pointing up to 10° (20° full-cone angle) is allowed for by using a slow spiral scan search pattern in acquisition. The maximum search time is three minutes. The subsystem described here is the communications portion of the Ku-band integrated radar and communications subsystem for the Space Shuttle orbiter.

Note that Links (1) and (2) have less than 40% real-time coverage, whereas Links (3) and (4) have more than 95% due to SPS Test Article II being in low earth orbit and the good coverage given by TDRSS.

Data Management

The subsystem described in Section 2.2.3 is essentially the same as required on this satellite with the exception of the data bus which, because of its considerably shorter routing requirements, will permit the use of either fiber optic or metallic buses. Routing of cables may parallel the power harnesses although they would be separated by the width of the main support structural beams.

3.2.4 ATTITUDE AND VELOCITY CONTROL SUBSYSTEM

Summary

The main features and characteristics of the attitude and velocity control subsystem (AVCS) are summarized in Figure 3.2-11.

The AVCS is designed to perform several post-construction functions. It controls the vehicle's attitude, points the microwave antenna, controls orbit transfer maneuvers, and regulates the vehicle velocity to maintain proper spacing with the co-orbiting rectenna.

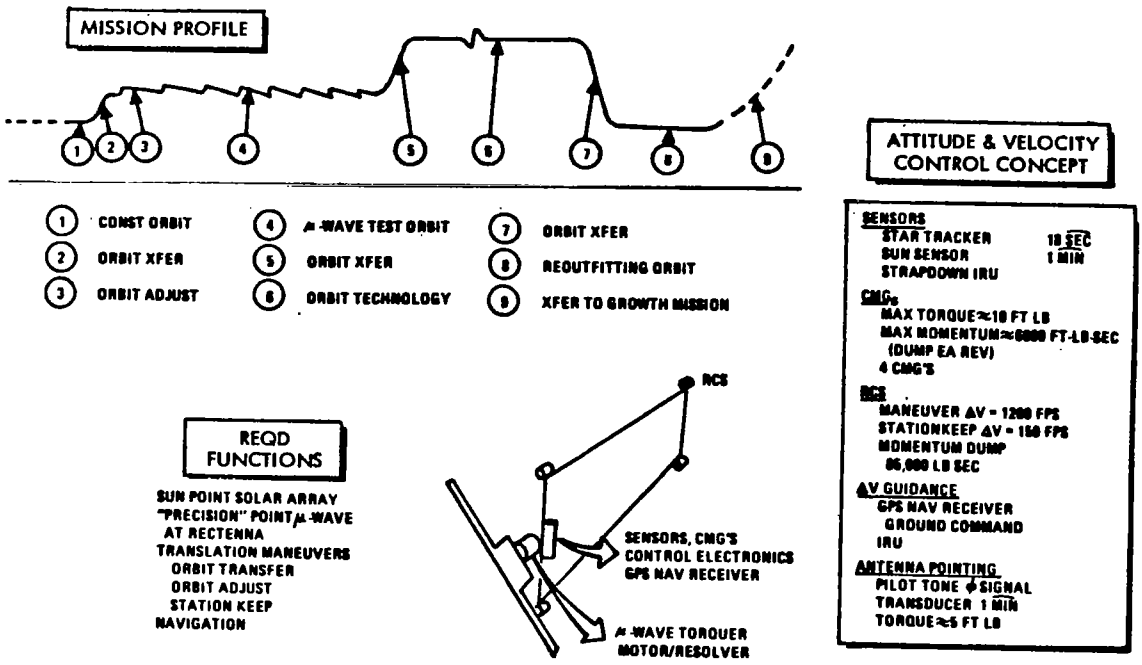

Figure 3.2-11. AVCS Summary—SPS Test Article II

The AVCS is designed to perform during the following phases of flight following construction and checkout: orbit transfer from the 250-nmi construction orbit to the 300-nmi operational orbit, six months of antenna testing, transfer from the operational orbit to a 400-nmi holding orbit, a prolonged period in storage, and transfer back down to the 250-nmi construction orbit. Subsequent flight phases, starting with reoutfitting the vehicle for another mission, are not considered here.

A primary function of the AVCS is to control the angular orientation of the SPS Test Article II. The attitude control requirements are different for each flight phase, and all phases (orbit transfer, experiment operation, and storage) must be considered in selecting an attitude control scheme.

Details of the AVCS are presented in Figures 3.2-12 and -13. The control system consists of an attitude reference system (Figure 3.2-13) and four CMG's in a conic configuration. The control moment gyros (CMG's) are single-degree-of freedom devices, the characteristics of which are summarized in Figure 3.2-12. The precision attitude reference is comprised of the inertial reference unit (IRU) and star tracker. The information from the IRU and star tracker is processed by the attitude reference algorithm which provides attitude and attitude rate signals used to generate the CMG commands. The sun sensor is used during attitude acquisition to initialize the star tracker.

AVCS Requirements

An important consideration in selecting a preferred attitude control concept is the required orientation accuracy. Two attitude control requirements must be met. The solar array must be oriented toward the sun, and the bearing

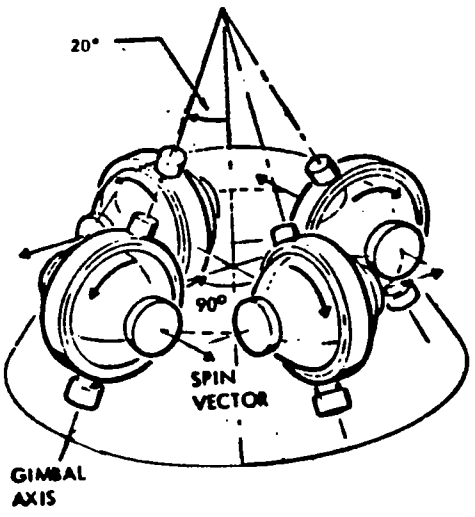

CHARACTERISTICS OF EACH CMG	
• CMG WEIGHT (BASE GIMBAL INCLUDED)	195 LB
• ANGULAR MOMENTUM	1600 FT-LB-SEC
• POWER REQUIREMENTS	
PEAK GYRO INPUT POWER	50 W
PEAK DURING RUN-UP	200 W
STEADY-STATE RUNNING	40 W @ 5300 RPM
• WHEEL OPERATING SPEED	7000 RPM
• SPIN BEARINGS BALL BEARINGS	204H DF PAIR
• TORQUER OUTPUT	15 FT-LB
CMG SIZE	40.1×27.0×30.5 IN.
• TOTAL WEIGHT (INCL. ELECTRONICS)	206 LB

Figure 3.2-12. CMG's for Test Article II Attitude Control

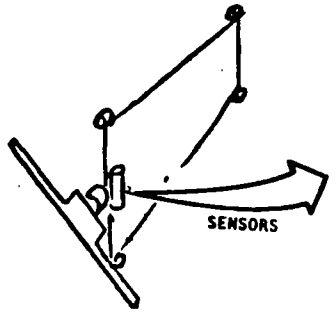

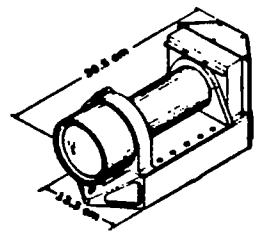

STAR SENSORS

TYPE	TRACKER
FOV	8×8 DEG
POWER	4 WATTS
ACCURACY	10 SEC (1σ)

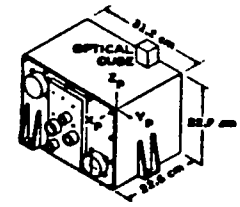

INERTIAL REFERENCE UNIT

POWER	7.5 W/CHANNEL
RANDOM DRIFT	0.015 DEG/HR (3σ)

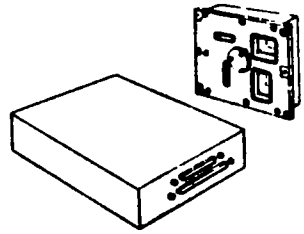

TWO-AXIS SUN SENSOR

FOV	±32 DEG
POWER	2.5 W
RESOL.	<15 SEC
STAB.	1 MIN

Figure 3.2-13. Sensors for Test Article II Attitude Control

axis of the microwave antenna must be oriented so that the antenna can be accurately pointing toward the co-orbiting rectenna. These requirements are satisfied by aligning the long axis of the vehicle perpendicular to the orbit and orienting the solar arrays toward the sun with accuracies listed in Figure 3.2-14. The requirements are (1) roll, ±5°; (2) pitch, ±8°, and (3) yaw, ±3°; and (4) microwave antenna pointing control, 13 arc-min.

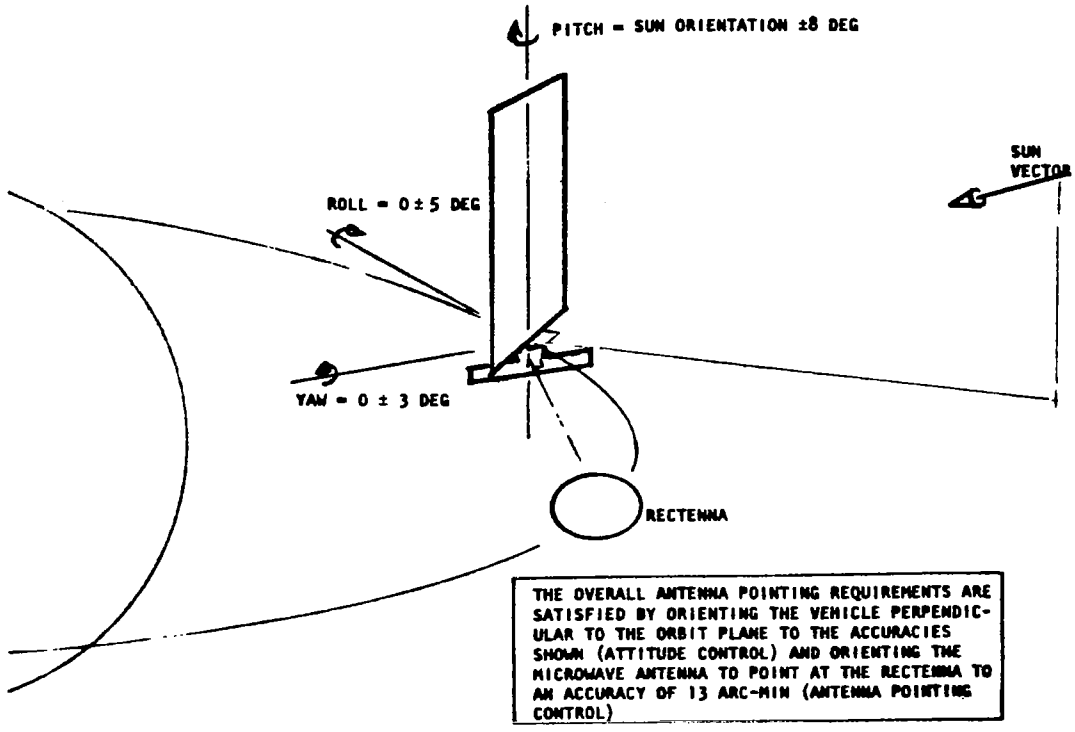

Figure 3.2-14. Attitude Control Requirements for SPS Test Article II

The control system selected achieves pointing accuracies less than those required. Control of the antenna pointing attitude to an accuracy in arc-sec is achieved by the attitude reference system. A three-axis CMG control system is a high-accuracy system with pointing accuracies of 0.01-0.1° easily achievable, for the antenna.

AVCS Definition

Attitude Control

An important consideration in determining the control system design is the environmental disturbance torques. The major disturbances—gravity gradient, aerodynamic and solar pressure—are illustrated in Figure 3.2-15. These torque-time histories serve as the basis for AVCS design.

Control wheels can be used in a variety of ways. A logical concept for the SPS Test Article II is to store (exchange) the angular momentum caused by cyclic disturbance torques and rely on the reaction jets to counter the secular

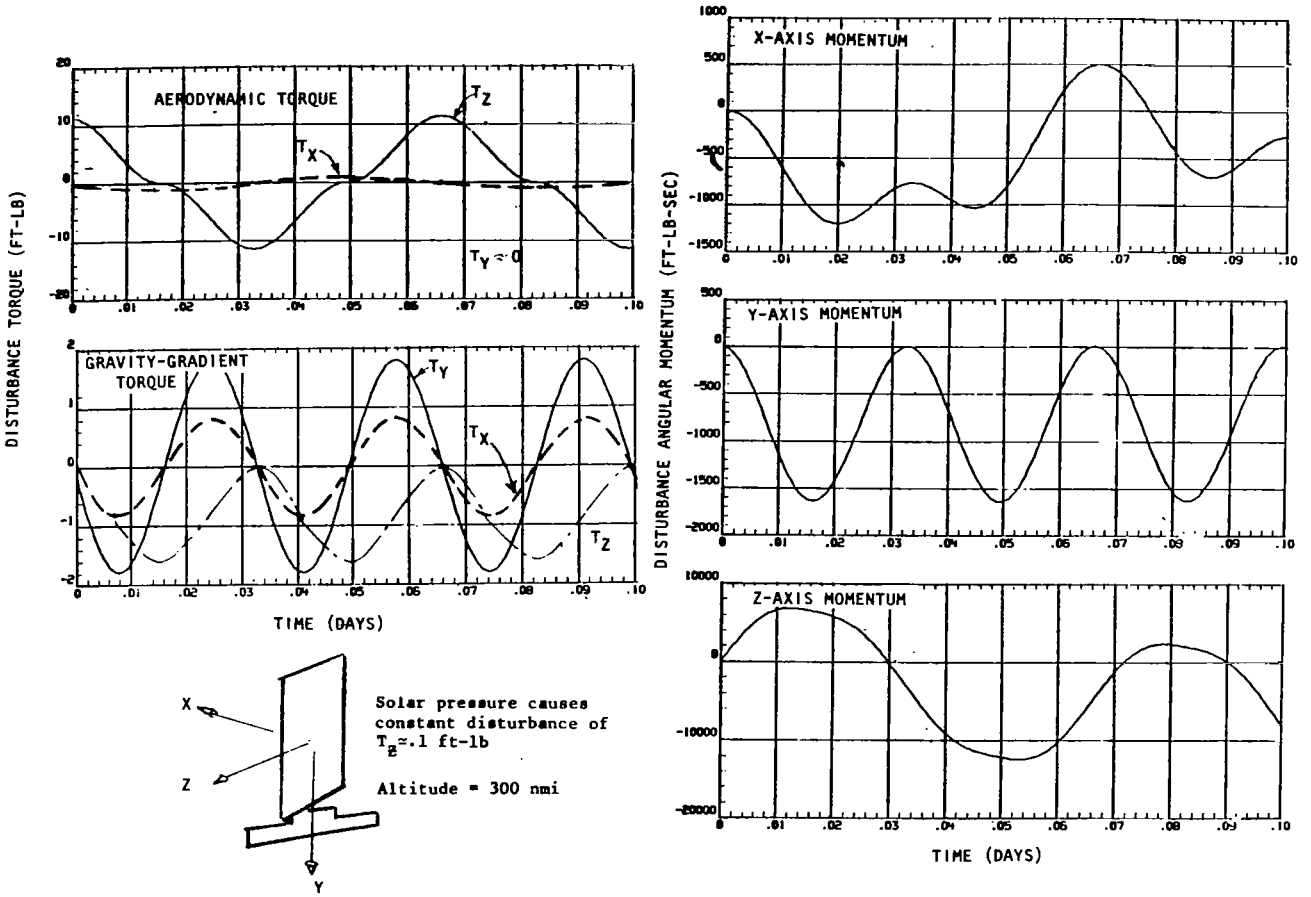

Figure 3.2-15. Environmental Disturbances—
SPS Test Article II

components of the environmental torques. With this concept, the propellant requirements for six months of attitude control are 70 kg (150 lb). The CMG configuration capable of exchanging the environmentally induced cyclic momentum was illustrated in Figure 3.2-12. CMG's have some attractive features. They are the only devices presently available with very large momentum storage capability; and they have much larger torque capacities than momentum wheels, enabling them to settle transient disturbances faster.

The combination of CMG's to exchange cyclic momentum and APS jets to control the secular momentum buildup probably costs more than all-jet systems, but it provides more capability which may be required after the vehicle is reoutfitted for subsequent missions.

Antenna Pointing

Two control functions combine to aim the microwave antenna at the rectenna. The attitude control system orients the antenna's bearing axis perpendicular to the orbit plane to within 5° in roll and 3° in yaw (Figure 3.2-14). Then, the pointing control system orients the antenna about the bearing axis to point it toward the rectenna to an accuracy of at least 13 arc-min.

Fine pointing of the antenna is performed by a continuous drive torquer which nulls the pointing error measured by a directional antenna. The directional antenna is part of the microwave antenna payload. It receives a pilot signal transmitted from the rectenna at two locations displaced from one another. Angular errors much less than 13 arc-min are sensed by comparing the phase differences between the two signals.

An angle measurement transducer is included in the pointing control system to provide antenna angle relative to the solar array. The transducer, together with the star sensor/IRU is used for open-loop pointing of the antenna with sufficient accuracy to get within the directional antenna's field of view. The angle transducer is also available for controlling the antenna's relative orientation during other phases of flight.

The drive motor must have sufficient torque to overcome friction and environmental disturbance torques, and to accelerate the antenna to track the rectenna. A peak drive torque capacity of 7.0 N m is sufficient as indicated in Table 3.2-8.

Table 3.2-8. Antenna Pointing Drive Torque Requirements, SPS Test Article II

	Torque (N·m)
Friction	1.0
Gravity gradient	0.6
Aerodynamic	0.1
Solar pressure	Negl.
Tracking acceleration	3.0
50% contingency	2.3
Torque requirement	7.0 (5.2 ft-lb)

Orbit Transfer and Maintenance

The AVCS must perform guidance and attitude control functions during orbit transfer and velocity corrections for orbit maintenance. Most of the components required for these functions are required for other functions and have been discussed previously.

The additional equipment requirements include hardware to determine the vehicle's orbital parameters and its position relative to the rectenna, as well as sensors to measure the velocity change caused by orbit transfer thrusting maneuvers. The most effective way to satisfy these requirements is to use the Global Positioning System (GPS) for navigation data.

GPS navigation data are provided by a small antenna, which receives information from four GPS spacecraft, and on-board electronics to process data. This system will locate the SPS Test Article II and the rectenna to an accuracy of less than 10 m.

Orbit transfer is achieved by first computing the required ΔV maneuver parameters on the ground, using GPS navigation data and vehicle attitude data. Maneuver parameters (attitude and velocity change) are transmitted to the vehicle. Then, the AVCS controls orbit transfer by using angle and angle rate data from the IRU together with the APS jets and CMG's to maintain the proper attitude.

Control System/Structural Dynamics Interaction

Special care is required to prevent unstable interactions between the AVCS and the vehicle's soft structure. The easiest method to ensure stable operation is to design the structure to be stiff when compared to the control system. Analyses for many other space vehicles indicate that stable operation is achieved if the vehicle's fundamental vibration frequency is at least 5 to 10 times greater than the control system's characteristic frequency. When sufficient structural stiffness does not exist, the AVCS control logic can be shaped to stabilize the low-frequency vibration modes. However, this approach can be risky when more than a few modes must be stabilized. The main concern grows out of the inability to accurately identify and measure motions of more than a few low-frequency modes.

The approach taken here is to develop adequate separation between the structural and control frequencies wherever possible and to actively stabilize low-frequency modes when separation is not possible. This approach is examined in the following text for the AVCS functions most likely to couple with structural vibrations—vehicle attitude control and antenna pointing during the microwave experiment.

Attitude Control

The potential for unstable interactions between the attitude control loops and the SPS test article's structure is again examined by comparing frequencies.

The lowest frequency mode liable to couple with the pitch control loop is a torsional mode at 0.010 Hz, and the mode most likely to couple with the roll and yaw control loops is the first transverse bending mode at 0.029 Hz. It is these frequencies which must be compared with the control frequencies.

The control frequencies of a simple attitude control system (i.e., control loops with rate and position feedback only) are established by two considerations—transient and steady-state response characteristics. The transient response requirements are easily met by assuring that the control frequency is at least two times greater than the fastest disturbance torque. A control frequency of 7×10^{-4} Hz ensures that the attitude control system can compensate for environmental disturbances without a significant transient response. A somewhat higher frequency is desirable to settle the transients caused by firing jets, but a frequency less than one tenth of the structural frequency is adequate.

The control frequency must also provide enough "stiffness" so that the attitude errors caused by the environmental torques do not exceed the allowable

values (5° in roll, 3° in yaw, and 8° in pitch). The required control stiffness and the vehicle's mass moment of inertia then establish the control system frequency. The control frequency requirements for adequate steady-state response are listed in Table 3.2-9 along with the transient control frequency requirement and the structural frequencies. The maximum control frequency requirement is compared to the structural frequency in the right-hand column. Note that a frequency separation greater than 10 can be achieved. Reasonable structural frequency requirements are: first torsional mode, >0.007 Hz; and first bending mode, >0.007 Hz.

Table 3.2-9. Attitude Control Frequency Separation

Axis	f_c, Control Frequency Requirement (Hz)		f_s, Structural Frequency (Hz)	f_s/f_c
	Steady State	Transient		
Roll	$\geq 4.4X10^{-5}$	$\geq 7X10^{-4}$	0.029	≤ 41
Pitch	$\geq 3.7X10^{-4}$	$\geq 7X10^{-4}$	0.010	≤ 14
Yaw	$\geq 1.7X10^{-4}$	$\geq 7X10^{-4}$	0.029	≤ 41

Antenna Pointing Control

The microwave antenna pointing control system can excite vibrations of the antenna and the solar array. However, only modes which can be excited by the drive motor and which can be sensed by the directional antenna (which is mounted on the microwave antenna) can interact with the control system.

The lowest frequency mode computed herein is a 0.010 Hz torsional mode of the vehicle, which nominally does not displace the directional antenna. However, stiffness and mass asymmetries, as well as drive axis friction, can cause a small amount of motion of the directional antenna in that mode. Thus, good design practice dictates that the pointing control frequency be less than 0.010 Hz. Because this motion can only occur as a second-order effect, a closer frequency spacing of 5 is permissible ($f_c \leq 0.0020$ Hz).

Next, the control frequency required to point the antenna accurately is determined and compared with the foregoing requirement. Again, the control frequency is established by the antenna's inertia and the "stiffness" needed to overcome the environmental disturbances to point accurately. In this case, the control system must be stiff enough to balance the gravity-gradient torque, which increases as the long axis of the antenna is rotated off of its local vertical orientation, plus the aerodynamic and solar pressure disturbances. The gravity gradient torque calculation is complicated because the maximum offset pointing angle is related to how well the orbit of the SPS test article is matched to that of the rectenna.

The control frequency required to achieve a residual error of 13 arc-min is plotted as a function of the altitude error between the two vehicles in Figure 3.2-16. Notice that the frequency requirement ($f_c \leq 0.0020$ Hz) is

satisfied when the altitude error is kept to less than 5 km. Matching orbits to this accuracy are readily achievable, as discussed earlier.

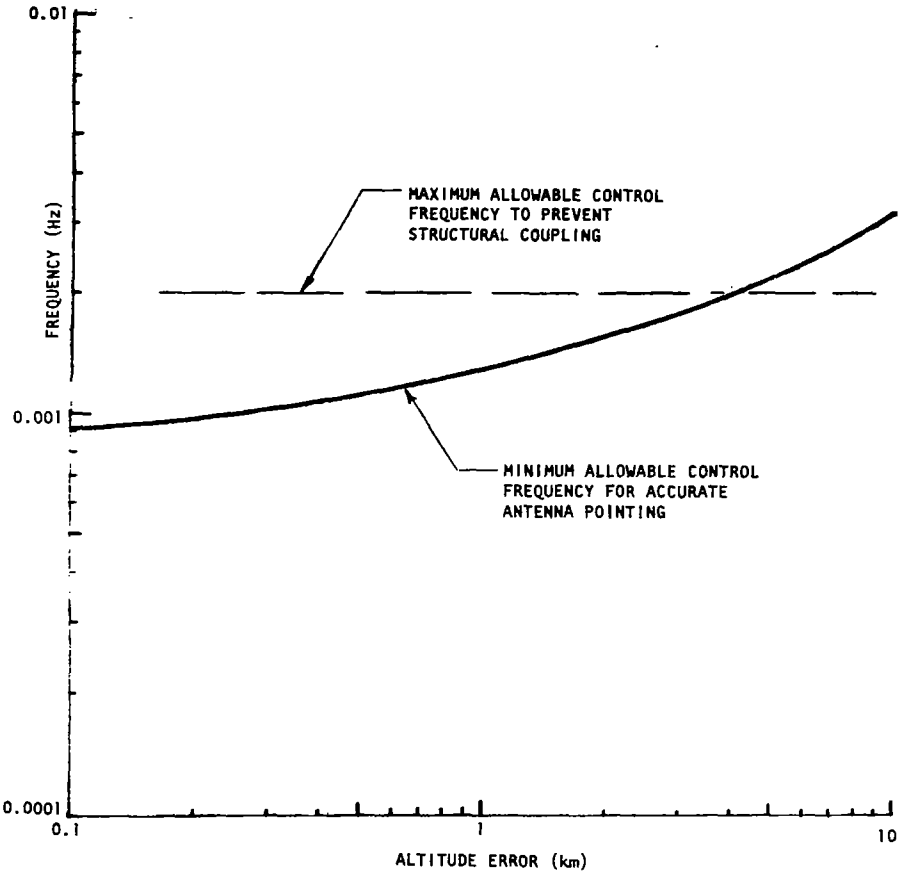

Figure 3.2-16. Antenna Pointing Control Frequency Requirements, SPS Test Article II

3.2.5 AUXILIARY PROPULSION

An auxiliary propulsion system (APS) is provided for control of SPS Test Article II in low earth orbit (LEO) during a six-month life, during which the microwave antenna is tested. The APS provides control for both translation maneuvers and for attitude orientation control in conjunction with the attitude and velocity control subsystem (AVCS).

Summary

The key features of the APS are summarized in Table 3.2-10. The APS module is illustrated in Figure 3.2-17.

Table 3.2-10. APS Summary

Propellants	N_2O_4/MMH
Pressurization Gas	Helium
Total Impulse	15.1 x 10^6N-sec (3.4 x 10^6 lb-sec)
Number of Modules	4
Number of Thrusters	20
Thrust, Each	
12 Thrusters	111 N (25 Lbf)
8 Thrusters	22 N (5 Lbf)
Total Weight	7,196 kg (15,830 Lb)

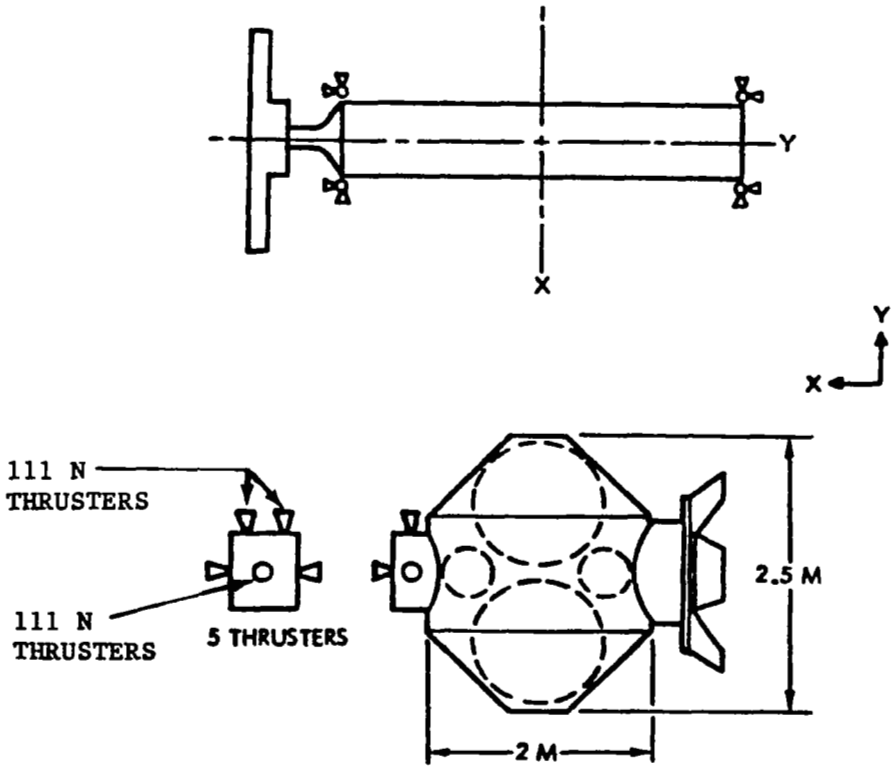

Figure 3.2-17. APS Module

Requirements

The translation functional requirements consist of (1) low altitude orbit transfer, (2) rendezvous with the rectenna, and (3) stationkeeping for six months. The APS attitude control functional requirements consist of periodic thrusting for momentum dumping of the control moment gyros (CMG's) about the pitch, yaw, and roll axes. These requirements in terms of delta-V (velocity increment) and total impulse are shown in Table 3.2-11. The delta-V for the orbit transfer maneuvers includes a 6% increase for low T/W [0.01 N/kg (0.001 lb_f/lb_m)] effects. The initial orbit transfer maneuver transports the platform from the construction orbit altitude up to operational test altitude [556 km (300 nmi)]. After the microwave test, the platform is transported to a holding orbit [741 km (400 nmi)] where it is parked until required; then later, the platform is returned to the construction altitude [463 km (250 nmi)] for reoutfitting, refurbishment, and resupply in preparation for a subsequent mission in GEO.

Table 3.2-11. APS Requirements

Function	Requirement	
	Delta-V	
	M/Sec	(Ft/Sec)
1. Translation Maneuvers		
a. Orbit Transfer	54.7	(180)
b. Rendezvous W/Rectenna	30.5	(100)
c. Stationkeeping 6 Months, 556 km (300 nmi)	45.7	(150)
d. Orbit Transfer, 544 to 741 km (294 to 400 nmi)	116.4	(382)
e. Orbit Transfer, 741 km to 463 km (400 to 250 nmi)	164.9	(541)
TOTAL TRANSLATION	412.2	(1,353)
	Total Impulse	
	N-Sec	(Lb-Sec)
2. Attitude Control CMG Momentum Dump (6 Months)		
a. Roll	36,862	(8,287)
b. Yaw	336,646	(75,681)
c. Pitch	2,633	(592)
TOTAL MOMENTUM DUMP	376,141	(84,560)

Description

A 20-thruster configuration, grouped in four modules with propellants and located at the four corners of the rectangular-shaped platform, provides an APS that meets the mission and functional requirements. The corner locations were selected to provide maximum length moment arms and to avoid thruster exhaust impingement on the vehicle structure and components.

Figure 3.2-17 illustrated a typical APS module containing an oxidizer tank, a fuel tank, and helium pressurization tanks located within a structural shell that acts as a micrometeoroid shield and provides for thermal control. On one side of the APS module, an assembly of five thrusters are located, with a docking port on the opposite side for mating and attachment to the platform structure.

The assembly of five thrusters (per module) consists of three 111 N (25 lb_f) thrusters and two opposing 22 N (5 lb_f) thrusters. Operation of the four-module APS consists of firing four 111 N thrusters at a time for low altitude orbit transfer, two 111 N thrusters at a time for yaw axis CMG momentum dump and stationkeeping, and two or four 22 N thrusters for pitch and roll CMG momentum dump.

Storable propellants (N_2O_4/mmH) were selected for the APS to be compatible with long-duration propellant storage for the six-month mission and still provide reasonable performance. Bi-propellant APS thrusters are being qualified that provide a steady-state specific impulse of 2750 N-sec/kg (280 sec) to 2893 N-sec/kg (295 sec). These performance values were used in sizing propellant quantities since relatively long pulse durations are required, with 90% of this propellant required for translation.

APS propellant requirements were based on a platform weight of 31,300 kg (69,000 lb) without APS and with APS, a platform weight to 38,600 kg (85,000 lb). A weight summary of the APS module is shown in Table 3.2-12.

Table 3.2-12. APS Module Weight Summary

Weight per Module	kg	lb
Propellant	1309	2,881
Inert	490	1,076
Total	1799	3,957
Total Weight (4 modules)		
Propellant	5239	11,525
Inert	1957	4,305
	7196	15,830

3.2.6 STRUCTURES

Summary

This section describes the structural analysis performed in support of the definition of the SPS Test Article II system, evaluation of the resulting structural system credibility, and for establishment of the significant structural requirements delineated in Section 3.1.5.

SPS Test Article II Structure Description

The SPS test article basic structure configuration is presented in Figure 3.1-11, using as an example (for illustration), a "ladder" configuration. The solar blanket support structure is 215 meters long and 20 meters wide to which the solar blanket panels are attached. The blankets are stretched to a minimum tension of 17.5 N/m (0.10 lb/in.) between the six laterals provided as shown. The four APS modules are mounted to the extremities of the end bay 20-meter laterals. The struts shown are provided to limit lateral deflection, during APS longitudinally directed thruster firing, to values compatible with the solar array blanket tension design.

A system support housing structure and bridge fitting are provided at the extremities of the solar blanket structure. The system support housing structure contains the control moment gyros, electrical power conditioning distribution panels, TT&C unit, battery packages, and docking port for attachment of the rotary joint. The joint delivers the electrical power and data management cables to the microwave antenna. The bridge fitting contains the docking port for fixture mounting of the solar electric pods for geosynchronous orbit transfer. While providing these required functions, the system support housing and bridge fitting also serve (for the ladder configuration) as strongbacks to increase the configuration torsional stiffness. The strongback bending stiffness significantly supplements the in-plane Vierendahl behavior of the ladder achieved by welding the laterals to longitudinal members at the four corners of each lap joint (Figure 3.2-18).

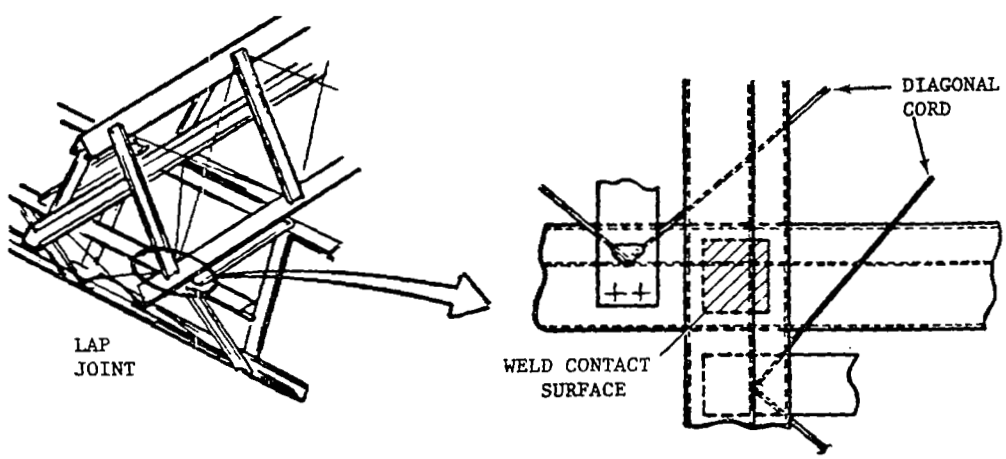

Figure 3.2-18. Lap Joint Design Features

The example structure also contains the discrete system of electrical power and data management cables, J-boxes, and EDC switching boxes.

Pertinent to the example structure, the ladder is extremely simple to construct, yet is structurally suitable since it is fabricated in the benign environment of space, and then subjected only to the low levels of loading described herein. The ladder is comprised to two longitudinal beams (215 m long) spaced 10 m apart and interconnected by a total of six lateral beams. The two longitudinal and six lateral beams shown are the baseline machine-made beams currently being developed by General Dynamics under Contract NAS9-15310 (Figure 3.2-19), except that the diameter of the diagonal cords (1 mm) has been increased to 2 mm (0.080 in.). Also, the cord pretension has been appropriately increased from 45 to 180 N (40 lb) to maintain the same cord pretension unit stress. Discussion with General Dynamics has confirmed the suitability of these modifications.

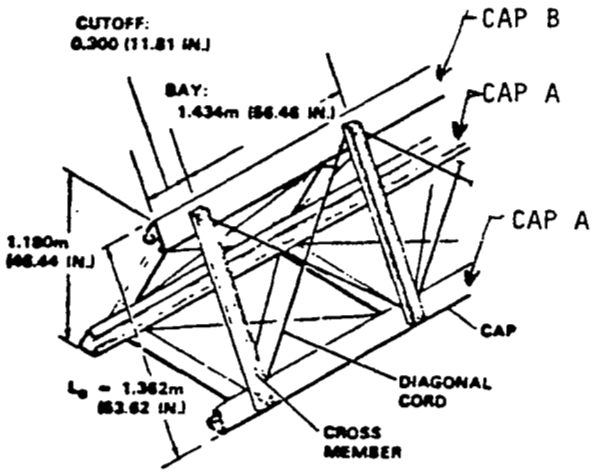

Typical Beam

Structural Characteristics

A	$4.43\times10^{-4}m^2$ (0.687 $in.^2$)
I	$1.205\times10^{-4}m^4$ (289.7 $in.^4$)
AE	63.41×10^6N (14.26×10^6 lb)
EI	$17.25\times10^6 Nm^2$ (6.014×10^9 lb-in^2)
GJ	$44.4\times10^3 Nm^2$ (3.87×10^6 lb-in^2)
KAG	89×10^3N (20×10^3 lb)

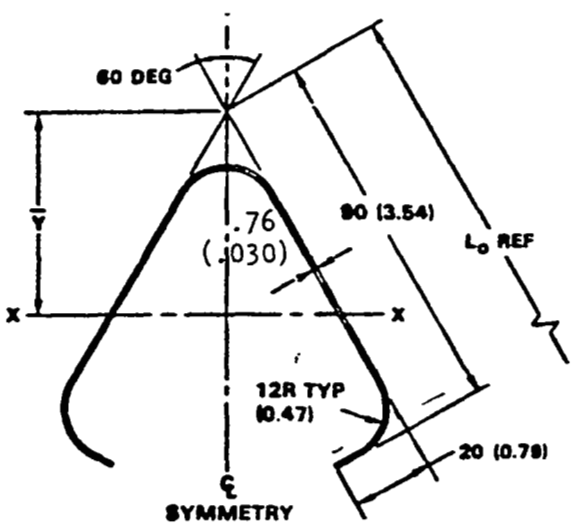

Cap Section

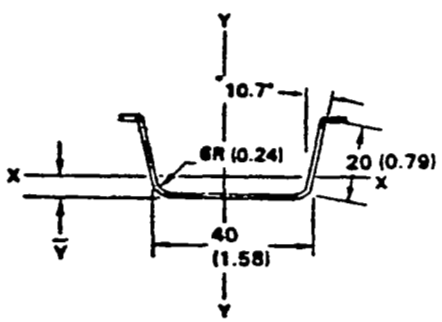

Cross-Member Section

Figure 3.2-19. Baseline Beam Structural Characteristics

SPS Test Article II Structure Concept Derivation

The SPS test article structural configuration was derived on the basis of the following:

- A solar blanket area of 4000 m^2 (520 kW) was required to provide power for the microwave antenna (279 kW) to accomplish the test objectives stated in Section 3.2.1.
- During construction from the orbiter-mounted fixture, installation of the solar blankets utilized the RMS with its reach limitation directing the structure width to essentially 20 m and a blanket length of 200 m.
- Satisfaction of the strength and stability, and minimum modal frequency requirements was possible with a structure of minimum space construction complexity.

Associated with the foregoing, iteration between the APS maneuver requirements of orbit transfer and attitude stabilization resulted in use of thrust levels compatible with the ladder structure capability, and thruster burn time and life requirements.

SPS Test Article II Requirements

The significant structural requirements established by the test article mission requirements, and equipment requirements that are pertinent to the overall solar blanket support structure, are listed below.

Solar Array Blanket Tension Loading

The structure must have sufficient rigidity to maintain a minimum limit solar array blanket pretension loading of 17.5 N/m (0.10 lb/in.) in each of the 4-m-wide blankets that comprise the 20-m-wide array.

Thermal Gradients

The structure must sustain the loads resulting from thermal gradients throughout the structure with the resulting deflections additional to construction induced deviations from straightness.

Stationkeeping and Attitude Control Loads

The structure must be capable of sustaining the orbit transfer, stationkeeping, and attitude control loads delineated in Table 3.2-13.

Control System Requirements

The structural stiffness of the configuration must be compatible with the control system design. The design of the control system has torsionally decoupled the solar array configuration from that of the antenna. The minimum

modal frequencies of the solar blanket array and microwave antenna structures must be greater than 0.0040 Hz.

Table 3.2-13. Stationkeeping and Attitude Control Loads

CASE / LOAD	LOAD CONDITIONS (NEWTONS)											
	STATIONKEEPING								ATTITUDE			
	1	2	3	4	5	6	7	8	9	10	11	12
1_x	222											
1_y			111							111		
1_z							22		-22			22
2_x	222											
2_y				111							111	
2_z							22		-22			-22
3_x		222										
3_y					111						111	
3_z								22	22			+22
4_x		222										
4_y						111				111		
4_z								22	22			-22

TIME DELAY BETWEEN FIRST AND LAST LOAD NOT TO EXCEED .020 SECOND.

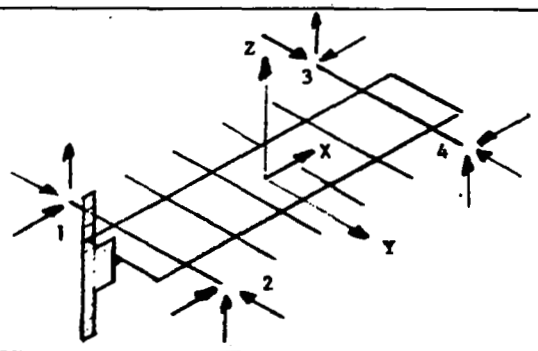

Miscellaneous Loads

The load sources contained herein for completeness have been reviewed and/or analyzed and found to be non-critical and, for reporting convenience, are contained herein. A "soft dock" concept utilizing the RMS will be employed.

Prior analyses for this concept (ATL/LSS program) indicated the loads will be less than the thruster loads shown in Table 3.2-13.

For transfer to synchronous orbit, the SPS system imposes loads that are negligible. Gravity-gradient, solar pressure, and atmospheric drag loads acting upon the structure directly are not significant.

Dimensional Stability

None.

Structural Analyses

The structural analyses performed to verify the credibility of satisfaction of the foregoing requirements, through demonstration of the suitability of the ladder structural configuration are delineated herein. All these analyses utilize a safety factor of 1.5 applied to limit load.

Solar Array Blanket Tension Loading

The structure must have sufficient rigidity to maintain a minimum limit solar array blanket pretension loading of 17.5 N/m (0.10 lb/in.) in each of the 4-m-wide blankets that comprise the 20-m-wide array. The ladder structure, therefore, allowing for thermal effects (see later section) must be capable of sustaining the resulting compression due to a peak limit blanket pretension loading of 26.2 N/m (0.15 lb/in.) across each 4-m blanket as discretely imposed during construction and in the final constructed state. The initial diagonal cord pretension-induced compression of the basic beam is, for convenience, included in this requirement. The pretension is 180 N (40 lb) for each cord.

Since the example design utilizes the baseline beam being developed by General Dynamics (except for the diagonal cord modifications), Figure 3.2-19 was included to present the basic beam structural characteristics. The characteristics shown are for the modified design (2 mm diagonal cords). The analysis presumes, pending a static test of the prototype beam, that the individual cap ultimate load capability is 6583 N (1480 lb), i.e., the value quoted in Reference 1. It is pertinent to note the feasibility of the concept is not dependent on that value since the basic cap can be significantly strengthened, if necessary, by increasing the basic effective cap gauge from 0.75 mm (0.030 in.) to 1.25 mm (0.050 in.). The associated structure weight increase of 225 kg (500 lb) with the 1.25 mm gauge would represent approximately 0.60% of the total low earth orbit SPS weight.

Euler Column Analysis

The total limit compression loading on each beam due to the combined limit pretension of 26.2 N/m (0.15 lb/in.)* the diagonal cord pretension of 180 N per cord (40 lb), and an APS total thrust of 444 N (100 lb) per beam (Case 2, Table 3.2-13) is shown on Figure 3.2-20. While the inertial reaction to the

**For this design, a pretension of 26.2 N/m ensures the minimum pretension of 17.5 N/m (see later discussion).*

APS thrust is primarily distributed over the array length, the total reaction is shown at the extreme end for convenience (and conservatism). The total limit compression, due to pretension of the six diagonal cords per bay of 748 N (168 lb), is included only for local cap stability. It does not affect Euler column capability nor produce deflection magnification since it is an internal load with each bay a closed-force system. The compression load from blanket tension (267 N) cannot produce deflection magnification, but its affect on Euler stability is questionable; hence, it is included in the analysis.

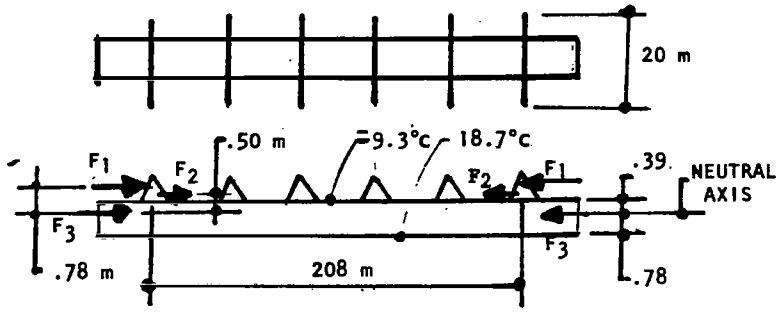

NOTE: F_1 includes dynamic amplification factor of 2.

F_1 is RCS thrust load = 444 N (100 lb)
F_2 is solar array tension load = 267 N (60 lb)
F_3 is diagonal cord tension load = 748 N (168 lb)
Temperatures quoted are relative to neutral axis.

Figure 3.2-20. Euler Column Loading Diagram (per Longitudinal)

The Euler column capability per longitudinal is determined from Reference 2 which includes the effect of shear deformation.

$$P_{cr} = \frac{\pi^2 EI}{\ell^2} \quad \frac{1}{1 + \frac{\pi^2 EI}{\ell^2} \frac{1}{A_d E \sin\phi \cos^2\phi}}$$

where $$\frac{\pi^2 EI}{\ell^2} = \frac{\pi^2 (17.25 \times 10^6)}{(208)^2} = 3935 \text{ N } (884 \text{ lb})$$

$$P_{cr} = 3935 \frac{1}{1 + \frac{3935}{4(71,200)(.35)}} = 3785 \text{ N } (850 \text{ lb})$$

To assure no significant magnification of load and deflection, the permissible ultimate axial load is limited to one half of the determined value; hence, for the total configuration this value is 3785 N (850 lb), and is greater than the total ultimate applied load of 2136 N (480 lb).

The combination of loads and thermal gradients is analyzed more rigorously as follows.

Referring to Figure 3.2-20 and Reference 2, the peak deflection y at the center of a beam column is determined from

$$y = \frac{M_T \ell^2}{8EI} \quad \frac{2(1 - \cos u)}{u^2 \cos u}$$

where $$u = \frac{\ell}{2} \sqrt{\frac{P}{EI}}$$

hence $$u = \frac{208}{2} \sqrt{\frac{712 \times 1.5}{17.25 \times 10^6}} = .818$$

Accounting for shear stiffness affects, u = 0.834; hence, y = 0.00439 M_T, where M_T is the total equivalent end moment due to the offset loads shown and the existing thermal gradient. For this condition M_T = 875 N.m (7747 lb-in.), for which the peak deflection is 0.38 m (15 in.). The maximum ultimate moment of 1126 N·m, in conjunction with the total ultimate axial load of 2190 N, induces a peak cap load of 1209 N (272 lb) on Cap A (Figure 2.3-19) which is well below the design capability. The effects of a fabrication deviation of 0.100 m will not be deleterious. The separate but additional loading due to APS firing is discussed later.

Cord Pretension Considerations

The intent of this section is to demonstrate the suitability of the selected diagonal cord pretension of 180 N, insofar as maintenance of pretension. The worst possible case visualized is a cord temperature increase of 11°K (200°F) concurrent with compression in the cap and vertical shear across the element (Figure 3.2-21). Although the peak 6583 N (1480 lb) compression will not occur at the same station as the peak shear, the analysis conservatively assumes that to occur.

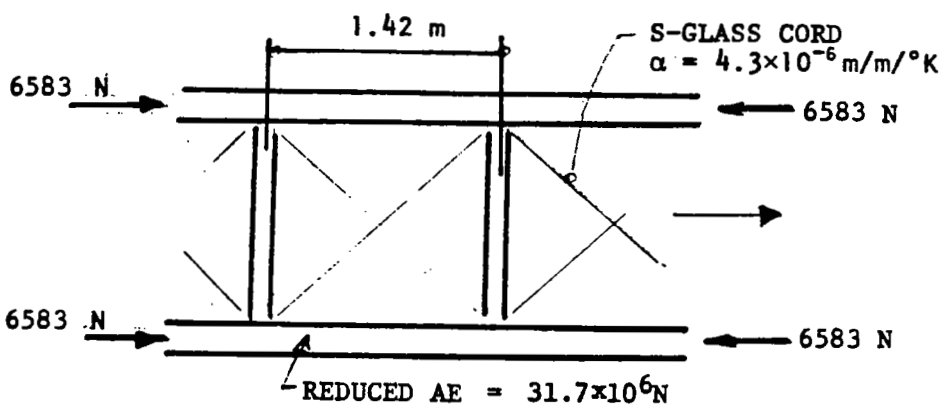

Figure 3.2-21. Diagonal Cord Configuration

- The cap shortening (6583 N compression) = 0.889 mm
- Cord thermal-induced length change along X-axis = 0.584
- Cord shear-induced length change along X-axis = 0.889

Peak relative length change = 2.36 mm

- Initial diagonal cord elongation along X-axis = 3.10 mm

Remaining elongation = 0.74 mm

The initial pretension appears adequate since creep is not expected to be significant for the stress level in the glass which is approximately 3 percent of ultimate.

Solar Array Blanket Structure—Strain Compatibility

The design of the spring tension system to comply with the differences in strain between the solar array blanket and the longitudinal beams is beyond the present stage of study scope. However, the performed conceptual evaluation efforts are discussed as follows.

It is reasonable to assume the blanket expansion over half of the 40 m bay is $18.50\times10^{-6}\times111\times20 = 0.041$ m (1.60 in.). The shortening of the beams due to thermal variation and/or compression loading is negligible by comparison. For each 4-m width containing three tension springs each, each spring is initially loaded to 35 N (7.9 lb). Using a spring constant of 297 N·m (1.7 lb-in.), the initial stretch = 0.118 m (4.65 in.). The remaining tension equals

$$\frac{0.118 - 0.041}{0.118} \times 26.2 = 17 \text{ N·m } (0.10 \text{ lb-in.})$$

During a peak g-load, normal to the array, of 0.001 (conservative), the solar array blanket static response would be as follows:

Referring to Figure 3.2-22, a basic membrane calculation indicates a deflection of 0.116 m (4.6 in.). This is considered to be reasonable. Incidentally, the basic blanket natural frequency with the minimum tension is 0.042 Hz.

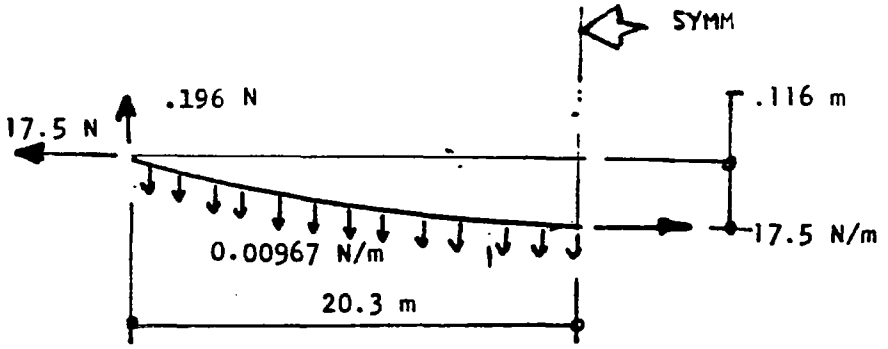

Figure 3.2-22. Solar Blanket Array Tension Loading

Along the same lines, it is very desirable for the lateral beams to be quite stiff to preclude tuning problems during blanket installation. An analysis of the lateral deflections (shear deformation predominates) of the beam indicated the following lateral deflection due to a limit tension of 26.2 N·m (0.15 lb-in.).

- Maximum cantilever tip deflection = 1.8 cm (0.70 in.)
- Maximum center span deflection = 1.8 cm
- Maximum deflection between 1.4-m support points = 0.51 cm (0.20 in.)

Modal Analysis

A modal analysis performed with the McNeal Schwendler version of NASTRAN upon the test article model shown in Figure 3.2-23 predicts first and second modal frequency values at 0.0104 and 0.0254 Hz. The next 25 modes have values of 0.039 to 0.043 Hz and represent (in contrast to the first two modes) the blanket behavior relative to the structure. The model contains the mass description and structural characteristics defined in Table 3.1-5 and Figure 3.2-19, with pretension of the cables (representing the solar blankets) to 17.5 N/m (0.10 lb/in.)

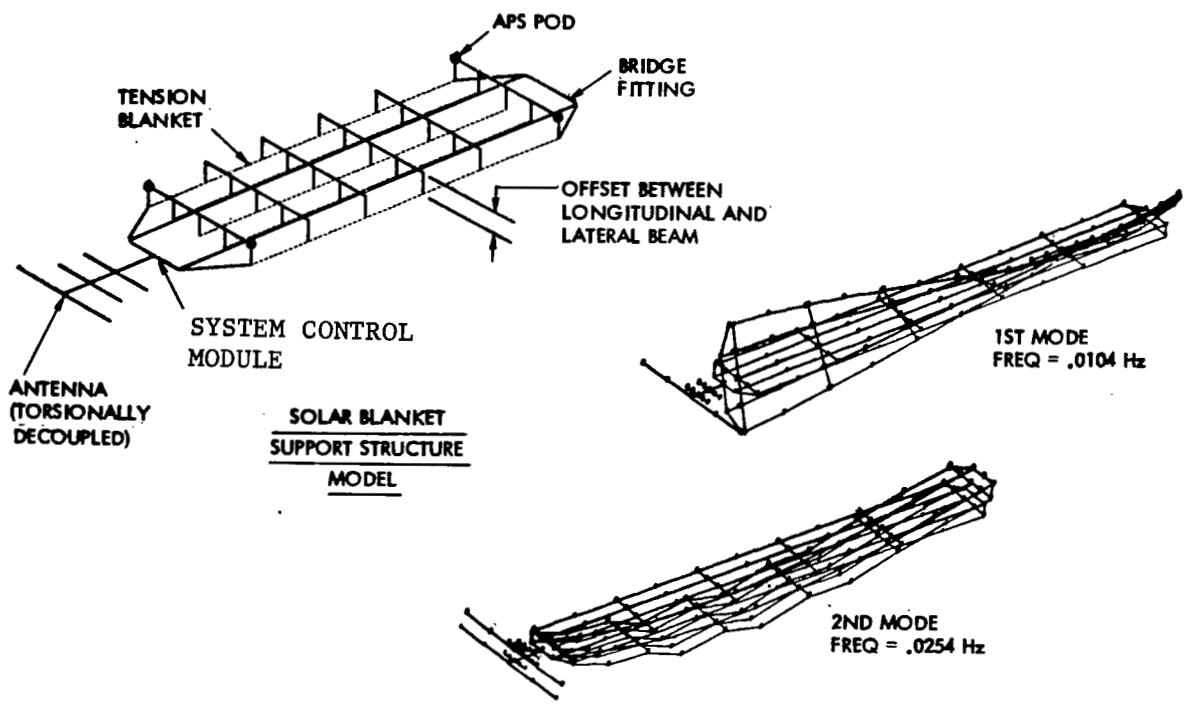

Figure 3.2-23. Solar Blanket Structure—Modal Analysis Results

Transient Analysis

In view of the significant torsional flexibility, the transient loads resulting from APS thruster time delay and thrust magnitude differences was of concern. A transient analysis of the two conditions shown in Figure 3.2-24

indicates a peak bending moment of 808 N/m (7147 lb/in.) which is well below the beam capability of 6470 N m. In this analysis, all of the beam bending and torsional moments were presented and reviewed. The significance is that the structural requirements presented in Section 3.1.5 are espected to be achievable in either deployable, erectable, or space construction designs.

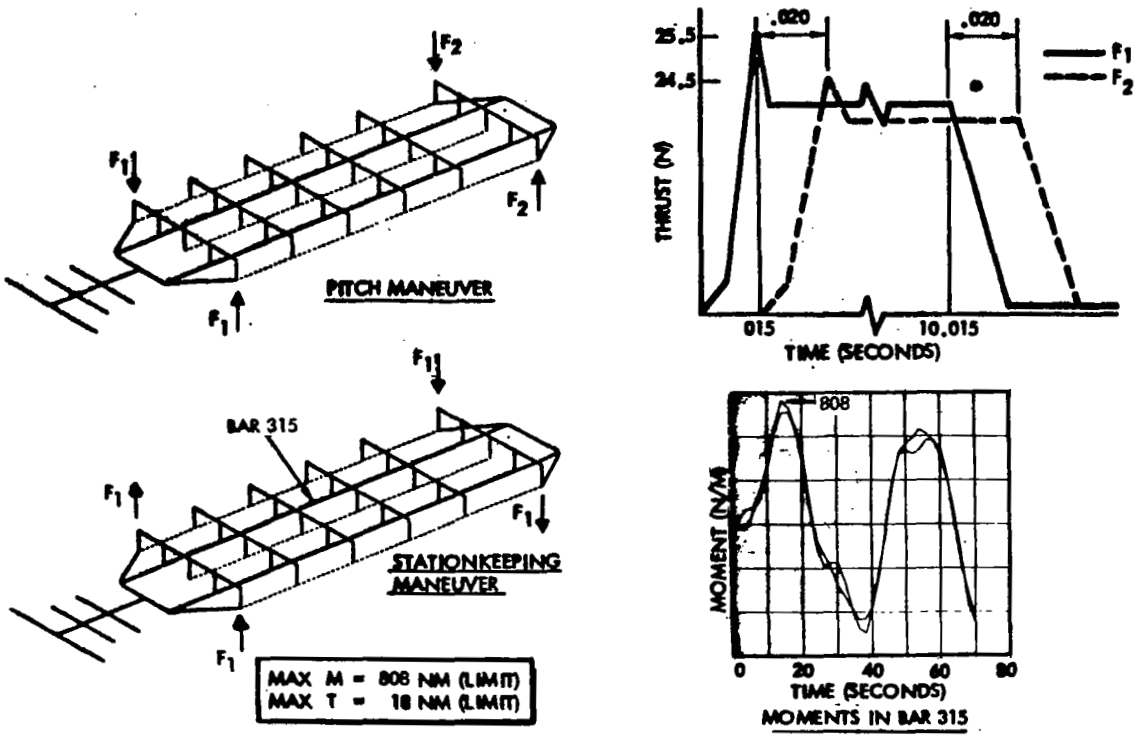

Figure 3.2-24. Transient Analysis Results

References

1. *Space Construction Automated Fabrication Experiment Definition Study (SCAFEDS)*, Convair Division, General Dynamics, CASD ASP77-0177 (26 May, 1978).

2. Timoshenko, S., *Theory of Elastic Stability*, New York, McGraw-Hill, Inc.

4.0 CONCLUSIONS

The basic study conclusions are presented below.

SPS TEST ARTICLE I

- Test article is a significant but "do-able" challenge. The fixture, constructed from the orbiter and capable of constructing the hexagonal frame and the control system, is an integral part of the challenge.

- The hexagonal frame is highly loaded (by space structures standards) with an ultimate stress of 17,000 psi. The design will, therefore, be primarily driven by the load and dimensional stability requirements, and not by systems installation requirements, which are minimal. Systems installation requirements will, however, be significant to the construction procedures.

- The hexagonal frame structure weight can vary from 50 to 75% of total satellite dry mass.

- Docking loads can be minimized to capability of structure. Of significance is the impact on construction of the additional parts for attachment of the docking ports.

SPS TEST ARTICLE II

- Structure is lightly loaded (ultimate stress, 3000 psi).

- Construction driven most by fabrication and equipment support accommodation.

- Berthing loads (using RMS) not expected to have significant design impact.

- Solar blanket basic support structure mass: 2-1/2% of total satellite.

APPENDIX A.
SPS TEST ARTICLES I AND II DRAWINGS

42635-18029	SPS Test Article I, Hex. Frame Antenna Configuration
42635-18031	SPS Test Article I, Interface Diagram, Hexagon Frame Antenna
42635-18030	SPS Test Article II, Ladder Configuration, Preliminary Arrangement
42635-18032	SPS Test Article II, Interface Diagram, Ladder Configuration

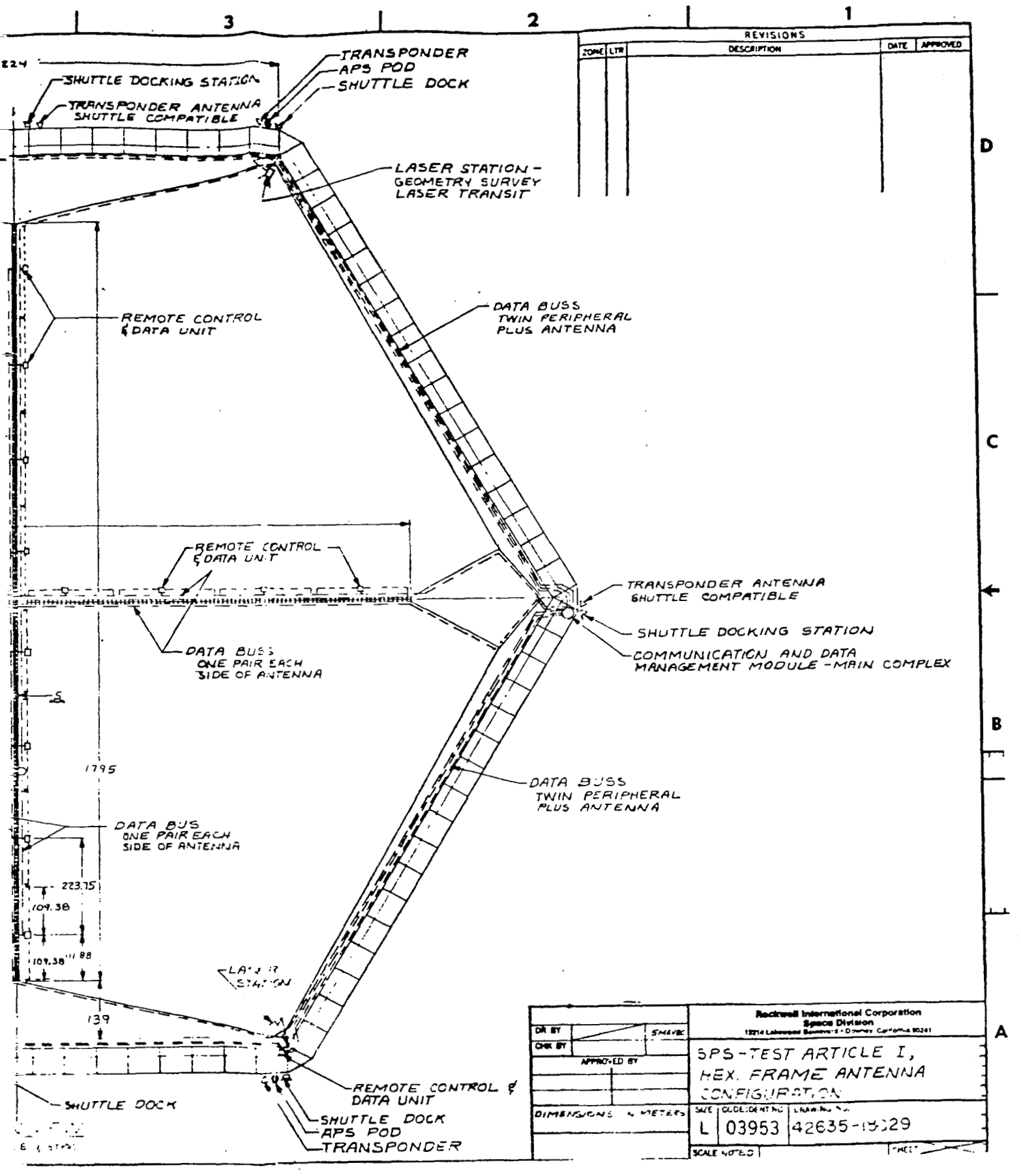
3
2
1
D
C
B
A
TRANSPONDER
APS POD
SHUTTLE DOCK
SHUTTLE DOCKING STATION
TRANSPONDER ANTENNA
SHUTTLE COMPATIBLE
LASER STATION -
GEOMETRY SURVEY
LASER TRANSIT
REMOTE CONTROL
& DATA UNIT
DATA BUSS
TWIN PERIPHERAL
PLUS ANTENNA
REMOTE CONTROL
& DATA UNIT
TRANSPONDER ANTENNA
SHUTTLE COMPATIBLE
SHUTTLE DOCKING STATION
COMMUNICATION AND DATA
MANAGEMENT MODULE - MAIN COMPLEX
DATA BUSS
ONE PAIR EACH
SIDE OF ANTENNA
1795
DATA BUSS
TWIN PERIPHERAL
PLUS ANTENNA
DATA BUSS
ONE PAIR EACH
SIDE OF ANTENNA
223.75
109.38
109.38
111.88
139
LASER
STATION
SHUTTLE DOCK
REMOTE CONTROL &
DATA UNIT
SHUTTLE DOCK
APS POD
TRANSPONDER
REVISIONS
ZONE
LTR
DESCRIPTION
DATE
APPROVED
DR BY
SHAVEC
CHK BY
APPROVED BY
DIMENSIONS IN METERS
Rockwell International Corporation
Space Division
SPS-TEST ARTICLE I,
HEX. FRAME ANTENNA
CONFIGURATION
SIZE
L
CODE IDENT NO
03953
42635-1029
SCALE NOTED
SHEET

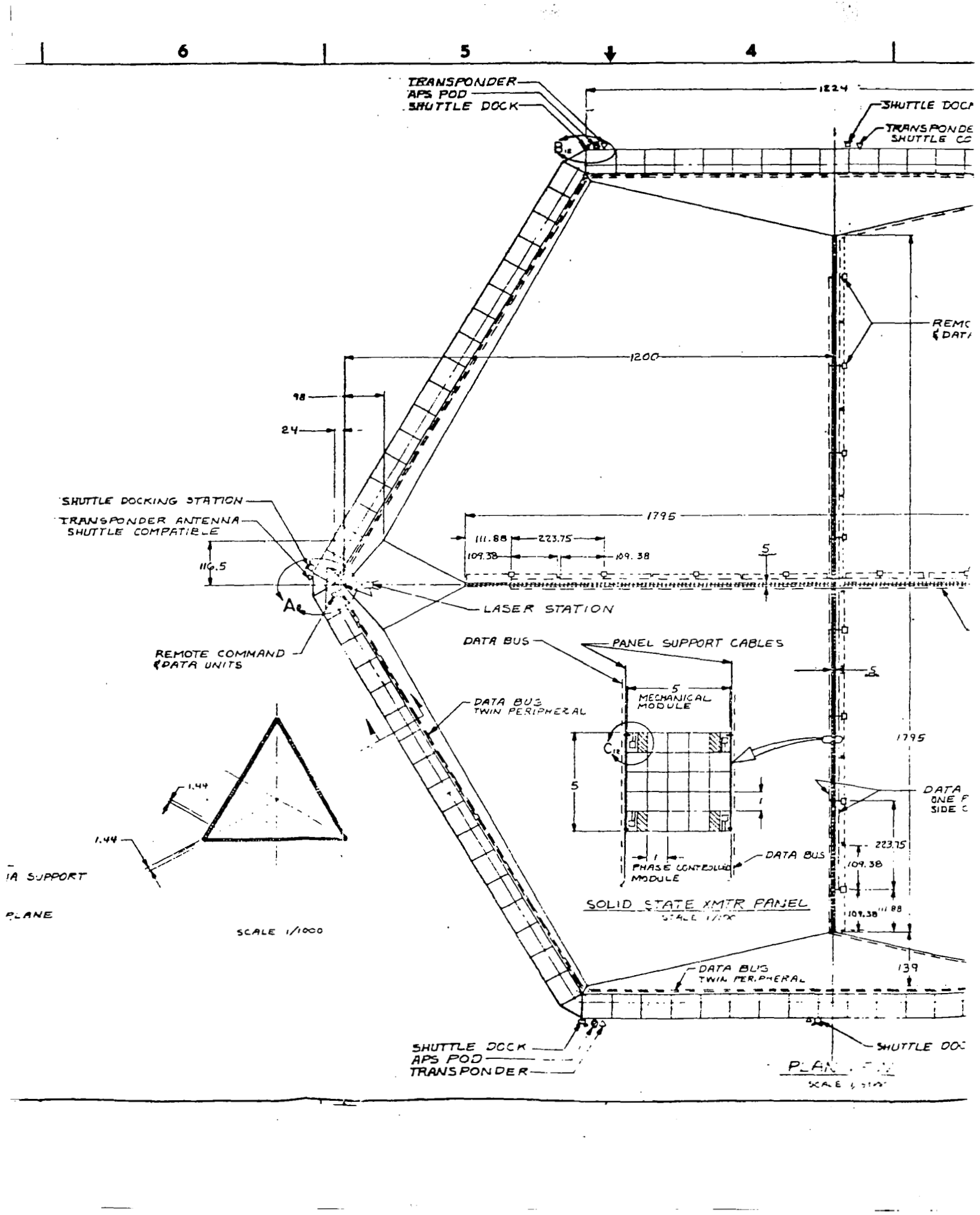
6
5
4
TRANSPONDER
APS POD
SHUTTLE DOCK
1224
SHUTTLE DOCK
TRANSPONDER
SHUTTLE CO
REMO
& DATA
1200
98
24
SHUTTLE DOCKING STATION
TRANSPONDER ANTENNA
SHUTTLE COMPATIBLE
116.5
1795
111.88
223.75
109.38
109.38
5
LASER STATION
REMOTE COMMAND
& DATA UNITS
DATA BUS
PANEL SUPPORT CABLES
5
MECHANICAL
MODULE
DATA BUS
TWIN PERIPHERAL
1795
5
1
DATA
ONE P
SIDE C
1.44
1.44
1
PHASE CONTROLLED
MODULE
DATA BUS
223.75
109.38
111.88
109.38
SOLID STATE XMTR PANEL
SCALE 1/1
IA SUPPORT
PLANE
SCALE 1/1000
DATA BUS
TWIN PERIPHERAL
139
SHUTTLE DOC
SHUTTLE DOCK
APS POD
TRANSPONDER
PLAN
SCALE 1/100

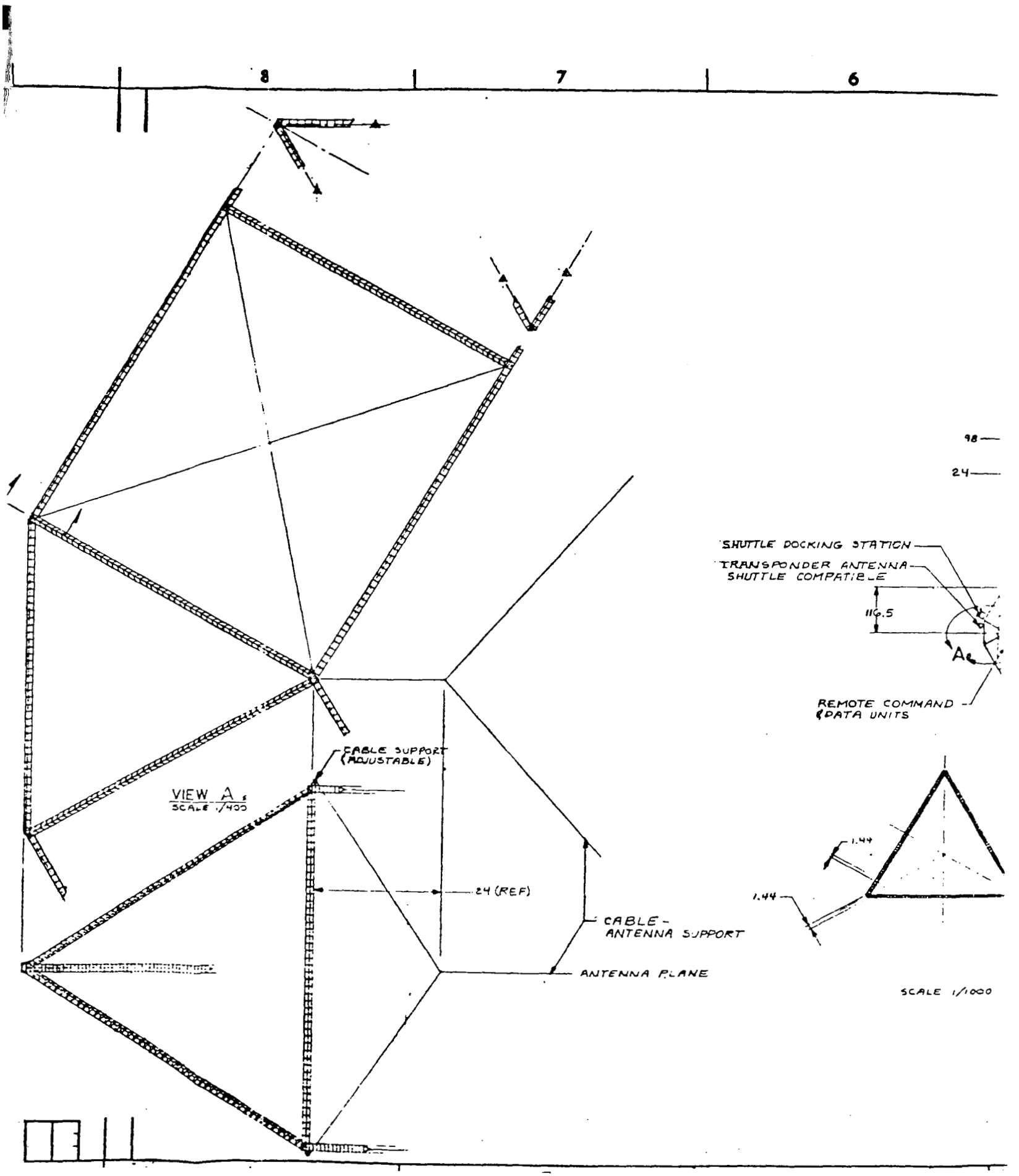
8
7
6
98
24
SHUTTLE DOCKING STATION
TRANSPONDER ANTENNA SHUTTLE COMPATIBLE
116.5
A
REMOTE COMMAND & DATA UNITS
CABLE SUPPORT (ADJUSTABLE)
VIEW A
SCALE 1/400
24 (REF)
CABLE - ANTENNA SUPPORT
ANTENNA PLANE
1.44
1.44
SCALE 1/1000

TERNATE LOCATIONS

CHARGER AND CONTROL

ATTACH FITTING

ALTERNATE LOCATION

IPPLY

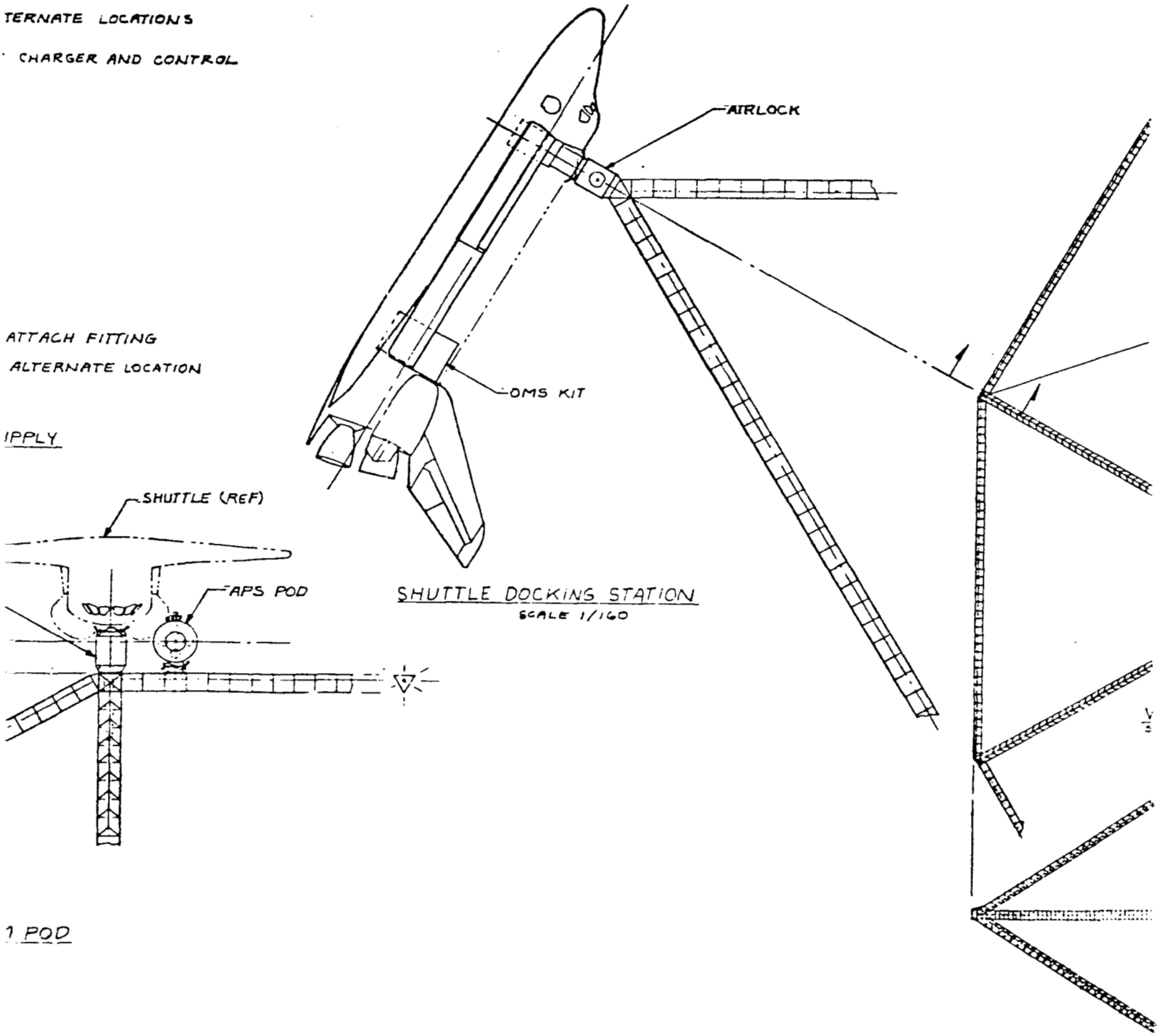

SHUTTLE DOCKING STATION

SCALE 1/160

1 POD

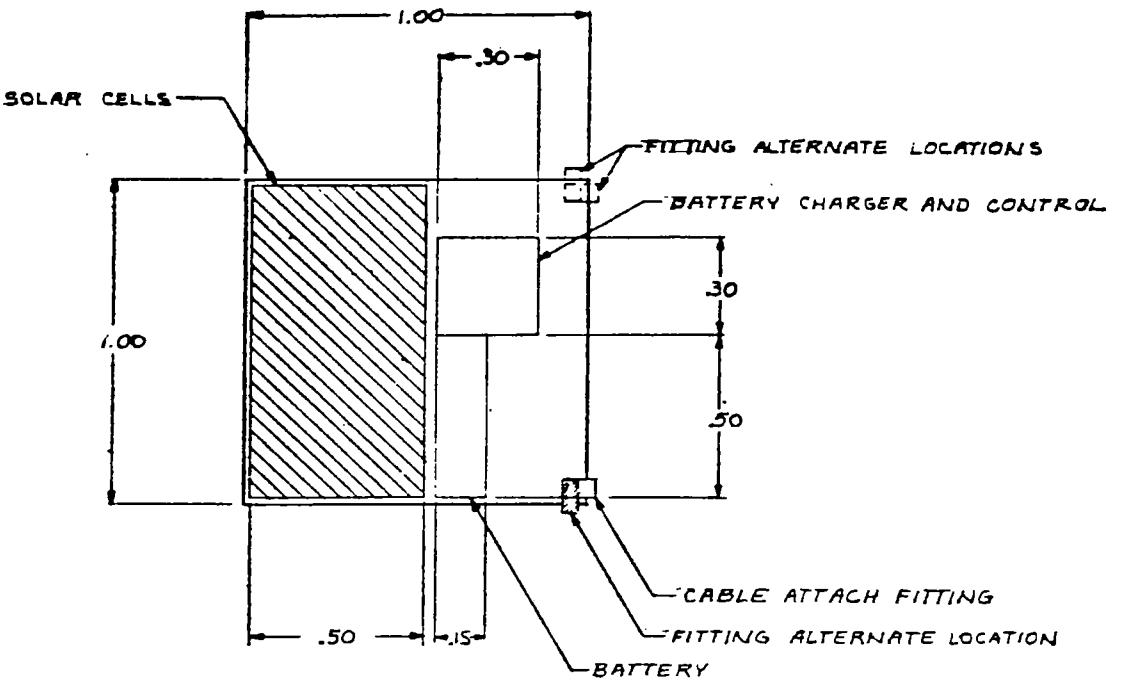

VIEW C, TRANSMITTER POWER SUPPLY
SCALE 1/100

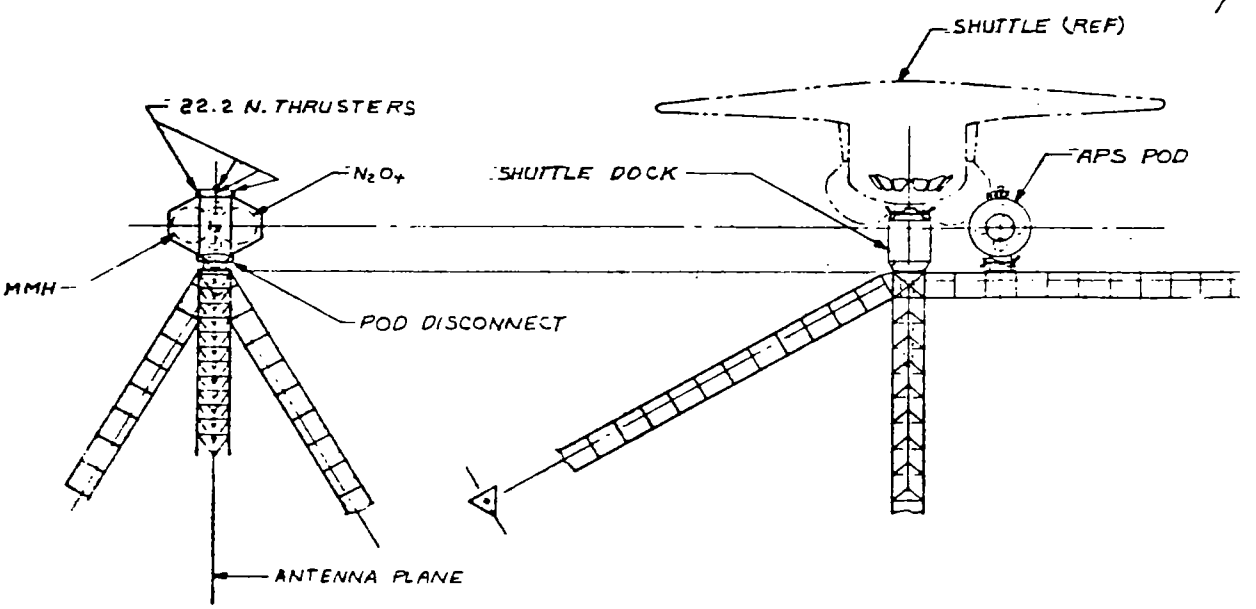

DETAIL B, - APS SYSTEM POD
SCALE 1/160

REVISIONS				
ZONE	LTR	DESCRIPTION	DATE	APPROVED

RAGE

ENT (2.1.3)

FACE
POD
TLE DOCK
SPONDER (2.2.3)
R PACK, TYPE B (2.2.2)

NOTES: UNLESS OTHERWISE SPECIFIED

1. THIS DRAWING IN CONJUNCTION WITH REPORT SD80-0102, SECTION 2.1.5 DEFINES THE FRAME STRUCTURAL REQUIREMENTS. (XX.X) EQUALS OTHER SECTIONS
2. ALL REMOTE DATA MANAGEMENT EQUIPMENT INSTALLATIONS SHALL USE TYPE E POWER PACKS.
3. A SOLAR CELL ARRAY AND RELATED POWER PACK HAVE POWER INTERCONNECTS WHETHER OR NOT SHOWN.

(1) INTERFACE
•CABLE ATTACH

(2) INTERFACE
•CABLE ATTACH

(4) INTERFACE
•SHUTTLE DOCK
•TRANSPONDER (2.2.3)
•POWER PACK, TYPE E (2.2.2)
•POTENTIAL CARGO STORAGE

(6) INTERFACE
• COMMUNICATION (2.2.3)
• DATA MANAGEMENT (2.2.3)
• POWER PACK, TYPE A (2.2.2)

(1) INTERFACE
•CABLE ATTACH

NT
OCK
ER (2.2.3)
K, TYPE B (2.2.2)

DR BY	JULY 80	Rockwell International Corporation, Space Division, 12214 Lakewood Boulevard · Downey, California 90241
CHK BY		
APPROVED BY		SPS-TEST ARTICLE I, INTERFACE DIAGRAM, HEXAGON FRAME ANTENNA
DIMENSIONS IN METERS		SIZE: L · CODE IDENT NO: 03953 · DRAWING NO: 42635-18031
		SCALE NONE · SHEET 1 OF 2

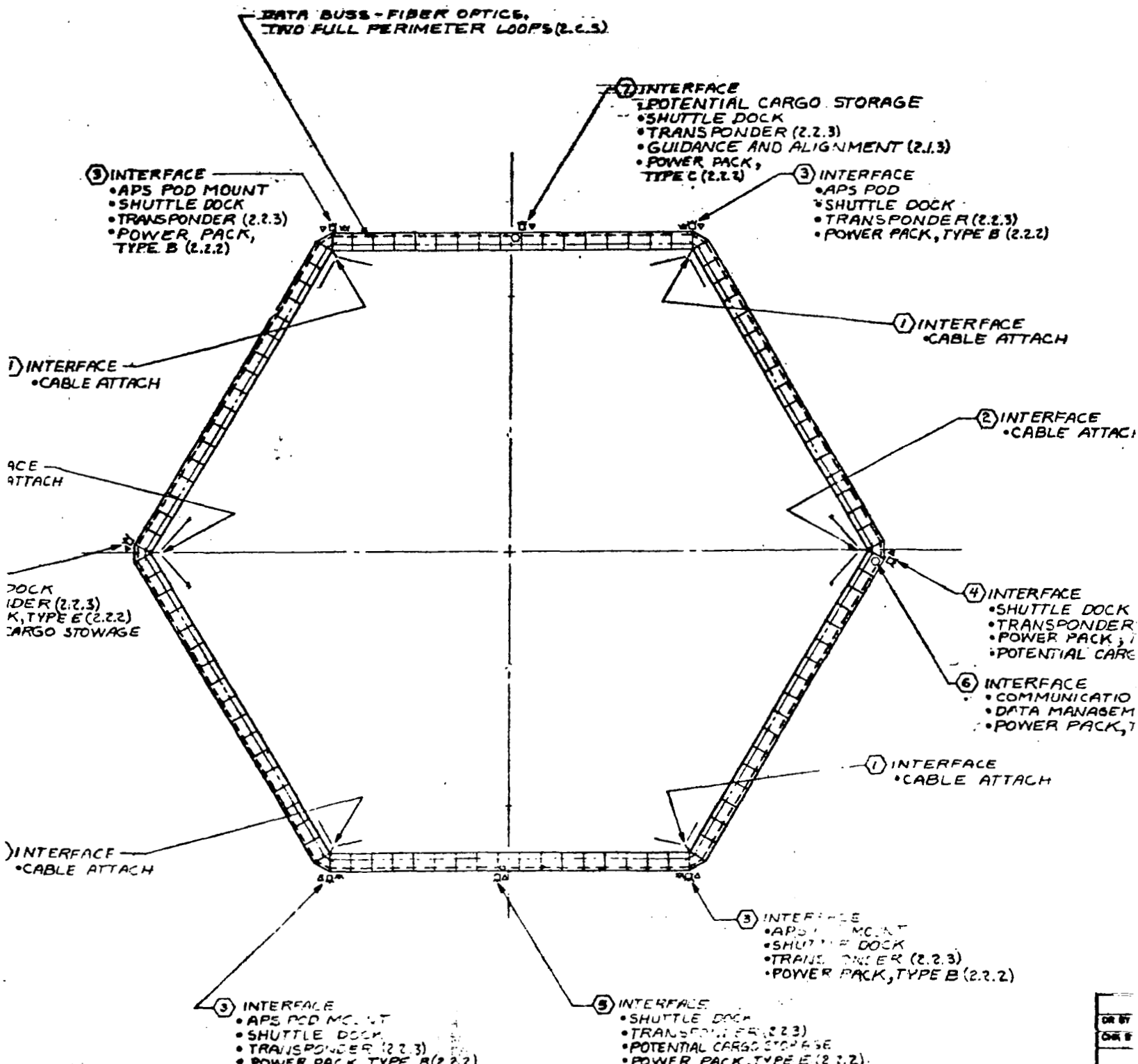
DATA BUSS - FIBER OPTICS, TWO FULL PERIMETER LOOPS (2.2.3)
7 INTERFACE
POTENTIAL CARGO STORAGE
•SHUTTLE DOCK
•TRANSPONDER (2.2.3)
•GUIDANCE AND ALIGNMENT (2.1.3)
•POWER PACK, TYPE C (2.2.2)
5 INTERFACE
•APS POD MOUNT
•SHUTTLE DOCK
•TRANSPONDER (2.2.3)
•POWER PACK, TYPE B (2.2.2)
3 INTERFACE
•APS POD
•SHUTTLE DOCK
•TRANSPONDER (2.2.3)
•POWER PACK, TYPE B (2.2.2)
1 INTERFACE
•CABLE ATTACH
1 INTERFACE
•CABLE ATTACH
2 INTERFACE
•CABLE ATTAC
4 INTERFACE
•SHUTTLE DOCK
•TRANSPONDER
•POWER PACK ;
•POTENTIAL CARG
6 INTERFACE
•COMMUNICATIO
•DATA MANAGEM
•POWER PACK,
1 INTERFACE
•CABLE ATTACH
3 INTERFACE
•APS POD MOUNT
•SHUTTLE DOCK
•TRANSPONDER (2.2.3)
•POWER PACK, TYPE B (2.2.2)
5 INTERFACE
•SHUTTLE DOCK
•TRANSPONDER (2.2.3)
•POTENTIAL CARGO STORAGE
•POWER PACK, TYPE E (2.2.2)
3 INTERFACE
•APS POD MOUNT
•SHUTTLE DOCK
•TRANSPONDER (2.2.3)
•POWER PACK, TYPE B (2.2.2)

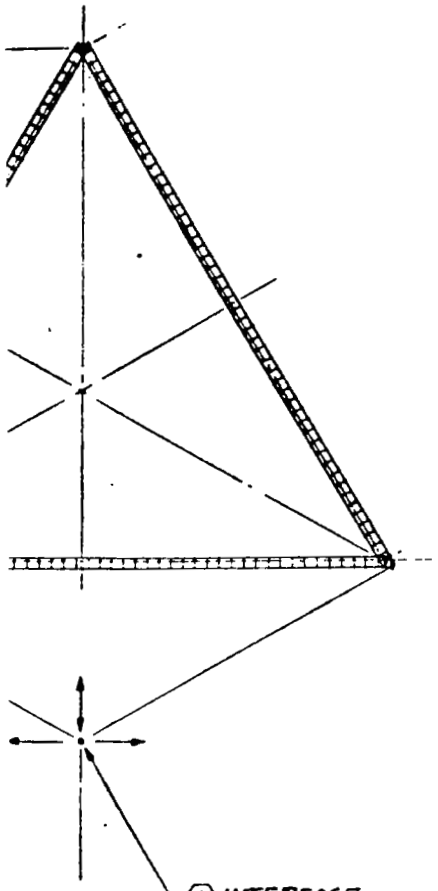

(1) INTERFACE
•CABLE ATTACH
PROVIDE ADJUSTMENT CAPABILITY CONSISTANT WITH CONSTRUCTION AND DIMENSIONAL STABILITY REQUIREMENTS.

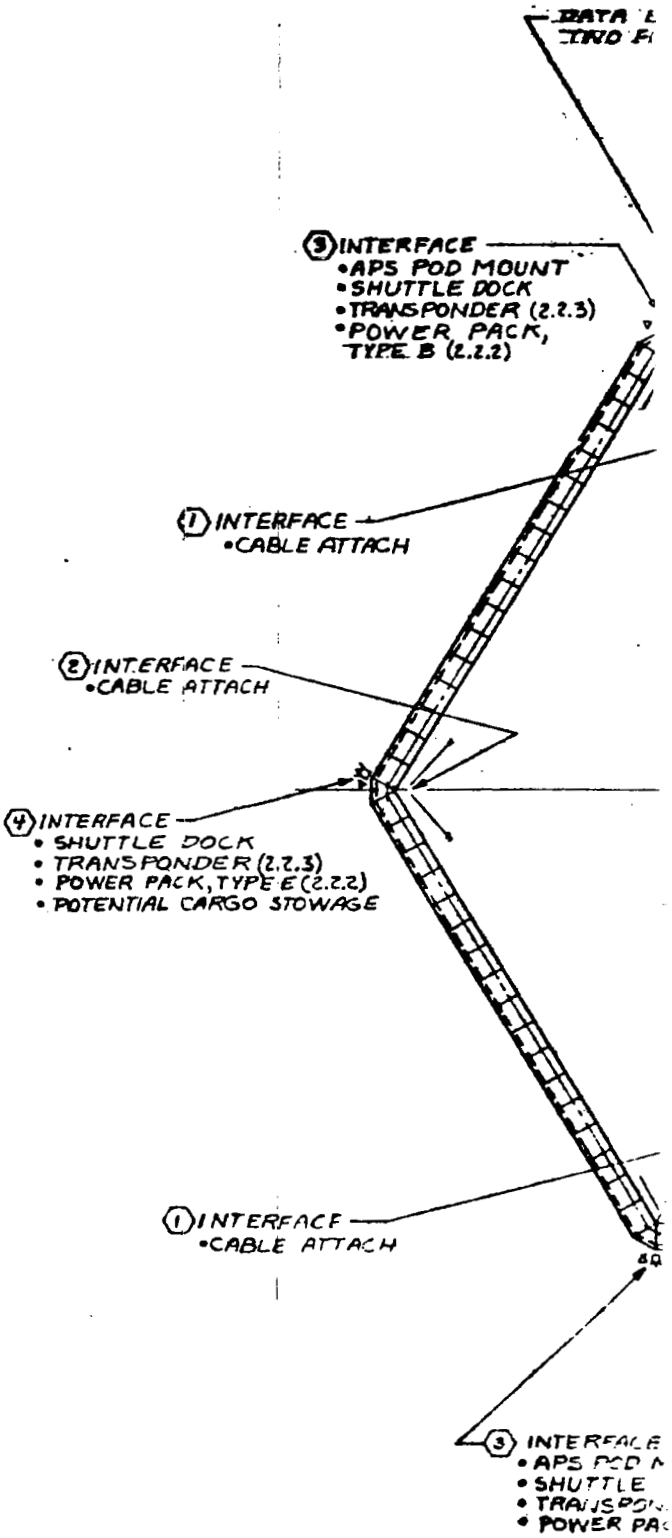

(3) INTERFACE
•APS POD MOUNT
•SHUTTLE DOCK
•TRANSPONDER (2.2.3)
•POWER PACK, TYPE B (2.2.2)

(1) INTERFACE
•CABLE ATTACH

(2) INTERFACE
•CABLE ATTACH

(4) INTERFACE
• SHUTTLE DOCK
• TRANSPONDER (2.2.3)
• POWER PACK, TYPE E (2.2.2)
• POTENTIAL CARGO STOWAGE

(1) INTERFACE
•CABLE ATTACH

(3) INTERFACE
• APS POD M
• SHUTTLE
• TRANSPON
• POWER PA

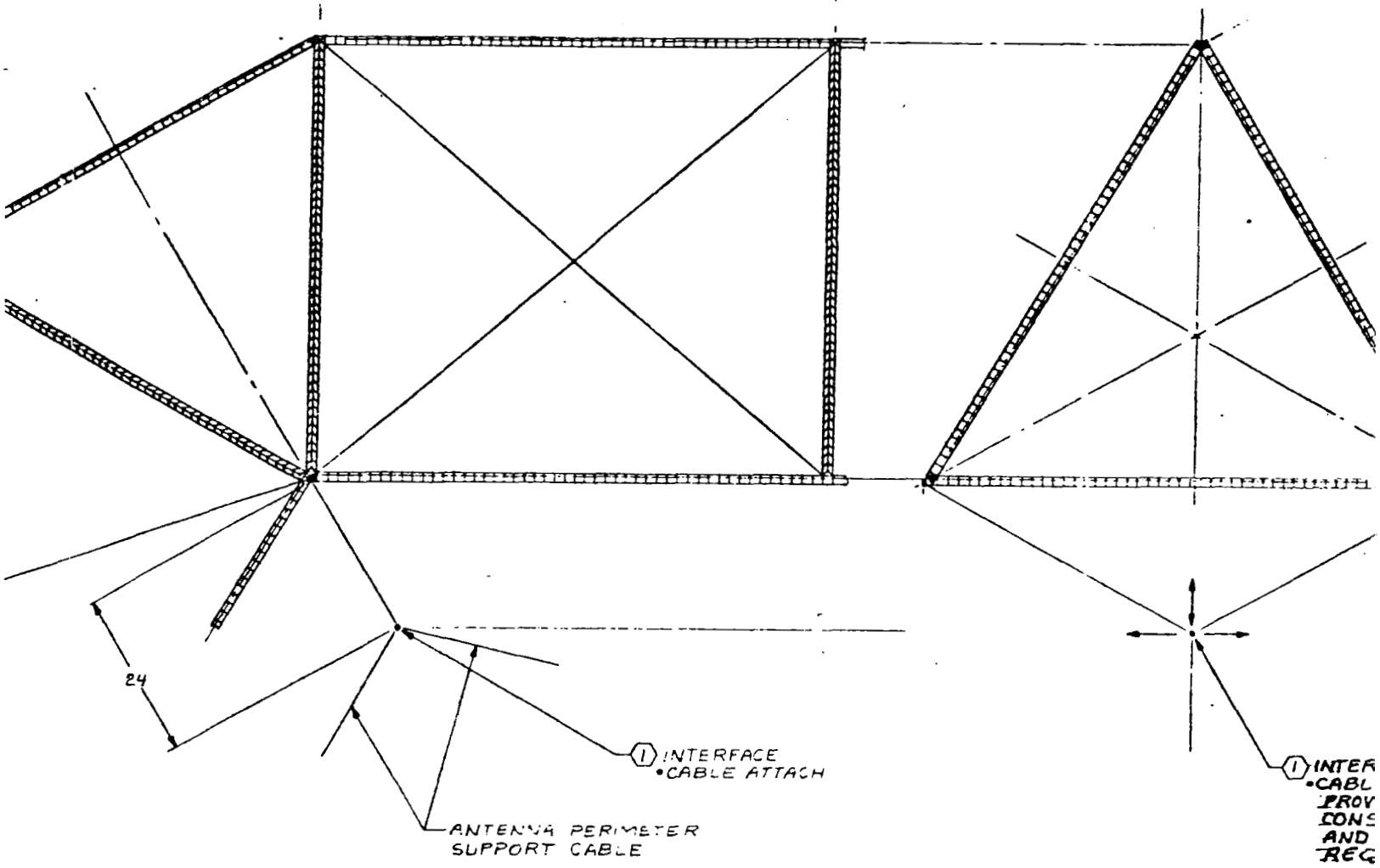

(1) INTERFACE DETAILS
SCALE 1/NOT

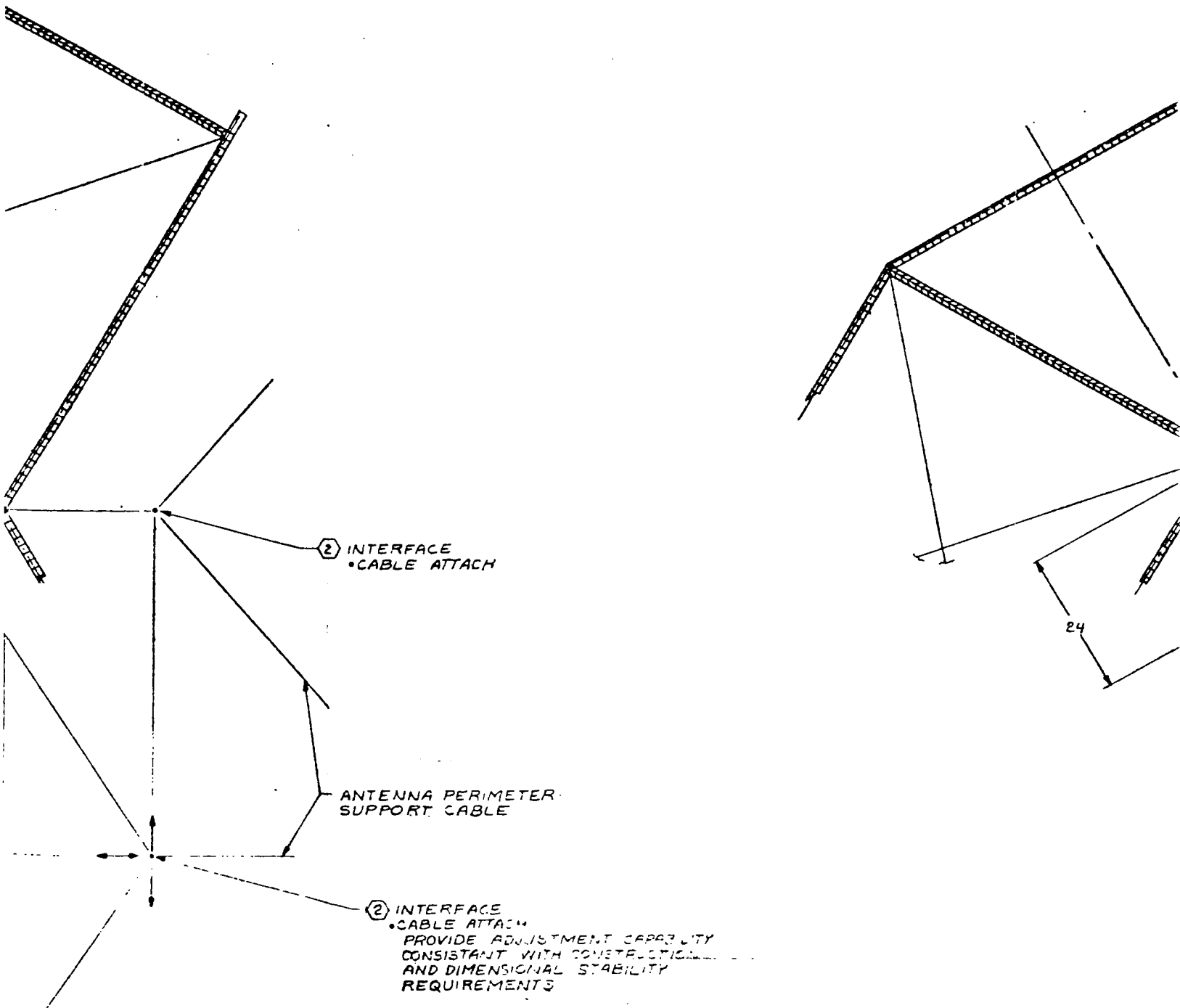
(2) INTERFACE
•CABLE ATTACH
ANTENNA PERIMETER
SUPPORT CABLE
(2) INTERFACE
•CABLE ATTACH
PROVIDE ADJUSTMENT CAPABILITY
CONSISTANT WITH CONSTRUCTIONAL
AND DIMENSIONAL STABILITY
REQUIREMENTS
24

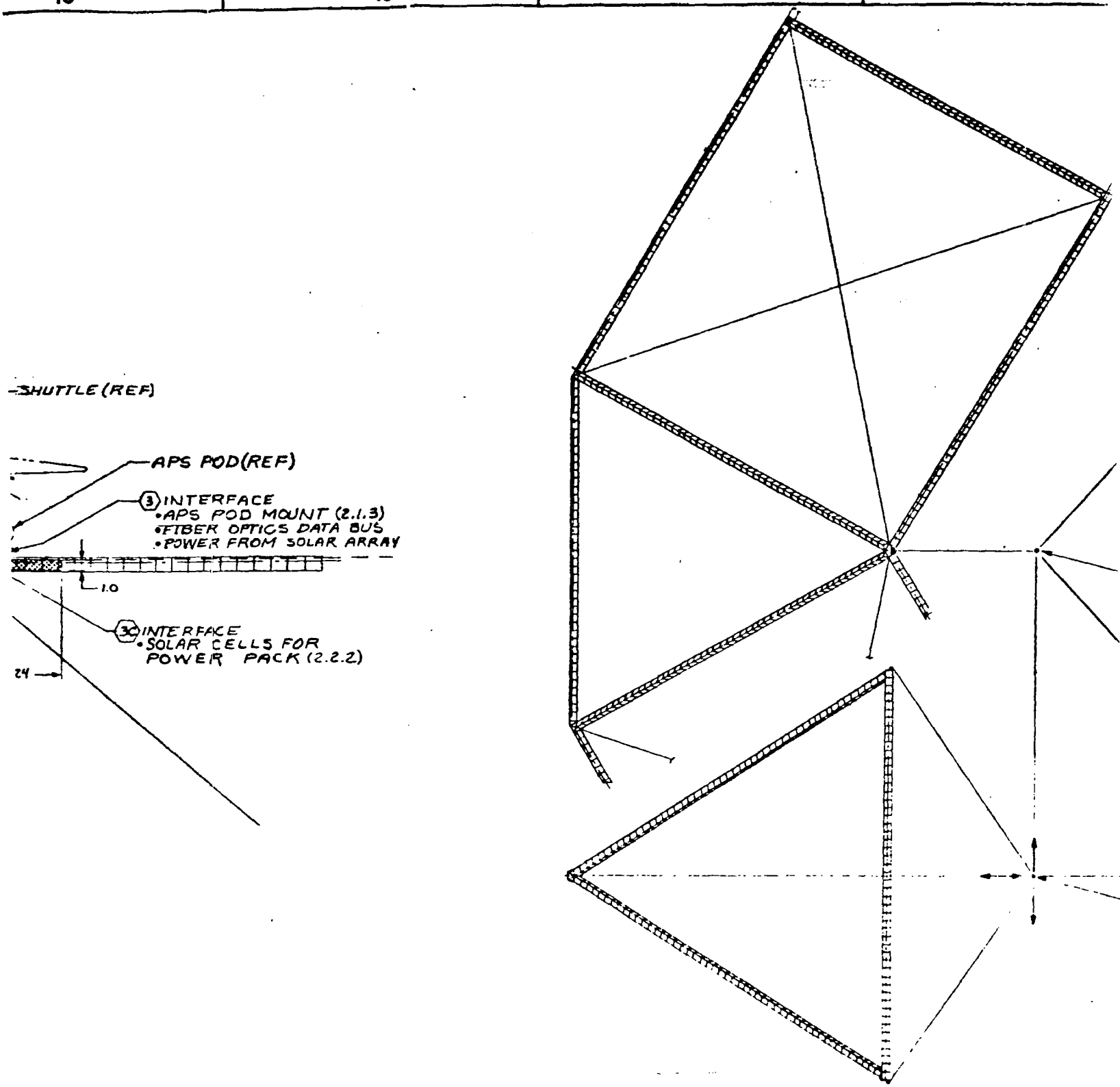

2 INTERFACE DETAILS

SCALE 1/4"=1'-0"

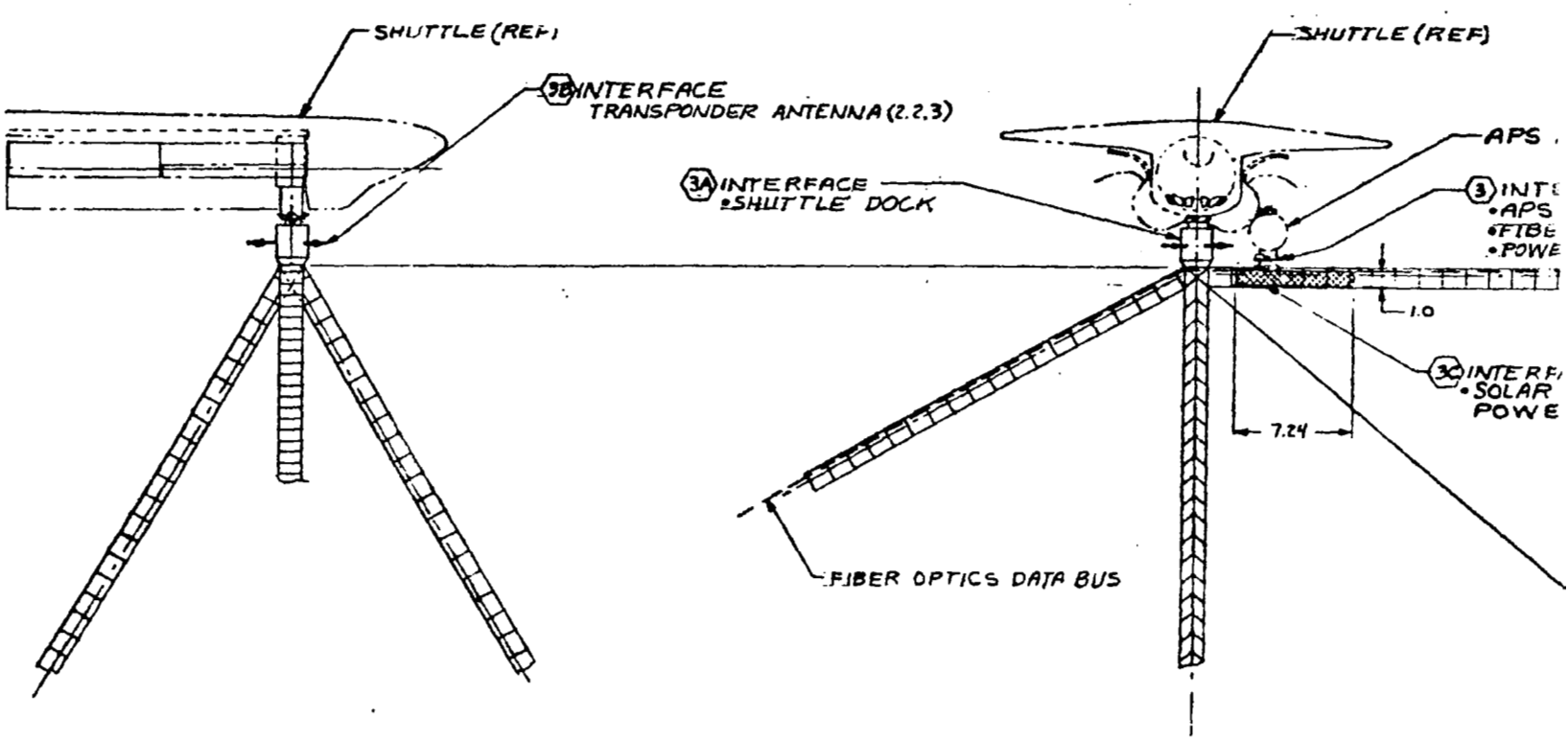

3 INTERFACE DETAILS
SCALE 1/200

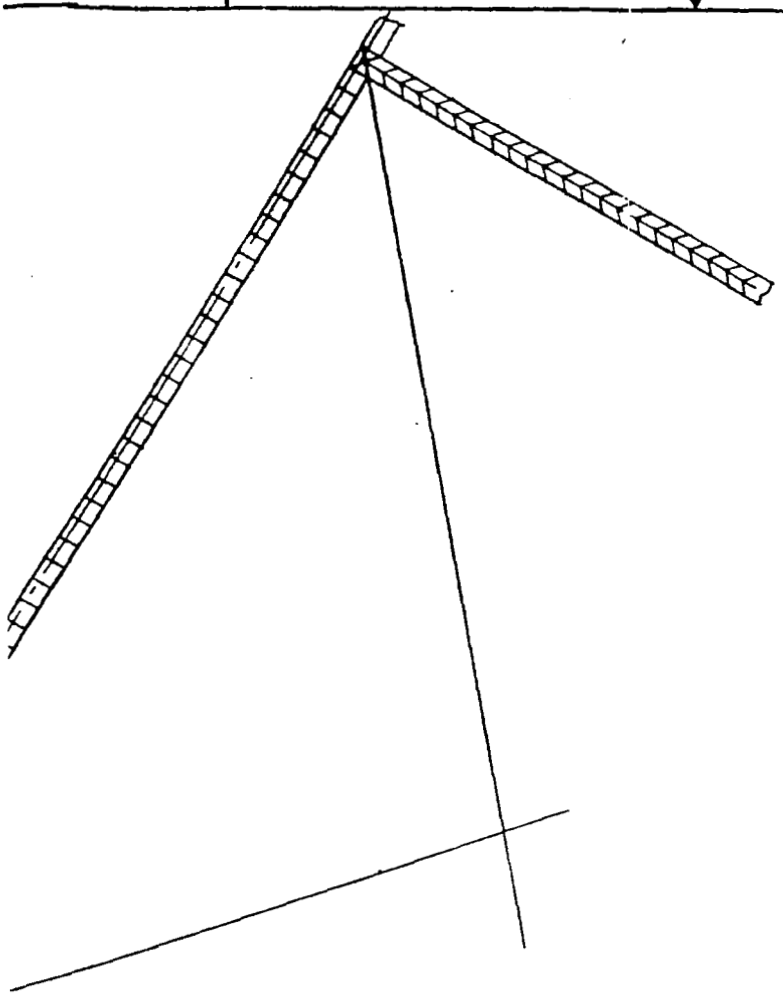

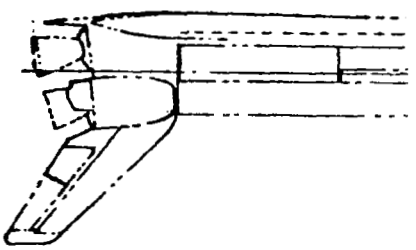

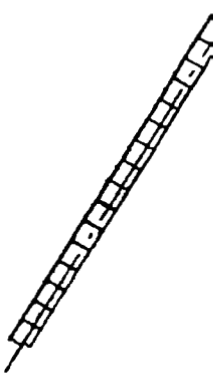

(4A) INTERFACE
• SOLAR CELLS FOR POWER PACK (2.2.2)

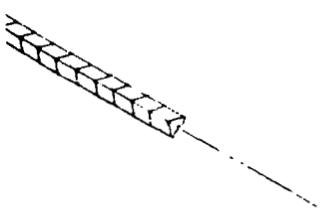

FACE DETAILS
SCALE 1/200

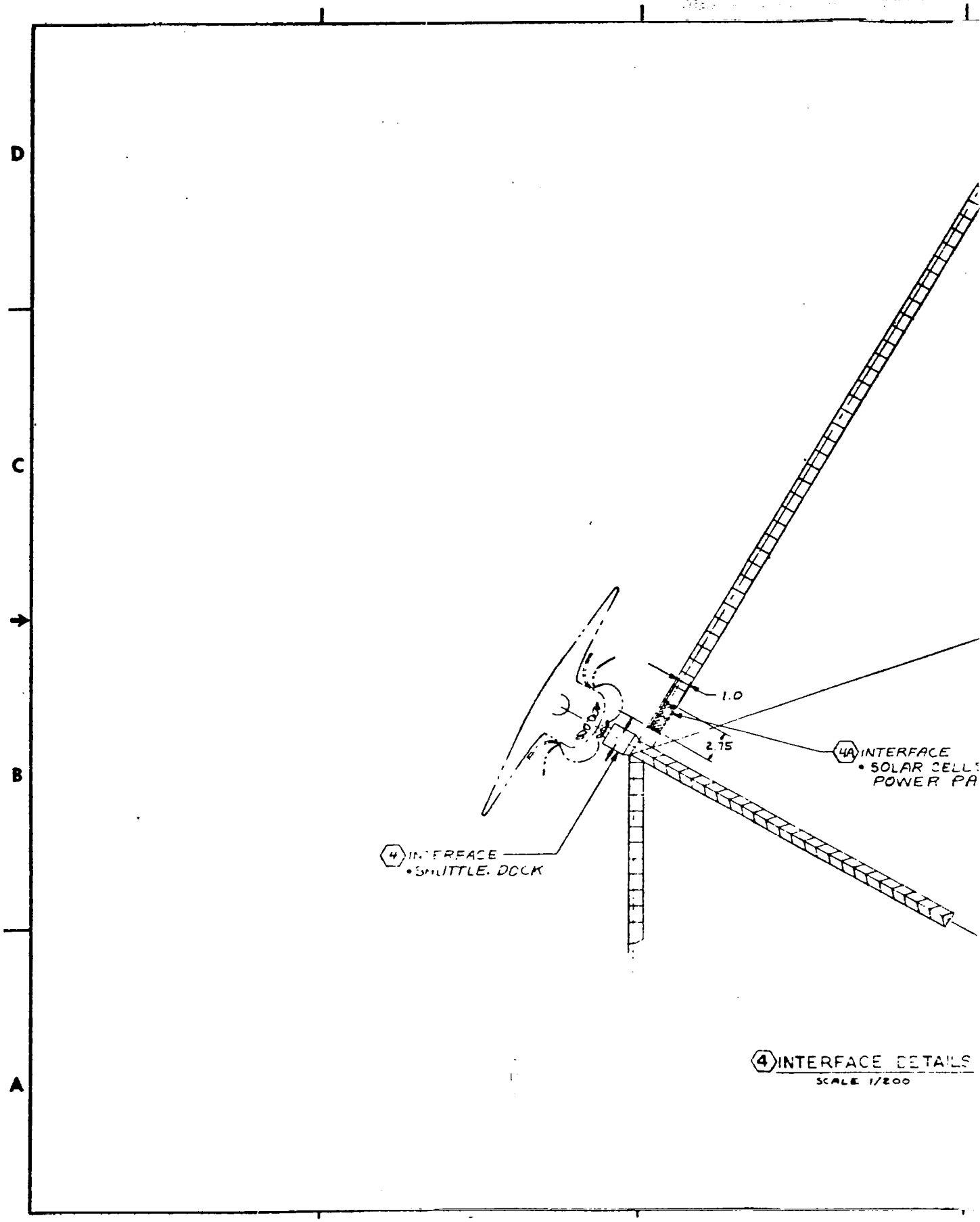

4 INTERFACE DETAILS
SCALE 1/200

REVISIONS				
ZONE	LTR	DESCRIPTION	DATE	APPROVED

JA REFERENCE PLANE

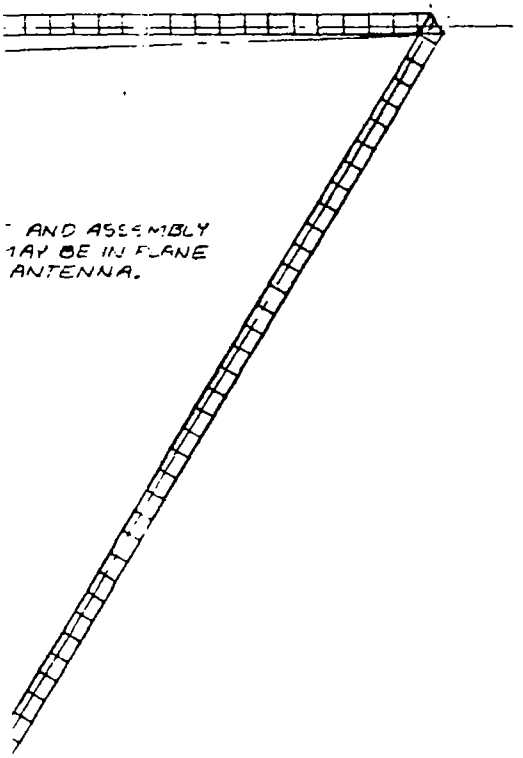

AND ASSEMBLY
MAY BE IN PLANE
ANTENNA.

D

C

B

A

SIZE	COOL IDENT NO	DRAWING NO
L	03953	42635-8031

SCALE NOTED SHEET 2 OF 2

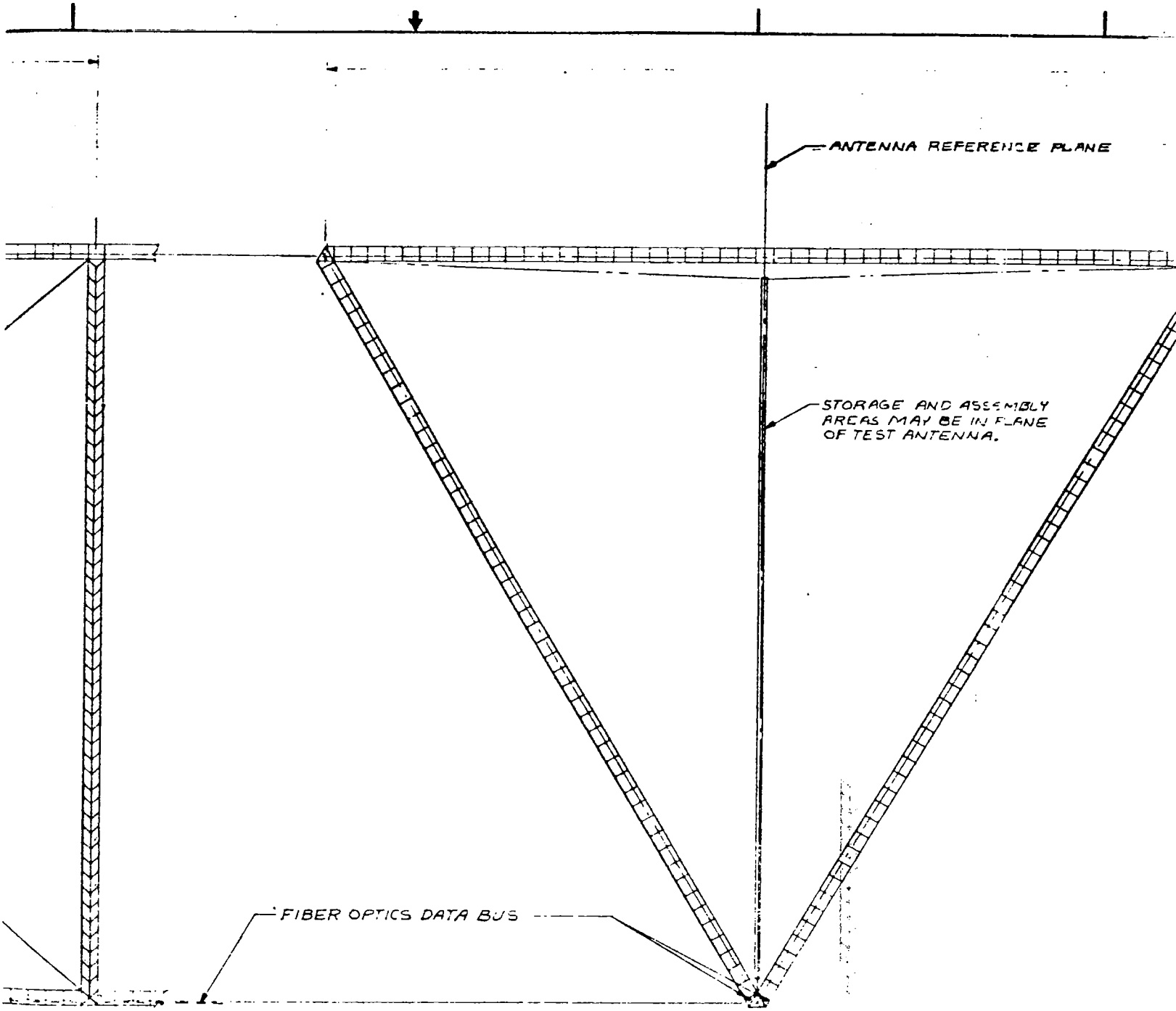

NA MAY
MBLE

BE USED.

(5) INTERFACE DETAILS
SCALE 1/200

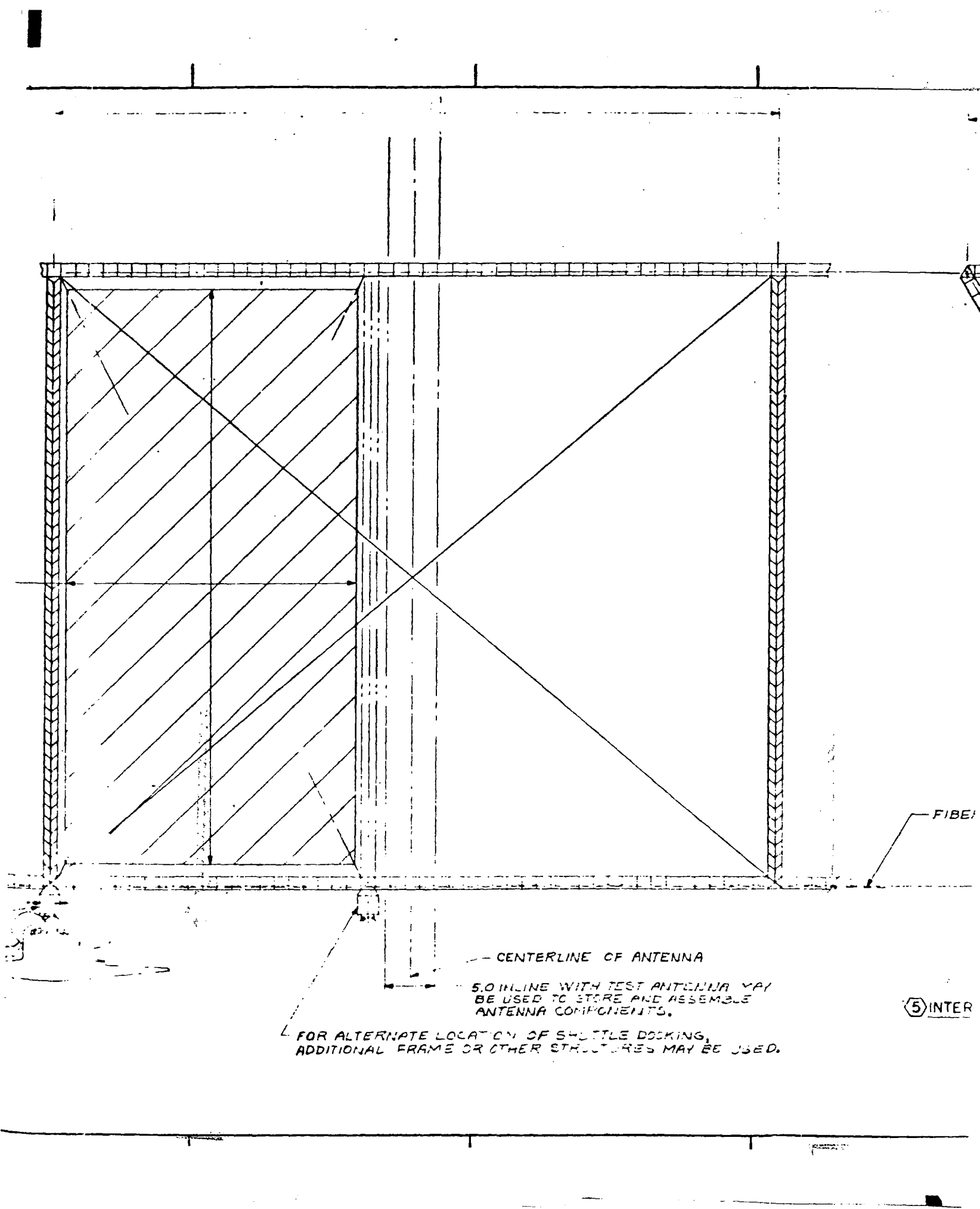
FIBE
CENTERLINE OF ANTENNA
5.0 IN LINE WITH TEST ANTENNA MAY BE USED TO STORE AND ASSEMBLE ANTENNA COMPONENTS.
FOR ALTERNATE LOCATION OF SHUTTLE DOCKING, ADDITIONAL FRAME OR OTHER STRUCTURES MAY BE USED.
5 INTER

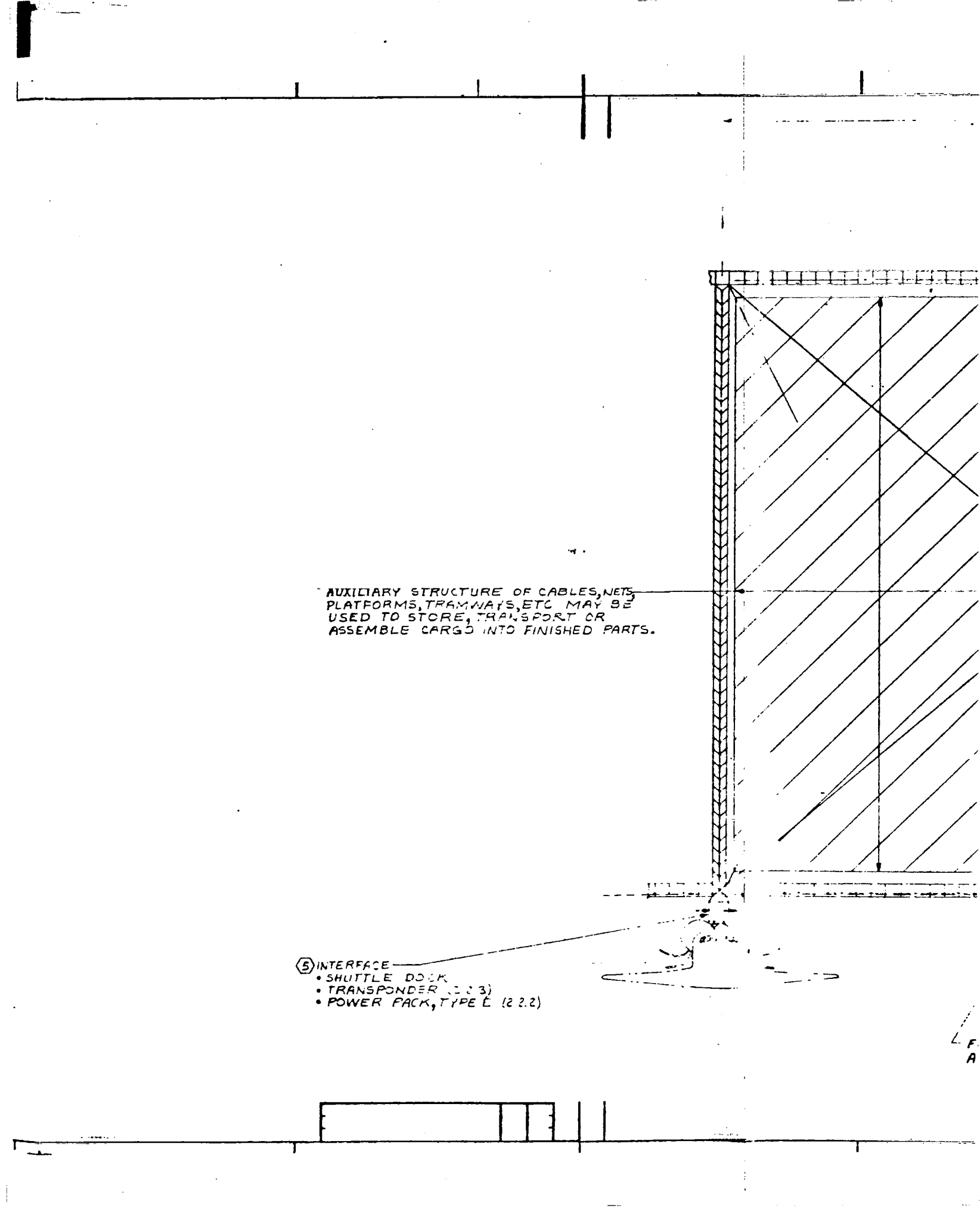
AUXILIARY STRUCTURE OF CABLES, NETS, PLATFORMS, TRAMWAYS, ETC MAY BE USED TO STORE, TRANSPORT OR ASSEMBLE CARGO INTO FINISHED PARTS.
(5) INTERFACE
• SHUTTLE DOCK
• TRANSPONDER (2.2.3)
• POWER PACK, TYPE E (2.2.2)

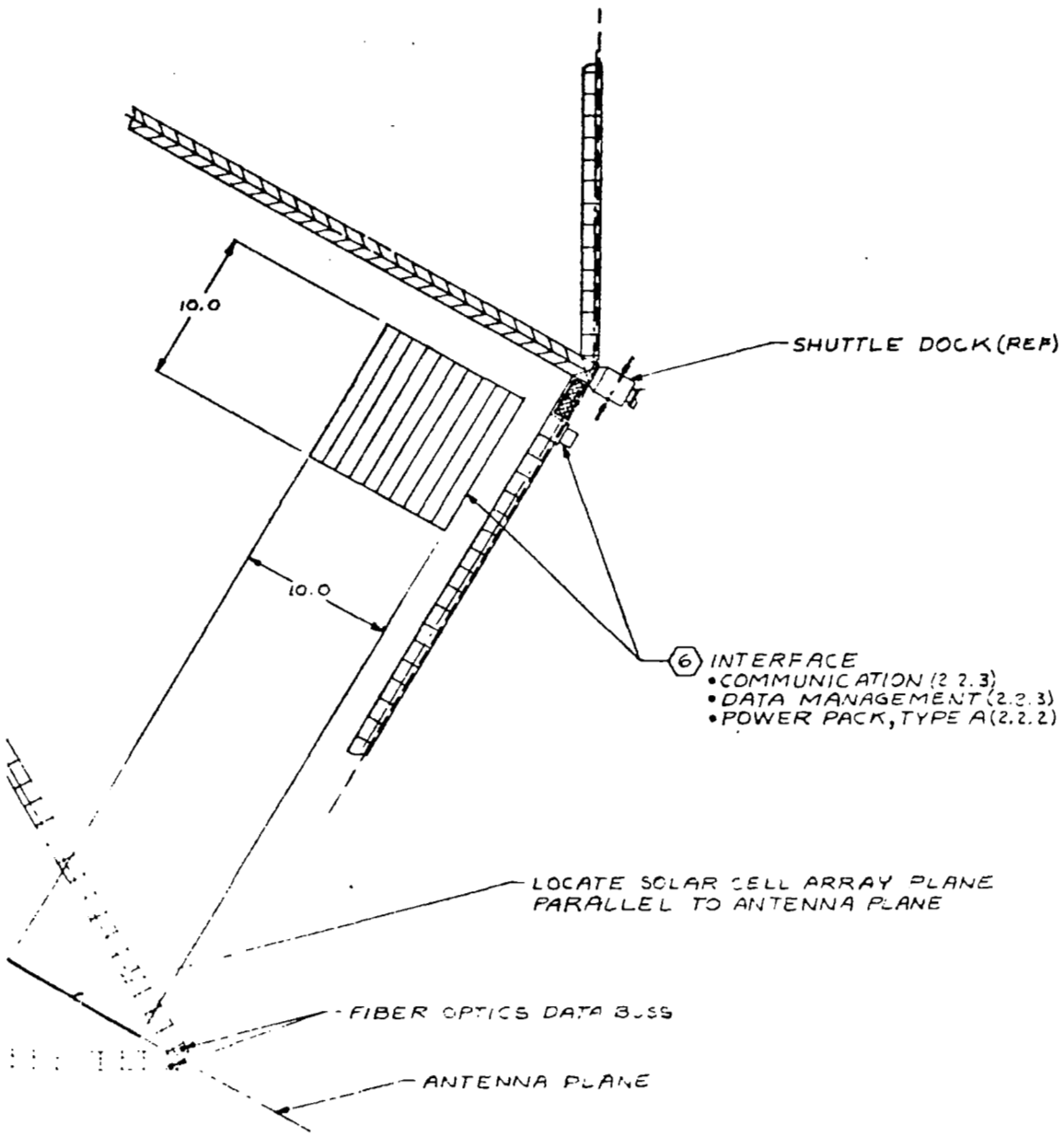

⑥ INTERFACE DETAILS
SCALE 1/200

CE
DOCK
ONDER(2.2.3)

CE
CE AND ALIGNMENT(2.1.3)
PACK, TYPE C(2.2.2)

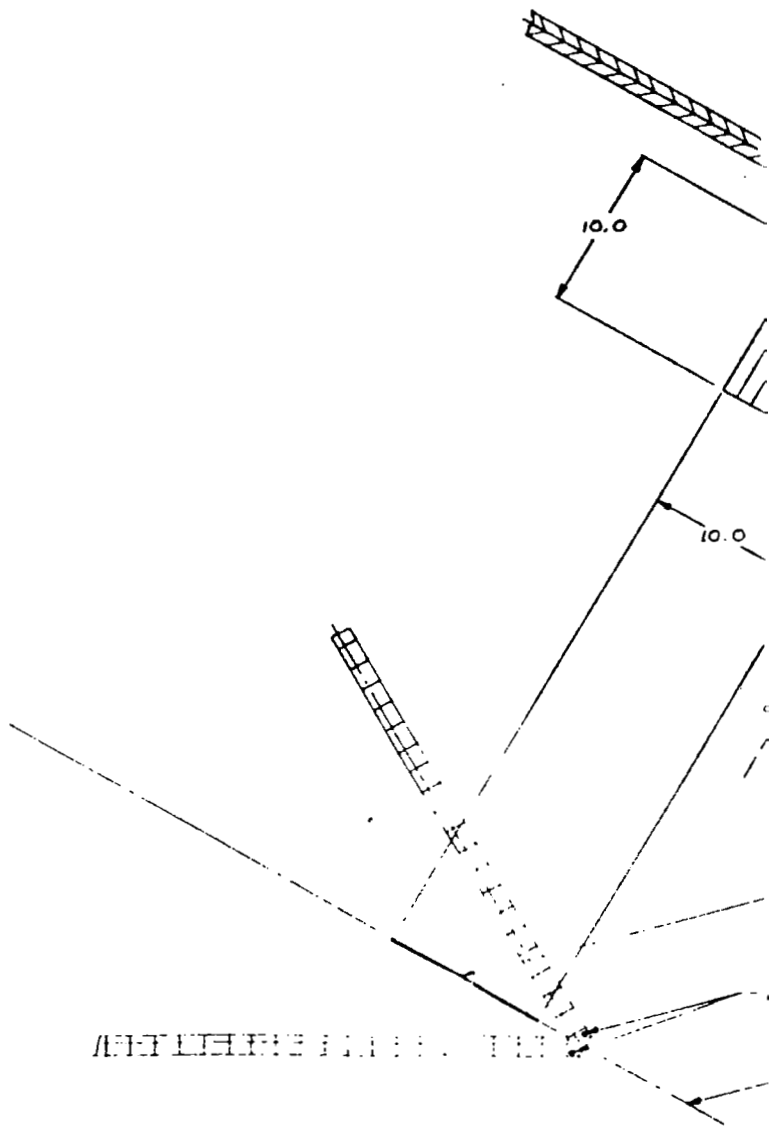

⑤

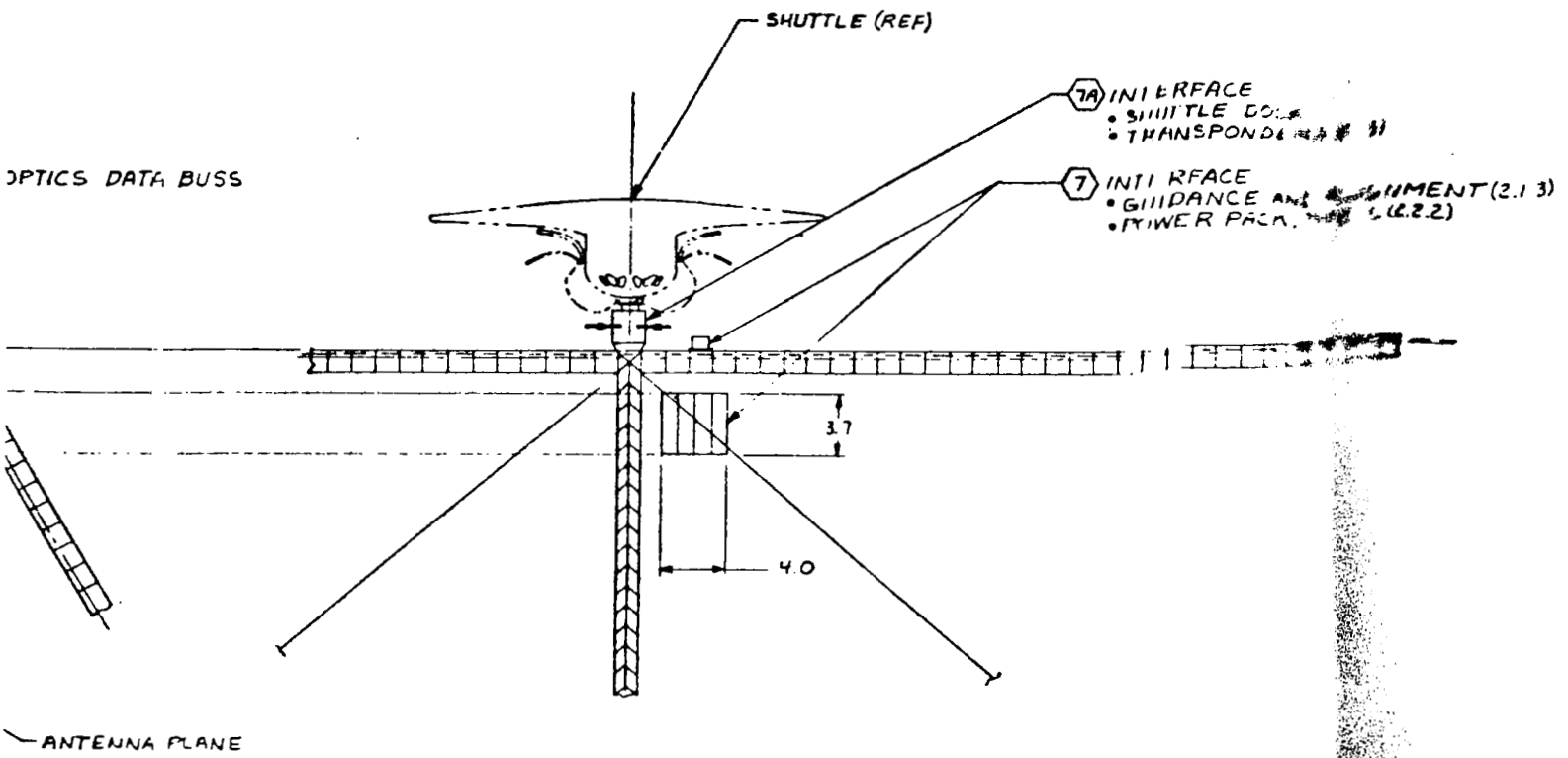

7 INTERFACE DETAILS
SCALE 1/200

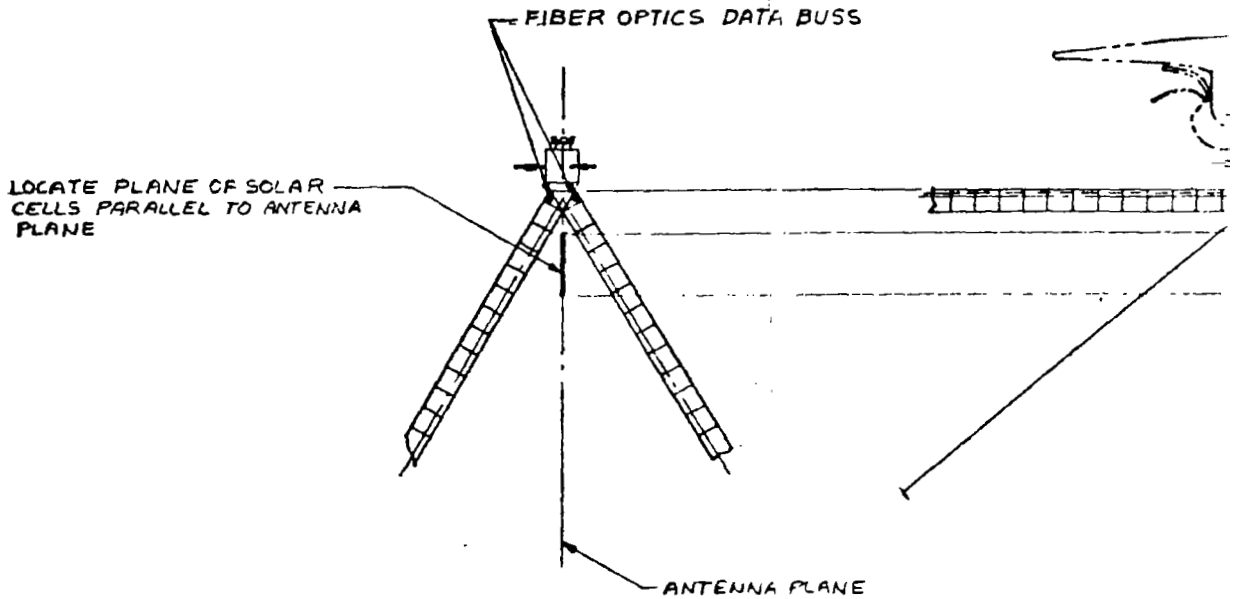

(7) INTERFACE DETAILS
SCALE 1/200

REVISIONS				
ZONE	LTR	DESCRIPTION	DATE	APPROVED

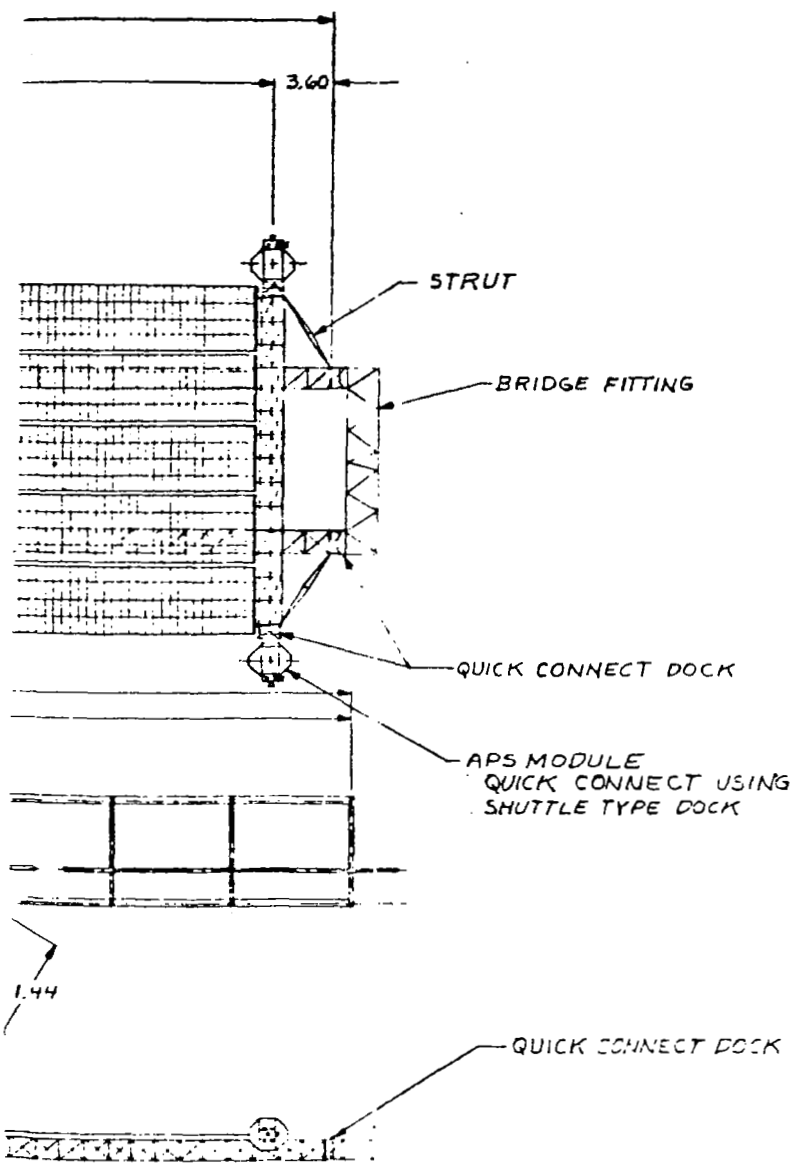

DR BY	Rockwell International Corporation Space Division	
CHK BY		
APPROVED BY	SPS-TEST ARTICLE II, LADDER CONFIGURATION, PRELIM. ARRANGEMENT	
DIMENSIONS IN METERS	SIZE: L CODE IDENT NO.: 03953 DRAWING NO.: 42635-18030	
	SCALE NONE	SHEET

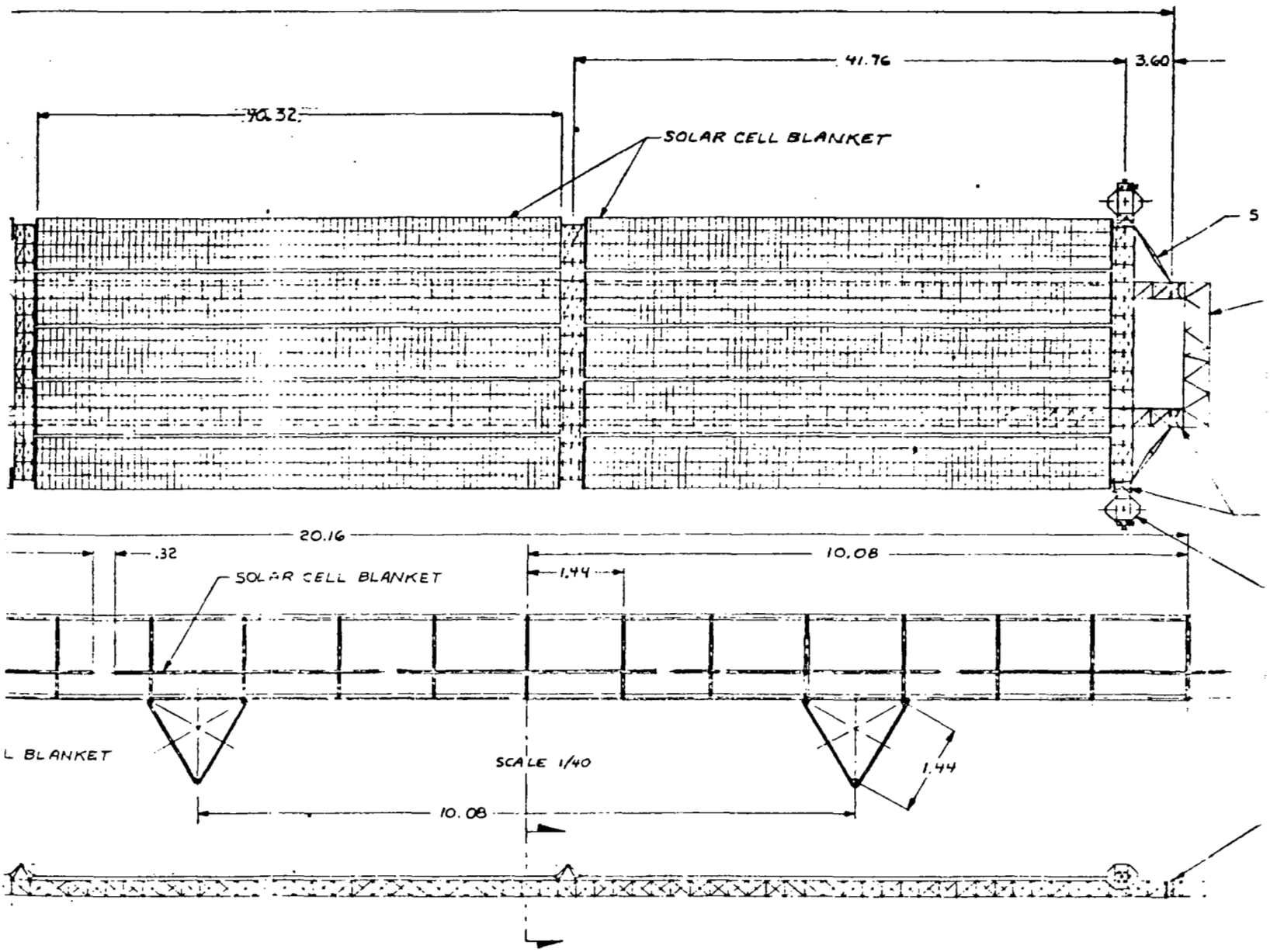
41.76
3.60
70.32
SOLAR CELL BLANKET
5
20.16
.32
SOLAR CELL BLANKET
10.08
1.44
L BLANKET
SCALE 1/40
1.44
10.08

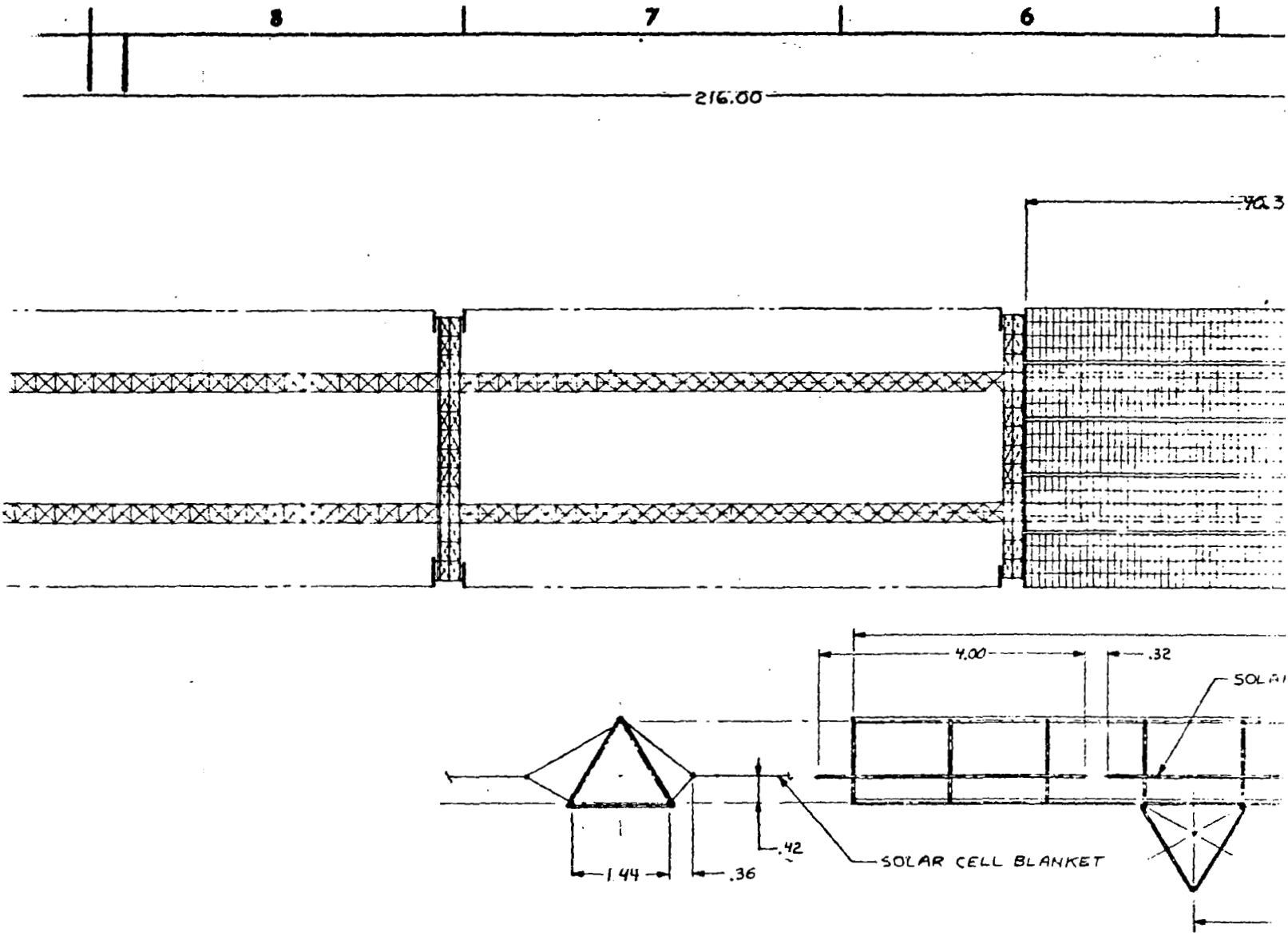
8
7
6
216.00
4.00
.32
1.44
.36
.42
SOLAR CELL BLANKET

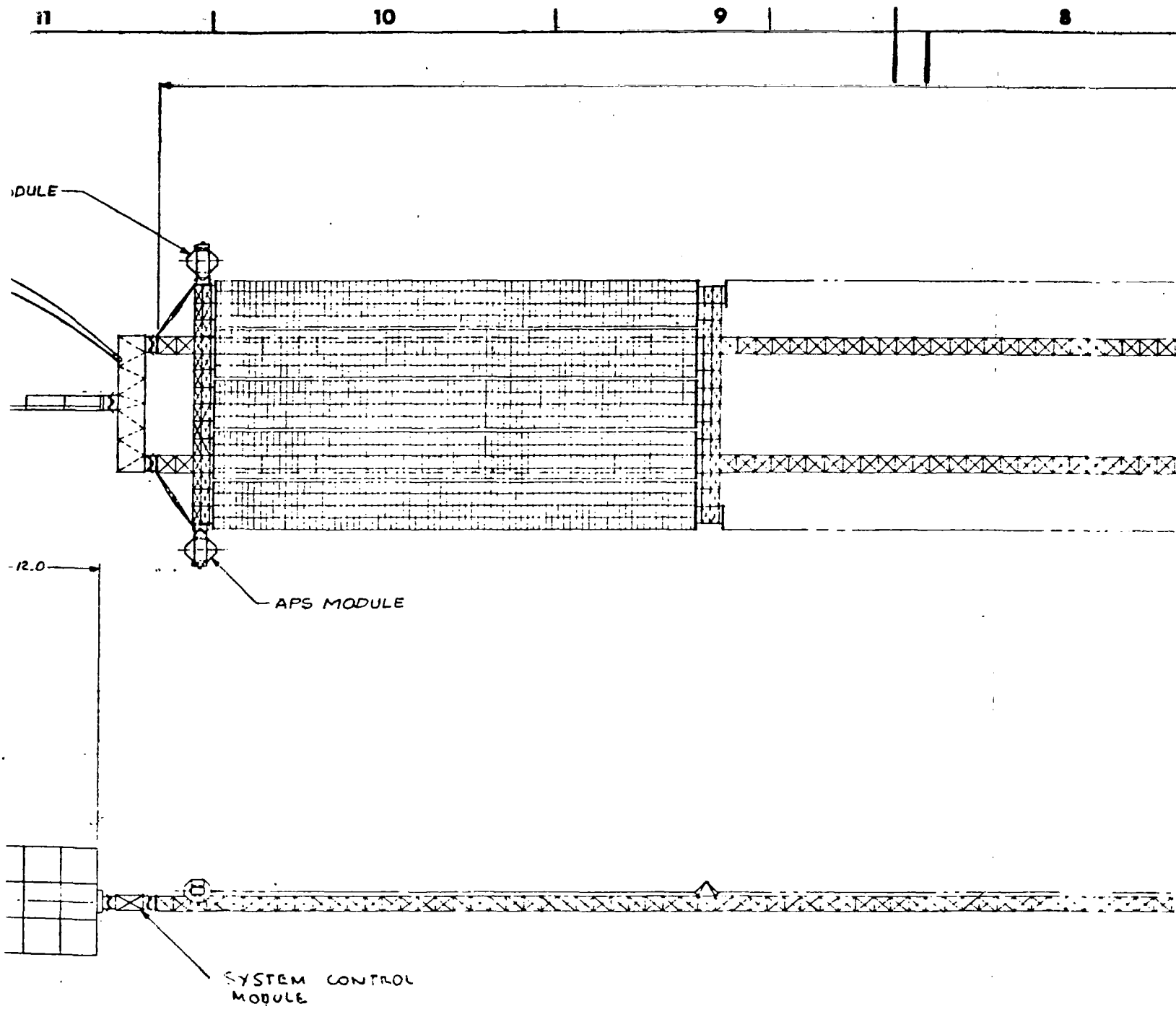
11
10
9
8
DULE
12.0
APS MODULE
SYSTEM CONTROL
MODULE

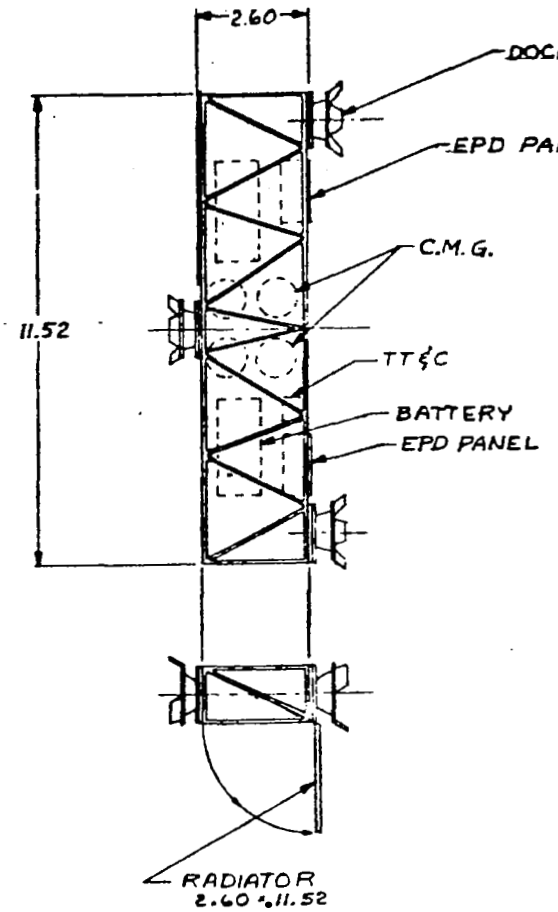

SYSTEM CONTROL MODULE
SCALE 1/80

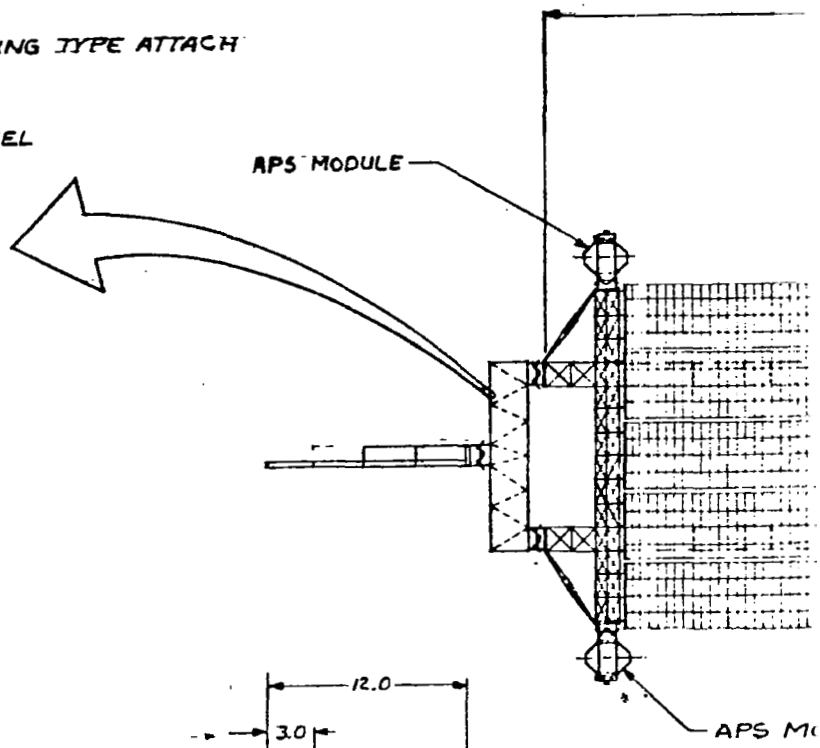

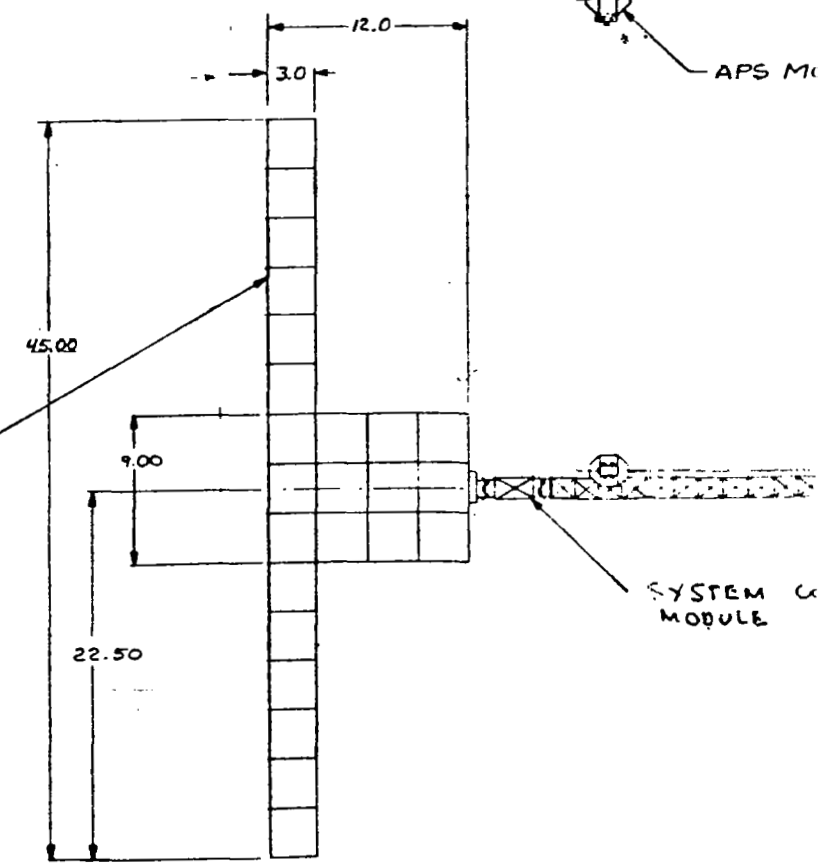

5 FIXTURE SIDE

ING PORT SIVE SIDE

5 BEAM

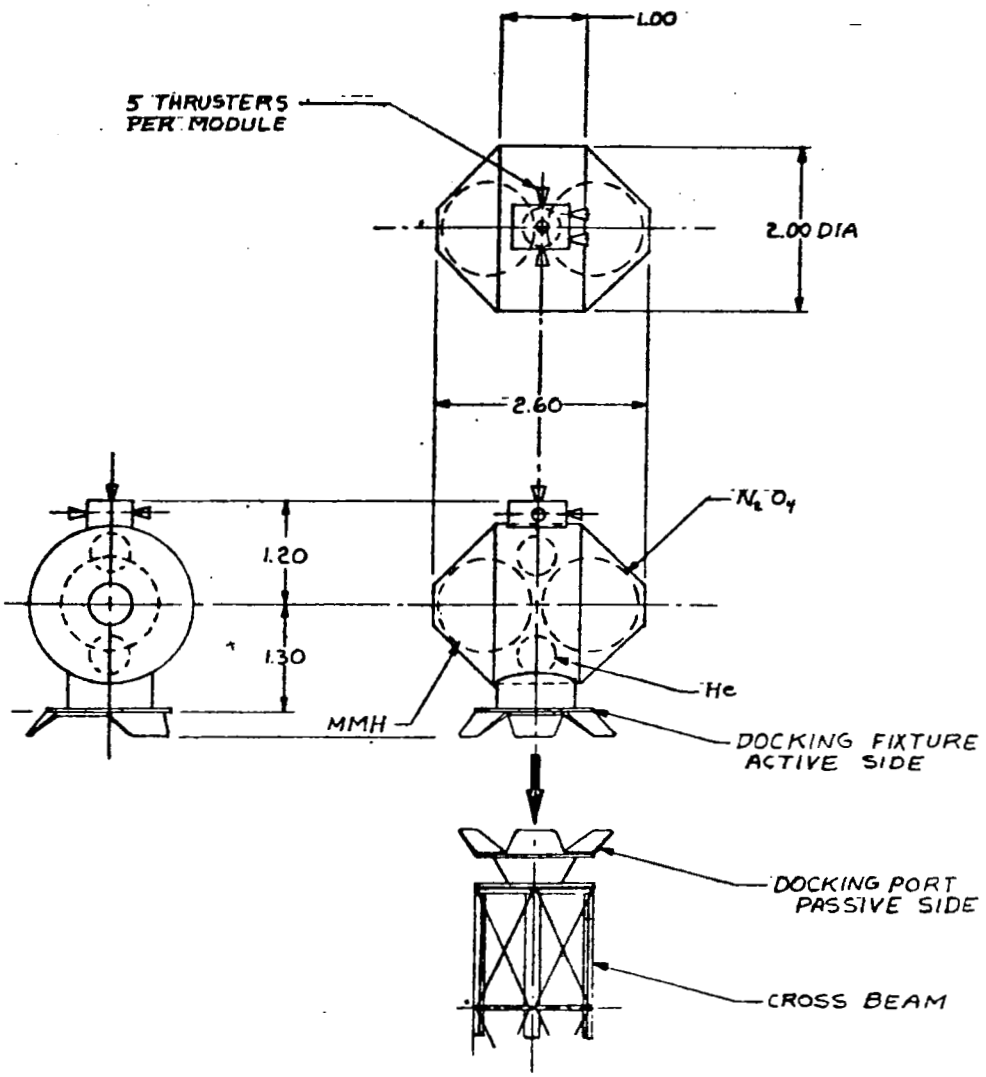

APS MODULE & DOCK PORT

SCALE 1/40

REVISIONS				
ZONE	LTR	DESCRIPTION	DATE	APPROVED

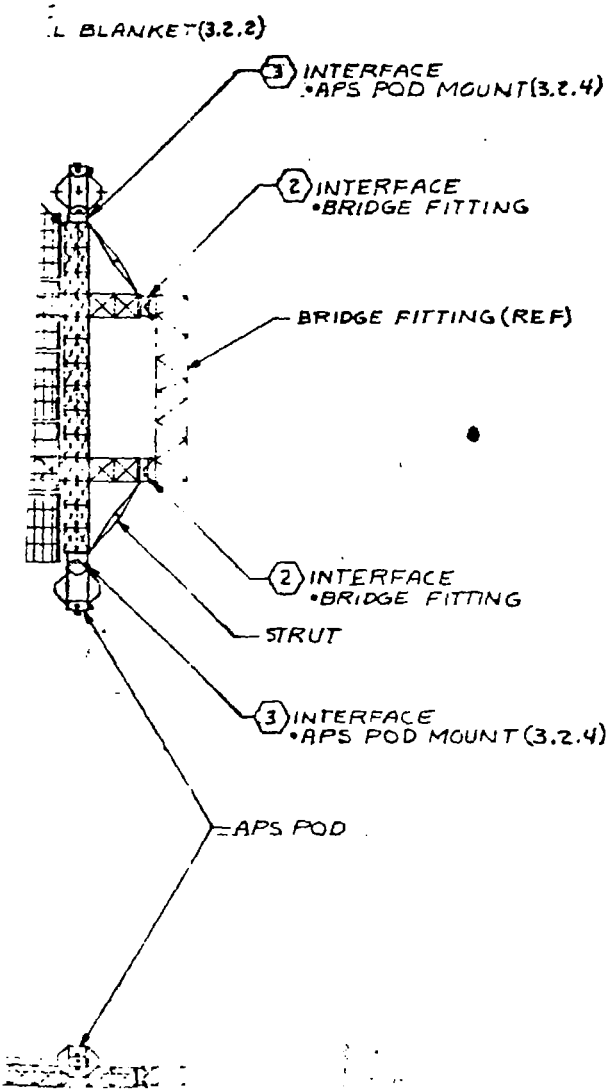

NOTES: UNLESS OTHERWISE SPECIFIED

1. THIS DRAWING IN CONJUNCTION WITH REPORT SD80-0102, SECTION 3.1.5 DEFINES THE FRAME STRUCTURAL REQUIREMENTS.
2. (X.X.X) DENOTES SECTION NUMBERS OF REPORT SD80-0102

DR BY		Rockwell International Corporation Space Division
CHK BY		
APPROVED BY		SPS-TEST ARTICAL II, INTERFACE DIAGRAM, LADDER CONFIGERATION
DIMENSIONS		SIZE: L; CODE IDENT NO: 03953; DRAWING NO: 42635-18032
		SCALE NOTED

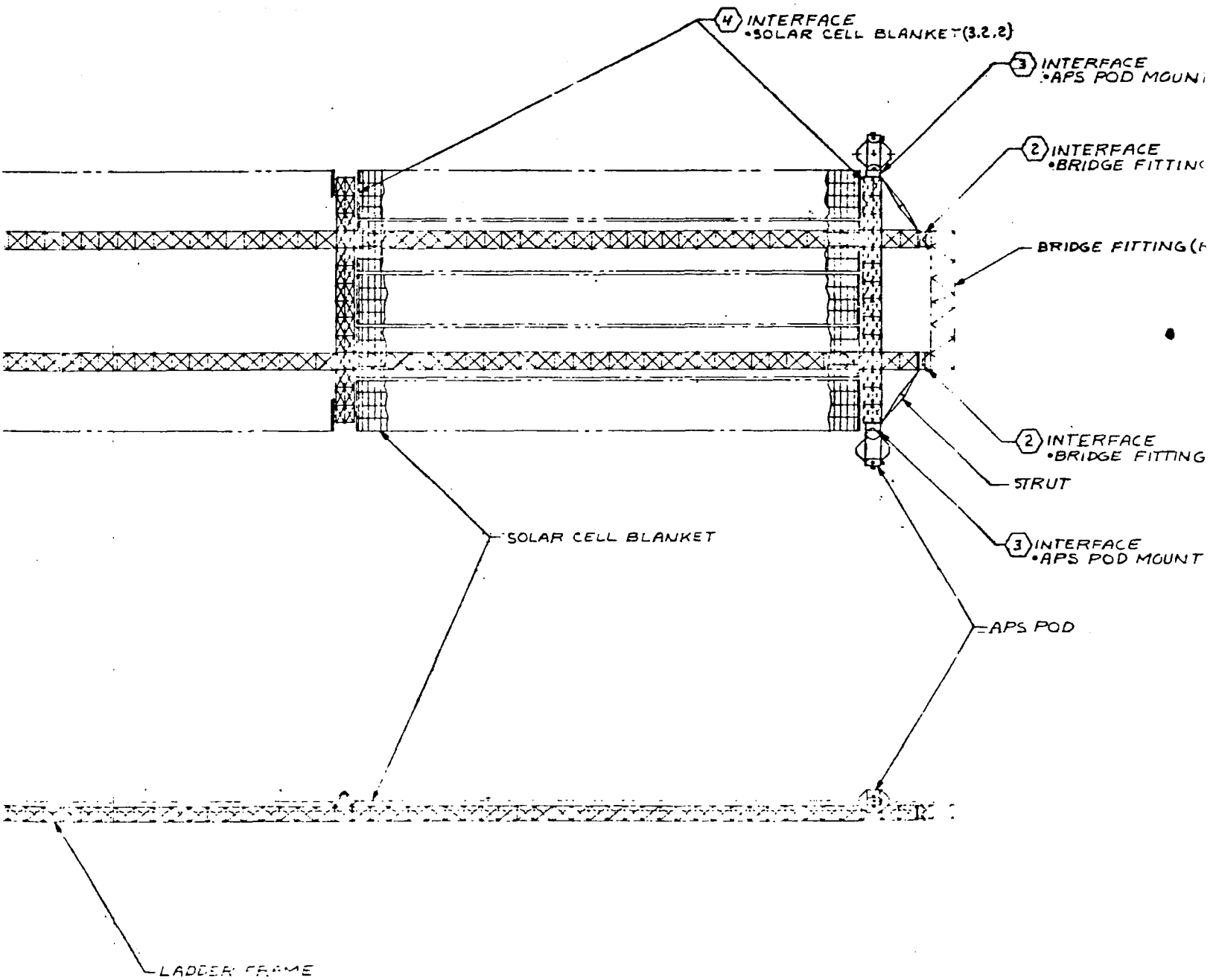
4 INTERFACE
•SOLAR CELL BLANKET (3.2.2)
3 INTERFACE
•APS POD MOUN
2 INTERFACE
•BRIDGE FITTIN
BRIDGE FITTING (
2 INTERFACE
•BRIDGE FITTING
STRUT
3 INTERFACE
•APS POD MOUNT
SOLAR CELL BLANKET
APS POD
LADDER FRAME

8 7 6 5

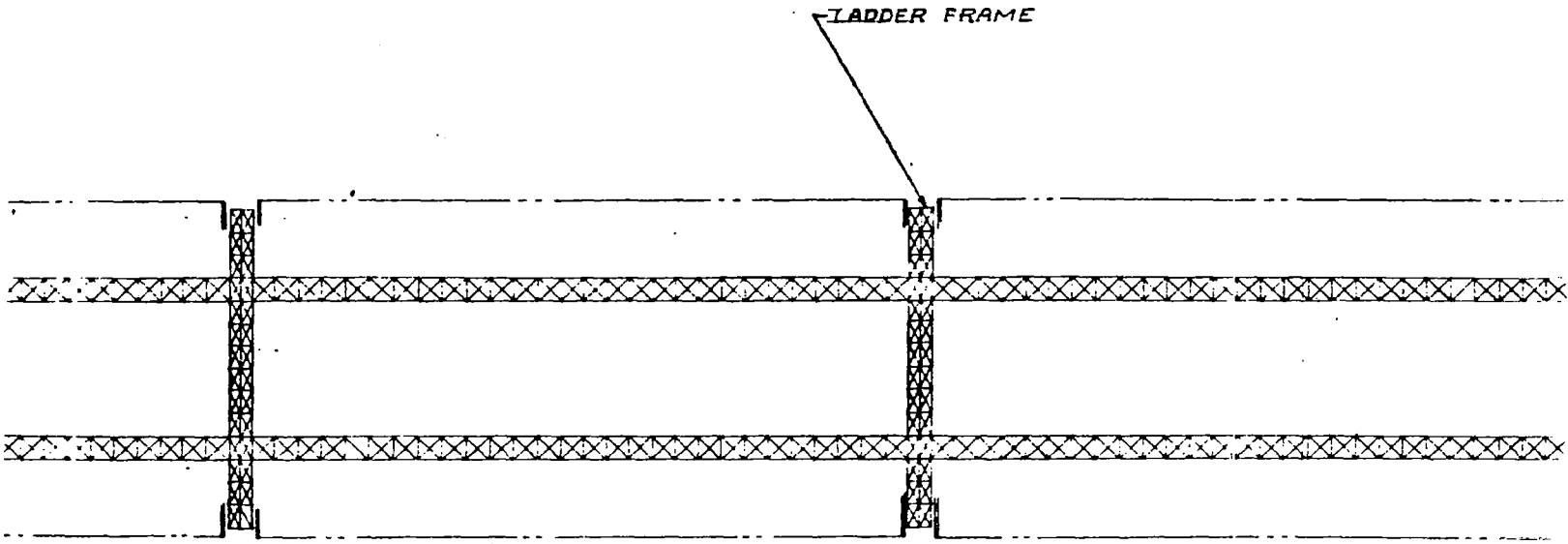

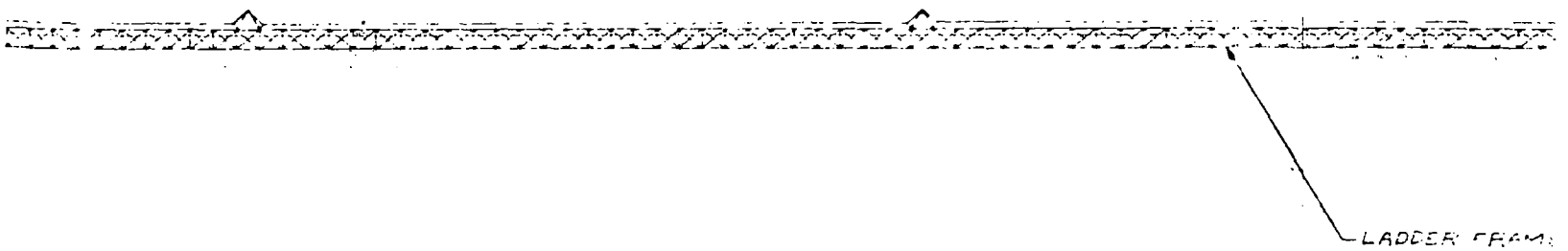

10 9 8 7

③ INTERFACE
• APS POD MOUNT (3, 2, 4)

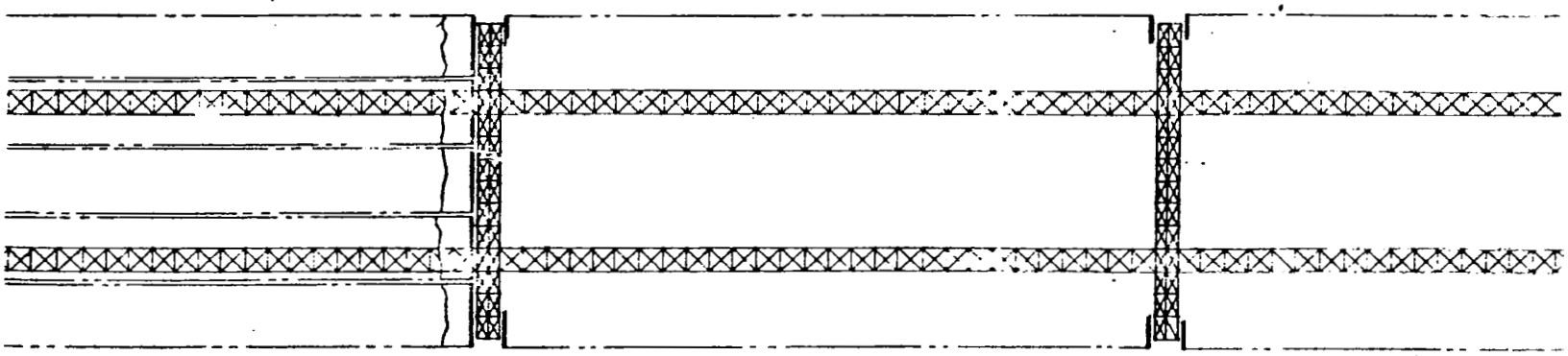

D(REF)

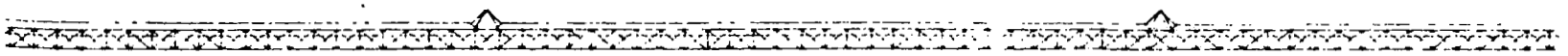

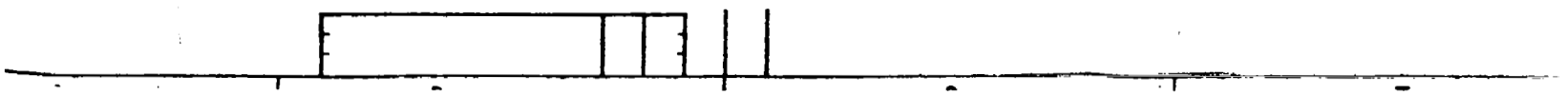

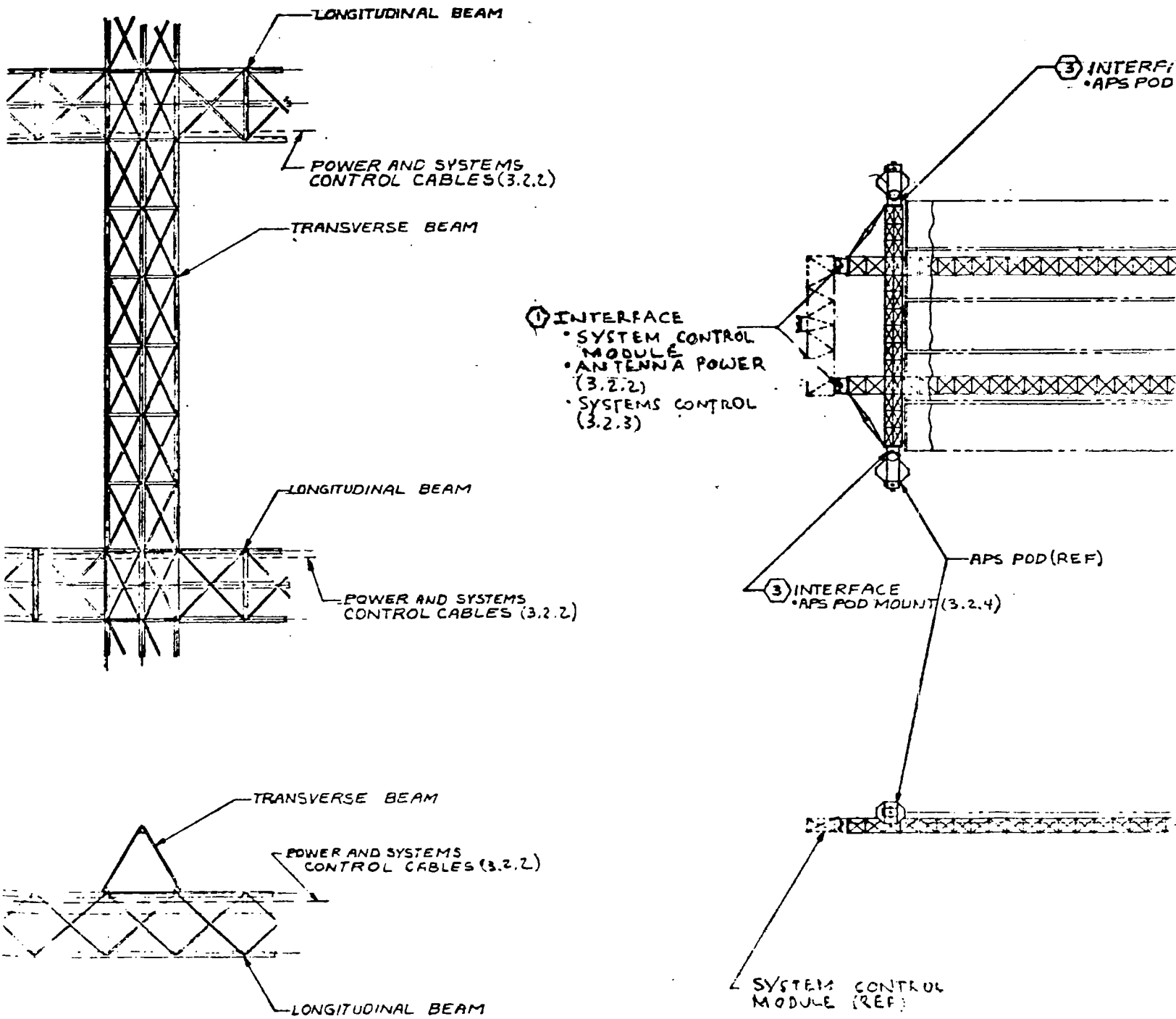

CE DETAILS

ALE 1/50

15 14 13

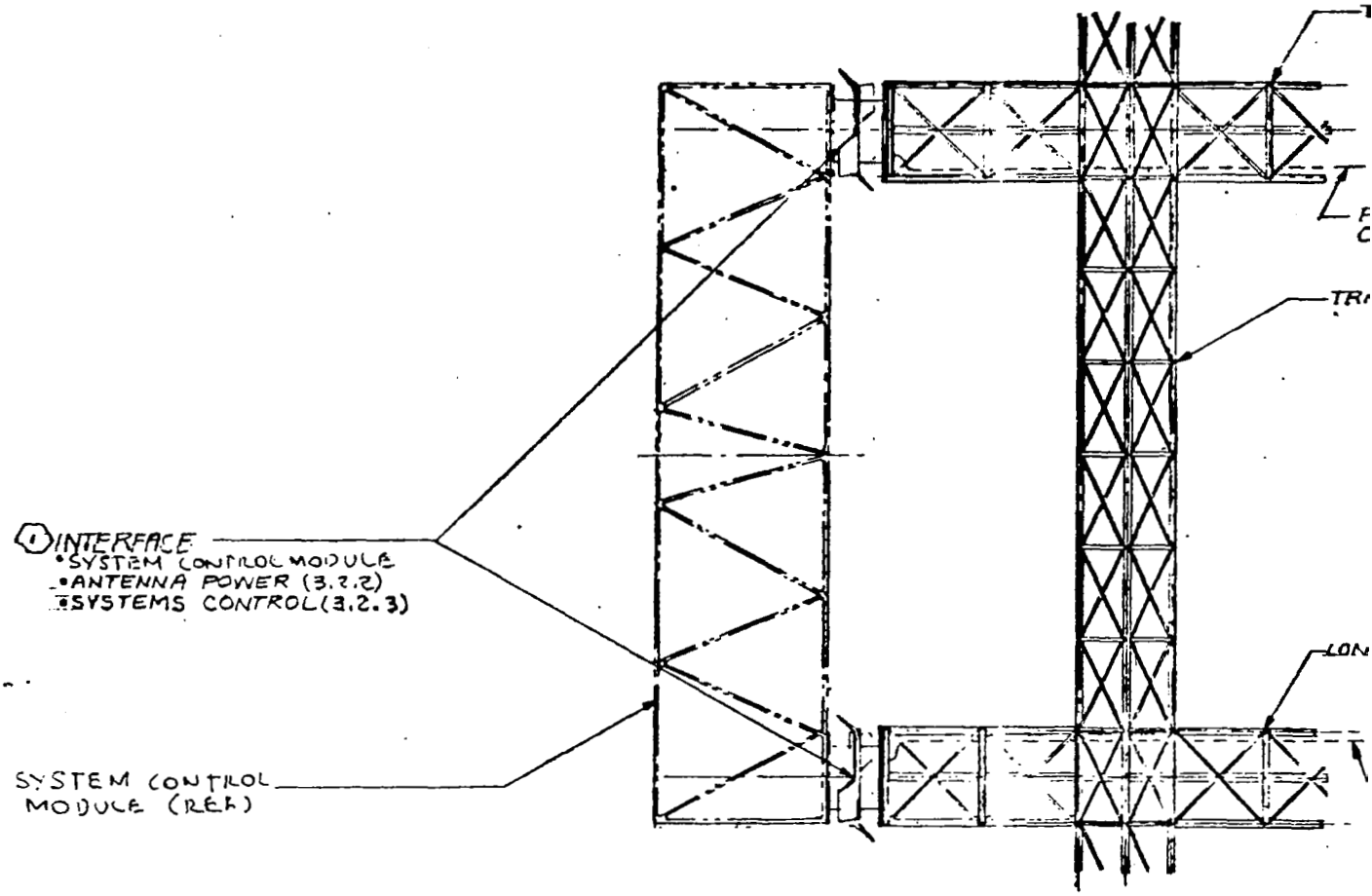

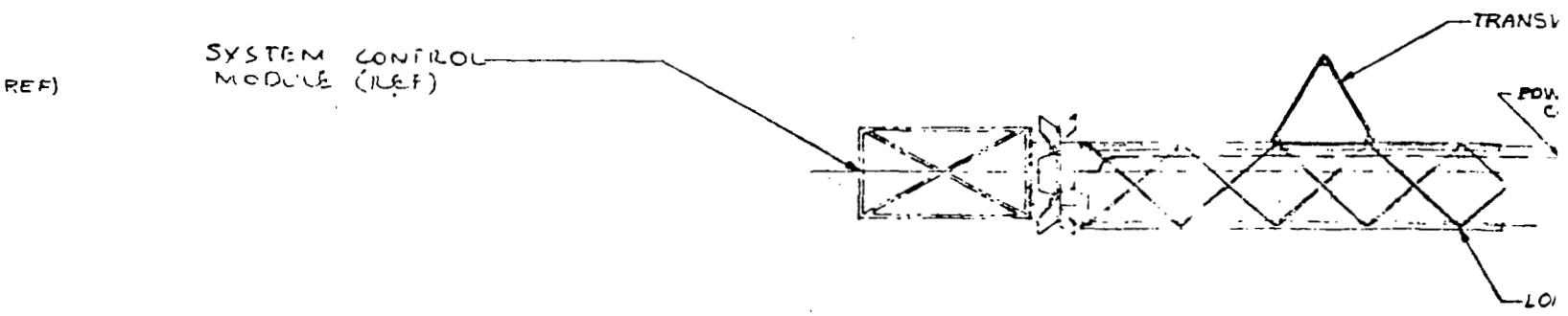

1 INTERFACE DETAILS
SCALE 1/50

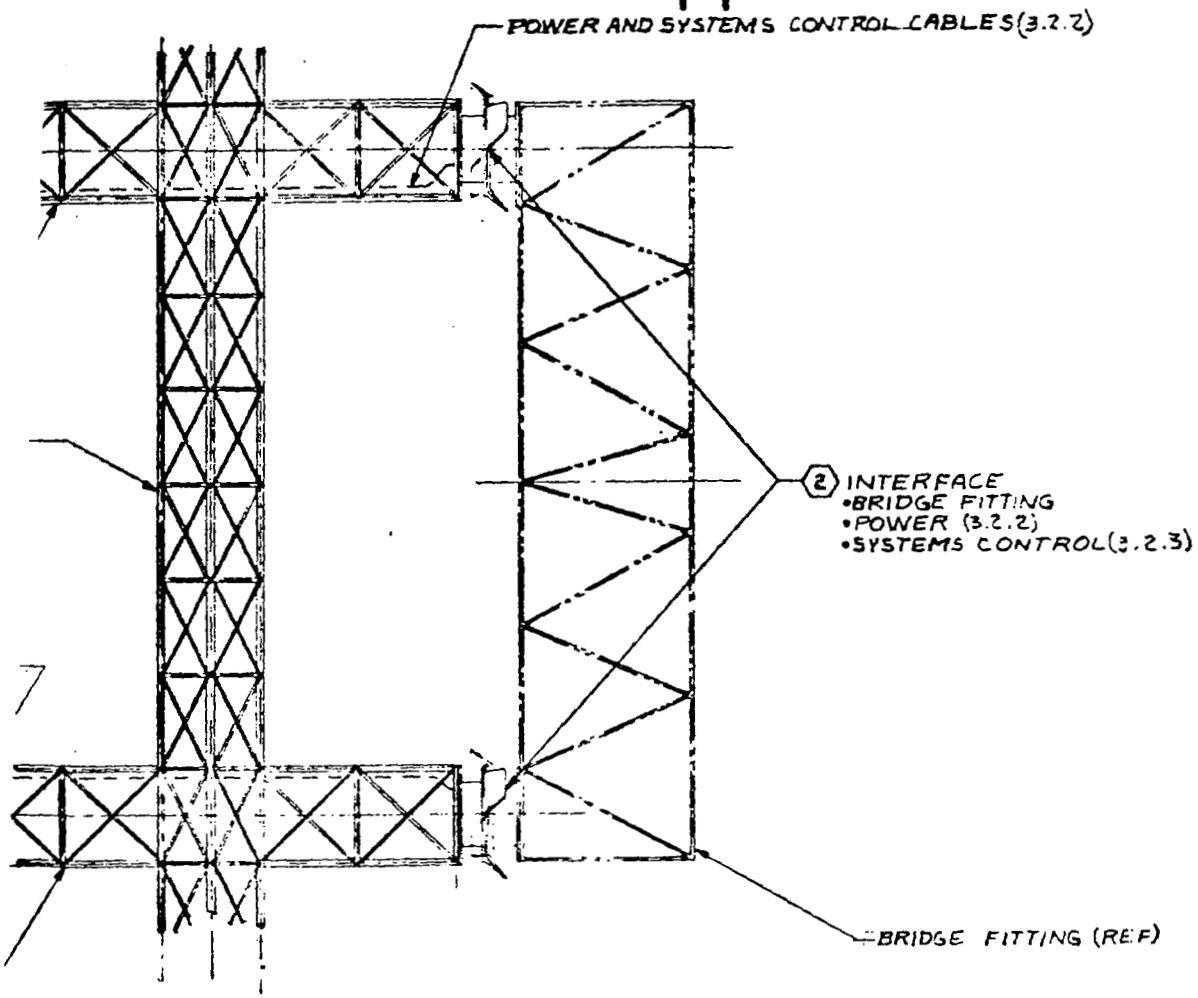

1 INTERFACE
•SYSTEM CONTROL MO
•ANTENNA POWER (
•SYSTEMS CONTROL

SYSTEM CONTROL MODULE (REF)

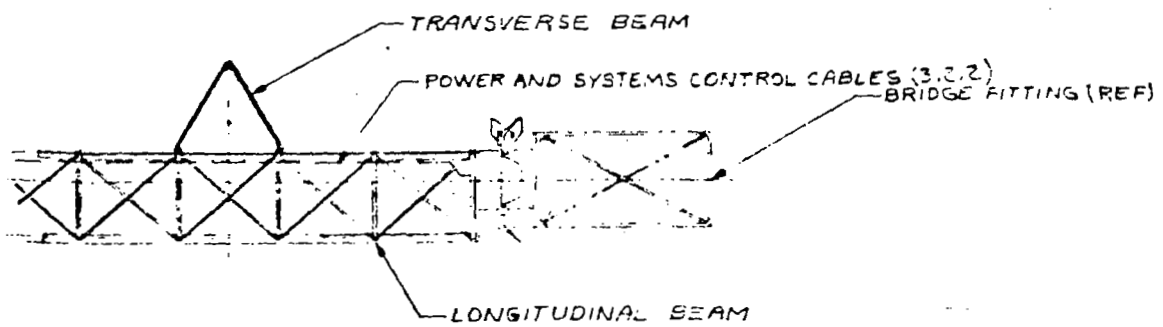

SYSTEM CONTROL MODULE (REF)

2 INTERFACE DETAILS
SCALE 1/50

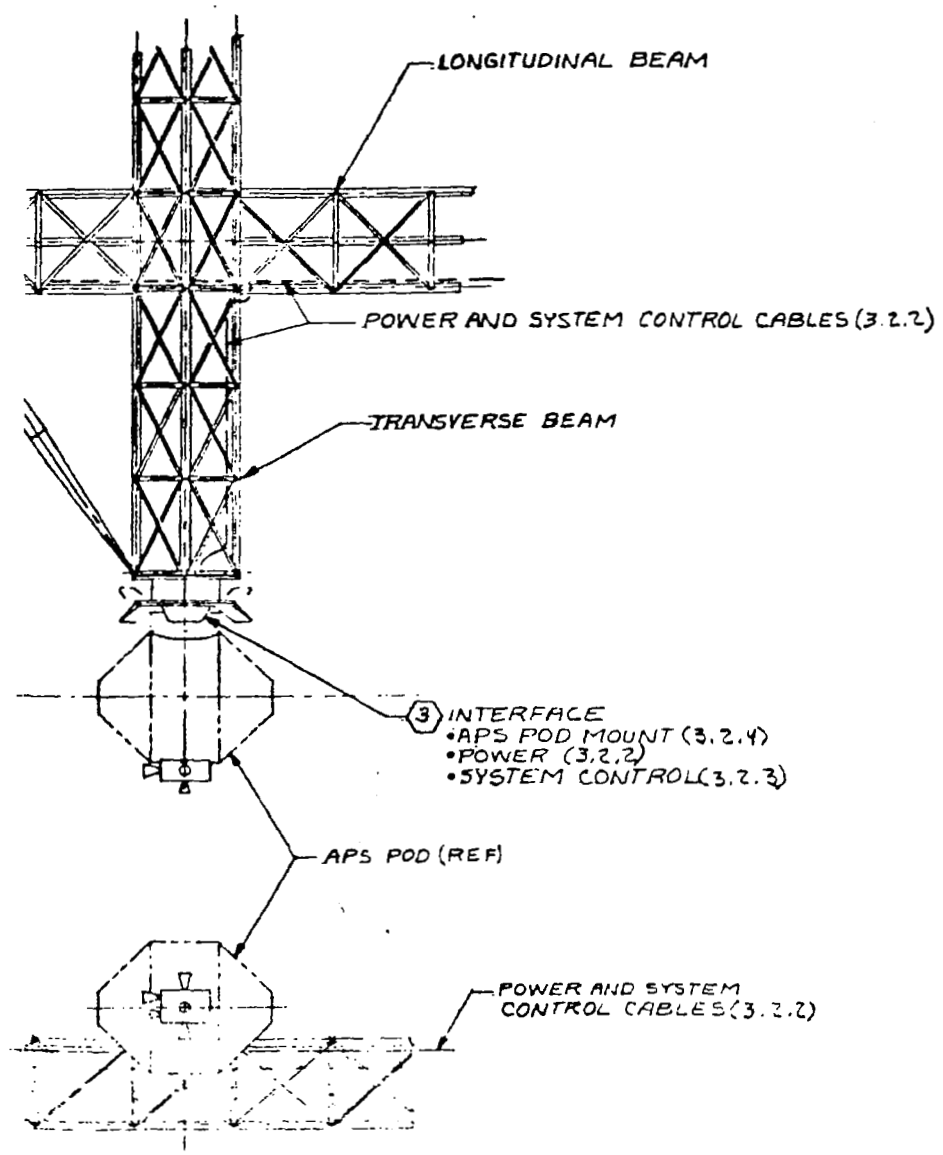

3 INTERFACE DETAILS
SCALE 1/50

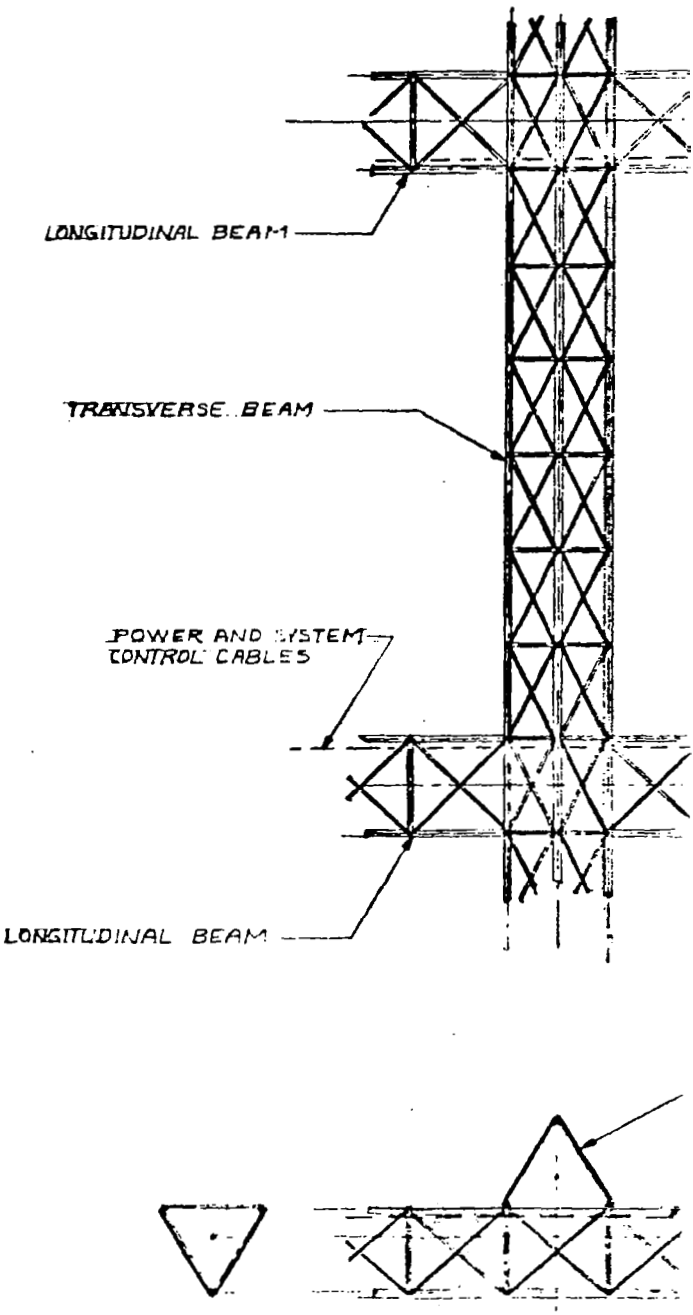

2 INTERFACE DETA
SCALE 1/50

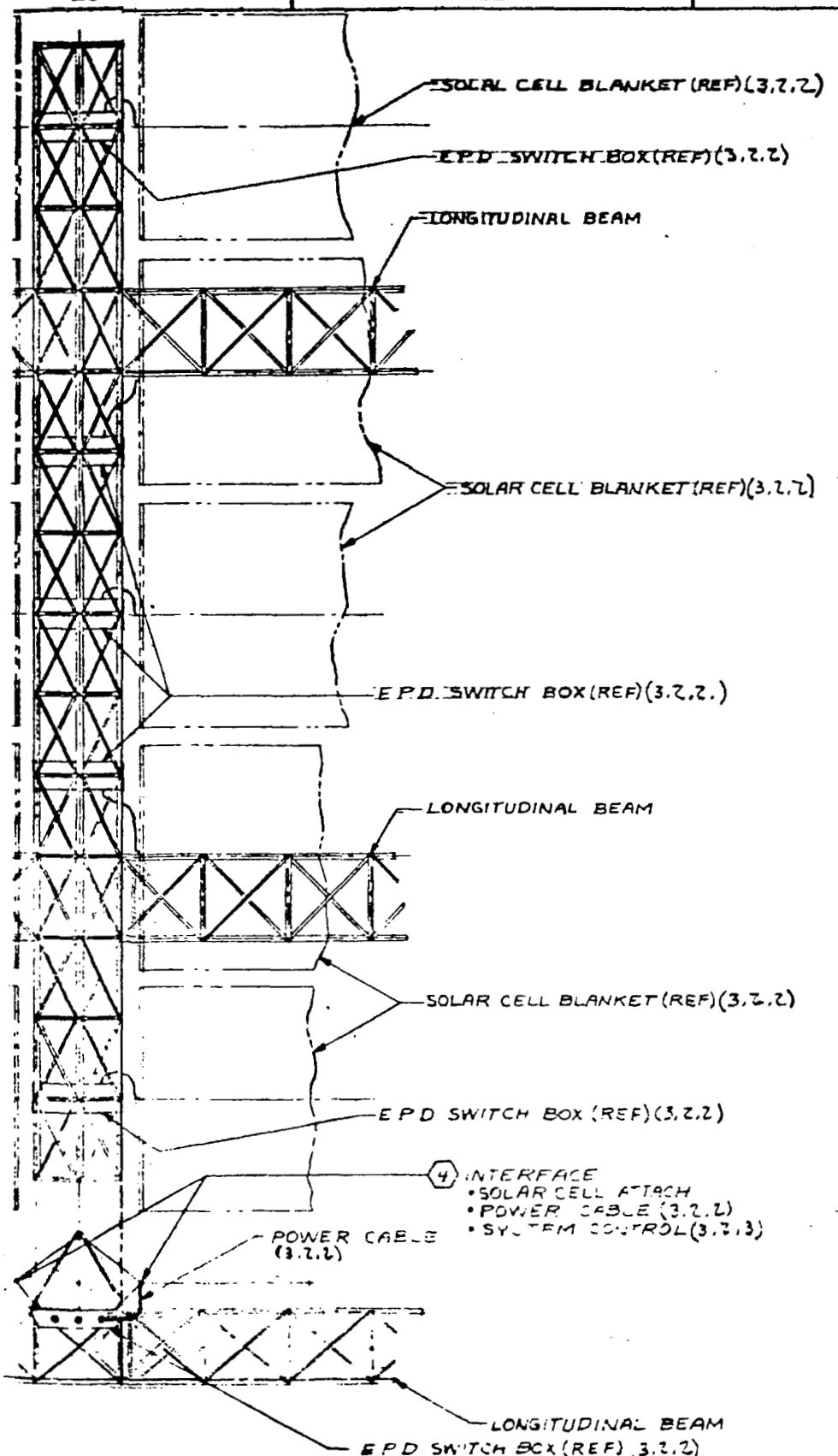

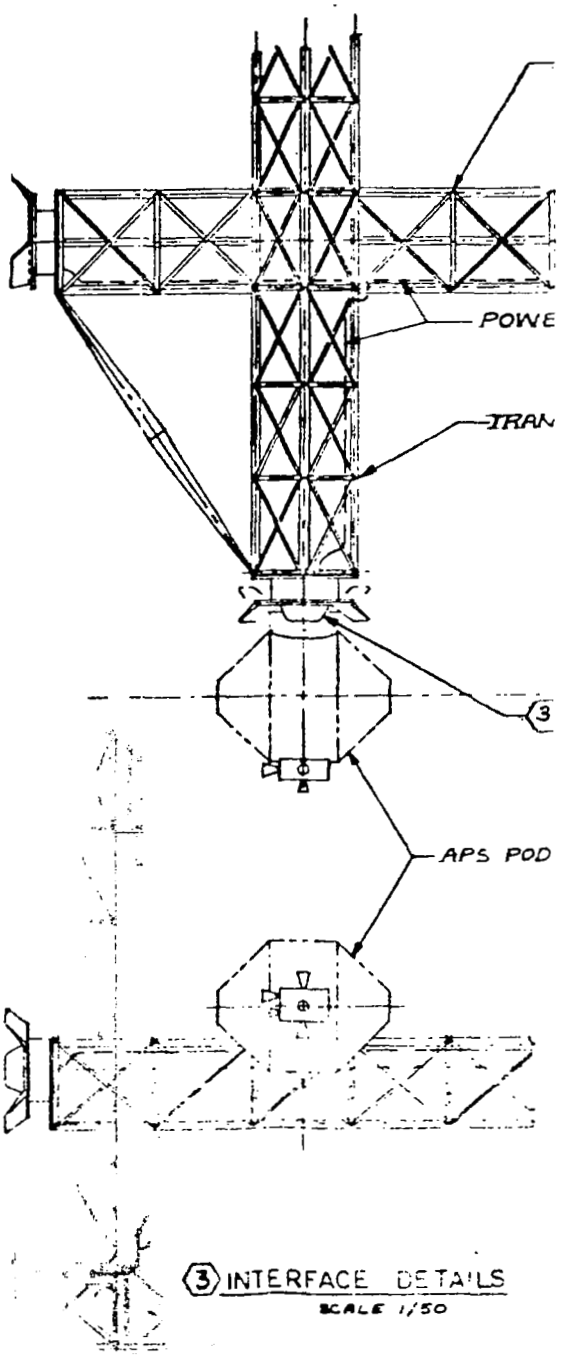

3 INTERFACE DETAILS
SCALE 1/50

RFACE DETAILS
SCALE 1/50

ELTA

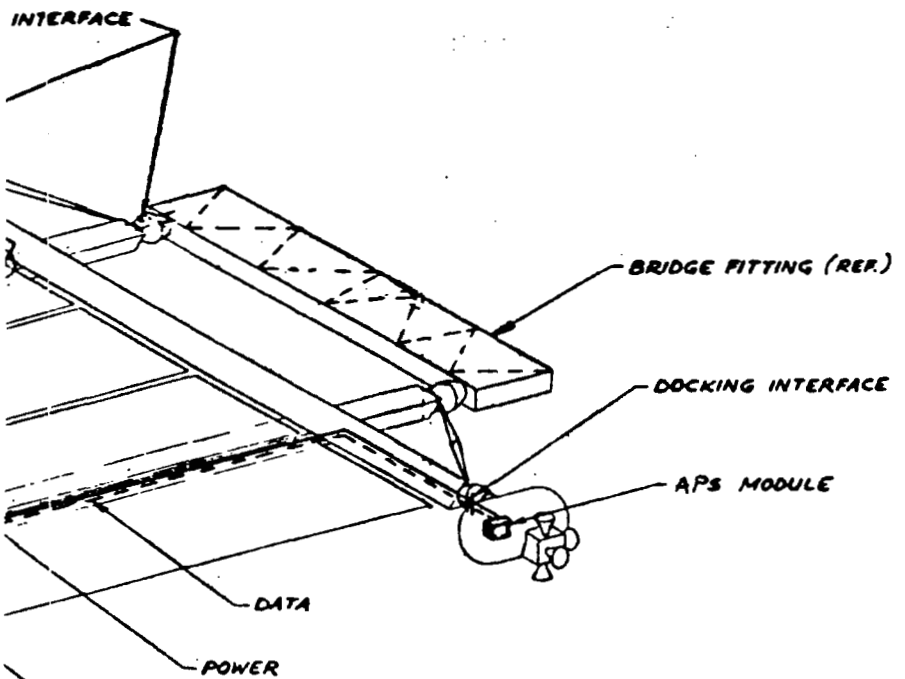

A LINES
SUPPORT
PPOSITE END
SION UNIT

OTE -
THE POWER OUTPUT FROM EACH SOLAR BLANKET SWITCH BOX IS AN INDIVIDUAL CABLE FEEDING DIRECTLY INTO THE DISTRIBUTION PANELS LOCATED IN THE SYSTEM SUPPORT HOUSING.

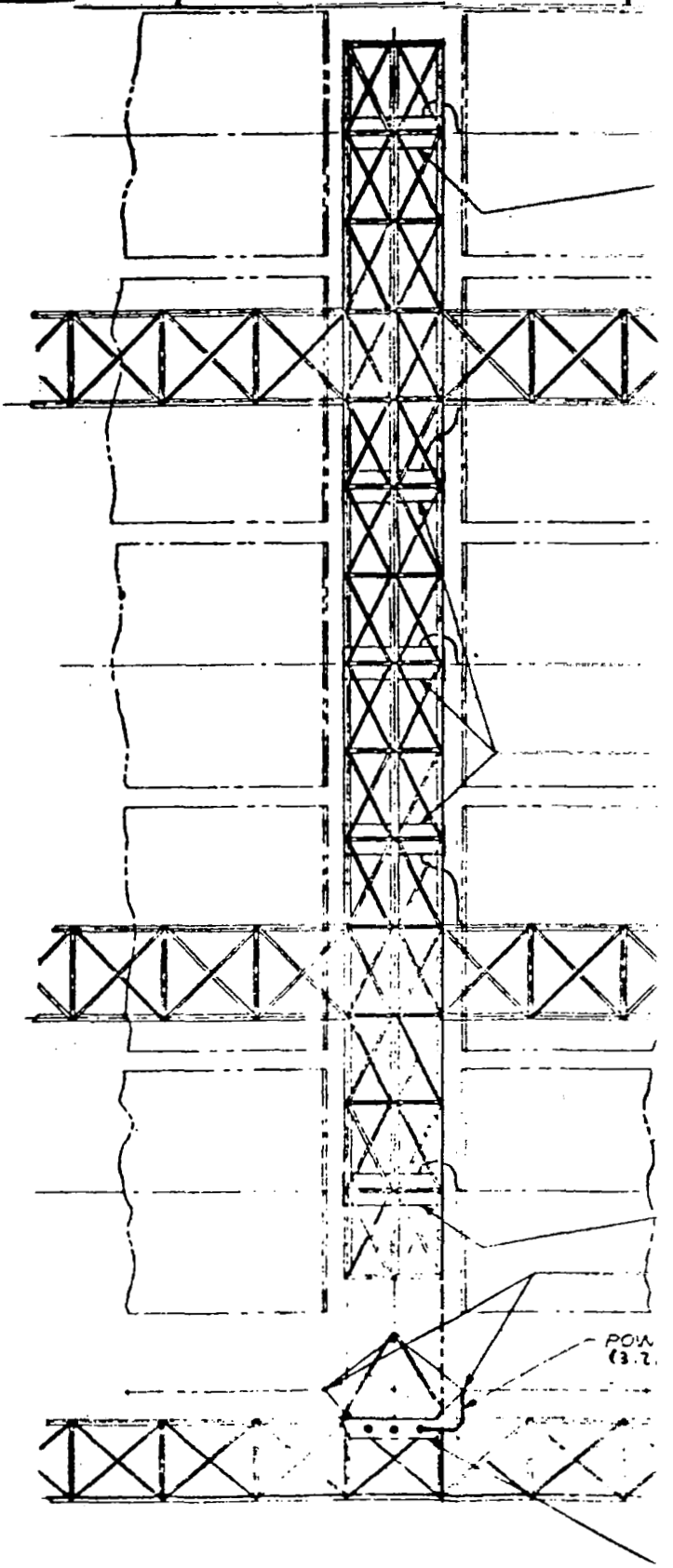

④ INTERFACE DETAILS
SCALE 1/50

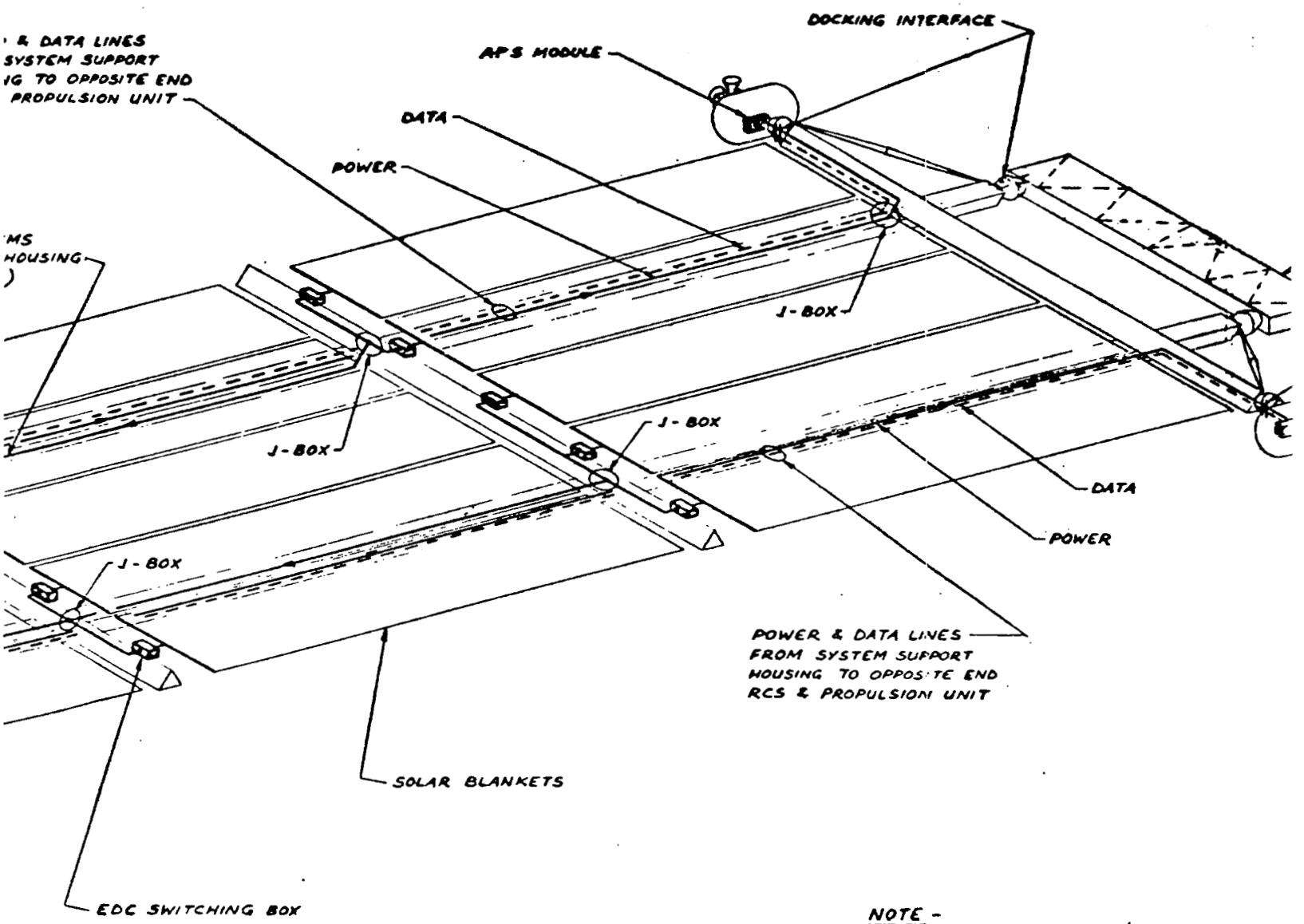

NOTE -
THE POWER OUTPUT FROM EACH SOLAR BLANKET SWITCH BOX IS AN INDIVIDUAL CABLE FEEDING DIRECTLY INTO THE DISTRIBUTION PANELS LOCATED IN THE SYSTEM SUPPORT HOUSING.

VIRE ROUTING SCHEMATIC

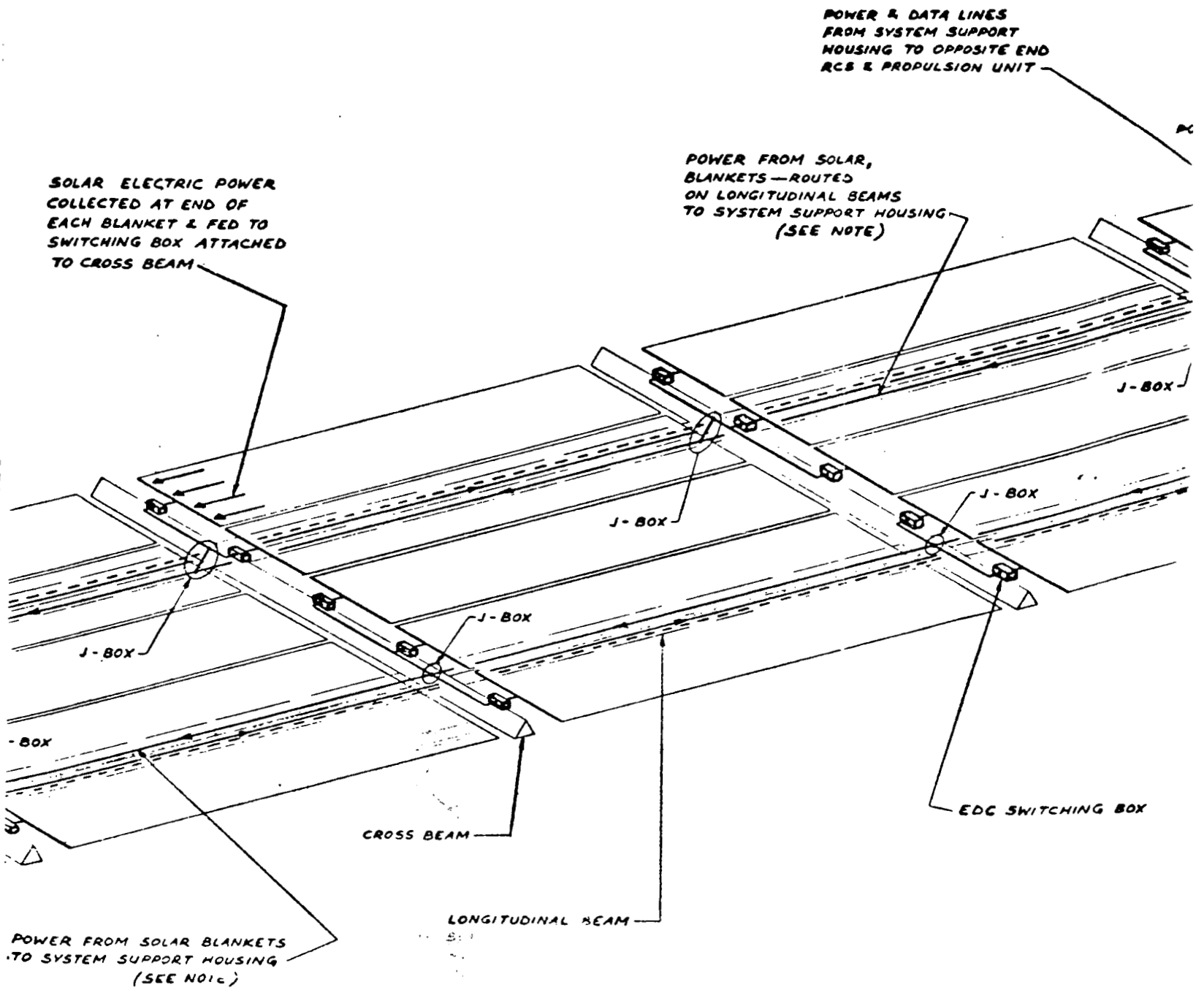

WIRE ROUTING SCHEM

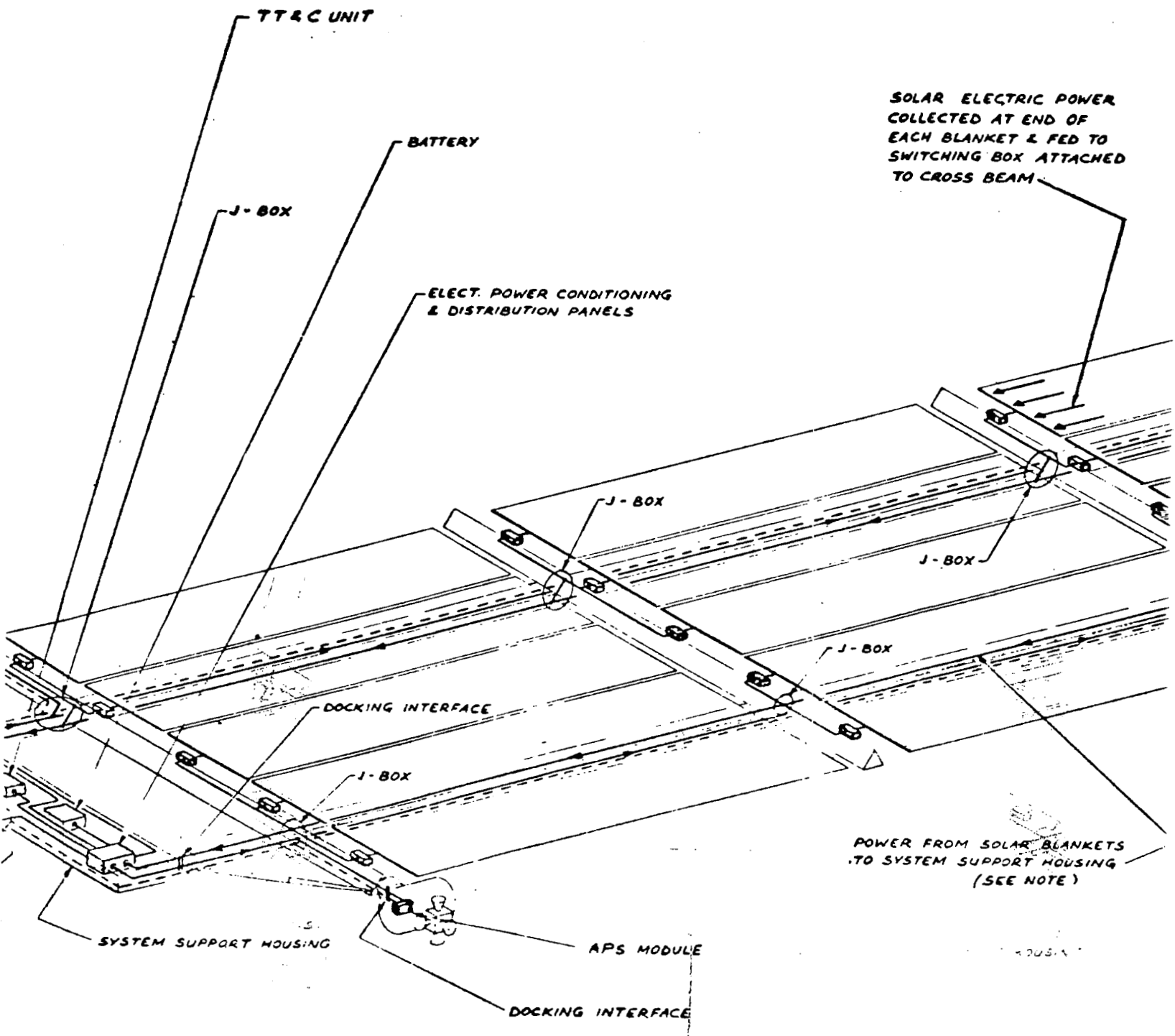
T T & C UNIT
BATTERY
J - BOX
ELECT. POWER CONDITIONING & DISTRIBUTION PANELS
SOLAR ELECTRIC POWER COLLECTED AT END OF EACH BLANKET & FED TO SWITCHING BOX ATTACHED TO CROSS BEAM
J - BOX
J - BOX
J - BOX
DOCKING INTERFACE
J - BOX
POWER FROM SOLAR BLANKETS TO SYSTEM SUPPORT HOUSING (SEE NOTE)
SYSTEM SUPPORT HOUSING
APS MODULE
DOCKING INTERFACE

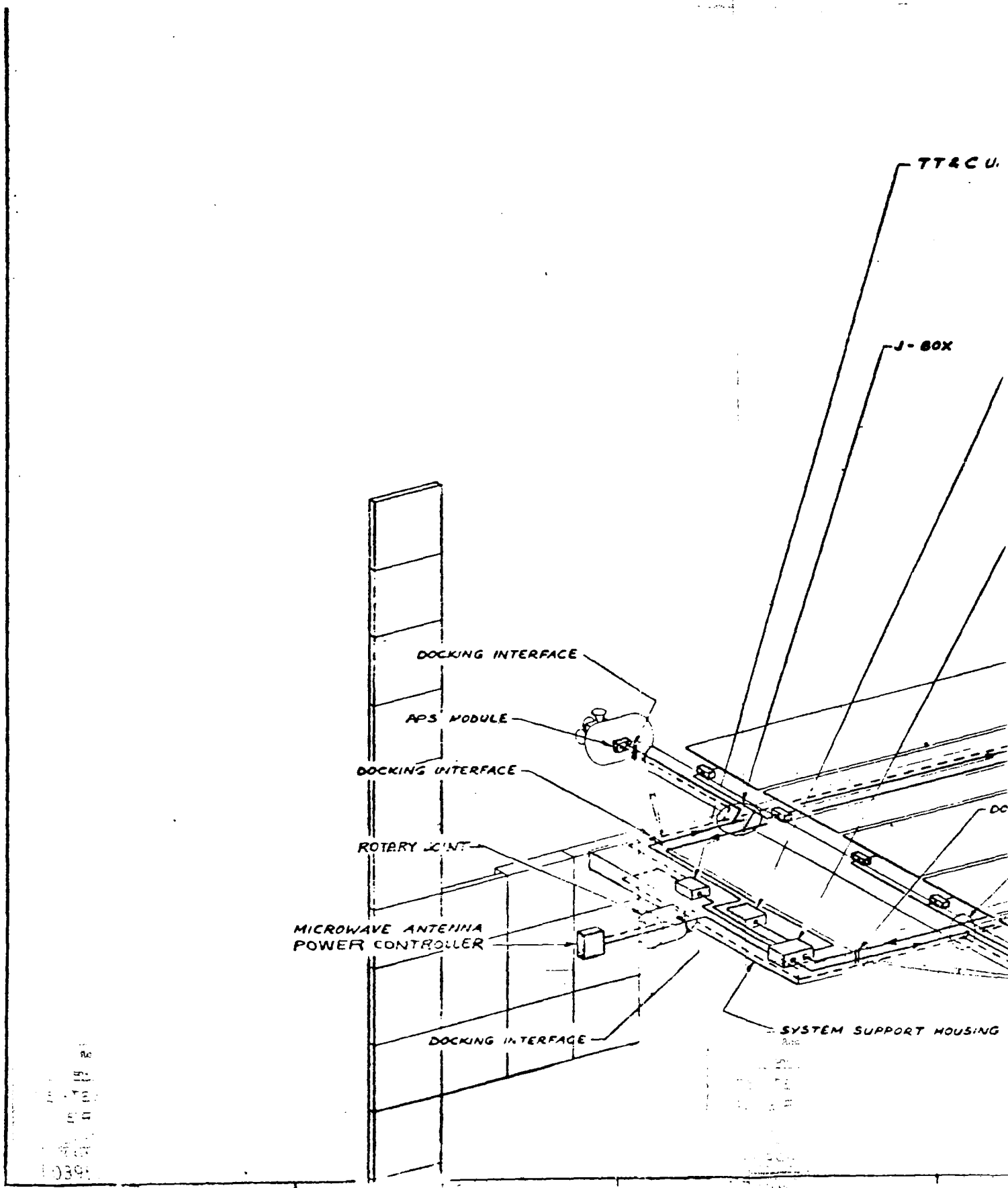
TT&C U.
J-BOX
DOCKING INTERFACE
APS MODULE
DOCKING INTERFACE
ROTARY JOINT
MICROWAVE ANTENNA
POWER CONTROLLER
DOCKING INTERFACE
SYSTEM SUPPORT HOUSING

TECHNICAL REPORT STANDARD TITLE PAGE

1. REPORT NO.	2. GOVERNMENT ACCESSION NO.	3. RECIPIENT'S CATALOG NO.
NASA CR-3375		

4. TITLE AND SUBTITLE	5. REPORT DATE
Satellite Power Systems (SPS) - LSST Systems Analysis and Integration Task for SPS Flight Test Article	February 1981
	6. PERFORMING ORGANIZATION CODE
7. AUTHOR(S)	8. PERFORMING ORGANIZATION REPORT #
H. S. Greenberg	SSD 80-0102
9. PERFORMING ORGANIZATION NAME AND ADDRESS	10. WORK UNIT NO.
Rockwell International, Space Division 12214 Lakewood Boulevard Downey, CA 90241	M-315
	11. CONTRACT OR GRANT NO. NAS8-32475
12. SPONSORING AGENCY NAME AND ADDRESS	13. TYPE OF REPORT & PERIOD COVERED
National Aeronautics and Space Administration Washington, DC 20546	Contractor Report
	14. SPONSORING AGENCY CODE

15. SUPPLEMENTARY NOTES

Marshall Technical Monitor: James K. Harrison
Final Report

16. ABSTRACT

This research activity emphasizes the systems definition and resulting structural requirements for the primary structure of two potential SPS large space structure test articles. These test articles represent potential steps in the SPS research and technology development.

17. KEY WORDS	18. DISTRIBUTION STATEMENT
Satellite Power Systems LSST Space Structures Systems Analysis Test Articles	Unclassified - Unlimited Subject Category 44

19. SECURITY CLASSIF. (of this report)	20. SECURITY CLASSIF. (of this page)	21. NO. OF PAGES	22. PRICE
Unclassified	Unclassified	141	A07

MSFC - Form 3292 (Rev. December 1972)

For sale by National Technical Information Service, Springfield, Virginia 22161

☆ U. S. GOVERNMENT PRINTING OFFICE : 1981—736-223

2 1 1U,E, 022381 S00903DS
DEPT OF THE AIR FORCE
AF WEAPONS LABORATORY
ATTN: TECHNICAL LIBRARY (SUL)
KIRTLAND AFB NM 87117